People's Democratic Republic of Algeria
Ministry of Higher Education and Scientific Research
University of Oum El Bouaghi
Faculty of: Exact Sciences and Nature and Life Sciences

Thesis

Presented to obtain

3rd Cycle Doctorate

Branch: Mathematics

Specialty: Applied Mathematics

Title :

On Nonlinear Fractional-Order Neural Networks

Presented by :
Amel Hioual

Publicly defended on 26/02/2025 in front of the following committee members:

N°	first and last name	Grade	University	Quality
01	Sofiane Dehilis	MCA	University of OumEl Bouaghi	President
02	Taki Eddine Oussaeif	Prof.	University of OumEl Bouaghi	Supervisor
03	Adel Ouannas	Prof.	University of OumEl Bouaghi	Co-reporter
04	Imed Rezzoug	Prof.	University of OumEl Bouaghi	Examiner
05	Ahlem Gasri	MCA	University of Tebessa	Examiner
06	Nadjet Abada	MCA	Assia Djebbar Higher Normal School of Constantine	Examiner

"Mathematics is the music of reason."

— James Joseph Sylvester

In the name of Allah, the Most Gracious, the Most Merciful.

To my dearest mother, my first and everlasting love. Your boundless affection and steadfast support have been the cornerstone of all my achievements. Your encouragement has been my guiding light, and your endless love has been my strength. Without you, none of this would have been possible.

To my late father, my first teacher and eternal guide. Though you are no longer with us, your wisdom, strength, and exemplary life continue to inspire me every day. Your teachings and love have shaped the person I am, and your memory fuels my determination to excel.

To my beloved sister and brother, whose countinuous support and faith in me have been a source of immense strength and motivation. Your belief in my potential has carried me through the most challenging times.

To my cherished husband, my partner and confidant. Your love, patience, and unwavering belief in our shared dreams have given me the courage to pursue my aspirations with passion and determination. Your presence in my life is a blessing beyond measure.

To my dear friends, whose loyalty and companionship have been a constant source of joy and support. Your encouragement and belief in me have enriched my journey.

And to all my family, who have stood by me with love and support. Each of you has played an integral part in my journey, and I am deeply grateful for your presence in my life.

Acknowledgment

Throughout the journey of my PhD studies, I have been blessed with an immense amount of support and assistance, for which I am profoundly indebted. This thesis, along with much of the related research, was carried out under the esteemed guidance of Professor Adel Ouannas.

Professor Ouannas, you have been the epitome of an ideal teacher, mentor, and thesis supervisor, offering a perfect blend of wisdom, insight, and humor. Your guidance has been a beacon, and your encouragement has been a cornerstone of my achievements. I am deeply honored and grateful for the opportunity to have worked under your supervision. I extend my heartfelt appreciation to Doctor Taki Eddine Oussaeif. Your invaluable assistance, profound insights, and unwavering support have been instrumental in the completion of this thesis. Your expertise and guidance have greatly enhanced the quality and depth of my work, and for that, I am deeply grateful.

My sincere thanks are due to the distinguished members of the dissertation jury, whose willingness to examine and evaluate my work has been invaluable. Your insightful feedback has significantly elevated the quality of this thesis: President of the Jury, Professor Imad Rezzoug, for your enlightenment, information, and guidance, during my PhD studies. Doctor Abada Nadjet, for your invaluable guidance and advice, drawn from your extensive experience, which has been a guiding light. Doctor Ahlem Gasri, for your dedication, energy, and efforts in evaluating and enhancing the quality of this work.

I also extend my deepest gratitude to my family, whose love and support have been my bedrock throughout this journey. To Mahmoud my late father, whose memory has been a constant source of strength and inspiration—your values and dreams for me have driven my determination and perseverance. To my amazing mother Halima, whose endless love, sacrifices, and encouragement have been my anchor. Your unwavering belief in me has been a source of immense strength, and I owe this accomplishment to you.

To my sister Nour El Houda, for her support and encouragement, always being there to listen and offer advice. To my brother Ayoub, for his constant belief in my abilities and his motivating words that kept me going during challenging times. Your support has been invaluable, and I am profoundly grateful.

To my dear husband Houssem Eddine Bousba, for his incredible patience, understanding, and steadfast support. Your encouragement and love have been my source of comfort and motivation. You have walked this journey with me, sharing in the highs and lows, and for that, I am eternally grateful.

Additionally, I would like to thank my friends and colleagues for their camaraderie, encouragement, and invaluable discussions that have contributed significantly to this work. A special thank you to my dear friends Zineb Laouar and Rahma Bounas. Zineb Laouar, your constant support, insightful advice, and belief in me have been a guiding light. The countless hours spent discussing research ideas and life challenges have been invaluable. Rahma Bounas, your friendship has been a source of great strength. Your enthusiasm and encouragement have kept me motivated, and your ability to find humor in even the most challenging situations has been a great relief.

To all of you, I express my deepest gratitude and appreciation.

Contents

List of Figures

General Introduction

Within the vast field of mathematical analysis, continuous fractional calculus boasts a significant and storied history. This branch of calculus is nearly as ancient as the well-known integer-order calculus, with its origins tracing back to the late 17th century. The concept of fractional derivatives was first introduced in 1695 when the Marquis de L'Hôpital posed a question to Gottfried Wilhelm Leibniz regarding the interpretation of a one-half derivative [1, 2]. This inquiry marked the inception of fractional calculus. However, it wasn't until the 19th century that a rigorous and comprehensive theoretical framework for fractional calculus was established. Mathematicians such as Joseph Fourier, Niels Henrik Abel, and others contributed to the foundational principles that underpin this field today [3, 4].

In the modern era, fractional calculus is being extensively investigated for its theoretical and practical applications [5, 6]. Its theoretical allure lies in its ability to generalize classical calculus, providing tools to model and analyze processes that exhibit anomalous behavior, such as those with memory effects and hereditary properties. These characteristics are particularly relevant in systems where the future state depends not only on the present state but also on the history of the system. This property of fractional systems makes fractional calculus a powerful tool for capturing the complexities of real-world phenomena [7, 8, 9].

The exploration of fractional-order dynamical systems has recently evolved into a prominent and multidisciplinary research effort. Scholars across diverse fields such as mechanics, viscoelasticity, electrical circuits, and engineering control have been captivated by the potential of fractional calculus to provide deeper insights into system dynamics [10, 11, 12]. These systems are characterized by their unique properties of infinite memory and hereditary traits, which differentiate them from classical integer-order systems. As a result, fractional-order models are increasingly being used to describe complex processes in various scientific and engineering disciplines.

In the topic of engineering control, fractional calculus provides more accurate models for systems with memory and hereditary properties, leading to the development of more robust and efficient control strategies [12]. Control systems designed using fractional calculus can better accommodate the dynamic behaviors of complex systems, resulting in improved performance and reliability in applications ranging from robotics to aerospace engineering. In mechanics, for instance, fractional calculus is utilized to model materials with viscoelastic properties, which exhibit both viscous and elastic behavior over time [13]. This is crucial for understanding and predicting the behavior of materials under different stress and strain conditions. In the field of electrical engineering, fractional-order circuits are employed to design filters, oscillators, and other electronic components with enhanced performance characteristics [14]. These circuits leverage the memory prop-

erties of fractional derivatives to achieve superior stability and response characteristics compared to their integer-order counterparts.

Innovative contributions by researchers, notably Yang and others, have played an important role in refining and extending the theory of fractional calculus. These efforts have been particularly significant in the topic of local fractional calculus [15, 16, 17]. Local fractional calculus deals with functions that are not differentiable in the traditional sense, enabling the analysis of fractal structures and other complex geometries. This branch of fractional calculus has opened up new avenues for research, providing deeper insights into the behavior of complex systems with non-integer dimensions.

Variable-order calculus offers a fresh approach to mathematical analysis, drawing from established fractional calculus techniques. It introduces the concept of variable-order differential and integral operations, which opens up new possibilities in understanding complex real-world phenomena [18, 19, 20, 21, 22, 23]. By adjusting the order of operations, variable-order calculus simplifies problem-solving and can reveal hidden patterns in data. This approach prompts us to reconsider traditional methods and explore nonlinear behavior in systems previously thought to be linear. Ultimately, variable-order calculus provides a promising avenue for modeling systems with memory effects, offering new insights and solutions to scientific problems.

Despite the existence of a well-established mathematical theory for continuous fractional calculus, until recently, there had been no significant parallel development in the topic of discrete fractional calculus [24, 25, 26]. However, over the past five to seven years, there has been a burgeoning interest in this area, leading to substantial advancements. This newfound focus on discrete fractional calculus has unveiled a host of unforeseen challenges and technical difficulties, which researchers are actively addressing.

Exploring further the foundational theories, the domain of discrete fractional calculus and fractional difference operators has garnered considerable attention among mathematicians [28, 29]. This interest has been driven by the potential to extend the concepts of continuous fractional calculus to discrete settings, thereby enabling the analysis of systems that evolve in discrete time steps. The development of discrete fractional operators has opened up new avenues for modeling and analyzing complex systems that exhibit fractional-order dynamics [30, 31].

One notable area of exploration is the integration of chaotic maps into discrete fractional calculus. As demonstrated in references [32, 33], this approach has not only expanded our understanding of discrete fractional systems but has also highlighted the persistence of chaotic characteristics within this framework. For instance, the study of the synchronization of chaotic dynamics in discrete fractional logistic maps [33] has provided valuable insights into the behavior of such systems and their potential applications. Similarly, the investigation of equilibrium properties in discrete non-autonomous systems [34] has further enriched the field by revealing the complex interactions and stability considerations in these systems.

In recent years, the exploration of incommensurate discrete fractional-order systems has emerged as a critical area of investigation [35, 36, 37]. These systems, characterized by their non-integer-order dynamics in discrete time steps, pose unique challenges and opportunities for stability and synchronization analysis. Researchers are actively studying

the stability criteria and synchronization phenomena within these systems [38, 39], aiming to extend the insights gained from continuous fractional calculus to discrete settings.

Understanding stability in fractional discrete systems involves distinguishing between commensurate and incommensurate cases. Commensurate systems have orders that can be expressed as ratios of integers, whereas incommensurate systems have orders that cannot be expressed as such ratios. The stability analysis of commensurate fractional discrete systems often relies on traditional methods adapted from integer-order calculus, albeit with adjustments to account for fractional dynamics [40, 41, 42]. These systems exhibit stability characteristics that are more predictable and easier to analyze due to their periodic or quasi-periodic nature.

On the other hand, incommensurate fractional discrete systems present more complex stability challenges. Their non-integer-order dynamics do not align with simple periodicity, leading to irregular behaviors that require specialized analytical techniques. Stability criteria for incommensurate systems often involve sophisticated mathematical tools such as Lyapunov exponents, bifurcation analysis, and numerical simulations [43, 44, 45]. These systems may exhibit chaotic or quasi-chaotic behaviors depending on their specific fractional orders and initial conditions, necessitating a deeper understanding of their stability properties. The exploration of stability in both commensurate and incommensurate fractional discrete systems represents a frontier in mathematical analysis and engineering applications. Advances in this area not only contribute to the theoretical foundation of fractional calculus but also pave the way for innovative applications in diverse fields such as signal processing, control systems, and data science. By elucidating the stability criteria and dynamics of fractional discrete systems, researchers can harness the unique properties of fractional calculus to solve real-world problems more effectively.

Moreover, researchers have introduced novel criteria to ensure the asymptotic stability of nonlinear fractional-order systems in a discrete nabla setting. As evidenced by the research presented in [46, 47, 48], these criteria are crucial for developing robust and reliable models of discrete fractional systems. The discrete nabla calculus offers a powerful tool for analyzing the stability and dynamics of such systems. This has significant implications for various applications, ranging from control theory to signal processing.

In recent years, synchronization phenomena in fractional discrete systems have garnered significant attention due to their implications for various applications in science and engineering. Synchronization, defined as the phenomenon where multiple systems achieve a coordinated behavior over time, plays a crucial role in enhancing the robustness and functionality of networked systems [49, 50, 51][52]-[109]. Unlike their integer-order counterparts, fractional-order systems exhibit complex dynamics that include memory effects and non-local interactions, making synchronization analysis non-trivial. Recent research has focused on understanding synchronization in discrete fractional systems, exploring how system parameters and initial conditions influence synchronization stability and dynamics [110, 111][112]-[136].

Neural networks, also known as artificial neural networks, are computational models inspired by the structure and function of biological neural networks in the human brain. They consist of interconnected nodes, called neurons or units, organized into layers. These layers typically include an input layer, one or more hidden layers, and an output layer

[137, 138, 139].

The neural network operates by receiving input data through the input layer, which is then processed through the hidden layers using weighted connections and activation functions. Each neuron in the hidden layers aggregates the input data, applies weights to them, and passes the result through an activation function to introduce nonlinearity into the system. The output layer produces the final result or prediction based on the processed information.

Neural networks are trained using a process called backpropagation, where the network adjusts its internal parameters (weights and biases) iteratively to minimize the difference between the predicted output and the actual output for a given set of training data [140, 141]. This training process involves feeding the network with labeled input-output pairs and updating the weights and biases based on the calculated error.

Neural networks have demonstrated remarkable capabilities in various tasks, including pattern recognition, image classification, natural language processing, and regression analysis [142, 143, 144]. They have found applications in diverse fields such as finance, healthcare, marketing, robotics, and autonomous vehicles, among others [145, 146, 147].

Stability analysis of neural networks is crucial for assessing their behavior under different conditions and ensuring their robustness and reliability in real-world applications [148]. It involves examining how small perturbations or changes in the networks parameters affect its performance and stability over time. Understanding the stability properties of neural networks is essential for designing efficient learning algorithms, optimizing network architectures, and deploying neural networks in safety-critical systems [149].

Research into dynamical system and network stability analysis has made significant advancements, particularly since the 1990s. Recent decades have seen a surge in research focusing on the stability analysis of fractional neural networks, which serve as mathematical models mirroring the behaviors of organic nervous systems across continuous and discrete-time domains [150, 151, 152, 153]. However, due to the absence of complete analytical solutions, stability analysis remains one of the most challenging areas of study today.

The allure of stability, particularly in finite-time scenarios, has attracted scholars from diverse fields, leading to the formulation of numerous theoretical frameworks [154, 155, 156, 157, 158, 159]. For instance, investigations into finite-time stability in fractional-order disdcrete neural networks reflect the widespread interest in applying fractional calculus concepts to real-world problems [160]. Similarly, research on finite-time stability has extended to fractional-order complex-valued neural networks, providing valuable insights into critical aspects of system behavior[161, 162].

In neural networks, synchronization phenomena are crucial for understanding information processing, learning, and decision-making processes [163, 164]. Neural networks with fractional-order dynamics exhibit rich synchronization behaviors that are not observed in integer-order networks. Synchronization in these networks can enhance information transfer, improve computational efficiency, and mitigate noise and perturbations in networked environments [165, 166, 167]. Studies have demonstrated synchronization in fractional-order neural networks across different architectures, including recurrent, feedforward, and complex-valued networks [168, 169, 170]. Theoretical frameworks for

analyzing synchronization stability, such as Lyapunov exponents and phase coherence measures, have been adapted to fractional-order networks to quantify synchronization robustness and predict emergent behaviors [171].

The thesis is structured into two main parts, each focusing on different aspects of discrete fractional calculus and its applications in neural networks:

Part I: Mathematical Considerations

Chapter 1 serves as a foundational introduction, offering a comprehensive overview of the notation and key concepts of discrete fractional calculus. It also presents essential theorems that provide numerical formulas for evaluating fractional discrete maps, laying the groundwork for subsequent analysis.

Chapter 2 delves into the stability analysis of fractional discrete maps, presenting fundamental results, methodologies, and stability criteria for assessing the behavior of these maps. This chapter explores asymptotic stability conditions, particularly focusing on the zero equilibrium of generic fractional discrete maps.

Chapter 3 shifts the focus to fractional-order neural networks and discrete-time fractional-order neural networks. It provides an overview of these networks, including their architecture and properties, and discusses key results related to the stability analysis of discrete-time fractional-order neural networks.

Part II: Applications

Chapter 4 showcases the asymptotic stability analysis of various discrete neural network models, considering both commensurate and incommensurate fractional and variable orders. It demonstrates how these models behave under different stability conditions, providing insights into their long-term behavior.

Chapter 5 delves into the finite-time stability analysis of discrete neural network models, extending the investigation to encompass commensurate and incommensurate fractional and variable orders. This chapter explores the transient dynamics of these models and their stability within finite time frames.

Chapter 6 introduces and explores two additional stability criteria, namely Ulam-Hyers stability and uniform stability, within the context of discrete neural network models with fractional variable orders. It elucidates the conditions under which these models exhibit stability and provides practical insights into their applications.

Chapter 7 concludes the thesis by examining the synchronization phenomenon in discrete neural network models, considering both commensurate and incommensurate fractional and variable orders. It explores how synchronization emerges and evolves within these networks, shedding light on their complex dynamics and behaviors.

Part I

Mathematical Considerations

Chapter 1

Analytical Aspects of Discrete Fractional Calculus

1.1 Introduction

Fractional calculus serves as an extension of classical calculus to non-integer orders, offering a powerful set of tools for modeling and controlling systems characterized by complexity, self-similarity, scale-free attributes, and inverse power law behavior. Particularly, fractional-order derivatives have emerged as instrumental in capturing memory and hereditary properties across various materials and processes. This versatile framework finds applications in diverse fields such as high-energy physics, anomalous diffusion, complex viscoelastic materials, rheology, geophysics, biomedical engineering, and economics [5, 6, 7]. Consequently, FC establishes a robust theoretical foundation for modeling and controlling complex systems, progressively becoming a pivotal research instrument in both natural and social sciences [8, 9].

In recent times, discrete fractional calculus has garnered substantial attention from researchers. The introduction of fractional sums with the delta operator and fractional differences with nabla operators in [28] marked the inception of this theoretical domain. Subsequent extensive developments are documented in [29, 30, 31].Investigations into the monotonicity properties of delta and nabla fractional operators have been explored in [181, 182, 183]. Notably, Atici et al. in [184] explored the monotonicity properties of delta fractional differences, establishing a delta-fractional difference variant of the mean-value theorem. Recent works [186, 187, 188, 191, 192] have explored fractional operators with Mittag–Leffler and exponential "non-singular" kernels, along with their discrete counterparts, investigating monotonicity within this context

Inspired by this extensive range of studies, this chapter unfolds by presenting fundamental concepts of discrete fractional calculus. It encompasses Delta and Nabla type fractional operators with both singular and non-singular kernels, elucidating different transformation methods employed for exploring fractional difference equations.

1.2 Fundamental Concepts in Discrete Calculus

The functions we consider are frequently defined on a set of the form

$$\mathbb{N}_a = \{a, a+1, a+2, ...\},$$

where $a \in \mathbb{R}$; or a set of the form

$$\mathbb{N}_a^b = \{a, a+1, a+2, ..., b\},$$

where $a, b \in \mathbb{R}$ and $b - a$ is a positive integer.

1.2.1 Delta Calculus

We will go through the fundamentals of delta calculus.

Definition 1.1. *[27] Assume $x : \mathbb{N}_a^b \to \mathbb{R}$ If $b > a$, then we define the forward difference operator Δ by*

$$\Delta x(t) = x(t+1) - x(t), \quad t \in \mathbb{N}_a^{b-1}. \tag{1.1}$$

Definition 1.2. *[27] We define the forward jump operator σ on $\mathbb{N}_a^{b-a}$ a by*

$$\sigma(t) = t + 1. \tag{1.2}$$

We present some important properties of the forward difference operator in the following theorem.

Theorem 1.1. *[27] Assume $x, y : \mathbb{N}_a^b \to \mathbb{R}$ and $\alpha, \beta \in \mathbb{R}$, then for $t \in \mathbb{N}_a^{b-1}$*

- $\Delta\alpha = 0.$
- $\Delta\alpha x(t) = \alpha\Delta x(t).$
- $\Delta[x + y](t) = \Delta x(t) + \Delta y(t).$
- $\Delta\alpha^{t+\beta} = (\alpha - 1)^{t+\beta}.$
- $\Delta[xy](t) = x(\sigma(t))\Delta y(t) + \Delta x(t)y(t).$
- $\Delta\left[\frac{x}{y}\right](t) = \frac{y(t)\Delta x(t) - x(t)\Delta y(t)}{y(t)\sigma(y(t))}, \qquad y(t) \neq 0.$

The subsequent function to be introduced is the falling function.

Definition 1.3. *[27] For n a positive integer we define the falling function, $t^{(n)}$, read t to the n falling, by*

$$t^{(n)} := t(t-1)(t-2)...(t-n+1), \tag{1.3}$$

and we let $t^{(0)} := 1$.

The falling function is defined in a manner that adheres to the power rule described below.

Theorem 1.2. *[27] The power rule*

$$\Delta t^{(n)} = nt^{(n-1)}, \tag{1.4}$$

holds for $n = 1, 2, 3, ...$

The gamma function, a highly significant mathematical function, is defined as follows:

Definition 1.4. *[27] For complex numbers z with a positive real part, the gamma function is defined as:*

$$\Gamma(z) = \int_0^\infty e^{-t} t^{z-1} dt, \tag{1.5}$$

where the function exhibits a fundamental property:

$$\Gamma(z+1) = z\Gamma(z). \tag{1.6}$$

Inspired by the definition and the fundamental property of the gamma function, we broaden the domain of the falling function in the subsequent definition:

Definition 1.5. *[27] The generalized falling function is formally expressed as:*

$$t^{(r)} = \frac{\Gamma(t+1)}{\Gamma(t-r+1)}. \tag{1.7}$$

For values of t and r such that the right-hand side of this equation is well-defined, we extend this definition by adopting the convention that $t^{(r)} = 0$ when $t-r+1$ is a nonpositive integer and $t+1$ is not a nonpositive integer.

We proceed to articulate and establish the generalized power rules.

Definition 1.6. *[27] The succeeding (extended) power rules:*

$$\Delta(t+\alpha)^{(r)} = r(t+\alpha)^{(r-1)}, \tag{1.8}$$

and

$$\Delta(t-\alpha)^{(r)} = -r(\alpha-\sigma(t))^{(r-1)}, \tag{1.9}$$

apply as long as the expressions in the respective formulas are well-defined.

The generalized binomial coefficient is defined as follows:

Definition 1.7. *[27] The expression $\binom{t}{r}$ denotes the generalized binomial coefficient and is defined as follows:*

$$\binom{t}{r} = \frac{t^{(r)}}{\Gamma(r+1)}. \tag{1.10}$$

For valid combinations of t and r such that the right-hand side is well-defined, we adopt the convention that if the denominator is undefined but the numerator is defined, then $\binom{t}{r} = 0$.

The properties of the generalized binomial coefficient are presented in the following theorem.

Theorem 1.3. *[27] The following properties hold:*

- $\Delta \binom{t}{r} = \binom{t}{r-1}$.
- $\Delta \binom{r+t}{t} = \binom{r+t}{t+1}$.

- $\Delta\Gamma(t) = (t-1)\Gamma(t)$.

Definition 1.8. *[27] The expressions $e_\nu(\kappa, t-a)$ and $e_{\nu,\nu}(\kappa, t-a)$ represent Mittag–Leffler functions with one and two parameters, respectively. They are mathematically defined as follows:*

$$e_\nu(\kappa, t-a) = \sum_{k=0}^{\infty} \kappa^k \frac{(t-a+k(\nu-1))^{(k\nu)}}{\Gamma(k\nu+1)}, \quad t \in \mathbb{N}_a, \tag{1.11}$$

and

$$e_{\nu,\nu}(\kappa, t-a) = \sum_{k=0}^{\infty} \kappa^k \frac{(t-a+k(\nu-1))^{(k\nu+\nu-1)}}{\Gamma(k\nu+\nu)}, \quad |\kappa| < \nu,\ t \in \mathbb{N}_{a+\nu-1}. \tag{1.12}$$

Lemme 1.1. *[27] For both Mittag–Leffler functions, the following holds:*

$$e_\nu(\kappa, t-a) > 0, \quad e_{\nu,\nu}(\kappa, t-a) > 0, \quad -\nu < \kappa < 0, \tag{1.13}$$

and

$$\lim_{t\to+\infty} e_\nu(\kappa, t-a) = 0, \quad \lim_{t\to+\infty} e_{\nu,\nu}(\kappa, t-a) = 0, \quad -\nu < \kappa < 0. \tag{1.14}$$

1.2.2 Nabla Calculus

We introduce notation and present fundamental results related to nabla calculus.

Definition 1.9. *[27] We define the nabla operator, also known as the backward difference operator, denoted by ∇, as follows:*

$$\nabla x(t) = x(t) - x(t-1), \quad t \in \mathbb{N}_{a+1}. \tag{1.15}$$

Next, we introduce the backward jump operator.

Definition 1.10. *[27] The operator representing the backward jump, denoted as ρ, is defined as follows:*

$$\rho(t) = t - 1. \tag{1.16}$$

The following theorem outlines several properties of the nabla difference operator.

Theorem 1.4. *[27] Under the assumption $x, y : \mathbb{N}_a \to \mathbb{R}$ and $\alpha, \beta \in \mathbb{R}$. Then, for $t \in \mathbb{N}_{a+1}$*

- $\nabla\alpha = 0$.
- $\nabla\alpha x(t) = \alpha\nabla x(t)$.
- $\nabla[x(t) + y(t)] = \nabla x(t) + \nabla y(t)$.
- $\nabla\alpha^{t+\beta} = \dfrac{\alpha-1}{\alpha}\alpha^{t+\beta}$ *when* $\alpha \neq 0$.
- $\nabla[xy](t) = x(\rho(t))\nabla y(t) + \nabla x(t)y(t)$.
- $\nabla\left[\dfrac{x(t)}{y(t)}\right] = \dfrac{y(t)\nabla x(t) - x(t)\nabla y(t)}{y(t)y(\rho(t))}$, *when* $y(t) \neq 0$.

Now, we proceed to define the rising function.

Definition 1.11. *[27] Let n be a positive integer and $t \in \mathbb{R}$. We define the rising function, denoted as $t^{\overline{n}}$, by:*

$$t^{\overline{n}} = t(t+1)(t+2)...(t+n-1). \tag{1.17}$$

The rising function is defined in such a way that it satisfies the following power rule:

Definition 1.12. *[27] For $n \in \mathbb{N}_1$ and $\alpha \in \mathbb{R}$, the Nabla Power Rule is defined as follows:*

$$\nabla(t+\alpha)^{\overline{n}} = n(t+\alpha)^{\overline{n-1}}, \qquad t \in \mathbb{R}. \tag{1.18}$$

In light of the Nabla Power Rule definition and the Gamma function, we proceed to introduce the generalized rising function in the following manner:

Definition 1.13. *[27] The generalized rising function, denoted as $t^{\overline{n}}_{\alpha}$, is defined as follows:*

$$t^{\overline{r}} = \frac{\Gamma(t+r)}{\Gamma(t)}. \tag{1.19}$$

For valid values of t and r, such that the right-hand side is meaningful, the generalized rising function $t^{\overline{r}}_{\alpha}$ is defined. Additionally, we adopt the convention that if t is a nonpositive integer while $t+r$ is not a nonpositive integer, then $t^{\overline{r}} = 0$.

We obtain the following generalized power rules:

Theorem 1.5. *[27] The formulas*

$$\nabla(t+\alpha)^{\overline{r}} = r(t+\alpha)^{\overline{r-1}}, \tag{1.20}$$

and

$$\nabla(t-\alpha)^{\overline{r}} = -r(\alpha-\rho(t))^{\overline{r-1}}, \tag{1.21}$$

are valid under the conditions where t, r, and α are chosen such that the expressions in the formulas are well-defined. Specifically, the case $t^0 = 1$ holds, and for nonpositive integers $t = -1, -2, \ldots$.

The importance of nabla discrete Mittag-Leffler functions cannot be overstated, and we delve deeper into their significance.

Definition 1.14. *[27] Formulated with parameters κ belonging to the real numbers and $\delta, \beta, \gamma, \eta$ as complex values, where the real part of δ is greater than zero, the nabla discrete generalized Mittag-Leffler function is represented by:*

$$E^{\delta}_{\overline{\gamma},\beta}(\kappa,\eta) := \sum_{n=0}^{\infty} \kappa^n \frac{\eta^{\overline{n\delta+\beta-1}}(\gamma)_n}{\Gamma(n\delta+\beta)n!}, \quad |\kappa| < 1. \tag{1.22}$$

In this context, $(\gamma)_n = \gamma(\gamma+1)\ldots(\gamma+n-1)$ signifies the Pochhammer symbol. Notably, when $\gamma = 1$, the expression transforms into the nabla discrete two-parameter Mittag-Leffler function:

$$E_{\overline{\gamma},\beta}(\kappa,\eta) := E^{1}_{\overline{\gamma},\beta}(\kappa,\eta) = \sum_{n=0}^{\infty} \kappa^n \frac{\eta^{\overline{n\delta+\beta-1}}}{\Gamma(n\delta+\beta)}, \quad |\kappa| < 1. \tag{1.23}$$

For $\beta = \gamma = 1$, the resulting function corresponds to the nabla discrete one-parameter Mittag-Leffler function:

$$E_{\overline{\delta}}(\kappa,\eta) := E^{1}_{\overline{\gamma},1}(\kappa,\eta) = \sum_{n=0}^{\infty} \kappa^n \frac{\eta^{\overline{n\delta}}}{\Gamma(n\delta+1)}, \quad |\kappa| < 1. \tag{1.24}$$

Lemme 1.2. *[27] For any positive real number $\delta > 0$, parameters $\beta > -1$, $\gamma, \eta \in \mathbb{C}$, and $\kappa \in \mathbb{R}$ satisfying $|\kappa| < 1$, the following relationship holds:*

$$\nabla^n E^{\delta}_{\overline{\gamma,\beta+n}}(\kappa,\eta) = E^{\delta}_{\overline{\gamma,\beta}}(\kappa,\eta), \quad \beta 0. \tag{1.25}$$

Remarque 1.1. *(i) For any $\kappa = -\frac{\delta}{1-\delta}$, where $0 < \delta < \frac{1}{2}$, $\eta \in \mathbb{N}$, and $0 < \gamma \leq 1$, the two-parameter Mittag-Leffler function $E^{\delta}_{\overline{\gamma,1}}(\kappa,\eta)$ exhibits monotonic decrease. The initial values of $E^{\delta}_{\overline{\gamma,1}}(\kappa,\eta)$ are as follows:*

$$\begin{aligned} E^{\delta}_{\overline{\gamma,1}}(\kappa,0) &= 1, \\ E^{\delta}_{\overline{\gamma,1}}(\kappa,1) &= (1-\delta)^{\gamma}, \\ E^{\delta}_{\overline{\gamma,1}}(\kappa,2) &= (1-\delta)^{\gamma}(1-\delta^2\gamma), \\ E^{\delta}_{\overline{\gamma,1}}(\kappa,3) &= \frac{1-\delta}{2}(\delta^4\gamma(\gamma+1) - \delta^3\gamma - 3\delta^2\gamma + 2). \end{aligned} \tag{1.26}$$

*(ii) Considering (i) and Definition **??**, we observe that:*

$$\begin{aligned} \nabla E^{\delta}_{\overline{\gamma,1}}(\kappa,\eta) &= \sum_{k=0}^{\infty} \kappa^k \frac{k\delta\eta^{\overline{k\delta-1}}(\gamma)_k}{\Gamma(k\delta+1)k!} = \sum_{k=0}^{\infty} \kappa^k \frac{\eta^{\overline{k\delta-1}}}{\Gamma(k\delta)k!}, \\ &= \kappa \sum_{k=0}^{\infty} \kappa^k \frac{\eta^{\overline{k\delta+\delta-1}}(\gamma)_{k+1}}{\Gamma(k\delta+\delta)(k+1)!} := \kappa E^{\gamma}_{\overline{\delta}}(\kappa,\eta) < 0. \end{aligned} \tag{1.27}$$

As a consequence, $E^{\gamma}_{\overline{\delta}}(\kappa,\eta)$ maintains strict positivity for $\kappa < 0$.

Definition 1.15. *[27] The discrete exponential kernel in the nabla calculus is expressed as*

$${}_h\hat{e}_{\kappa}(t,\rho(s)) = \left(\frac{1}{1-\kappa h}\right)^{\frac{t-\rho}{h}} = \left(\frac{1-\nu}{1-\nu+\nu h}\right)^{\frac{t-\rho}{h}}, \tag{1.28}$$

where $\kappa = \dfrac{-\nu}{1-\nu}$.

Additionally, by utilizing $\ominus s = \dfrac{-s}{1-hs}$, we define

$${}_h\hat{e}_{\ominus s}(t,a) = (1-hs)^{\frac{t-a}{h}} \quad \text{for} \quad t \in \mathbb{N}_{a,h}.$$

1.2.3 h-Discrete Calculus

For $h > 0$, we will use the notations

$$\mathbb{N}_{a,h} = \{a, a+h, a+2h, \ldots\},$$

and

$$\mathbb{N}^{b}_{a,h} = \{a, a+h, a+2h, \ldots\ b\}.$$

We present various definitions and introduce notation.

Definition 1.16 ([196]). *The backward jump operator on the time scale $h\mathbb{Z}$ is given by:*

$$\rho_h(t) = t - h. \tag{1.29}$$

The forward jump operator on the time scale $h\mathbb{Z}$ is given by:

$$\sigma_h(t) = t + h. \tag{1.30}$$

Definition 1.17 ([196]). *Let h be strictly positive real number, and consider $x : \mathbb{N}_{h,a} \to \mathbb{R}$. We define the forward h-difference operator as:*

$$\Delta_h x(t) = \frac{x(\sigma_h(t)) - x(t)}{h}. \tag{1.31}$$

Definition 1.18 ([196]). *The backward difference operator over $h\mathbb{Z}$ is specified by:*

$$\nabla_h x(t) = \frac{x(t) - x(\rho_h(t))}{h}. \tag{1.32}$$

Definition 1.19 ([196]). *The h-falling factorial function of real order ν is characterized by:*

$$t_h^{(r)} = h^r \frac{\Gamma(\frac{t}{h} + 1)}{\Gamma(\frac{t}{h} + 1 - r)}, \quad t \in \mathbb{R}. \tag{1.33}$$

When $h = 1$, the h-falling factorial function is identical to the falling factorial function defined by equation (1.33). It is anticipated that t_h^r converges to t^r as h tends to zero.

Proposition 1.1 ([196]). *For $t \geq 0$ and $r \in \mathbb{R}$*

$$\lim_{h \to 0} t_h^{(r)} = t^r. \tag{1.34}$$

Definition 1.20 ([196]). *For $h > 0$ and $r \in \mathbb{R}$, the increasing h-polynomial factorial function is defined as follows:*

$$t_h^{\overline{r}} = \frac{h^r \Gamma(\frac{t}{h} + r)}{\Gamma(\frac{t}{h})}. \tag{1.35}$$

Considering the division at a pole results in zero. In the case where μ is a positive integer, then

$$t^{\overline{\mu h}} = t(t + h)(t + 2h) \cdots (t + (\mu - 1)h). \tag{1.36}$$

Proposition 1.2 ([196]). *When $r \neq 0$, the following relations are valid:*

$$\Delta_h (t - a)_h^{(r)} = r(t - a)^{(r-1)}. \tag{1.37}$$

$$\nabla_h (t - a)_h^{\overline{r}} = r(t - a)^{\overline{r-1}}. \tag{1.38}$$

Definition 1.21 ([196]). *For $k \in \mathbb{R}$, $|k| < 1$, and $h, , t, q \in \mathbb{C}$ with $Re(\cdot)h > 0$, the nabla h-discrete Mittag–Leffler functions are defined by:*

$${}_h E_{\overline{\theta,\beta}}^{\rho}(\kappa, t) = \sum_{k=0}^{\infty} \kappa^k \frac{t_h^{\overline{k\theta+\beta-1}}(\rho)_k}{\Gamma(\theta k + \beta)k!}. \tag{1.39}$$

When $h = \beta = \rho = 1$, one may consult the definition of the nabla Mittag-Leffler in (1.24).

1.3 Delta Type Fractional Discrete Operators

1.3.1 Fundamental Results in Fractional Delta Sums

To effectively leverage fractional difference calculus, we introduce the right inverse operator of the fractional difference operator in this section, referred to as the "fractional sum." Consider the Cauchy function,

Definition 1.22 ([203]). *Define the fractional sum of f with respect to ν as*

$$\Delta^{-\nu} f(t) = \frac{1}{\Gamma(\nu)} \sum_{s=a}^{t-\nu} (t - \sigma(s))^{(\nu-1)} f(s). \tag{1.40}$$

Next, we will present and demonstrate the law of exponents for fractional sums.

Theorem 1.6 ([202]). *Consider a real-valued function f and let $\mu, \nu > 0$. For all t such that*

$$\Delta_{a+\nu}^{-\nu} \Delta_a^{-\mu} f(t) = \Delta_a^{-(\nu+\mu)} f(t) = \Delta_{a+\mu}^{-\mu} \Delta_a^{-\nu} f(t). \tag{1.41}$$

Proof. Using the definition of the fractional sum, we can represent the given expression as

$$\begin{aligned}
\Delta_{a+\nu}^{-\nu} \Delta_a^{-\mu} f(t) &= \frac{1}{\Gamma(\nu)} \sum_{r=0}^{t-\nu} (t - \sigma(r))^{(\nu-1)} f(r), \\
&= \frac{1}{\Gamma(\nu)\Gamma(\mu)} \sum_{s=\nu}^{t-\mu} \sum_{r=0}^{s-\nu} (t - \sigma(s))^{(\mu-1)} (s - \sigma(r))^{(\nu-1)} f(r), \\
&= \frac{1}{\Gamma(\nu)\Gamma(\mu)} \sum_{r=0}^{t-(\nu+\mu)} \sum_{s=r+\nu}^{t-\nu} (t - \sigma(s))^{(\mu-1)} (s - \sigma(r))^{\nu-1} f(r), \\
&= \frac{1}{\Gamma(\nu)\Gamma(\mu)} \sum_{r=0}^{t-(\mu+\nu)} \left(\sum_{x=\nu-1}^{t-\sigma(r)-\mu} (t - \sigma(r) - \sigma(x))^{(\mu-1)} x^{(\nu-1)} \right) f(r), \\
&= \frac{1}{\Gamma(\nu)} \sum_{r=0}^{t-(\mu+\nu)} (\Delta^{-\mu})(t - \sigma(r))^{(\nu-1)} f(r), \\
&= \frac{1}{\Gamma(\nu)} \sum_{r=0}^{t-(\mu+\nu)} \left(\frac{\Gamma(\nu)}{\Gamma(\nu+\mu)} (t - \sigma(r))^{(\nu+\mu-1)} f(r), \right. \\
&= \Delta_a^{-(\nu+\mu)} f(t).
\end{aligned} \tag{1.42}$$

The demonstration is now finished. □

Remarque 1.2. *Replace ν with $\nu + 1$ in (1.40) and apply Theorem 1.6 to obtain:*

$$\Delta^{-\nu-1} \Delta f(t) = \Delta^{-\nu} f(t) - \frac{(t-a)^{(\nu)}}{\Gamma(\nu+1)} f(a). \tag{1.43}$$

This results in:

$$\Delta^{-\nu} f(t) = \Delta^{-\nu-1} \Delta f(t) + \frac{(t-a)^{(\nu)}}{\Gamma(\nu+1)} f(a). \tag{1.44}$$

Remarque 1.3. *Consider $p-1<\nu<p$, where p is a positive integer. According to Theorem 1.6, we can infer that:*

$$\begin{aligned}
\Delta\Delta^{\nu}f(t) &= \Delta\Delta^{p}(\Delta^{-(p-\nu)}f(t)),\\
&= \Delta^{p+1}(\Delta^{-(p-\nu)}f(t)),\\
&= \Delta^{p}(\Delta\Delta^{-(p-\nu)}f(t)),\\
&= \Delta^{p}[\Delta^{-(p-\nu)}\Delta f(t)+\frac{(t-a)(p-\nu-1)}{\Gamma(p-\nu)}f(a)],\\
&= \Delta^{p}\Delta^{-(p-\nu)}\Delta f(t)+\Delta^{p}\frac{(t-a)(p-\nu-1)}{\Gamma(p-\nu)}f(a),\\
&= \Delta^{\nu}\Delta f(t)+\frac{(t-a)(-\nu-1)}{\Gamma(-\nu)}f(a).
\end{aligned}$$

Therefore, we conclude that Theorem 1.6 holds for any real number ν.

Theorem 1.7 ([202])**.** *For a function f defined on $\mathbb{N}_a$, the subsequent equality holds for any real number ν and any positive integer p:*

$$\Delta^{-\nu}\Delta^{p}f(t)=\Delta^{p}\Delta^{\nu}f(t)-\sum_{p-1}^{k=0}\frac{(t-a)^{\nu-p+k}}{\Gamma(\nu+k-p+1)}\Delta^{k}f(a). \tag{1.45}$$

Proof. We replace f with Δf in equation (1.44):

$$\begin{aligned}
\Delta^{-\nu}\Delta^{2}f(t) &= \Delta\Delta^{-\nu}\Delta f(t)-\frac{(t-a)^{(\nu-1)}}{\Gamma(\nu)}\Delta f(a),\\
&= \Delta\left[\Delta\Delta^{-\nu}f(t)-\frac{(t-a)^{(\nu-1)}}{\Gamma(\nu)}f(a)\right]-\frac{(t-a)^{(\nu-1)}}{\Gamma(\nu)}\Delta f(a),\\
&= \Delta^{2}\Delta^{-\nu}f(t)-\frac{(t-a)^{(\nu-2)}}{\Gamma(\nu)}f(a)-\frac{(t-a)^{(\nu-1)}}{\Gamma(\nu)}\Delta f(a),\\
&= \Delta^{2}\Delta^{-\nu}f(t)-\sum_{k=0}^{1}\frac{(t-a)^{(\nu-2+k)}}{\Gamma(\nu+k-1)}\Delta^{k}f(a).
\end{aligned} \tag{1.46}$$

Continuing with subsequent iterations leads to the desired result. □

Remarque 1.4. *Replace ν with $\nu+p$ in equation (1.45) and apply Theorem 1.6 to obtain:*

$$\Delta^{-\nu}f(t)=\Delta^{-\nu-p}\Delta^{p}f(t)+\sum_{k=0}^{(p-1)}\frac{(t-a)^{(\nu+k)}}{\Gamma(\nu+k+1)}\Delta^{k}f(a). \tag{1.47}$$

Next, we derive a power rule

Lemme 1.3 ([202])**.** *Let $\mu\in\mathbb{R}\{...,-2,-1\}$*

$$\Delta^{-\nu}t^{\mu}=\frac{\Gamma(\mu+1)}{\Gamma(\mu+\nu+1)}t^{\mu+\nu}. \tag{1.48}$$

1.3.2 Delta Fractional Differences

1. **Riemann fractional difference operator**
In the realm of fractional calculus, we introduce the Riemann left fractional difference operator, represented as ${}^{RL}\Delta_a^{\nu}$,

Definition 1.23 ([203]). *For $\nu > 0$, where $f : \mathbb{N}_a \to \mathbb{R}$, and $n-1 < \nu < n$, where n is a positive integer, the operator is defined as follows:*

$$ {}^{RL}\Delta_a^{\nu} f(t) = \Delta^n \Delta_a^{(n-\nu)} f(t) = \frac{1}{\Gamma(n-\nu)} \Delta^n \left(\sum_{s=a}^{t-(n-\nu)} (t-\sigma(s))^{(n-\nu-1)} f(t) \right). \quad (1.49) $$

We also introduce the Riemann operator of order $\nu > 0$ as

$$ \Delta_a^{\nu} f(t) = \begin{cases} \frac{1}{\Gamma(-\nu)} \sum_{k=0}^{t+\nu} (t-\sigma(k))^{-\nu-1} f(s), & n-1 < \nu < n, \\ \Delta^n f(t), & \nu = n, \end{cases} \quad (1.50) $$

where $t \in \mathbb{N}_{a+n-\nu}$.

Proposition 1.3 ([203]). *Asserts that when considering a function $f : \mathbb{N}_a \to \mathbb{R}$, the Riemann operator of order $\nu > 0$ is specified as:*

$$ \Delta_a^{\nu} f(t) = \sum_{k=0}^{\nu+t-a} (-1)^k \binom{\nu}{k} f(t+\nu-k), \quad (1.51) $$

where $t \in \mathbb{N}_{a+n-\nu}$.

Now, let's explore the fractional difference of the power rule function $(t-a)^{\nu}$.

Lemme 1.4 ([202]). *for $t \in \mathbb{N}_{a+\mu+n-\nu}$, the following hold:*

$$ \Delta_{a+\mu}^{\nu} (t-a)^{(\mu)} = \frac{\Gamma(\mu+1)}{\Gamma(\mu+1+n-\nu)} \frac{\Gamma(\mu+n-\nu+1)}{\Gamma(\mu+1-\nu)} (t-a)^{\mu-\nu}. \quad (1.52) $$

Continuing, we delve into the correlation between Riemann left fractional operators and fractional differences.

Proposition 1.4 ([202]). *Examining a function f defined on the natural numbers starting from a and mapping to real numbers, we assume positive values for both ν and μ, where $n-1 < \nu \leq n$. In this particular situation,*

$$ {}^{RL}\Delta_{a+\mu}^{\nu} \Delta_a^{-\mu} f(t) = \Delta_a^{\nu-\mu} f(t), \quad (1.53) $$

for $t \in \mathbb{N}_{a+\mu+n-\nu}$.

Proof. Assuming the definitions of f, ν, n, and μ from the theorem, consider $t \in \mathbb{N}_{a+\mu+n-\nu}$. Subsequently,

$$ \Delta_{a+\mu}^{\nu} \Delta_a^{-\mu} f(t) = \Delta^n \Delta_{a+\mu}^{-(n-\nu)} \Delta_a^{-\mu} f(t) = \Delta^n \Delta_a^{-(n-\nu+\mu)} f(t). \quad (1.54) $$

Utilizing the composition rule from Theorem 1.6, we obtain:

$$\Delta_a^{n-(n-\nu+\mu)} f(t) = \Delta_a^{\nu-\mu} f(t). \tag{1.55}$$

When $\nu > 0$ and $f \in \mathbb{N}_a$, the left Riemann difference operator ${}^{RL}\Delta a + \nu^{\nu}$ yields operations that are inverses to the ν-th fractional sum operator $\Delta^{-\nu}$ given in (1.40), both from the left and the right. In particular, we observe the following situations. □

Now, let's emphasize the inverse operations of the ν-th fractional sum operator $\Delta^{-\nu}$ from both the left and the right:

Proposition 1.5 ([203]). *In the scenario where $\nu > 0$ and f is a function defined within the suitable domain $\mathbb{N}_a$, the subsequent relation is valid for t in $\mathbb{N}_{a+n}$, a subset of $\mathbb{N}_a$:*

$$ {}^{RL}\Delta_{a+\nu}^{\nu} \Delta^{-\nu} f(t) = f(t), \tag{1.56}$$

$$ \Delta_{a+n-\nu}^{-\nu} {}^{RL}\Delta \nu f(t) = f(t), \quad \nu \notin \mathbb{N}. \tag{1.57}$$

Proposition 1.6 ([202]). *For a function $f : \mathbb{N}_a \to \mathbb{R}$ and positive values of $\nu > 0$ and $\mu > 0$ with $0 < \mu \leq n$, the subsequent relation is valid for $t \in \mathbb{N}_{a+n-\mu+\nu}$:*

$$\Delta_{a+n-\mu}^{-\nu} \Delta_a^{\mu} f(t) = \Delta_a^{\mu-\nu} f(t) - \sum_{j=0}^{n-1} \frac{\Delta^{j-(n-\mu)} f(a+n-\mu)}{\Gamma(\nu-n+j+1)} (t-a-n+\mu)^{(\nu-n+j)}. \tag{1.58}$$

Proof. Let $\nu, \mu > 0$ with $n-1 < \mu \leq n$. Define

$$g(t) = \Delta_a^{(n-\mu)} f(t), \quad \text{and} \quad = a+n-\mu, \tag{1.59}$$

where is the first point of the g function. For $t \in \mathbb{N}_{a+n-\mu+\nu}$, we have,

$$\begin{aligned}
\Delta_{a+n-\mu}^{-\nu} \Delta_a^{\mu} f(t) &= \Delta_{a+n-\mu}^{\mu} g(t), \\
&= \Delta_{a+n-\mu}^{n-\nu} g(t) - \sum_{j=0}^{n-1} \frac{\Delta^j g()}{\Gamma(\nu-n+j+1)} (t-)^{\nu-n+j}, \\
&= \Delta_{a+n-\mu}^{n-\nu} \Delta_a^{-(n-\mu)} f(t) - \sum_{j=0}^{n-1} \frac{\Delta^j \Delta^{-(n-\mu)} f()}{\Gamma(\nu-n+j+1)} (t-)^{\nu-n+j}, \\
&= \Delta_a^{\mu-\nu} f(t) - \sum_{j=0}^{n-1} \frac{\Delta_a^{j-n+\mu} f(a+n-\mu)}{\Gamma(\nu-n+j+1)} (t-a-n+\mu)^{\nu-n+j}.
\end{aligned} \tag{1.60}$$

In the concluding step, we employed Proposition 1.4. In the scenario where $\nu > n$, we applied Theorem 1.6. □

Lemme 1.5 ([202]). *For any integer p and $\nu > 0$ with $n-1 < \nu \leq n$, we obtain*

$$\Delta^p \Delta_a^{\nu} = \Delta_a^{p+\nu} f(t), \quad t \in \mathbb{N}_{a+n-\nu}. \tag{1.61}$$

Proposition 1.7 ([202]i). *For $p-1 < \nu < p$ and $p \in \mathbb{N}$ we have*

$$\Delta \, {}^{RL}\Delta^{\nu} f(t) = {}^{RL}\Delta^{\nu} \Delta f(t) + \frac{(t-a)^{(-\nu-1)}}{\Gamma(-\nu)} f(a). \tag{1.62}$$

The extensive generalization to the fully fractional scenario, where μ is any positive real number, is elucidated in Theorem 4.6 [193]:

Theorem 1.8 ([202]). *For a given function $f : \mathbb{N}_a \to \mathbb{R}$, assuming $\nu, \mu > 0$ with $n-1 < \nu \leq n$ and $m-1 < \mu \leq m$, the following relation holds for $t \in \mathbb{N}_{a+m-\mu+n-\nu}$:*

$$\Delta^{\nu}_{a+m-\mu}\Delta^{\mu}_{a} f(t) = \Delta^{\nu+\mu} f(t) - \sum_{j=0}^{m-1} \frac{\Delta_a^{j-(n-\mu)} f(a+m-\mu)}{\Gamma(-\nu-m+j+1)}(t-a-m+\mu)^{(-\nu-m+j)}. \tag{1.63}$$

Proof. Let f, ν, and μ be as specified in the theorem. If $n-1 < \nu < n$, then for $t \in \mathbb{N}_{a+m-\mu+n-\nu}$,

$$\begin{aligned}
\Delta^{\nu}_{a+m-\mu}\Delta^{\mu}_{a} f(t) &= \Delta^{n}[\Delta^{-(n-\nu)}_{a+m-\mu}\Delta^{\mu}_{a} f(t), \\
&= \Delta^{n}\left[\Delta_a^{-n+\mu+\nu} f(a+m-\nu)\right] \\
&\quad - \sum_{j=0}^{m-1} \frac{\Delta^{j-m+\mu} f(a+m-\nu)}{\Gamma(n-\nu-m+j+1)}(t-a-m+\mu)^{n-\nu-m+j}, \\
&= \Delta^{\nu+\mu} f(t) - \sum_{j=0}^{m-1} \frac{\Delta^{j-m+\mu} f(a+m-\nu)}{\Gamma(\nu-m+j+1)}(t-a-m+\mu)^{-\nu-m+j}.
\end{aligned} \tag{1.64}$$

In a similar fashion to Theorem 1.8, we can express in reverse order:

$$\Delta^{\mu}_{a+n-\nu}\Delta^{\nu}_{a} f(t) = \Delta^{\mu+\nu} f(t) - \sum_{j=0}^{n-1} \frac{\Delta_a^{j-(m-\nu)} f(a+m-\mu)}{\Gamma(-\mu-n+j+1)}(t-a-n+\nu)^{-\mu-m+j}, \tag{1.65}$$

The terms within the summation become zero if $\mu \in \mathbb{N}_0$. □

2. **Caputo fractional difference operator**

The efficacy of the Riemann–Liouville left operator is limited when applied to model real-world phenomena through fractional difference equations. Consequently, we will investigate an alternative approach to fractional difference operators. Analogous to standard fractional calculus, we can define the left Caputo fractional difference of order ν. The initial concept of a discrete fractional operator was introduced in [30], where the operator emerged from a natural discretization of the traditional Caputo operator in fractional calculus. Originally introduced by mathematician Caputo in 1967 [194], the continuous Caputo operator provides a significant advantage: the need to specify the initial condition of the fractional order is eliminated when solving equations or systems of equations.

Definition 1.24 ([203]). *Consider $\nu > 0$ with $n-1 < \nu < n$, where $n = \lceil \nu \rceil + 1$. The definition of the ν-th fractional Caputo difference operator is as follows:*

$${}^{C}\Delta^{\nu}_{a} f(t) = \Delta^{n-\nu}_{a}\Delta^{n} f(t) = \frac{1}{\Gamma(n-\nu)} \sum_{s=a}^{t-(n-\nu)} (t-\sigma(s))^{(n-\nu-1)}(\Delta^{n}_{s} f)(s), \quad \forall t \in \mathbb{N}_{a+\nu}. \tag{1.66}$$

If $\nu = n \in \mathbb{N}$, then ${}^{C}\Delta_a^{\nu} f(t) = \Delta^n f(t)$. The formula for $\Delta^n f(t)$ is provided by:

$$\Delta^n f(t) = \sum_{r=0}^{n} (-1)^{r+1} \binom{n}{r} f(r+k). \tag{1.67}$$

Lemme 1.6 ([202]). *For the power rule function $f(t) = (t-a)^{(\mu)}$, the fractional difference is expressed as:*

$$\Delta_{a+\mu}^{\nu}(t-a)^{(\mu)} = \frac{\Gamma(\mu+1)}{\Gamma(\mu-\nu+1)}(t-a)^{(\mu-\nu)} \quad \text{for } t \in \mathbb{N}_{a+\mu+n-\nu}, \tag{1.68}$$

Here, $n = \lceil \nu \rceil$, and $\mu > n$. Equation (1.90) can be derived through a direct generalization of the Δ^n difference of f.

The relationship between the Riemann and Caputo fractional difference operators is stated as:

Theorem 1.9 ([203]). *The following conditions are fulfilled for any $\nu > 0$*

$${}^{C}\Delta_a^{\nu} f(t) = {}^{RL}\Delta_a^{\nu} f(t) - \sum_{k=0}^{n-1} \frac{(t-a)(k-\nu)}{\Gamma(k-\nu+1)} \Delta^k f(a). \tag{1.69}$$

Proof. As stated in Theorem 1.7, for $\nu > 0$ and a positive integer p, we have

$$\Delta^{-\nu}\Delta^p f(t) = \Delta^p \Delta^{-\nu} f(t) - \sum_{k=0}^{p-1} \frac{(t-a)^{\nu-p+k}}{\Gamma(\nu+k-p+1)} \Delta^k f(a). \tag{1.70}$$

If we substitute ν with $n-\nu$ and p with n, and set $n = [\nu]+1$, then we can establish

$$\Delta^{-(n-\nu)}\Delta^n f(t) = \Delta^n \Delta^{-(n-\nu)} f(t) - \sum_{k=0}^{n-1} \frac{(t-a)^{k-\nu}}{\Gamma(k-\nu+1)} \Delta^k f(a). \tag{1.71}$$

Hence, from equation (1.71), we obtain

$${}^{C}\Delta_a^{\nu} f(t) = {}^{RL}\Delta_a^{\nu} f(t) - \sum_{k=0}^{n-1} \frac{(t-a)^{k-\nu}}{\Gamma(k-\nu+1)} \Delta k f(a). \tag{1.72}$$

Specifically, when $0 < \nu < 1$, the relation (1.72) takes the following form:

$${}^{C}\Delta_a^{\nu} f(t) = {}^{RL}\Delta_a^{\nu} f(t) - \frac{(t-a)^{-\nu}}{\Gamma(1-\nu)} f(a). \tag{1.73}$$

□

Proposition 1.8 ([202]). *For $\nu > 0$ and a function f defined on suitable domains $\mathbb{N}_a$, the expression is as follows:*

$$\Delta_{a+(n-\nu)}^{-\nu} {}^{C}\Delta_a^{\nu} f(t) = f(t) - \sum_{k=0}^{n-1} \frac{(t-a)^k}{k!} \Delta^k f(a). \tag{1.74}$$

Especially when $0 < \nu \leq 1$, the relationship is expressed as:

$$\Delta_{a+(n-\nu)}^{-\nu} \Delta_a^{\nu} f(t) = f(t) - f(a). \tag{1.75}$$

Proof. To prove equation (1.74), we apply the relationship between the Riemann left operator and sum as stated in Proposition 1.5. □

Theorem 1.10 ([202]). *For $\mu > 0$, where μ is non-integer, $m = [\mu]$, and $\nu = m - \mu$, the ensuing expression is valid for $f(t)$ defined on $\mathbb{N}_a$ with $a \in \mathbb{Z}^+$ (where $\mathbb{Z}^+ := 0, 1, 2, \ldots$) and $t \in \mathbb{N}a + m$:*

$$f(t) = \sum_{k=0}^{m-1} \frac{(t-a)^k}{k!} \Delta^k f(a) + \frac{1}{\Gamma(\mu)} \sum_{a+\mu}^{s=t-\mu} (t-s-1)^{(\mu-1)} \Delta^\mu f(s). \tag{1.76}$$

Furthermore, when $0 < \nu < 1$, the Caputo generalized Taylor's formula (1.76) simplifies to:

$$f(t) = f(0) + \frac{1}{\Gamma(\nu)} \sum_{s=1-\nu}^{t-\nu} (t-s-1)^{(\nu-1)} \Delta^\nu f(s). \tag{1.77}$$

Proof. From the definition of the Caputo-left operator (1.66) and the commutativity property in Theorem 1.6, for all $t \in \mathbb{N}_{a+\nu+\mu}$ we obtain

$$\Delta^{-\nu} \Delta^\mu f(t) = \Delta^{-\nu} \Delta^{-(\mu-\nu)} (\Delta^\mu f(t)) = \Delta^{-(nu+(\mu-\nu))} (\Delta^\mu f(t)) = \Delta^{-\mu} (\Delta^\mu f(t)), \tag{1.78}$$

that is

$$\Delta^{-\nu} \Delta^\nu f(t) = \Delta^{-\mu} (\Delta^\mu f(t)), \quad \forall t \in \mathbb{N}_{a+\mu}. \tag{1.79}$$

It has been observed that

$$(t-s-1)^{(\mu-1)} = \frac{\Gamma(t-s)}{\Gamma(t-s-m+1)} = (t-s-1)(t-s-2)\ldots(t-s-m+1), \tag{1.80}$$

the falling factorial, where $t - s - m + 1 > 0$. Therefore, we obtain

$$\Delta^{-m} (\Delta^m f(t)) = \frac{1}{(m-1)!} \sum_{s=a}^{t-m} (t-s-1)^{(m-1)} \Delta^m f(s). \tag{1.81}$$

By employing the discrete Taylor formula previously mentioned in equation [195], one can derive

$$f(t) = \sum_{k=0}^{n-1} \frac{(t-a)^{(k)}}{k!} \Delta^k f(a) + \frac{1}{(m-1)!} \sum_{s=a}^{t-n} (t-s-1)^{(m-1)} \Delta^m f(s), \tag{1.82}$$

From the latter expression, we derive the Taylor formula

$$f(t) = \sum_{k=0}^{n-1} \frac{(t-a)^{(k)}}{k!} \Delta^k f(a) + \Delta^{-\nu} \Delta^\nu f(t), \tag{1.83}$$

where f is defined on $\mathbb{N}_a$, for all $t \in \mathbb{N}a + m$. □

Theorem 1.11 ([202]). *Consider $\mu > p$, where $p \in \mathbb{N}$, and μ is not an integer. Let $n = \lceil \mu \rceil$ and $\nu = n - \mu$. Then*

$$\Delta^p f(t) = \sum_{k=p}^{n-1} \frac{(t-a)^{(k-p)}}{(k-p)!} \Delta^k f(a) + \frac{1}{\Gamma(\mu-p)} (t-s-1)^{(\mu-p-1)} \Delta_*^\mu f(s), \tag{1.84}$$

for every $t \in \mathbb{N}_{a+n-p}$, where f is defined on $\mathbb{N}_a$.

Proposition 1.9 ([202]). *When $p = 0$ is inserted into (1.84) with $\mu > 0$, where μ is a non-integer, $n = \lceil \mu \rceil$, $\nu = n - \mu$, f defined on $\mathbb{N}_a$, and $\Delta^k f(a) = 0$ for $k = 0, \ldots, n-1$, we obtain*

$$f(t) = \frac{1}{\Gamma(\mu)} \sum_{s=a+\nu}^{t-\mu} (t - s - 1)^{(\mu-1)} \Delta_*^{\mu} f(s). \tag{1.85}$$

Proposition 1.10 ([202]). *Consider $\mu > p$, where p is a positive integer, μ is non-integer, $n = \lceil \mu \rceil$, and $\nu = n - \mu$. Suppose f is defined on $\mathbb{N}_a$, and additionally, assume that $\Delta^k f(a) = 0$ for $k = p, \ldots, n-1$. Then,*

$$\Delta^p f(t) = \frac{1}{\Gamma(\mu - p)} \sum_{s=a+\nu}^{t-\mu+p} (t - s - 1)^{(\mu-p-1)} \Delta_*^{\mu} f(s). \tag{1.86}$$

3. **Grunwald-Letnikov fractional difference operator**
In this part, we introduce the fractional discrete difference operator using the formulation based on the fractional order Grunwald-Letnikov approach.

Definition 1.25 ([204]). *The fractional order Grunwald-Letnikov difference operator ${}^{GL}\Delta^{\nu} f(t)$ is expressed as:*

$${}^{GL}\Delta^{\nu} f(t) = \frac{1}{h^{\nu}} \sum_{j=0}^{k} (-1)^j \binom{\nu}{j} f(k - j), \tag{1.87}$$

In the above formulations, the fractional order $\nu \in \mathbb{R}^+$, belonging to the set of strictly positive real numbers. Here, $h \in \mathbb{R}^+$ represents the sampling time, set to unity in subsequent discussions, and $k \in \mathbb{N}$ denotes the discrete time.
The coefficient $\binom{\nu}{j}$ is computed using the following relation:

$$\binom{\nu}{j} = \begin{cases} 1, & \text{for} \quad j = 0, \\ \dfrac{\nu(\nu-1)\ldots(\nu-j+1)}{j!}, & \text{for} \quad j > 0. \end{cases} \tag{1.88}$$

1.4 Nabla Type Fractional Operators

1.4.1 Essentiel Results in Fractional Nabla Sums

Definition 1.26 ([24]). *The left nabla fractional sum with order $\nu > 0$ (commencing at a) is explicitly defined as follows*

$$\nabla_a^{-\nu} f(t) = \frac{1}{\Gamma(\nu)} \sum_{s=a+1}^{t} (t - \rho(s))^{\overline{\nu-1}} f(s), \quad t \in \mathbb{N}_{a+1}. \tag{1.89}$$

Lemme 1.7 ([26]). *For any positive ν, the ensuing equality is satisfied:*

$$\nabla_a^{-\nu} \nabla f(t) = \nabla \nabla_a^{-\nu} f(t) - (t - a)^{\overline{\nu-1}} \frac{1}{\Gamma(\nu)} f(a). \tag{1.90}$$

Proof. Leveraging the subsequent identity obtained through integration by parts:

$$\begin{aligned}\nabla_s[(t-s)^{\overline{\nu-1}}f(s)] &= \nabla_s(t-s)^{\overline{\nu-1}}f(s) + \nabla(t-\rho(s))^{\overline{\nu-1}}\nabla_s f(s),\\ &= -(\nu-1)(t-\rho(s))^{\overline{\nu-2}}f(s) + (t-\rho(s))^{\overline{\nu-1}}\nabla_s f(s),\end{aligned} \tag{1.91}$$

we obtain

$$\begin{aligned}\nabla_a^{-\nu}\nabla f(t) &= \frac{1}{\Gamma(\nu)}\sum_{s=a+1}^{t}(t-\rho(s))^{\overline{\nu-1}}\nabla_s f(s),\\ &= \frac{1}{\Gamma(\nu)}\left[(t-s)^{\overline{\nu-1}}f(s)|_a + (\nu-1)\sum_{s=a+1}^{t}(t-\rho(s))^{\overline{\nu-1}}f(s)\right],\\ &= \frac{(t-a)^{\overline{\nu-1}}}{\Gamma(\nu)}f(a) + \frac{1}{\Gamma(\nu-1)}\sum_{s=a+1}^{t}(t-\rho(s))^{\overline{\nu-2}}f(s).\end{aligned} \tag{1.92}$$

However, we can express this as

$$\nabla\nabla_a^{-\nu}f(t) = \frac{1}{\Gamma(\nu)}\sum_{s=a+1}^{t}(t-\rho(s))^{\overline{\nu-1}}\nabla_s f(s) = \frac{1}{\Gamma(\nu-1)}\sum_{s=a+1}^{t}(t-\rho(s))^{\overline{\nu-2}}\nabla_s f(s). \tag{1.93}$$

Hence, we have successfully demonstrated the validity of Lemma 1.7.

□

Remarque 1.5. *Consider the case where $\nu > 0$ and $n = \lfloor\alpha\rfloor + 1$. With the aid of Lemma 1.7, we derive the following result:*

$$\nabla\nabla_a^{\nu}f(t) = \nabla\nabla^n\left[\nabla_a^{-(n-\nu)}f(t)\right] = \nabla^n\left[\nabla\nabla_a^{-(n-\nu)}f(t)\right]. \tag{1.94}$$

Alternatively,

$$\nabla\nabla_a^{\nu}f(t) = \nabla^n\left[\nabla_a^{-(n-\nu)}\nabla f(t)\right] + \frac{(t-a)^{\overline{n-\nu-1}}}{\Gamma(n-\nu)}f(a). \tag{1.95}$$

By employing the identity

$$\nabla^n\frac{(t-a)^{\overline{n-\nu-1}}}{\Gamma(n-\nu)} = \frac{(t-a)^{\overline{-\nu-1}}}{\Gamma(n-\nu)}. \tag{1.96}$$

We deduce that (1.95) holds true for all real values of ν.

Leveraging Lemma 1.7 and Remark 1.5, we systematically deduce the subsequent generalization through induction.

Theorem 1.12 ([26])**.** *For every real number ν and any positive integer p, the ensuing equality is established:*

$$\nabla_a^{-\nu}\nabla^p f(t) = \nabla^p\nabla_a^{-\nu}f(t) - \sum_{k=0}^{p-1}\frac{(t-a)^{\overline{\nu-p+k}}}{\Gamma(\nu+k-p+1)}\nabla^k f(a), \tag{1.97}$$

where the function f is defined over $\mathbb{N}_a$ and at some points preceding a.

Theorem 1.13 ([26]). *The given equation is satisfied for any real number ν and any positive integer p :*

$$\nabla_{a+p-1}^{-\nu}\nabla^{p}f(t)=\nabla^{p}\nabla_{a+p-1}^{-\nu}f(t)-\sum_{k=0}^{p-1}\frac{(t-(a+p-1))^{\overline{\nu-p+k}}}{\Gamma(\nu+k-p+1)}\nabla^{k}f(a+p-1), \tag{1.98}$$

here the function f is defined solely on $\mathbb{N}_a$.

Proof. The proof proceeds by iteratively applying Remark 1.5. The subsequent theorem is established. □

Lemme 1.8 ([30]). *Suppose $0\leq n-1<\nu\leq n$, and let $f(t)$ be defined over $\mathbb{N}_{\nu-n}$. The following statements are affirmed:*

- $\nabla_a^{\nu}f(t)=(\Delta_a^{\nu})f(t-\nu)$ *for* $t\in\mathbb{N}_{n+a}$.
- $\nabla_a^{\nu}f(t)=(\Delta_a^{\nu})f(t+\nu)$ *for* $t\in\mathbb{N}_{n}$.

Proposition 1.11 ([26]). *Suppose f is a real-valued function defined over $\mathbb{N}_a$, and let $\nu,\mu>0$. Then,*

$$\nabla_a^{-\nu}\nabla_a^{-\mu}f(t)=\nabla_a^{-(\nu+\mu)}f(t)=\nabla_a^{-\mu}\nabla_a^{-\nu}f(t). \tag{1.99}$$

Proof. The demonstration proceeds by employing Lemma 1.8 and the aforementioned Theorem 1.6. Indeed,

$$\begin{aligned}\nabla_a^{-\nu}\left(\nabla_a^{-\mu}f(t)\right)&=\nabla_a^{-\nu}\left(\Delta_a^{-\mu}f(t+\mu)\right),\\&=\Delta_a^{-\nu}\left(\Delta_a^{-\mu}f(t+(\mu+\nu)\right),\\&=\Delta_a^{-(\nu+\mu)}f\left(t+(\nu+\mu)\right),\\&=\Delta_a^{-(\nu+\mu)}f\left(t+(\nu+\mu)\right),\\&=\nabla_a^{-(\nu+\mu)}f(t).\end{aligned} \tag{1.100}$$

□

The upcoming power rule governing left fractional differences holds a crucial significance.

Proposition 1.12 ([26]). *Consider $\nu>0$ and $\mu>-1$. Then, for $t\in\mathbb{N}_a$, the following holds:*

$$\nabla_a^{-\nu}(t-a)^{\overline{\mu}}=\frac{\mu+1}{\nu+\mu+1}(t-a)^{\overline{\nu+\mu}}. \tag{1.101}$$

1.4.2 Nabla Fractional Differences

Definition 1.27. *[24] The fractional difference ∇ of order ν $(n-1<\nu<n)$ of the Riemann-Liouville type is given by:*

$${}^{RL}\nabla_a^{\nu}f(t)=\frac{\nabla^{n}}{\Gamma(n-\nu)}\sum_{s=a+1}^{t}(t-\rho(s))^{\overline{n-\nu-1}}(f(s))\quad t\in\mathbb{N}_{a+n}. \tag{1.102}$$

Definition 1.28 ([24]). *For f belonging to $\mathbb{N}_{a+n}$, the fractional difference ∇ of order ν $(n-1<\nu<n)$ in the Liouville-Caputo type is expressed as:*

$$ {}^{C}\nabla_a^{\nu} f(t) = \frac{1}{\Gamma(n-\nu)} \sum_{s=a+1}^{t} (t-\rho(s))^{\overline{n-\nu-1}} \nabla^n f(s), \quad t \in \mathbb{N}_{a+n}. \tag{1.103} $$

The subsequent proposition establishes connections between the nabla fractional differences of both the Riemann-Liouville and Liouville-Caputo types for a higher order ν.

Proposition 1.13 ([29]). *For t within $\mathbb{N}a+n-\nu$, and further, for $f \in \mathbb{N}_a$, it is affirmed that:*

$$ {}^{C}\nabla_a^{\nu} f(t) = {}^{RL}\nabla_a^{\nu} f(t) - \sum_{\ell=0}^{n-1} \frac{(t-a)^{\overline{-\nu+\ell}}}{\Gamma(-\nu+\ell+1)} \nabla^{\ell} f(a). \tag{1.104} $$

1.5 h-Difference Fractional Operators

1.5.1 Left Delta Fractional Sums and Differences on $h\mathbb{Z}$

Definition 1.29 ([197]). *Let f be defined on $\mathbb{N}_{a,h}$, and assume $k \in \mathbb{N}$. The left h-Caputo fractional delta sum of order $\nu > 0$ is given by:*

$$ \begin{aligned} ({}_a\Delta_h^{-\nu} f)(t) &= \frac{1}{\Gamma(\nu)} \int_a^{\sigma(t-\nu h)} (t-\sigma(s))_h^{\nu-1} f(s) \Delta_h s \\ &= \frac{1}{\Gamma(\nu)} \sum_{k=\frac{a}{h}}^{\frac{t}{h}-\nu} (t-\sigma(kh))_h^{\nu-1} f(kh) h, \quad t \in \mathbb{N}_{a,h}. \end{aligned} \tag{1.105} $$

Lemme 1.9 ([197]). *Let $\nu > 0$. For any $t \in \mathbb{N}_{a,h}$, the following hold true:*

$$ \lim_{\nu \to 0} ({}_a\Delta_h^{-\nu} f)(t+\nu h) = f(t). \tag{1.106} $$

Definition 1.30 ([197]). *consider f be defined on $\mathbb{N}_{a,h}$. The left h-Caputo fractional difference of order $\nu > 0$ is expressed as:*

$$ ({}_a\Delta_h^{\nu} f)(t) = (\Delta_h \, {}_a\Delta_h^{-(n-\nu)} f)(t), \quad {}_t \in \mathbb{N}_{a+(n-\nu)h,h}. \tag{1.107} $$

Definition 1.31 ([197]). *Let f be defined on $\mathbb{N}_{a,h}$. The left delta Caputo h-fractional difference of order $\nu > 0$ is defined by*

$$ ({}_a^{C}\Delta_h^{\nu} f)(t) = ({}_a\Delta_h^{-(n-\nu)} \Delta_h^n f)(t), \quad t \in \mathbb{N}_{a+(n-\nu)h,h}. \tag{1.108} $$

Lemme 1.10. *[[197]] Given $\nu > 0$, $\mu > 0$, and $h > 0$,*

$$ {}_{a+\mu h}\Delta_h^{-\nu} (t-a)_h^{\mu-1} = \frac{\Gamma(\mu)}{\Gamma(\mu+\nu)} (t-a)_h^{\nu+\mu-1}. \tag{1.109} $$

Theorem 1.14 ([197]). *For $\nu > 0$, $\mu > 0$, and $h > 0$, if f is defined on $\mathbb{N}a, h$, then for all $t \in \mathbb{N}a + h(\nu+\mu), h$, we have*

$$ ({}_{a+\nu h}\Delta_h^{-\mu} \, {}_a\Delta_h^{-\nu} f)(t) = ({}_a\Delta_h^{-(\nu+\mu)} f)(t) = ({}_{a+\nu h}\Delta_h^{-\nu} \, {}_a\Delta_h^{-\mu} f)(t). \tag{1.110} $$

Proof. Now, let's establish the validity of the left part. We can observe that

$$\begin{aligned}
({}_{a+\nu h}\Delta_h^{-\mu}\,{}_a\Delta_h^{-\nu} f)(t) &= \frac{1}{\Gamma(\nu)}\int_{a+\nu h}^{\sigma(t-\mu h)}(t-\sigma(r))_h^{\mu-1}\frac{1}{\Gamma(\mu)}\int_a^{\sigma-r-\alpha h)}(r-\sigma(s))_h^{\mu-1}f(s)\Delta_h r,\\
&= \frac{1}{\Gamma(\nu)}\int_a^{\sigma(t-(\nu+\mu)h)}\frac{1}{\Gamma(\mu)}\int_{s+\nu h}^{\sigma(t-\mu h)}(a+r-\sigma(s)-a)_h^{\nu-1}(t-\sigma(r))_h^{\mu-1}\Delta_h r f(s)\Delta_h s,\\
&= \frac{1}{\Gamma(\nu)}\int_a^{\sigma(t-(\nu+\mu)h)} f(s)\frac{1}{\Gamma(\mu)}\int_{a+(\nu-1)h}^{a+t-\mu h-s}(u-a)_h^{\nu-1}(t+a-\sigma(s)-\sigma(u))_h^{\mu-1}\Delta_h u\Delta_h s,\\
&= \frac{1}{\Gamma(\nu)}\int_{\sigma(t-(\nu+\mu)h)}^{a}{}_{a+(\nu-1)h}\Delta_h^{-\mu}(u-a)_h^{\nu-1}\Big|_{u=t+a-\sigma(s)} f(s)\Delta_h s.
\end{aligned} \tag{1.111}$$

Applying Lemma 1.10, we derive the following:

$$({}_{a+\nu h}\Delta_h^{-\mu}\,{}_a\Delta_h^{-\nu} f)(t) = \frac{1}{\Gamma(\nu+\mu)}\int_{\sigma(t-(\nu+\mu)h)}^{a}(t-\sigma(s))_h^{\nu+\mu-1}f(s)\Delta_h s. \tag{1.112}$$

This completes the proof, as the right-hand side of (1.112) is $({}_{a+\alpha}\Delta_h^{\nu+\mu}f)(t)$.

□

Lemme 1.11 ([197]). *The following holds for any $\nu > 0$:*

$$({}_a\Delta_h^{-\nu}\Delta_h f)(t) = (\Delta_h\,{}_a\Delta_h^{-\nu} f)(t) - \frac{(t-a)_h^{(\nu-1)}}{\Gamma(\nu)}f(a), \tag{1.113}$$

here f is defined on $\mathbb{N}_{a,h}$.

Proof. The verification of (1.113) is accomplished by performing Δ_h-integration by parts on the time scale $\mathbb{N}_{a,h}$, taking advantage of the property $(\nu h - h)_h^{(\nu-1)} = \Gamma(\nu)$.

□

Theorem 1.15 ([197]). *For any real number ν and any positive integer p, the following equality is valid*

$$({}_a\Delta_h^{-\nu}\Delta_h^p\psi)(t) = (\Delta_h^p\,{}_a\Delta_h^{-\nu} f)(t) - \sum_{k=0}^{p-1})\frac{(t-a)_h^{(\nu-p+k}}{\Gamma(\nu+k-p+1)}\Delta_h^k f(a). \tag{1.114}$$

Applying Theorem 1.15 with $p = n$ and substituting ν with $n-\nu$, we can represent:

Proposition 1.14 ([197]). *Assuming f is defined on $\mathbb{N}_{a,h}$, for $\nu > 0$, we have:*

$$({}_a^C\Delta_h^\nu\psi)(t) = ({}_a\Delta_h^\nu f)(t) - \sum_{k=0}^{n-1}\frac{(t-a)_h\{(k-\nu)}{\Gamma(k-\nu+1)}\Delta_h^k f(a), \quad n = [\nu]+1. \tag{1.115}$$

In particular, when $0 < \nu < 1$, we get:

$$({}_a^C\Delta_h^\nu f)(t) = ({}_a\Delta_h^\nu f)(t) - \frac{(t-a)_h\{(-\nu)}{\Gamma(1-\nu+1)}f(a). \tag{1.116}$$

Proposition 1.15 ([197]). *For $\nu > 0$, $h > 0$, and f defined on $\mathbb{N}_{a,h}$, consider $t \in \mathbb{N}_{a+nh,h} \subset \mathbb{N}_{a,h}$. Then,*

$$({}_{a-\nu h}\Delta_h^{\nu}\, {}_a\Delta_h^{-\nu}\psi)(t) = f(t), \tag{1.117}$$

$$({}_{a+(n-\nu)h-h}\Delta_h^{-\nu}\, {}_a\Delta_h^{\nu} f)(t) = f(t), \quad \nu \in \mathbb{N}, \tag{1.118}$$

and

$$({}_a\Delta_h^{-\nu}\, {}_a\Delta_h^{\nu} f)(t) = f(t) - \sum_{k=0}^{n-1} \frac{(t-a)_h^k}{k!} \Delta_h^k h f(a), \quad \nu \in \mathbb{N}, \tag{1.119}$$

where $n = \lfloor \nu \rfloor + 1$.

Proof. The proof relies on Theorem 1.15 ((1.114)), Theorem 1.14 ((1.110)), and the acknowledgment that ${}_a\Delta^{-(n-\nu)}\psi(a + (n-\nu)h - h) = 0$. This completes the proof. □

Proposition 1.16. *Let $\nu > 0$, $h > 0$, and f be defined on $\mathbb{N}_{a,h}$. Then,*

$$({}_{a+(n-\nu)h}\Delta_h^{-\nu}\, {}_a^C\Delta_h^{\nu} f)(t) = f(t) - \sum_{k=0}^{n-1} \frac{(t-a)_h^k}{k!} \Delta_h^k f(a). \tag{1.120}$$

Proof. The derivation of (1.120) follows from the definition, (1.117) in Proposition 1.15, and Theorem 1.14. This completes the proof.

□

1.5.2 Left Nabla Fractional Sums and Differences on $h\mathbb{Z}$

Definition 1.32 (Nabla h-Fractional Sums[196]). *: Consider a function $f : \mathbb{N}_{a,h} \to \mathbb{R}$. We introduce the nabla left h-fractional sum of order $\nu > 0$ as follows:*

$${}_a\nabla_h^{-\nu} f(t) = \frac{1}{\Gamma(\nu)} \int_a^t (t - \rho_h(s))^{\overline{\nu-1}}_h f(s) \nabla_h s = \frac{1}{\Gamma(\nu)} \sum_{k=\frac{a}{h}+1}^{\frac{t}{h}} (t - \rho_h(s))^{\overline{\nu-1}}_h f(kh) h, \tag{1.121}$$

where $t \in \mathbb{N}_{a,h}$.

Definition 1.33 (Nabla h-RL Fractional Differences[196]). *For a given function $f : \mathbb{N}_{a,h} \to \mathbb{R}$, the nabla left h-fractional sum of order $\nu > 0$ is defined as:*

$${}_a\nabla_h^{\nu} f(t) = (\nabla_h\, {}_a\nabla_h^{-(1-\nu)} f)(t), \tag{1.122}$$

this operator is represented by the expression:

$${}_a\nabla_h^{\nu} f(t) = \frac{1}{\Gamma(1-\nu)} \nabla_h \sum_{k=\frac{a}{h}+1}^{\frac{t}{h}} (t - \rho_h(kh))^{\overline{-\nu}}_h f(kh) h, \tag{1.123}$$

where $t \in \mathbb{N}_{a+h,h}$.

Definition 1.34 (Nabla h-Caputo Fractional Differences[196]). *Let $0 < \nu \leq 1$, $0 < h \leq 1$, $a \in \mathbb{R}$. If f is defined on $\mathbb{N}_{a,h}$, the h-Caputo fractional difference of order ν starting at a is given by:*

$${}_a^C\nabla_h^{\nu} f(t) = ({}_a\nabla_h^{-(1-\nu)} \nabla_h f)(t), \quad t \in \mathbb{N}_{a+h,h}. \tag{1.124}$$

Proposition 1.17 (Relation between Nabla h-RL Fractional Difference and h-Caputo Fractional Difference[196])**.**

$$ {}^{C}_{a}\nabla^{\nu}_{h} f(t) = \nabla^{\nu}_{h} f(t) - \frac{1}{\Gamma(1-\nu)}(t-a)^{\overline{-\nu}}_{h} f(a). \tag{1.125} $$

Proof.

$$
\begin{aligned}
{}^{C}_{a}\nabla^{\nu}_{h} f(t) &= {}_{a}\nabla^{-(1-\nu)}_{h}\nabla_{h} f(t), \\
&= {}_{a}\nabla^{-(1-\nu)}_{h}\left(\frac{f(t)-f(t-h)}{h}\right), \\
&= {}_{a}\nabla^{-(1-\nu)}_{h}\left(\frac{f(t)}{h}\right) - {}_{a}\nabla^{-(1-\nu)}_{h}\left(\frac{f(t-h)}{h}\right), \\
&= \frac{1}{\Gamma(1-\nu)}\sum_{k=\frac{a}{h}+1}^{\frac{t}{h}}(t-\rho_h(kh))^{\overline{-\nu}}_{h}\frac{f(kh)}{h}h - \frac{1}{\Gamma(1-\alpha)}\sum_{k=\frac{a-h}{h}+1}^{\frac{t}{h}-1}(t-h-\rho_h(kh))^{\overline{-\nu}}_{h}\frac{f(kh)}{h}h, \\
&= \frac{1}{h\Gamma(1-\nu)}\sum_{k=\frac{a}{h}+1}^{\frac{t}{h}}(t-\rho_h(kh))^{\overline{-\nu}}_{h} f(kh)h - \frac{1}{h\Gamma(1-\nu)}\sum_{k=\frac{a}{h}}^{\frac{t}{h}-1}((t-h)-(kh-h))^{\overline{-\nu}}_{h} f(kh)h, \\
&= \frac{1}{h\Gamma(1-\nu)}\sum_{k=\frac{a}{h}+1}^{\frac{t}{h}}(t-\rho_h(kh))^{\overline{-\nu}}_{h} f(kh)h - \frac{1}{h\Gamma(1-\nu)}\sum_{k=\frac{a}{h}}^{\frac{t}{h}-1}(t-h-\rho_h(kh))^{\overline{-\nu}}_{h} f(kh)h, \\
&\quad - \frac{1}{h\Gamma(1-\nu)}\left(t-h-\frac{a}{h}(h+h)\right)^{\overline{-\nu}}_{h} f\left(\frac{a}{h}h\right)h, \\
&= \frac{1}{\Gamma(1-\nu)}\frac{\sum_{k=\frac{a}{h}+1}^{\frac{t}{h}}(t-\rho_h(kh))^{\overline{-\nu}}_{h} f(kh)h - \sum_{k=\frac{a}{h}+1}^{\frac{t}{h}}((t-h)-\rho_h(kh))^{\overline{-\nu}}_{h} f(kh)h}{h}, \\
&\quad - \frac{1}{\Gamma(1-\nu)}(t-a)^{\overline{-\nu}}_{h} f(a), \\
&\quad - \frac{1}{\Gamma(1-\nu)}\nabla_{h}\sum_{k=\frac{a}{h}+1}^{\frac{t}{h}}(t-h-\rho_h(kh))^{\overline{-\nu}}_{h} f(kh)h - \frac{1}{\Gamma(1-\nu)}(t-a)^{\overline{-\nu}}_{h} f(a), \\
&= ({}_{a}\nabla^{a}_{h} f)(t) - \frac{1}{\Gamma(1-\nu)}(t-a)^{\overline{-\nu}}_{h} f(a).
\end{aligned}
\tag{1.126}
$$

□

Lemme 1.12 ([196])**.** *For $\nu > 0$, $\mu > -1$, $h > 0$, and $t \in \mathbb{N}_{a,h}$, the following relation holds:*

$$ {}_{a}\nabla^{-\nu}_{h}(t-a)^{\overline{\mu}}_{h} = \frac{\Gamma(\mu+1)}{\Gamma(\mu+1+\nu)}(t-a)^{\overline{\nu+\mu}}_{h}. \tag{1.127} $$

Theorem 1.16 ([196])**.** *Let $\nu > 0$, $\mu > 0$, $h > 0$. If f is defined on $\mathbb{N}^{h}_{a}$, then for all $t \in \mathbb{N}^{h}_{a+h}$, we have*

$$ {}_{a}\nabla^{-\mu}_{h}\,{}_{a}\nabla^{-\nu}_{h} f(t) = {}_{a}\nabla^{-(\nu+\mu)}_{h} f(t) = {}_{a}\nabla^{-\nu}_{h}\,{}_{a}\nabla^{-\mu}_{h} f(t). \tag{1.128} $$

Proof. The proof follows a similar approach to Theorem 1.14, incorporating the insights from Lemma 1.12. □

Lemme 1.13 ([196]). *For any $\nu > 0$, we have*

$$ {}_a\nabla_h^{-\nu}\nabla_h f(t) = \nabla_h\, {}_a\nabla_h^{-\nu} f(t) - \frac{(t-a)_h^{\overline{\nu-1}}}{\Gamma(\nu)} f(a). \tag{1.129}$$

Where f is defined on $\mathbb{N}_a^h$.

Proposition 1.18 ([196]). *For $\nu > 0$, $h > 0$, and f defined on $\mathbb{N}_a^h$, we have*

- ${}_a\nabla_h^{\nu}\, {}_a\nabla_h^{-\nu} f(t) = f(t)$.
- ${}_a\nabla_h^{-\nu}\, {}_a\nabla_h^{\nu} f(t) = f(t) - \sum_{k=0}^{n-1} \frac{(t-a)_h^k}{k!} \nabla_h^k f(a), \quad \nu \in \mathbb{N}$.

1.5.3 Nabla h-Discrete Fractional Defferences with Exponential Kernels

In this part, we thoroughly revisit and enhance the presented results. Specifically, we choose ν such that $0 < \nu < \min(1, \beta)$, where β is subject to the condition $|\kappa h^{\beta}| < 1$, with $\kappa = \dfrac{-\beta}{1-\beta}$. Our exposition incorporates the established time scale notation [199].

Here, we propose the following discrete versions:

Definition 1.35 ([196]). *For $\nu \in (0,1)$ and f defined on $\mathbb{N}_{a,h}$, let*

$$ H(\nu, h) = B(\nu)\left[\frac{\nu}{h} + (1-\nu)\right].$$

We introduce:

- *The left h-nabla CFC fractional difference is defined by:*

$$\begin{aligned} ({}_a^{CFC}\nabla_h^{\nu} f)(t) &= H(\nu,h)\left(\frac{1-\nu+\nu h}{1-\nu}\right) \sum_{k=\frac{a}{h}+1}^{\frac{t}{h}} h(\nabla_h f)(kh) \left(\frac{1-\nu}{1-\nu+\nu h}\right)^{\frac{t-\rho(kh)}{h}}, \\ &= H(\nu,h) \sum_{k=\frac{a}{h}+1}^{\frac{t}{h}} h(\nabla_h f)(kh) \left(\frac{1-\nu}{1-\nu+\nu h}\right)^{\frac{t-kh}{h}}, \end{aligned} \tag{1.130}$$

  where $t \in \mathbb{N}_{a+h,h}$.

- *The h-nabla CFR difference is defined by:*

$$\begin{aligned} ({}_a^{CFR}\nabla_h^{\nu} f)(t) &= H(\nu,h)\left(\frac{1-\nu+\nu h}{1-\nu}\right) \nabla_h \sum_{k=\frac{a}{h}+1}^{\frac{t}{h}} hf(kh) \left(\frac{1-\nu}{1-\nu+\nu h}\right)^{\frac{t-\rho(kh)}{h}}, \\ &= H(\nu,h)\nabla_h \sum_{k=\frac{a}{h}+1}^{\frac{t}{h}} hf(kh) \left(\frac{1-\nu}{1-\nu+\nu h}\right)^{\frac{t-kh}{h}}, \end{aligned} \tag{1.131}$$

  where $t \in \mathbb{N}_{a+h,h}$.

Remarque 1.6. *Observing that $H(0,h)=1$ and $H(1,h)=\frac{1}{h}$, in the limiting cases as $\nu\to 0$ and $\nu\to 1$, we find:*

- $({}^{CFC}_{a}\nabla^{\nu}_{h}f)(t)\to f(t)-f(a)$ *as* $\nu\to 0$, *and* $({}^{CFC}_{a}\nabla^{\nu}_{h}f)(t)\to \nabla_h f(t)$ *as* $\nu\to 1$.
- $({}^{CFR}_{a}\nabla^{\nu}_{h}f)(t)\to f(t)$ *as* $\nu\to 0$, *and* $({}^{CFR}_{a}\nabla^{\nu}_{h}f)(t)\to \nabla_h f(t)$ *as* $\nu\to 1$.

Additionally, it's worth noting that when $h=1$, all the definitions proposed in [?] are recovered.

Definition 1.36 ([196]). *We can establish the corresponding left discrete fractional integral of $({}^{CF}_{a}\nabla^{-\nu}_{h})$ as follows:*

$$\begin{aligned}({}^{CF}_{a}\nabla^{-\nu}_{h}f)(t)&=\frac{1-\nu}{H(\nu,h)(1-\nu+\nu h)}f(t)+\frac{\nu}{H(\nu,h)(1-\nu+\nu h)}\sum_{s=\frac{a}{h}+1}^{\frac{t}{h}}hf(hs),\\&=\frac{(1-\nu)}{H(\nu,h)(1-\nu+\nu h)}u(t)+\frac{\nu}{H(\nu,h)(1-\nu+\nu h)}\sum_{s=\frac{a}{h}+1}^{\frac{t}{h}}f(s)\Delta_h s.\end{aligned}\tag{1.132}$$

Proposition 1.19 ([196]). *The relation between Riemann and Caputo type h-fractional differences with exponential kernels*

$$({}^{CFC}_{a}\nabla^{\alpha\nu}_{h}f)(t)=({}^{CFR}_{a}\nabla^{\nu}_{h}f)(t)--\frac{H(\nu,h)(1-\nu+\nu h)}{1-\nu}f(a)\left(\frac{1-\nu}{1-\nu+\nu h}\right)^{\frac{(t-a)}{h}}.\tag{1.133}$$

1.5.4 Nabla h-Fractional Differences Operators with Discrete Mittag-Leffler Kernels

We provide here a revised and modified discussion building upon the work in [?]. Throughout our notation, we consistently set $\kappa=-\frac{\nu}{1-\nu}$ and $\rho(t)=t-h$.

Definition 1.37 ([196]). *For a function f defined on $\mathbb{N}a,h$, and for $\nu\in[0,1]$ such that $|\kappa h\nu|<1$, the nabla ABC fractional difference (in the sense of Atangana and Baleanu) is defined as follows:*

$$\begin{aligned}({}^{ABC}_{a}\nabla^{\nu}_{h}f)(t)&=H(\nu,h)\frac{1-\alpha\nu+\nu h}{1-\nu}\sum_{k=\frac{a}{h}+1}^{\frac{t}{h}}h\nabla_h f(kh)\,{}_hE_{\overline{\nu}}(\kappa,t-\rho(kh)),\\&=H(\nu,h)\frac{1-\nu+\nu h}{1-\nu}\nabla_h\left[f(t)*{}_hE_{\overline{\nu}}(\kappa,t-a)\right].\end{aligned}\tag{1.134}$$

Similarly, in the Riemann sense, the nabla ABC fractional sum is defined as:

$$\begin{aligned}({}^{ABR}_{a}\nabla^{\nu}_{h}f)(t)&=H(\nu,h)\frac{1-\nu+\nu h}{1-\nu}\nabla_h\sum_{k=\frac{a}{h}+1}^{\frac{t}{h}}hf(kh)\,{}_h,E_{\overline{\nu}}(\kappa,t-\rho(kh)),\\&=H(\nu,h)\frac{1-\nu+\nu h}{1-\nu}\nabla_h\left[f(t)*{}_hE_{\overline{\nu}}(\kappa,t-a)\right].\end{aligned}\tag{1.135}$$

Definition 1.38 ([196]). *The left h-fractional sum associated with* $({}_a^{ABR}\nabla_h^{\nu} f(t))$ *with order* $0 < \nu < 1$ *is defined on* $\mathbb{N}_{a,h}$ *as:*

$$({}_a^{AB}\nabla_h^{-\nu} f)(t) = \frac{(1-\nu)}{H(\alpha,h)(1-\nu+\nu h)} f(t) + \frac{\nu}{H(\nu,h)(1-\nu+\nu h)} ({}_a\nabla_h^{-\nu} f)(t). \quad (1.136)$$

It is evident that $\nu = 0$ yields the function f, and $\nu = 1$ results in ${}_a\nabla_h^{-1} f(t) = \sum_{i=\frac{a}{h}+1}^{\frac{t}{h}} f(ih)$. The case $h = 1$ reproduces the fractional sum defined in [**?**].

Conversely, solving $({}_a^{AB}\nabla_h^{-\nu} g)(t) = f(t)$ reveals that $g(t) = ({}_{ABR}\nabla_h^{\nu} f)(t)$.

Theorem 1.17 ([196]). *The relation between the Caputo and Riemann fractional differences with Mittag-Leffler (ML) kernels is given by:*

$$({}_a^{ABC}\nabla_h^{\nu} f)(t) = ({}_a^{ABR}\nabla_h^{\nu} f)(t) - f(a)\frac{H(\nu,h)(1-\nu+\nu h)}{1-\nu} {}_hE_{\overline{\nu}}(\kappa, t-a). \quad (1.137)$$

1.6 Laplace Transform Applications for Discrete Fractional Calculus

Since the late 18th century, Pierre Laplace's transform has played a crucial role in solving elementary differential equations. However, contemporary challenges often demand an extension of Laplace's approach to handle more intricate conditions. In this section, we apply the Laplace transform to address a fractional initial value problem defined on natural numbers.

1.6.1 Laplace Transforms for the Delta-Difference Operator

This section introduces the Laplace transform derived from the general theory of time scales, providing a transform suitable for functions defined on arbitrary, closed subsets of the real numbers (refer to [200, 201]). The concepts and lemmas articulated in this section are primarily extracted from the influential publications cited in reference [198]. The Laplace transform for a regulated function $f : \mathbb{T}_a \to \mathbb{R}$ on a time scale $\mathbb{T}_a$ is defined as follows:

$$L_a\{f\}(s) := \int_a^{\infty} e_{\ominus s}^{\sigma}(t,a) f(t) \Delta t, \quad (1.138)$$

with a special focus on the isolated time scale. The Laplace transform of function g is presented, emphasizing the significance of the preceding results:

$$L\{f\}(s) = \sum_{k=0}^{\infty} \frac{f(k+t_0)}{(s+1)^{k+1}}. \quad (1.139)$$

A key consideration when exploring the Laplace transform (1.140) is determining the set of $s \in \mathbb{C} \setminus \{-1\}$ for which the transform converges. Gaining insights into the properties of the function f becomes crucial in addressing this fundamental question.

Definition 1.39 ([198]). *A function* $f : \mathbb{N}_a \to \mathbb{R}$ *is considered to have exponential order* $r > 0$ *if there exists a positive constant* $D > 0$ *such that*

$$|f(t)| \leq Dr^t, \quad (1.140)$$

for t *sufficiently large in the set* $\mathbb{N}_a$.

We introduce now the Taylor monomial and its Laplace transform. The full-order Taylor monomials, as explored in [200], offer significant advantages in the application of the Laplace transform to discrete fractional calculus. This set of monomials is defined recursively as follows:

$$\begin{cases} h_0(t,a) = 1; \\ h_{n+1}(t,a) = \dfrac{\Gamma(t-a)^n}{n!}, \quad n \in \mathbb{N}_a. \end{cases} \tag{1.141}$$

Definition 1.40 ([198]). *For every $\mu \in \mathbb{R} \setminus -\mathbb{N}$, let's define the μth Taylor Monomial as follows:*

$$h_\mu(t,a) = \frac{\Gamma(t-a)^{(\mu)}}{\Gamma(\mu+1)}, \quad n \in \mathbb{N}_a. \tag{1.142}$$

Lemme 1.14 ([198]). *Assume $\mu \in \mathbb{R} \setminus -\mathbb{N}$, and let $a, b \in \mathbb{R}$ such that $b - a = \mu$. Then, for $s \in \mathbb{C} \setminus \overline{B}_{-1}(1)$, we obtain:*

$$L\left\{h_\mu(t,a)\right\}(s) = \frac{(s+1)^\mu}{s^{\mu+1}}. \tag{1.143}$$

Equation (1.144) for convolution corresponds to the convolution defined in [200] for general time scales, yet it exhibits a distinct domain compared to the convolution introduced by Atici and Eloe in [**?**]. Numerous benefits underscore the rationale for embracing the definition provided in (1.144).

Definition 1.41 ([198]). *Consider functions $f, g : \mathbb{N}_a \to \mathbb{R}$. We define the convolution of f and g as follows:*

$$(f * g)(t) = \sum_{r=a}^{t-1} f(r) g(t-1-r+a) \quad t \in \mathbb{N}_a. \tag{1.144}$$

Lemme 1.15 ([198]). *Suppose $f, g : \mathbb{N}_a \to \mathbb{R}$ are functions of exponential order $r > 0$. Then,*

$$L\left\{f * g\right\}(s) = L\left\{f\right\}(s) L\left\{g\right\}(s) \quad s \in \mathbb{C}\overline{B_{-1}(r)}. \tag{1.145}$$

Consider a function $f : \mathbb{N}_a \to \mathbb{R}$ and a positive parameter $\nu > 0$. Choose $N \in \mathbb{N}$ such that $N - 1 < \nu \leq N$. It's noteworthy that within the realm of Laplace transform theory, the following outcomes are firmly established: For $N \in \mathbb{N}$,

$$L\left\{\Delta_a^{-N} g\right\}(s) = \frac{L\left\{f\right\}(s)}{s^N}, \tag{1.146}$$

$$L\left\{\Delta_a^{N} f\right\}(s) = s^N L\left\{f\right\}(s) - \sum_{j=0}^{N-1} s^j \Delta^{N-1-j} f(a). \tag{1.147}$$

Expanding upon equations (1.146) and (1.147) we proceed to apply the Laplace transform to fractional-order sums and differences.
To commence, it is essential to delineate the connection between the exponential order of f and the exponential orders associated with $\Delta_a^{-\nu}$ and Δ_a^{ν}. The ensuing lemma furnishes an exhaustive depiction of this interrelation:

Lemme 1.16 ([198]). *Assume that $f : \mathbb{N}_a \to \mathbb{R}$ possesses exponential order $r \geq 1$, and consider a given parameter $\nu > 0$. For any fixed $\epsilon > 0$, both $\Delta_a^{-\nu} f$ and $\Delta_a^{\nu} f$ exhibit exponential order $r + \epsilon$.*

Lemme 1.17 ([198]). *Assume that $f : \mathbb{N}_a \to \mathbb{R}$ is of exponential order $r \geq 1$, and let $\nu > 0$ be given such that $N - 1 < \nu \leq N$. Then both $La + \beta - N \left\{\Delta_a^{-\beta} f\right\}(s)$ and $L_{a+\beta-N} \left\{\Delta_a^{\nu} f\right\}(s)$ converge for all $s \in \mathbb{C} \setminus \overline{B_{-1}(r)}$.*

Now, equipped with Lemma 1.17 to guarantee the correct domain of convergence for the Laplace transform of any fractional operator, we can formulate expressions for applying the Laplace transform to fractional operators.

Lemme 1.18 ([198]). *Assume that $f : \mathbb{N}a \to \mathbb{R}$ is of exponential order $r \geq 1$, and let $\nu > 0$ be given such that $N - 1 < \nu \leq N$. Then, for $s \in \mathbb{C} \setminus \overline{B_{-1}(r)}$,*

$$L_{a+\nu} \left\{\Delta_a^{\nu} f\right\}(s) = \frac{(s+1)^{\nu}}{s^{\nu}} L_a \left\{f\right\}(s), \tag{1.148}$$

and

$$L_{a+\nu-N} \left\{\Delta_a^{-\nu} f\right\}(s) = \frac{(s+1)^{\nu-N}}{s^{\nu}} L_a \left\{f\right\}(s). \tag{1.149}$$

Proof. Let f, r, ν, and N be given as in the statement of the theorem. Observe that f being of exponential order $r \in (0, 1)$ implies that f is of exponential order 1.
The assumption of $r \geq 1$ is not intended to exclude functions f of exponential order $r \in (0, 1)$. Instead, it ensures that Lemma 1.14, applied below, will hold whenever s is in the domain of convergence for $L_{a+\nu}\Delta_a^{-\nu} f$.
To elucidate the relationship between (1.148) and (1.149), we apply the following shift formula :

$$L_{a-m}\{f\}(s) = \frac{1}{(s+1)^m} L_a\{f\}(s) + \sum_{k=0}^{m-1} \frac{f(k+a-m)}{(s+1)^{k+1}}, \quad f : \mathbb{N}_{a-m} \to \mathbb{R}. \tag{1.150}$$

Specifically, for each $s \in \mathbb{C} \setminus \overline{B_{-1}(r)}$,

$$\begin{aligned} L_{a+\nu-N}\{\Delta_a^{-\nu} f\}(s) &= \frac{1}{(s+1)^N} L_{a+\nu}\{\Delta_a^{-\nu} f\}(s) + \sum_{k=0}^{N-1} \frac{\Delta_a^{-\beta} f(k+a+\nu-N)}{(s+1)^{k+1}}, \\ &= \frac{1}{(s+1)^N} L_{a+\nu}\{\Delta_a^{-\nu} f\}(s), \end{aligned} \tag{1.151}$$

considering the zeros of $\Delta_a^{-\nu} f$. Additionally,

$$\begin{aligned}
L_{a+\nu}\{\Delta_a^{-\nu} f\}(s) &= \sum_{k=0}^{\infty} \frac{\Delta_a^{-\nu} f(k+a+\nu)}{(s+1)^{k+1}}, \\
&= \sum_{k=0}^{\infty} \frac{1}{(s+1)^{k+1}} \frac{(k+a+\nu-\sigma(r))^{(\nu-1)}}{\Gamma(\nu)} f(r), \\
&= \sum_{k=0}^{\infty} \frac{1}{(s+1)^{k+1}} f(r) h_{\nu-1}((k+1)-r+a, a-(\nu-1)), \\
&= \sum_{k=0}^{\infty} \frac{(f * h_{\nu-1}(t, a-(\nu-1)))(k+a+1)}{(s+1)^{k+1}}, \\
&= L_{a+1}\{f * h_{\nu-1}(t, a-(\nu-1))\}(s), \\
&= (s+1) L_a\{f * h_{\nu-1}(t, a-(\nu-1))\}(s), \\
&= (s+1) L_a\{f\}(s) L_a\{h_{\nu-1}(t, a-(\nu-1))\}(s), \\
&= (s+1)^{\nu} s^{-\nu} L_a\{f\}(s), \quad \text{applying (7)}, \quad \text{since} \quad r \geq 1.
\end{aligned} \tag{1.152}$$

Furthermore, by applying the shift formula (1.150), we obtain

$$L_{a+\beta-N}\{\Delta_a^{-\beta} f\}(s) = \frac{1}{(s+1)^N} L_{a+\beta}\{\Delta_a^{-\beta} f\}(s) = \frac{(s+1)^{\beta-N}}{s^{-\beta}} L_a\{f\}(s), \tag{1.153}$$

for $s \in \mathbb{C} \setminus \overline{B_{-1}(r)}$, proving (1.149). □

Lemme 1.19 ([198]). *Assume that $f : \mathbb{N}a \to \mathbb{R}$ is of exponential order $r \geq 1$, and let $\nu > 0$ be given such that $N - 1 < \nu \leq N$. Then, for $s \in \mathbb{C} \setminus \overline{B_{-1}(r)}$,*

$$L_{a+\nu-N}\left\{\Delta_a^{\nu} f\right\}(s) = s^{\nu}(s+1)^{\nu+N} L_a\left\{f\right\}(s) - \sum_{j=0}^{N-1} s^j \Delta_a^{\nu-1-j} f(a+N-\beta), \tag{1.154}$$

1.6.2 Laplace Transforms for the Nabla-Difference Operator

In this section, we will focus on clarifying various aspects of the Laplace transform to establish a groundwork for addressing initial-value problems related to fractional nabla difference equations.

Inspired by the time scale-based definition of the Laplace transform provided in [178], we introduce the (nabla) Laplace transform operator N in the following manner:

Definition 1.42 ([178]). *Consider a function f mapping from $\mathbb{N}_a$ to $\mathbb{R}$ and let s be an element of $\mathbb{R}$. The Laplace transform of f is defined as:*

$$N_a\{f\}(s) := \int_a^1 e_{\rho \ominus s}(t; a) f(t)\, dt. \tag{1.155}$$

Although this representation will be convenient on certain occasions, it is equally crucial to contemplate its equivalent expression.

$$N_a\{f\}(s) = \frac{1}{1-s} \sum_{k=1}^{\infty} (1-s)^{k-1} f(a+k), \tag{1.156}$$

This property is easily confirmed. The linearity of this transformation can be deduced from the aforementioned form. Nevertheless, what may not be immediately apparent is the existence and uniqueness of this transformation, a matter that we establish in the subsequent theorem.

Theorem 1.18 ([178]). *If we have a function with an exponential order denoted by α, the Laplace transform of this function exists within the range where $\left|\frac{1-s}{1-\alpha}\right| < 1$.*

We introduce the concept of nabla Taylor monomials and subsequently extend their definition to non-integer orders. Following this, we will explore and derive their Laplace transforms.

Definition 1.43 ([178]). *The n-th nabla Taylor monomial $h_n(t,a)$, for all non-negative integers n, is defined through the following recursive formulation:*

$$\begin{cases} h_0(t,a) := 1, \\ h_n(t,a) := \int_a^t h_{n-1}(\tau,a)\nabla^\tau d\tau, \quad n \geq 1. \end{cases} \tag{1.157}$$

The following theorem provides a formula for the nabla Taylor monomials.

Theorem 1.19 ([178]). *For all non-negative integers n, the nabla Taylor monomial $h_n(t,a)$ is defined as follows:*

$$h_n(t,a) = \frac{(t-a)^n}{n!}. \tag{1.158}$$

Before extending the Taylor monomials to arbitrary values of n, let's start by finding the Laplace transform of the integer-order Taylor monomials.

Theorem 1.20 ([178]). *egative integer n and $|1-s| < 1$, the Laplace transform of the n-th nabla Taylor monomial $h_n(t,a)$ is given by:*

$$N_a\{h_n(\cdot,a)\}(s) = \frac{1}{s^{n+1}}. \tag{1.159}$$

Now, let's introduce the nabla Taylor monomials for fractional orders.

Definition 1.44 ([178]). *For any $\beta \in \mathbb{R}\backslash -1,-2,\ldots$, the corresponding Taylor monomial is expressed as:*

$$h_\beta(t,a) = \frac{(t-a)^{\overline{\beta}}}{\Gamma(\beta+1)}. \tag{1.160}$$

Now, let's find the Laplace transform of the fractional order Taylor monomial.

Theorem 1.21 ([178]). *For a non-integer real number β and $|1-s| < 1$, the Laplace transform of the β-th nabla Taylor monomial is given by:*

$$N_a\{h_\beta(\cdot,a)\}(s) = \frac{1}{s^{\beta+1}}. \tag{1.161}$$

The motivation behind the definition of convolution arises from the intention to represent fractional nabla sums and fractional nabla differences as convolutions involving arbitrary functions and Taylor monomials. Consequently, the properties that emerge from this definition align with those of the standard convolution.

Definition 1.45 ([178]). *The convolution of functions f and $g : \mathbb{N}_a \to \mathbb{R}$ and $t \in \mathbb{N}_{a+1}$, is defined as:*

$$(f * g)(t) := \int_t^a f(t - \rho(s) + a)g(s)\nabla^s \, ds. \tag{1.162}$$

Theorem 1.22 ([178]). *For functions $f, g : \mathbb{N}_a \to \mathbb{R}$, consider the following:*

$$N_a\{f * g\}(s) = N_a\{f\}(s).N_a\{g\}(s). \tag{1.163}$$

Now, we aim is to establish various properties of the Laplace transform.

Theorem 1.23 ([178]). *For a function $f : \mathbb{N}_a \to \mathbb{R}$, the following holds:*

$$N_{a+1}\{\nabla f\}(s) = sN_{a+1}\{f\}(s) - f(a + 1). \tag{1.164}$$

We can extend this result to an arbitrary number of nabla differences.

Theorem 1.24 ([178]). *For $f : \mathbb{N}_a \to \mathbb{R}$, we obtain*

$$N_{a+n}\{\nabla^n f\}(s) = s^n N_{a+n}\{f\}(s) - \sum_{k=1}^{n} s^{n-k}\nabla^{k-1} f(a + n). \tag{1.165}$$

Before delving into the Laplace transform of a νth order difference where $0 < \nu < 1$, we need to establish a useful lemma.

Lemme 1.20 ([178]). *For a function $f : \mathbb{N}_a \to \mathbb{R}$, the Shifting formula is expressed as:*

$$N_{a+1}\{f\}(s) = \frac{1}{1 - s}N_a\{f\}(s) - \frac{1}{1 - s}f(a + 1). \tag{1.166}$$

Theorem 1.25 ([178]). *For a function $f : \mathbb{N}_a \to \mathbb{R}$ and $\nu \in \mathbb{R}^+$, the Laplace transform of the ν-th order difference is given by:*

$$N_a\{\nabla_a^{-\nu} f\}(s) = \frac{1}{s^\beta}N_a\{f\}(s). \tag{1.167}$$

Proof.

$$\begin{aligned} N_a\{\Delta_a^{-\nu} f\}(s) &= N\{h_{\nu-1}(\cdot; a) * f\}(s), \\ &= N\{h_{\nu-1}(\cdot; a)\}(s)N_a\{f\}(s), \\ &= \frac{1}{s^\nu}N_a\{f\}(s). \end{aligned} \tag{1.168}$$

□

Having reached this point, we are prepared to present the comprehensive expression for the Laplace transform of a fractional-order difference of order ν, where $0 < \nu < 1$.

Theorem 1.26 ([178]). *For a function $f : \mathbb{N}_a \to \mathbb{R}$ and $0 < \nu < 1$, the Laplace transform of a νth order fractional nabla difference is given by*

$$N_{a+1}\{\nabla^\nu f\}(s) = s^\nu N_{a+1}\{f\}(s) - \frac{1 - s^\nu}{(1 - s)^\nu}f(a + 1). \tag{1.169}$$

Proof. We consider the following expression:

$$N_{a+1}\{\nabla_a^{\nu} f\}(s) = N_{a+1}\{\nabla \nabla_a^{1-\nu} f\}(s) = sN_{a+1}\{\nabla^{-(1-\nu)}\}(s) - \nabla_a^{-(1-\nu)} f(a+1). \quad (1.170)$$

The previous step is a consequence of Theorem 1.23. Additionally, we note that

$$\nabla_a^{-(1-\nu)} f(a+1) = f(a+1), \quad (1.171)$$

and, applying Lemma 25, we get

$$N_{a+1}\{\nabla_a^{\nu} f\}(s) = s\left(\frac{1}{1-s} N_a\{\nabla_a^{-(1-\nu)} f\}(s) - \frac{1}{1-s} f(a+1)\right) - f(a+1). \quad (1.172)$$

After additional simplification, the desired result is obtained. □

Theorem 1.27 ([178]). *Assuming $|p| < 1$, $\alpha > 0$, $\beta \in \mathbb{R}$, $|1-s| < 1$, and $|s^{\alpha}| > |p|$, the Laplace transform of the Mittag-Leffler Function is given by:*

$$N_a\{E_{p,\alpha,\beta}(\cdot, a)\}(s) = \frac{s^{\alpha-\beta-1}}{s^{\alpha} - p}. \quad (1.173)$$

1.6.3 Laplace Transforms for the h-Difference Operator

We define the discrete Laplace transform on $\mathbb{N}_{a,h}$ as follows:

Definition 1.46 ([196]). *Let $f(t)$ be a function defined on $\mathbb{N}_{a,h}$. The h-discrete Laplace transform of f is denoted by $N_{a,h}\{f(t)\}(s)$ and given by:*

$$\begin{aligned} N_{a,h}\{f(t)\}(s) \int_a^{\infty} {}_h e_{\ominus s}^{\rho}(t,a) f(t) \nabla_h t, \\ &= \int_a^{\infty} \frac{{}_h e_{\ominus s}^{\rho}(t,a)}{1-hs} f(t) \nabla_h t, \\ &= \int_a^{\infty} (1-hs)^{\frac{t-a-h}{h}} f(t) \nabla_h t, \\ &= h \sum_{t=\frac{a}{h}+1}^{\infty} (1-hs)^{t-\frac{a}{h}-1} f(ht). \end{aligned} \quad (1.174)$$

In the case where $a = 0$, we express

$$N_{0,h}\{f(t)\}(s) = N_h\{f(t)\}(s) = h\sum_{t=1}^{\infty} (1-hs)^{t-1} f(ht). \quad (1.175)$$

Definition 1.47 ([196]). *Let $s \in \mathbb{R}$, $0 < \alpha < 1$, and consider functions $f, g : \mathbb{N}_{a,h} \to \mathbb{R}$. The nabla h-discrete convolution of f and g is formally defined as*

$$(f * g)(t) = \sum_{k=\frac{a}{h}+1}^{\frac{t}{h}} g(t - \rho(kh) + a) f(kh). \quad (1.176)$$

Given the definition of nabla h-discrete convolution, we derive the following convolution theorem:

Theorem 1.28 ([196]). *Considering any $\alpha \in \mathbb{R}$ excluding $\{..., -2, -1, 0\}$, $s \in \mathbb{R}$, and functions f, g defined on $\mathbb{N}_{a,h}$, we obtain the following convolution theorem:*

$$N_{a,h}\{(f * g)(t)\}(s) = N_{a,h}\{f(t)\}(s) \cdot N_{a,h}\{g(t)\}(s). \tag{1.177}$$

Lemme 1.21 ([196]). *Assuming f is defined on $\mathbb{N}_{a,h}$, we have:*

$$N_{a,h}\{\nabla_h f(t)\}(s) = sN_{a,h}\{f(t)\}(s) - f(a). \tag{1.178}$$

Lemme 1.22 ([196]). *Consider any $\nu \in \mathbb{R} \setminus \{..., -2, -1, 0\}$, and assume $|1 - hs| < 1$. Then,*

$$N_h\{t_h^{\overline{\nu-1}}\}(s) = \frac{\Gamma(\nu)}{s^\nu}. \tag{1.179}$$

Indeed,

$$N_{a,h}\{(t-a)_h^{\overline{\beta-1}}\}(s) = \frac{\Gamma(\beta)}{s^\beta}. \tag{1.180}$$

Lemme 1.23 ([196]). *Considering complex numbers α, β, κ with $Re(\beta) > 0$, and s in the complex plane with $Re(s) > 0$ and $|\kappa s - \alpha| < 1$, the following expression holds*

$$N_h\{{}_hE_{\overline{\alpha,\beta}}(\kappa, t)\}(s) = s^{-\beta}[1 - \kappa s^{-\alpha}]^{-1}. \tag{1.181}$$

Certainly,

$$N_{a,h}\{{}_hE_{\overline{\alpha,\beta}}(\kappa, t-a)\}(s) = s^{-\beta}[1 - \kappa s^{-\alpha}]^{-1}. \tag{1.182}$$

Proof. By utilizing the h-Laplace transform and applying Lemma 1.22, we observe that

$$N_h\{{}_hE_{\overline{\alpha,\beta}}(\kappa, t)\}(s) = s^{-\beta}\sum_{k=0}^{\infty}\left(\frac{\kappa}{s^\alpha}\right)^k, \tag{1.183}$$

and thus, the proof is concluded. □

Lemme 1.24 ([196]). *For any positive ν, we get*

$$N_{a,h}\{({}_a\Delta_h^{-\nu} f)(t)\}(s) = s^{-\nu}N_{a,h}\{f(t)\}(s). \tag{1.184}$$

Proof. With the assistance of Lemma 1.22, we obtain

$$\begin{aligned} N_{a,h}\{({}_a\Delta_h^{-\nu} f)(t)\}(s) &= N_{a,h}\left\{\frac{1}{\Gamma(\nu)}f(t) * (t-a)_h^{\overline{\nu-1}}\right\}(s), \\ &= \frac{1}{\Gamma(\nu)}N_{a,h}\{f(t)\}(s)\frac{\Gamma(\nu)}{s^\nu} = s^{-\nu}N_{a,h}\{f(t)\}(s). \end{aligned} \tag{1.185}$$

□

Lemme 1.25 ([196]). *For the function $f(t)$ defined on $\mathbb{N}_{a,h}$ with $n - 1 < \nu \leq n$, the expression is given by*

$$N_{a,h}\{{}_a^C\nabla_h^\nu f(t)\}(s) = s^\nu N_{a,h}\{f(t)\}(s) - \sum_{k=0}^{n-1} s^{(\nu-1)-k}\nabla_h^k\{f(a)\}. \tag{1.186}$$

For the positive integer n, the expression becomes

$$N_{a,h}\{{}_a\nabla_h^n f(t)\}(s) = s^n N_{a,h}\{f(t)\}(s) - \sum_{k=0}^{n-1} s^{n-1-k}\nabla_h^k\{f(a)\}. \tag{1.187}$$

1.7 Z-Transform Method

In this section, we aim to explore the Z-transform of the presented fractional h-difference summation and operators. The subsequent definition outlines the Z-transform of a discrete sequence drawn from the comprehensive studies found in reference [207].

Definition 1.48 ([207]). *The Z-transform of a sequence $x(n)$, where $x(n)$ is zero for negative integers (i.e., $x(n) = 0$ for $n = -1, -2, \ldots$), is given by:*

$$Z(x(n)) = \sum_{j=0}^{\infty} x(n) z^{-n}, \quad z \in \mathbb{Z}. \tag{1.188}$$

Assuming that

$$R = \lim_{j\to\infty} \left| \frac{x(j+1)}{x(j)} \right|. \tag{1.189}$$

The infinite series (1.188) converges when

$$\lim_{j\to\infty} \left| \frac{x(j+1)z^{-j-1}}{x(j)z^{-j}} \right| < 1, \tag{1.190}$$

and diverges when

$$\lim_{j\to\infty} \left| \frac{x(j+1)z^{-j-1}}{x(j)z^{-j}} \right| > 1. \tag{1.191}$$

Therefore, the series (1.188) converges for $|z| > R$ and diverges for $|z| < R$.

1. **The Z-Transform for the Fractional Summation**
   Now, let's compute the Z-transform of the fractional difference summation. We consider binomial functions defined on $\mathbb{Z}$ and parameterized by $\nu \in \mathbb{R}$. These binomial functions, denoted as $\phi_\nu(n)$, are given by $\binom{n+\nu-1}{n}$ for $n \in \mathbb{N}_0$ and $\phi\nu(n) = 0$ for $n < 0$. We can employ these functions to calculate:

   $$\phi_\nu(n) = (-1)^n \binom{-\nu}{n}, \tag{1.192}$$

   and express the fractional difference operator as the convolution of ϕ_ν and $x(a+th)$, yielding:

   $${}_a\Delta_h^\nu x(t) = h^\nu (\phi_\nu * x(a+th))(n), \tag{1.193}$$

   where we have,

   $$(\phi_\nu * x(a+nh))(n) = \sum_{s=0}^{n} \binom{n-s+\nu-1}{n-s} \overline{x}(s). \tag{1.194}$$

   Based on this, we proceed to derive a general formula for the fractional sum, as documented in reference [207].

   Proposition 1.20 ([207]). *Consider $t = a + \nu h + nh \in (h\mathbb{Z})^{a+\nu h}$. Let $y(n) = {}_a\Delta_h^\nu x(t)$ and $\overline{x}(n) = x(a+nh)$. Then,*

   $$Z[y](z) = \left(\frac{hz}{z-1} \right)^\nu Z[\overline{x}](z). \tag{1.195}$$

2. **The Z-Transform for the Fractional Riemann Difference**
We also devise a set of functions essential for solving systems involving the Riemann-Liouville-type operator. Let's define the function family $\phi_{k,\nu} : \mathbb{Z} \to \mathbb{R}$, where $k \in \mathbb{N}_0$ and $\nu \in (0, 1]$. These functions are characterized by the following values:

$$\phi_{k,\nu} = \begin{cases} \binom{n-k+k\nu+\nu-1}{n-k} & \text{for } n \in \mathbb{N}_k, \\ 0 & \text{for } n < k. \end{cases} \tag{1.196}$$

Proposition 1.21 ([207]). *Consider $\phi_{k,\nu}$ as the function defined by (1.196). Then,*

$$Z[\phi_{k,\nu}](z) = \frac{1}{z^k}\left(\frac{z}{z--1}\right)^{k\nu+\nu}, \quad \text{for } |z| > 1. \tag{1.197}$$

Proposition 1.22 ([207]). *Let a be a real number and ν lie in the interval $(0, 1]$. Define $y(n) = {}_{,a}^{RL}\Delta_h^\nu x(t)$, where t belongs to $(h\mathbb{N})^{a+(1-\nu)h}$ and is expressed as $t = a + (1-\nu)h + nh$.*

$$Z[y](z) = z\left(\frac{hz}{z-1}\right)^{-\nu} Z[x(a+nh)](z) - zh^{-\nu}x(a), \tag{1.198}$$

3. **The Z-Transform for the Fractional Caputo Difference**
Initially, let's examine the Caputo-type h-difference operator ${}_a^C\Delta_h^\nu$ as presented in (1.124). By utilizing the binomial function ϕ defined in (1.192), we express the Caputo-type difference as follows:

$${}_a^C\Delta_h^\nu x(t) = h^{-\nu}(\phi_{1-\nu} * \Delta x(a+nh))(n), \tag{1.199}$$

where $t = a + (1-\nu)h + nh$.

Proposition 1.23 ([207]). *Consider a in $\mathbb{R}$ and ν in $(0, 1]$. Define $y(n) = {}_a^C\Delta_h^\nu x(t)$, where $t \in (h\mathbb{N})^{a+(1-\nu)h}$ and is given by $t = a + (1-\nu)h + nh$. Then,*

$$Z[y](z) = h^{-\nu}\left(\frac{hz}{z-1}\right)^{1-\nu}((z-1)Z[x(a+nh)](z) - zx(a)), \tag{1.200}$$

4. **Z-Transform Analysis for the Fractional Grünwald-Letnikov Difference**
Now, we turn our attention to the Grunwald-Letnikov-type fractional h-difference operator.

Proposition 1.24 ([207]). *Consider a in $\mathbb{R}$ and ν in $(0, 1]$. Define $y(n) = \Delta_h^\nu(t)$, where $t \in (h\mathbb{N})^a$ and is given by $t = a + nh, n \in \mathbb{N}_0$. Then,*

$$Z[y](z) = z\left(\frac{hz}{z-1}\right)^{-\nu} Z[x(a+nh)](z), \tag{1.201}$$

1.8 Discrete Variable-Order Calculus

In 1993, Samko and Ross made significant strides by exploring integrals and derivatives where the order varies, laying the groundwork for variable-order fractional calculus [208, 209, 210]. Subsequently, a multitude of scholarly and have contributed to advancing the theory of variable-order fractional calculus, spanning various mathematical and applied domains [211, 212, 213, 214, 215, 216]. In this section, we embark on an exploration of novel fractional operators characterized by variable order, particularly focusing on isolated time scales. These operators exhibit a unique blend of singular and Mittag–Leffler kernels, offering rich insights into dynamic systems with nuanced temporal dependencies [217].
To commence, let's elucidate the concept of nabla fractional sums characterized by variable orders.

Definition 1.49. *Let $f : \mathbb{N}_a \to \mathbb{R}$ be a function where $0 < \nu(t) \leq 1$ for all $t \in \mathbb{N}_a$. We define the left nabla fractional sum of order $\nu(t)$ as:*

$$\nabla_a^{-\nu(t)} f(t) = \frac{1}{\Gamma(\nu(t))} \sum_{s=a+1}^{t} (t - \rho(s))^{\overline{\nu(t)-1}} f(s), \quad t \in \mathbb{N}_{a+1}, \tag{1.202}$$

In accordance with the reference [218], we proceed to introduce a discrete adaptation of the left generalized nabla fractional variable-order difference operators.

Definition 1.50 ([217])**.**

$${}^{C}\nabla_a^{\nu(t)} f(t) = \frac{1}{\Gamma(1-\nu(t))} \sum_{s=a+1}^{t} (t - \rho(s))^{-\nu(t)} \nabla f(s), \quad t \in \mathbb{N}_{a+1}. \tag{1.203}$$

Definition 1.51 ([218])**.** *For any function $\phi : \mathbb{N}_a \to \mathbb{R}$, where $0 < \nu(t) < \frac{1}{2}$ for all $t \in \mathbb{N}_a$, the discrete left generalized fractional integral operator is defined as follows:*

$$E_{\overline{\nu(t),1},\frac{-\nu(t)}{1-\nu(t)}} \phi(t) = \frac{B(\nu(t))}{1-\nu(t)} \sum_{s=a+1}^{t} E_{\nu(t)} \left(\frac{-\nu(t)}{1-\nu(t)}, t - \rho(s) \right) \phi(s), \quad t \in \mathbb{N}_{a+1}. \tag{1.204}$$

Now, let's introduce the fractional sum and difference of variable order based on the framework proposed by Atangana–Baleanu [219], commonly referred to as the AB operators.

Definition 1.52 ([219])**.** *Consider $0 < \nu(t) \leq 1$ for all $t \in \mathbb{N}a$. Now, let's define the left AB nabla fractional sum of order $\nu(t)$ for a function $f : \mathbb{N}_a \to \mathbb{R}$ as follows:*

$$\begin{aligned} {}_a^{AB}\nabla^{-\nu(t)} f(t) &= \frac{1-\nu(t)}{B(\nu(t))} f(t) + \frac{\nu(t)}{B(\nu(t))\Gamma(\nu(t))} \sum_{s=a+1}^{t} (t - \rho(s))^{\overline{\nu(t)-1}} f(s), \\ &= \frac{1-\nu(t)}{B(\nu(t))} f(t) + \frac{\nu(t)}{B(\nu(t))} \nabla^{-\nu(t)} f(t), \quad t \in \mathbb{N}_{a+1}. \end{aligned} \tag{1.205}$$

Remarque 1.7. *It's important to note that in Definitions 7 and 8, if $\nu(t) = 0$, we retrieve the initial function. Conversely, when $\nu(t) = 1$, the result corresponds to the standard summation.*

Definition 1.53 ([219]). *For any $t \in \mathbb{N}_a$, where $0 < \nu(t) < \frac{1}{2}$, and a function $f : \mathbb{N}_a \to \mathbb{R}$, the left Riemann–Liouville AB nabla fractional difference of order $\nu(t)$ is given by:*

$$ {}^{ABR}_{a}\nabla^{\nu(t)} f(t) = \nabla E_{\overline{\nu(t),1},\frac{-\nu(t)}{1-\nu(t)}} f(t), \quad t \in \mathbb{N}_{a+1}. \tag{1.206} $$

Definition 1.54 ([219]). *For every $t \in \mathbb{N}a$, where $0 < \nu(t) < \frac{1}{2}$, and for a function $f : \mathbb{N}_a \to \mathbb{R}$, the left Caputo AB nabla fractional difference with order $\nu(t)$ is given by:*

$$ {}^{ABC}_{a}\nabla^{\nu(t)} f(t) = E_{\overline{\nu(t),1},\frac{-\nu(t)}{1-\nu(t)}} \nabla f(t), \quad t \in \mathbb{N}_{a+1}. \tag{1.207} $$

1.9 Conclusion

This chapter has highlighted the significant advancements and applications of discrete fractional calculus, emphasizing its critical role in modeling and controlling complex systems characterized by memory and hereditary properties. The discussion has showcased the broad utility of fractional-order differences and sums across various scientific disciplines through the implementation of delta and nabla operators.

The comprehensive review of monotonicity properties associated with these discrete fractional operators and their implications in various contexts underscores the depth and breadth of this research area. The exploration of monotonicity within the framework of discrete fractional operators has revealed relationships that enhance our understanding of dynamic behaviors in complex systems. Notably, the chapter has axplored the delta-fractional difference variant of the mean-value theorem.

Furthermore, this chapter has provided an in-depth examination of the discrete generalized Gronwall inequality, which serves as a fundamental tool for stability analysis in discrete fractional-order systems. The analysis of positivity and Mittag–Leffler stabilities has enriched our repertoire of methodologies, allowing for a more nuanced and comprehensive approach to stability assessment. These advancements push the boundaries of research, offering robust tools for tackling the inherent complexities of fractional-order systems.

By introducing fundamental concepts and transformation methods pertinent to discrete fractional calculus, this chapter lays a solid foundation for further investigations into fractional difference equations. The detailed exposition of both singular and non-singular kernels, and their respective transformation methods, equips researchers with the necessary tools to explore a wide range of applications and phenomena in various fields.

The chapter also serves as a comprehensive introduction to the evolving field of discrete fractional calculus, offering valuable insights and methodologies that propel the state-of-the-art in this critical area of research. Researchers and practitioners are encouraged to build upon this foundation, exploring new frontiers and applications of fractional calculus in diverse scientific and engineering disciplines.

Chapter 2

Stability of Discrete Fractional-Order Systems

2.1 Introduction

The pursuit of system stability is a fundamental cornerstone in the complex domain of dynamic system analysis and strategic design. In recent times, there has been a growing emphasis on discrete fractional-order systems, leading to the development of a sophisticated set of tools designed specifically for the comprehensive assessment of their stability. This toolkit includes fundamental methodologies such as the discrete generalized Gronwall inequality [220, 221, 222]. Moreover, explorations into the positivity of discrete fractional-order systems [223, 224, 225] and investigations on Mittag–Leffler stabilities [226, 227, 229] have collectively enriched the repertoire of tools available for stability analysis, pushing the boundaries of research in this dynamic domain.

An important advancement in this area has been the identification of positive definite quadratic forms as ideal candidates for Lyapunov functions in discrete fractional-order systems [230, 231, 232]. This revelation has sparked the widespread adoption of the second Lyapunov method, particularly in the context of commensurate discrete fractional-order systems. Yet, it's important to highlight the inherent constraints of this approach when dealing with the complex obstacles presented by incommensurate discrete fractional-order systems [233, 234, 235].

In the following chapters, we begin a comprehensive investigation into stability, with a deliberate focus on a specific class of discrete fractional-order systems that traverse both commensurate and incommensurate scenarios. The dynamical equations governing these systems exhibit a dual nature, featuring a combination of a linear component and a nonlinear term. This deliberate choice not only ensures that our analysis is methodologically robust but also broadly applicable, providing a nuanced understanding of stability in discrete fractional-order systems across diverse and real-world scenarios.

This chapter stands as a significant overview to the evolving landscape of stability analysis. By offering valuable insights and methodologies, our aim is to propel the state-of-the-art in this critical field, providing a solid foundation for further advancements in the dynamic study of system stability.

2.2 Notion of Stability

Let's examine the set of vector difference equations:

$$\begin{cases} x(t+1) = g(t, x(t)), \\ x(a) = x_a. \end{cases} \tag{2.1}$$

where $x(t) \in \mathbb{R}^n$, $g : \mathbb{Z}^+ \times \mathbb{R}^n \to \mathbb{R}^n$. We assume that $g(t, x)$ is continuous.

Definition 2.1 ([206]). *A point x^* in $\mathbb{R}^n$ is referred to as an equilibrium point of (2.1) if $g(t, x^*) = x^*$ for all $t \geq a$.*

Remarque 2.1. *Frequently, x^* is conventionally set to the origin 0 and denoted as the zero solution. This choice is substantiated by considering $z(t) = x(t) - x^*$, which transforms (2.1) into:*

$$z(t+1) = g(t, z(t) + x^*) - x^* = g(t, z(t)). \tag{2.2}$$

Consider the scenario where $z = 0$ aligns with $x = x^*$. We often find it more pragmatic to avoid this change of coordinates, and thus, we do not make the assumption that $x^* = 0$ unless it offers a more favorable approach.

Now, let's explore the various stability notions linked to the equilibrium point x^* of the system given by (2.1).

Definition 2.2 ([206]). *The equilibrium point x^* for the system described by (2.1) is characterized as:*

- *The equilibrium point x^* in (2.1) is classified as **stable** if, given any $\epsilon > 0$ and $a \geq 0$, there exists $\delta = \delta(\epsilon, a)$ such that $||x_0 - x^*|| < \delta$ implies $||x(t, a, x_a) - x^*|| < \epsilon$ for all $t \geq a$. If δ can be chosen without dependence on a, it is termed **uniformly stable**; otherwise, the equilibrium point is categorized as **unstable**.*
- *The equilibrium point x^* in (2.1) is designated as **asymptotically stable** if it is both stable and attracting. If these properties are uniform across different time instances, it is termed **uniformly asymptotically stable**.*
- *The equilibrium point x^* in (2.1) is considered **exponentially stable** if there exist constants $\delta > 0$, $M > 0$, and $\mu \in (0, 1)$ such that, for any initial condition x_a satisfying $||x_a - x^*|| < \delta$, the system follows the inequality $||x(t, a, x_a) - x^*|| \leq M||x_a - x^*||\mu^{t-a}$.*

2.3 Stability of Integer-Order Difference System

2.3.1 Stability of Linear Difference System

We explore the discrete system defined by integer-order differences:

$$\begin{cases} \Delta x(t) = Ax(t), \quad t \in \mathbb{N}, \\ x(0) = x_0, \quad x_0 \in \mathbb{R}^n, \end{cases} \tag{2.3}$$

where $x(t) = (x_1(t), x_2(t), \cdots, x_n(t))^T \in \mathbb{R}^n$ and A is an $n \times n$ constant matrix. The equilibrium point of (5.47) is located at the origin ($x = 0$). The solution of the linear system (5.47), initiated from x_0, can be expressed as follows:

$$x(t) = (A + I_n)^n x_0, \quad \forall t \in \mathbb{N}, \tag{2.4}$$

in the context of (5.47), where I_n denotes the identity matrix, we can ascertain the stability of the linear system using the following outcome.

Theorem 2.1 ([206]). *Should all the eigenvalues μ_i of A adhere to the condition $|\mu_i + 1| < 1$, for $1 \leq i \leq n$, the trivial solution of (5.47) attains global asymptotic stability over $\mathbb{N}$ Moreover, in the presence of an eigenvalue μ belonging to A with $|\mu + 1| > 1$, the trivial solution of (5.47) exhibits instability over $\mathbb{N}$.*

Example 2.1. *Let's examine the linear difference system with integer order presented below:*

$$\Delta x(t) = Ax(t), \quad t \in \mathbb{N}, \tag{2.5}$$

where

$$A = \begin{pmatrix} 0 & -5 \\ \frac{1}{4} & -2 \end{pmatrix}. \tag{2.6}$$

The matrix A possesses eigenvalues $\mu_1 = -1 + \frac{i}{2}$ and $\mu_2 = -1 - \frac{i}{2}$. Since

$$|\mu_1 + 1| = |\mu_2 + 1| = \frac{1}{2} < 1. \tag{2.7}$$

Consequently, based on Theorem 2.1, the solution of the system achieves global asymptotic stability on $\mathbb{N}$.

2.3.2 Stability of Nonlinear Difference System

Examining the following non-linear system:

$$\begin{cases} \Delta x(t) = g(x(t)), \quad t \in \mathbb{N}, \\ x(0) = x_0, \quad y_0 \in \mathbb{R}^n, \end{cases} \tag{2.8}$$

where $g : \mathbb{R}^n \to \mathbb{R}^n$ is a continuously differentiable function with $g(0) = 0$. This implies that $x = 0$ serves as an equilibrium point for the system outlined by (2.8).

1. **Linearisation method**
   A fundamental technique for analyzing nonlinear discrete dynamical systems involves linearizing the system around a trivial solution. The linearization of the system described by (2.8) is achieved through the Jacobian matrix of the function g, as demonstrated in the following theorem.

   Theorem 2.2 ([206]). *Let J represent the Jacobian matrix of g at 0. If all eigenvalues μ_i, where $1 \leq i \leq n$, of J satisfy $|\mu_i + 1| < 1$, then the trivial solution of (2.8) is asymptotically stable on $\mathbb{N}$. Additionally, if there exists an eigenvalue μ of J with $|\mu + 1| > 1$, then the trivial solution of (2.8) is unstable on $\mathbb{N}$.*

Example 2.2. *Let's examine the given non-linear difference system:*

$$\begin{cases} \Delta x_1(t) = g_1(x(t)), \\ \Delta x_2(t) = g_2(x(t)). \end{cases} \tag{2.9}$$

Let

$$\begin{cases} g_1(x(t)) = \dfrac{2x_2(t)}{(1+x_1^2(t))} - x_1(t), \\ g_2(x(t)) = \dfrac{x_1(t)}{(1+x_2^2(t))} - x_2(t). \end{cases} \tag{2.10}$$

The Jacobian matrix is expressed as follows:

$$J = \begin{pmatrix} \dfrac{\partial g_1(0)}{\partial x_1} & \dfrac{\partial g_1(0)}{\partial x_2} \\ \dfrac{\partial g_2(0)}{\partial x_1} & \dfrac{\partial g_2(0)}{\partial x_2} \end{pmatrix} = \begin{pmatrix} 0 & 2 \\ 1 & 0 \end{pmatrix}. \tag{2.11}$$

Thus, we find that the eigenvalues of J are $\mu_1 = -\sqrt{2}$ and $\mu_2 = \sqrt{2}$, and $|\mu_1 + 1| = 1 - \sqrt{2} < 1$.
As a result of Theorem 2.2, the solution to (2.9) exhibits instability over the set $\mathbb{N}$.

2. **Lyapunov direct method**
The Lyapunov direct method stands as a potent tool in stability theory, providing a means to investigate the stability of solutions without the need to explicitly determine these solutions. This method plays a crucial role in analyzing the behavior and stability of dynamic systems, offering valuable insights into the overall system dynamics. By leveraging Lyapunov functions, researchers and engineers can assess the stability properties of various systems, contributing to a deeper understanding of their behavior and aiding in the design of stable and reliable systems. We now follow [206] and illustrate the method with Theorem 2.3:

Theorem 2.3 ([206]). *If there exists a function $V : \mathbb{R}^n \to \mathbb{R}_+$, this function is continuous and satisfies the following properties:*

$$\begin{aligned} &V(0) = 0 \text{ and } V(x(t)) > 0, \ \forall x(t) \neq 0, \\ &\Delta V(x(t)) \leq 0, \ \forall t \in \mathbb{N}. \end{aligned} \tag{2.12}$$

Then, the trivial solution of (2.8) is stable. Additionally if

$$\Delta V(x(t)) =< 0, \ \forall t \in \mathbb{N}. \tag{2.13}$$

Additionally, the trivial solution of (2.8) exhibits asymptotic stability.

Example 2.3. *We examine the nonlinear discrete-time system:*

$$\begin{cases} \Delta x_1(t) = g_1(x(t)) \dfrac{2x_2(t)}{(1+x_1^2(t))} - x_1(t), \\ \Delta x_2(t) = g_2(x(t)) \dfrac{x_1(t)}{(1+x_2^2(t))} - x_2(t). \end{cases} \tag{2.14}$$

where $g(x(t)) = (g_1(x(t)), g_2(x(t)))^T = \left(\dfrac{x_2(t)}{1+x_1^2(t)} - x_1(t), \dfrac{x_1(t)}{1+x_1^2(t)} - x_2(t) \right)^T$.
Defining the Lyapunov function as:

$$V(x(t)) = x_1^2(t) + x_2^2(t). \tag{2.15}$$

Certainly, we observe that

$$\Delta V(x(t)) = V(x(t)) \left(\frac{1}{(1 + x_1^2(t))^2} - 1 \right) < 0. \tag{2.16}$$

Thus, according to Theorem 2.3, the trivial solution of (2.14) is asymptotically stable.

2.4 Stability of Caputo Fractional-Order Difference Systems

This section aims to investigate the stability of linear fractional-order discrete systems using the Caputo difference operator. Both commensurate and incommensurate fractional-orders will be considered in the analysis.
The foundational definitions and lemmas in this section are all adapted from the authoritative sources listed in [228], [229] and [233, 234], reflecting the critical insights from these key works.

2.4.1 Stability of Linear Caputo Fractional-Order Discrete Systems

1. **Commensurate Caputo linear fractional discrete system**
   Let's examine the general form of a linear fractional difference problem using the Caputo operator.

$$\begin{cases} {}^{C}\Delta_a^{\alpha} x(t) = Ax(t + \alpha - 1), \\ x(0) = x_0. \end{cases} \tag{2.17}$$

In this context, let matrix $A \in \mathbb{R}^{n.n}$ and ${}^{C}\Delta_a^{\alpha}$ represent the Caputo fractional-order difference operator of order α, where $0 < \alpha < 1$. Subsequently, the following result can be established:

Theorem 2.4 ([229]). *Consider $\alpha \in (0, 1]$ and matrix $A \in \mathbb{R}^{n.n}$. The system described by (2.17) is asymptotically stable if and only if the isolated zeros on the non-negative real axis satisfy:*

$$det(1 - w^{-1}(1 - w^{-1})^{-\alpha} A), \tag{2.18}$$

reside within the unit circle.

Proof. First, let's derive the discrete solution of the system (2.17). Utilizing the Taylor series expansion, we obtain:

$$x(t) = \sum_{p=0}^{m-1} \frac{(t - a - \alpha + m)^p}{p!} a + \frac{1}{\gamma(\alpha)} \sum_{s=a}^{t-\alpha} (t - s - 1)^{\alpha - 1} Ax(s + \alpha - m)). \tag{2.19}$$

For $t = a + N + 1$, where $N = 0, 1, 2, \ldots$, we can simplify equation (2.19) to:

$$x_N = x_{-1} + \sum_{s=0}^{N} B(N - s) x_{s-1}, \tag{2.20}$$

here the kernel function $B(N-s)$ is expressed as:

$$B(N) = \frac{A}{(N)!}\prod_{j=1}^{N}(\alpha+j-1) \quad \text{and} \quad x_N = x(a+N+\alpha), \quad k=-1,0,1,.... \tag{2.21}$$

Observe that (2.20) takes the form of a non-homogeneous Volterra difference equation with convolution. This equation will be instrumental in our subsequent analysis. Focusing on the scalar case where $A=\mu$, we make the assumption, without loss of generality, that $x_{-1}=1$.

- If $\mu=0$, then $x_N = y_{-1}$ for $N=1,2,....$ and analyze the sign of μ.
- If $\mu>0$. Since $x_N>1$ for $N\leq 0$,

$$x_N > 1+\mu\sum_{s=0}^{N}\frac{1}{(N-s)!}\left(\prod_{j=1}^{N-s}(\alpha+j-1)\right) = 1+\mu\sum_{s=0}^{N}\frac{1}{s!}\left(\prod_{j=1}^{s}(\alpha+j-1)\right). \tag{2.22}$$

But since

$$\frac{\dfrac{\prod_{j=1}^{s}(\alpha+j-1)}{s!}}{\dfrac{1}{(\alpha+s)}} = \alpha\frac{\prod_{j=1}^{s}(\alpha+j)}{s!} > \alpha, \tag{2.23}$$

Hence, we can deduce

$$y_N > 1+\mu\sum_{s=0}^{N}\frac{\alpha}{(\alpha+s)}, \tag{2.24}$$

Thus, through a straightforward comparison, we observe that the solution x_N of (2.14) diverges to infinity.

- If $\mu<0$,
  Let $\tilde{x}(z) = Z(x_N)$ represent the unilateral Z-transform of the sequence x_N. Then,

$$\tilde{x}(z) = (1-z^{-1})^{-1} + \mu(1-z^{-1})^{-\alpha}(1+z^{-1}\tilde{x}(z)), \quad |z|>R\geq 1. \tag{2.25}$$

Expressing $\tilde{x}$ in terms of z produces:

$$\tilde{x}(z) = \frac{(1-z^{-1})^{-1}+\mu(1-z^{-1})^{-\alpha}}{1-\mu z^{-1}(1-z^{-1})^{-\alpha}} = \frac{\dfrac{z}{z-1}+\mu\left(\dfrac{z}{z-1}\right)^{\alpha}}{1-\mu\dfrac{1}{z}\left(\dfrac{z}{z-1}\right)^{\alpha}}. \tag{2.26}$$

This implies

$$x_N = \frac{1}{2\pi i}\int_A z^{N-1}\tilde{x}(z)dz,$$

In the context of complex analysis, A denotes any positively-oriented simple-closed contour within the analyticity region of $\tilde{x}$ that encloses all singular points of $\tilde{x}(z)$. To elaborate, we examine the specific contour $A\rho$, where the

inner circles have a radius of ρ, chosen sufficiently small to ensure that all isolated singularities of $\tilde{x}$ lie within $A\rho$.

As ρ tends to zero, the line integrals of $z^{N-1}\tilde{x}(z)$ over the inner circles approach zero.

$$\int_A z^{N-1}\tilde{x}(z)dz = \lim_{\rho\to 0}\int_{A_\rho} z^{N-1}\tilde{x}(z)dz. \tag{2.27}$$

However, invoking the Residue Theorem,

$$\tilde{x}_N = \frac{1}{2\pi i}\int_{A_\rho} z^{N-1}\tilde{x}(z)dz = \sum_i Res(z^{N-1}\tilde{x}(z), z_i) = \sum_i z_i^{N-1} Res(\tilde{x}(z), z_i), \tag{2.28}$$

The z_i's represent the isolated singularities of $\tilde{x}(z)$, precisely simple poles corresponding to the zeros of

$$Q(z) = 1 - \mu\frac{1}{z}\left(\frac{z}{z-1}\right)^\alpha. \tag{2.29}$$

To illustrate this, consider z_i as a root of $Q(z)$. The presence of the factor $(z - z_i)$ in $Q(z)$ signifies that the function $\tilde{x}(z)$ possesses a simple pole at $z = z_i$, and conversely.n

$$\mu\left(\frac{z_i}{z_i-1}\right)^\alpha = z_i, \tag{2.30}$$

hence

$$Q'(z_i) = \frac{1-\alpha-z_i}{z_i(1-z_i)} \neq 0, \tag{2.31}$$

as $Q(1-\alpha) \neq 0$ for $0 < \alpha < 1$. Additionally, in conjunction with $P(z) = \frac{z}{(z-1)} + \mu(\frac{z}{(z-a)})^\alpha$, and $P(z_i) = \frac{z_i}{z_i - 1} + z_i \neq 0$.

The "function" $\left(\frac{z}{z-1}\right)^\alpha = \frac{z^\alpha}{(z-1)^\alpha}$ is multi-valued. In light of the branch cut shown in Figure 2.1, consider the branch of function $f_\alpha(z)$ with a branch cut along the interval $(-\infty, 0]$. By traversing a small counterclockwise loop around the origin, the function acquires a phase factor of $e^{2\pi i\alpha}$. This behavior is consistent with the fractional power z^α on the branch cut, and it ensures the continuity of the function in the complex plane. The branch cut allows us to define a consistent behavior for the fractional power function, ensuring its analyticity and usefulness in the context of the Laplace transform.

With this branch cut, we ensure the continuous and well-defined behavior of $\left(\frac{z}{z-1}\right)^\alpha$ across the complex plane, and it aligns with the conventions used in the theory of fractional calculus. This consideration is crucial for the analytical treatment and manipulation of fractional-order systems.

Now, let's explore the properties of this branch cut and how it affects the behavior of the function.

$$z = |z|\, e^{i\theta} \quad \text{and} \quad z - 1 = |z-1|\, e^{i\phi}, \tag{2.32}$$

here

$$|z|\,, |z-1| > 0 \quad \text{and} \quad -\pi \leq \theta, \phi < \pi. \tag{2.33}$$

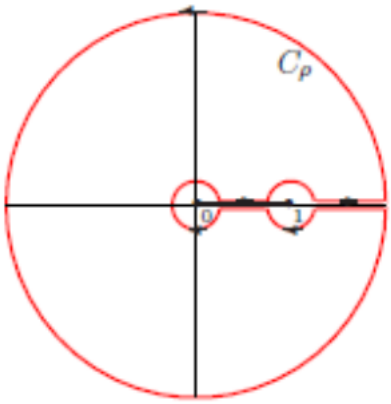

Figure 2.1: The contour A_ρ.

Which means,

$$Q(z) = 0 \qquad \Leftrightarrow \mu \frac{|z|^{\alpha-1}}{|z-1|^{\alpha}} e^{-i[(1-\alpha)\theta+\alpha\phi]} = 1 \Leftrightarrow (1-\alpha)\theta + \alpha\phi = -\pi$$
$$\text{and} \quad \mu \frac{|z|^{\alpha-1}}{|z-1|^{\alpha}} = -1. \tag{2.34}$$

Moreover, as $-\pi \leq \theta \leq \phi < \pi$, it follows that $\theta = \phi = -\pi$. Consequently, $|z-1| = |z| + 1$.

Revisiting the previous argument, there exist a finite number of poles inside A_ρ, and the residue of each is finite. Consequently, this leads to the desired result.

□

An alternative interpretation of Theorem 2.4 can be articulated as follows:

Theorem 2.5 ([229]). *The zero equilibrium point of the linear fractional-order discrete system (2.17) exhibits asymptotic stability if*

$$\mu_i \in \left\{ w \in \mathbb{C} : |w| < \left(\cos \frac{|arg(w) - \pi|}{2-\alpha} \right) \ \text{and} \ |arg(w)| > \frac{\alpha\pi}{2} \right\}, \tag{2.35}$$

where μ_i represents the eigenvalues of the matrix A.

Example 2.4. *Consider the linear commensurate fractional discrete system given by:*

$$\begin{cases} {}^{C}\Delta_0^{\alpha} x_1(t) = -\frac{1}{2} x_1(t+\alpha-1) + x_2(t+\alpha-1), \\ {}^{C}\Delta_0^{\alpha} x_2(t) = -\frac{1}{2} x_2(t+\alpha-1). \end{cases} \tag{2.36}$$

where $t \in \mathbb{N}_{a+1-\alpha}$ and the matrix A is defined as:

$$A = \begin{pmatrix} -\frac{1}{2} & 1 \\ 0 & -\frac{1}{2} \end{pmatrix}. \tag{2.37}$$

The matrix A has eigenvalues $\mu_1 = \mu_2 = -\frac{1}{2}$.

Thus, in accordance with Theorem 2.5, the zero equilibrium of the system (2.36) is asymptotically stable. The time evolution of the system states for the initial condition $x_0 = (1, -1)^T$ is depicted in Figure 2.2.

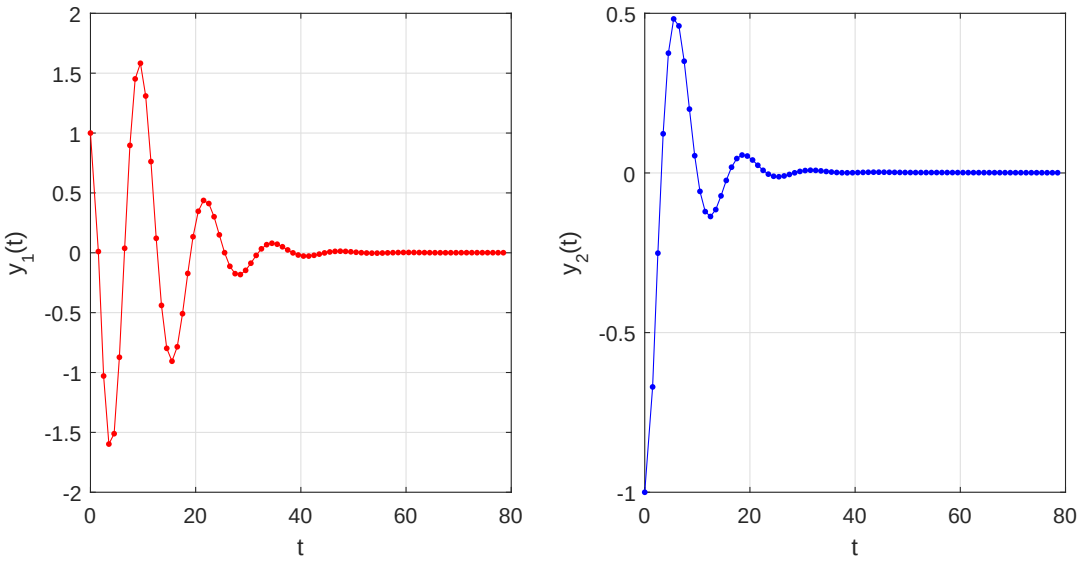

Figure 2.2: Asymptotic stability of states x_1 and x_2 for $\alpha = 0.6$.

2. **Incommensurate Caputo linear fractional discrete system**
Explore the unconventional fractional-order discrete system with a distinctive nonlinear character.

$$\begin{cases} {}^{C}\Delta_0^{\alpha_1} x_1(t) = c_{11}x_1(t+\alpha-1) + c_{12}x_2(t+\alpha-1) + ... + c_{1n}x_n(t+\alpha-1), \\ {}^{C}\Delta_0^{\alpha_2} x_2(t) = c_{21}x_1(t+\alpha-1) + c_{22}x_2(t+\alpha-1) + ... + c_{2n}x_n(t+\alpha-1), \\ ... \\ {}^{C}\Delta_0^{\alpha_n} x_n(t) = c_{n1}x_1(t+\alpha-1) + c_{n2}x_2(t+\alpha-1) + ... + c_{nn}x_n(t+\alpha-1). \end{cases} \tag{2.38}$$

Suppose $\mathbf{x}(t) = (\mathbf{x}_1(t), \ldots, \mathbf{x}_n(t)^T \in \mathbb{R}^n$. In light of this, the subsequent observation pertains to the stability assessment of linear fractional-order systems with incommensurate properties.

Theorem 2.6 ([233]). *If all the roots of the characteristic equation (2.39)*

$$det\left(diag\left(w\left(1-\frac{1}{w}\right)^{\alpha_1}, w\left(1-\frac{1}{w}\right)^{\alpha_2}, \ldots, w\left(1-\frac{1}{w}\right)^{\alpha_n}\right) - A\right) = 0, \tag{2.39}$$

reside within the unit circle, then the trivial solution of the system (2.38) associated with the initial condition $x(0) = x_0 \in \mathbb{R}^n$ is locally asymptotically stable, where J denotes the Jacobian matrix of g evaluated at 0.

Proof. When we substitute $s = t + \alpha_i - 1$ into system (2.38), it can be reformulated as follows:

$$({}^{C}\Delta_0^{\alpha_i} x_i)(s+1-\alpha) = \sum_{k=0}^{s} (-1)^{s-k+1} \binom{\alpha_i}{s-k+1} x(k) - (-1)^{s+1} \binom{\alpha_i - 1}{s+1} x(0) + x(s+1) \quad \forall i = 1, 2, \cdots, n. \tag{2.40}$$

Consequently,

$$x_i(s+1) = \sum_{k=0}^{s} (-1)^{s-k} \binom{\alpha_i}{s-k+1} x_i(k) + (-1)^{s+1} \binom{\alpha_i - 1}{s+1} x_i(0) + \sum_{j=1}^{n} c_{ij} x_j(s), k = 0, 1, \cdots. \tag{2.41}$$

Taking the Z-transform of (2.41) results in the following expression:

$$z\tilde{x}_i(z) - z x_i(0) = \left(z - z\left(1 - \frac{1}{z}\right)^{\alpha_i} \right) \tilde{x}_1(z) + \left(z\left(1 - \frac{1}{z}\right)^{\alpha_i - 1} - z \right) x_i(0) + \sum_{j=1}^{n} c_{ij} \tilde{x}_j(z), \tag{2.42}$$

Here, $\tilde{x}_i(z)$ represents the Z-transform of $x_i(s)$. Hence, we can express system (2.41) in the following manner:

$$M(z). \begin{pmatrix} \tilde{x}_1(z) \\ \tilde{x}_2(z) \\ \vdots \\ \tilde{x}_n(z) \end{pmatrix} = \begin{pmatrix} z\left(1 - \frac{1}{z}\right)^{\alpha_1 - 1} x_1(0) \\ z\left(1 - \frac{1}{z}\right)^{\alpha_2 - 1} x_2(0) \\ \vdots \\ z\left(1 - \frac{1}{z}\right)^{\alpha_n - 1} x_n(0) \end{pmatrix}, \tag{2.43}$$

in this context,

$$M(z) = \begin{pmatrix} z\left(1 - \frac{1}{z}\right)^{\alpha_1} - c_{11} & -c_{12} & \cdots & -c_{1n} \\ -c_{21} & z\left(1 - \frac{1}{z}\right)^{\alpha_2} - c_{22} & \cdots & -c_{2n} \\ \vdots & \vdots & \ddots & \vdots \\ -c_{n1} & -c_{n2} & \cdots & z\left(1 - \frac{1}{z}\right)^{\alpha_n} - c_{nn} \end{pmatrix}. \tag{2.44}$$

Employing the operation of multiplying both sides of (2.43) by $(z-1)$ yields:

$$M(z). \begin{pmatrix} (z-1)\tilde{x}_1(z) \\ (z-1)\tilde{x}_2(z) \\ \vdots \\ (z-1)\tilde{x}_n(z) \end{pmatrix} = \begin{pmatrix} z^2\left(1 - \frac{1}{z}\right)^{\alpha_1} x_1(0) \\ z^2\left(1 - \frac{1}{z}\right)^{\alpha_2} x_2(0) \\ \vdots \\ z^2\left(1 - \frac{1}{z}\right)^{\alpha_n} x_n(0) \end{pmatrix}. \tag{2.45}$$

It's worth noting that if all the roots of $\det M(z) = 0$ are confined within the unit disk, then system (3.7) is defined for z satisfying $|z| \geq R$, where $R \leq 1$ (where R represents the radius of convergence of $\tilde{x}(z)$). Essentially, within this bounded region, system (2.45) possesses a unique solution given by

$$((z-1)\tilde{x}1(z), (z-1)\tilde{x}2(z), \cdots, (z-1)\tilde{x}_n(z)).$$

Thus, we deduce:

$$\lim_{z\to 1}(z-1)\tilde{x}_i(z) = 0, \quad i = 1, 2, \cdots, n. \tag{2.46}$$

Given the assumption outlined in the initial part of this theorem, and also relying on the Final-Value Theorem linked with the Z-transform, we derive:

$$\lim_{k\to\infty} x_i(k) = \lim_{z\to 1}(z-1)\tilde{x}_i(z) = 0, \quad i = 1, 2, \cdots, n. \tag{2.47}$$

Alternatively, reflecting on the second part of this theorem suggests that the convergence radius R of the series:

$$\sum_{k=0}^{\infty} x(k)z^{-k} = \tilde{x}(z), \tag{2.48}$$

exceeds 1 (i.e., $R > 1$). Consequently, there exists an index i_0, where $1 \leq i_0 \leq n$, such that the convergence radius R_{i_0} of the series:

$$\sum_{k=0}^{\infty} x_{i_0}(k)z^{-k} = \tilde{x}_{i_0}(z), \tag{2.49}$$

is also greater than 1 (i.e., $R_{i_0} > 1$). Consequently, through the utilization of the Cauchy-Hadamard Theorem, we deduce:

$$R_{i_0} = \lim_{k\to\infty} \sup \sqrt[k]{|x_{i_0}(k)|} > 1. \tag{2.50}$$

As a result, $\lim_{k\to\infty} \sup |x_{i_0}(k)| = \infty$. This inference suggests that x will never be bounded, indicating that (2.45) is not stable. □

The subsequent theorem is a direct consequence of Theorem 2.6.

Theorem 2.7 ([233]). *Suppose $0 < \alpha_i \leq 1$, for $i = 1, ..., n$, and let M be the least common multiple of the denominators u_i of α_i's, where $\alpha_i = \frac{v_i}{u_i}$ with $(u_i, v_i) = 1$, and $v_i, u_i \in \mathbb{Z}_+$ for $i = 1, 2, ..., n$. If every root of the subsequent equation*

$$det(diag(\mu^{M\alpha_1}, ..., \mu^{M\alpha_n}) - (1-\mu^M) - A) = 0, \tag{2.51}$$

are contained within a set $\mathbb{C}/K^\sigma$, then the trivial solution of system (2.38) with $x(0) = x_0$ is asymptotically stable, where $A = (c_{ij}); 1 \leq i, j \leq n \in \mathbb{M}_n(\mathbb{R})$, $\sigma = \frac{1}{M}$, and

$$K^\sigma = \left\{ w \in \mathbb{C} : |w| \leq \left(2\cos\frac{|arg(w)|}{\sigma}\right)^\sigma \text{ and } |arg(w)| \leq \frac{\sigma\pi}{2} \right\}. \tag{2.52}$$

Example 2.5. *Explore the ensuing linear fractional discrete system with incommensurate characteristics:*

$$\begin{cases} {}^{C}\Delta_{0}^{\frac{1}{3}} x_1(t) = -x_1(t+\frac{1}{3}-1), \\ {}^{C}\Delta_{0}^{\frac{2}{3}} x_2(t) = 2.2x_1(t+\frac{2}{3}-1) - x_2(t+\frac{2}{3}-1), \\ {}^{C}\Delta_{0}^{\frac{1}{3}} x_n(t) = -x_3(t+\frac{1}{3}-1). \end{cases} \tag{2.53}$$

Observe that $M = 3$. *Subsequently,*

$$det\left(\begin{pmatrix} \mu & 0 & 0 \\ 0 & \mu^2 & 0 \\ 0 & 0 & \mu \end{pmatrix} - (1-\mu^3)\begin{pmatrix} -1 & 0 & 0 \\ 2.2 & -1 & 0 \\ 0 & 0 & -1 \end{pmatrix}\right) = 0. \tag{2.54}$$

For this purpose, we have:

$$-\mu^9 + \mu^8 + 2\mu^7 + \mu^6 - 3\mu^5 - 3\mu^4 - 3\mu^2 + \mu + 1 = 0. \tag{2.55}$$

Equation (2.55) yields the following solutions:

$$\begin{cases} \mu_1 = 1.6527 + 0.3232i, \\ \mu_2 = 1.6527 - 0.3232i, \\ \mu_3 = -0.8150 + 1.0140i, \\ \mu_4 = -0.8150 - 1.0140i, \\ \mu_5 = -1.1413 + 0.0000i, \\ \mu_6 = 0.1422 + 0.8386i, \\ \mu_7 = 0.1422 - 0.8386i, \\ \mu_8 = 0.6012 + 0.0000i, \\ \mu_9 = -0.4197 + 0.0000i. \end{cases} \tag{2.56}$$

Hence, in accordance with Theorem 2.6, the zero equilibrium point of the incommensurate system (2.53) achieves asymptotic stability. The numerical solution of system (2.53) with the initial condition $(0.1, -0.5, 0.3)^T$ *is illustrated in Figure 2.3.*

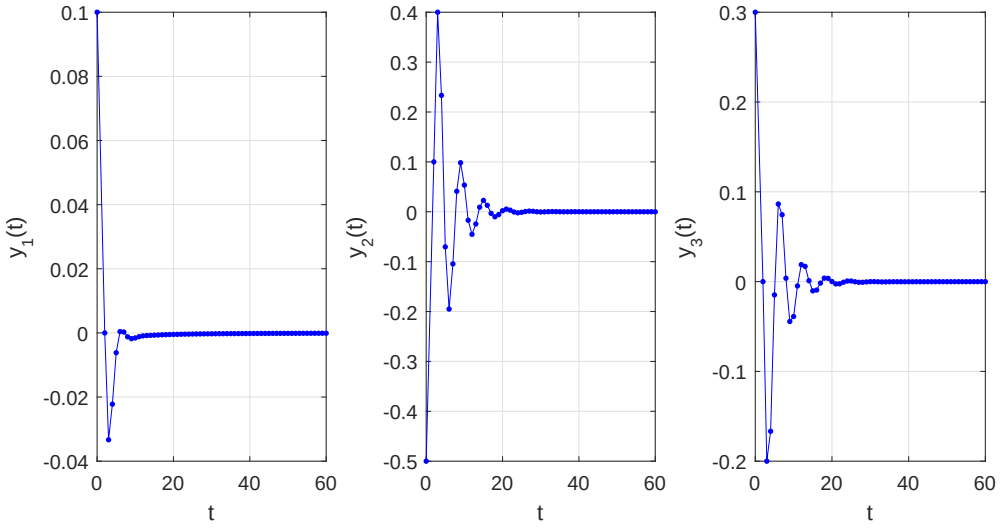

Figure 2.3: Assessing the Stability of the Zero Solution in System (2.53) with Varied Orders: $\alpha_1 = \frac{1}{3}$, $\alpha_2 = \frac{2}{3}$, and $\alpha_3 = \frac{1}{3}$.

2.4.2 Stability of Nonlinear Caputo Fractional-Order Difference Systems

1. **Caputo commensurate nonlinear fractional discrete system**
   Introducing the following nonlinear commensurate fractional discrete system:

$$\begin{cases} {}^{C}\Delta_a^{\alpha} x(t) = g(t+\alpha-1, x(t+\alpha-1)), \quad t \in \mathbb{N}_{a+1-\alpha}, \\ x(a) = x_a. \end{cases} \tag{2.57}$$

Definition 2.3 ([229]). *A function $\phi(r)$ falls into the category of $\mathcal{K}$ if it meets the conditions: $\phi \in C[(0,\rho), \mathbb{R}^+]$, $\phi(0) = 0$, and $\phi(r)$ strictly increases with r. If $\phi : \mathbb{R}^+ \to \mathbb{R}^+$, $\phi \in \mathcal{K}$, and $\lim_{r\to\infty} \phi(r) = \infty$, then ϕ is classified under $\mathcal{KR}$.*

Definition 2.4 ([229]). *A function $V(t,x)$, where $t \in \mathbb{N}\alpha$ and $x \in S\rho$ with $S_\rho = x \in \mathbb{R}^n : \|x\| \leq \rho$, is termed positive definite if $V(t,0) = 0$ for all $t \in \mathbb{N}_\alpha$, and if there exists a function $\phi(r) \in \mathcal{K}$ satisfying $\phi(r) \leq V(t,x)$ for $\|x\| = r$ and $(t,x) \in \mathbb{N}_a \times S_\rho$.*

Definition 2.5 ([229]). *A real-valued function $V(t,x)$, where $t \in \mathbb{N}\alpha$ and $x \in S\rho$ with $S_\rho = x \in \mathbb{R}^n : |x| \leq \rho$, is termed decrescent if $V(t,0) = 0$ for all $t \in \mathbb{N}\alpha$, and if there exists a function $\phi(r) \in \mathcal{K}$ such that $V(t,x) \leq \phi(r)$ for $|x| = r$ and $(t,x) \in \mathbb{N}\alpha \times S_\rho$.*

Now, we are ready to outline the theorems concerning the stability properties of solutions to system (2.57).

Theorem 2.8 ([229]). *Should a positive definite, decreasing scalar function $V(t,x) \in C[\mathbb{N}_a \times S\rho, \mathbb{R}_+)$ be present, with , ${}^{C}\Delta_a^{\alpha} V(t,x(t)) \leq 0$ for all $a \in \mathbb{N}_a$ and $(t,x) \in \mathbb{N}_0 \times S\rho$, then the trivial solution of (2.57) achieves uniform stability.*

Proof. Let $x(t) \to x(t,a,x_a)$ denote a solution trajectory of system (2.57). Assuming the positivity and monotonic decrease of $V(t,x)$, we can identify functions ϕ

and ψ from $\mathcal{K}$ such that $\phi(|x|) \leq V(t,x) \leq \psi(|x|)$ for all $(t,x) \in \mathbb{N}a \times S\rho$. Take any $\epsilon > 0$, where $0 < \epsilon < \rho$, and select $\delta = \delta(\epsilon)$ such that $\psi(\delta) < \phi(\epsilon)$. For any solution $x(t)$ of (2.57), it holds that $\phi(|x(t)|) \leq V(t,x(t)) \leq \phi(\epsilon)$ provided $|x_0| < \delta(\epsilon)$. Given ${}^{C}\Delta_a^{\alpha} V(t,x(t)) \leq 0$, we infer $V(t,x(t)) \leq V(a,x_a)$ for all $t \in \mathbb{N}_a$. As a result,

$$\phi(\|x(t)\|) \leq V(t,x(t)) \leq V(a,x_a) \leq \psi(\|x_a\|) < \psi(\delta) < \phi(\epsilon), \tag{2.58}$$

and thus $\|x(t)\| < \epsilon$ for all $t \in \mathbb{N}_a$.

□

Theorem 2.9 ([229]). *Suppose there exists a positive definite and decreasing scalar function $V(t,x) \in C[\mathbb{N}_a \times S\rho, \mathbb{R}_+)$ such that*

$${}^{C}\Delta_a^{\alpha} V(t,x(t)) \leq -\psi(\|x(t+\alpha-1)\|), \tag{2.59}$$

given that $\psi \in \mathcal{K}$ and for all $t \in \mathbb{N}_a$ along with $(t,x) \in \mathbb{N}_a \times S\rho$, the zero solution of (2.57) attains uniform asymptotic stability.

Proof. Given that all conditions of Theorem 3.24 are met, the zero solution of system (2.57) is uniformly stable. Let $0 < \epsilon < \rho$ and $\delta = \delta(\epsilon)$ be associated with uniform stability.
Choose a fixed $\epsilon_0 \leq \rho$ and $\delta_0 \to \delta(\epsilon_0) > 0$.
Now, for $\|x_a\| < \delta_0$ and $T(\epsilon)$ large enough so that

$$(T+a)^{\alpha} \geq \frac{\phi(\delta_0)}{\psi(\delta\epsilon_0)}\Gamma(\alpha+1). \tag{2.60}$$

Such a large T can be selected given that

$$\lim_{T\to\infty} \frac{\Gamma(T+\alpha)}{\Gamma(T)} = \infty. \tag{2.61}$$

Here, we assert that $\|x_{t,a,x_a}| < \delta(\epsilon)$ for all $t \in [a, a+T] \cap \mathbb{N}$.
If this assumption doesn't hold, according to (2.59), we obtain

$$\begin{aligned} V(t,x_{t,a,x_a}) &\leq V(a,x_a) - \frac{1}{\Gamma(\alpha)} \sum_{s=a+1-\alpha}^{t-\alpha} (t-\sigma(s))^{(\alpha-1)}\, \psi(\|x(s+\alpha-1)\|, \\ &\leq \phi(\|x_a\|) - \frac{\psi(\delta)}{\Gamma(\alpha)} \sum_{s=n_0}^{t-\alpha} (t-\sigma(s))^{(\alpha-1)}, \\ &\leq \phi(\delta_0) - \frac{\psi(\delta)}{\Gamma(\alpha+1)}(t-n_0)^{(\alpha)}. \end{aligned} \tag{2.62}$$

Upon substituting $t \in [a, a+T] \cap \mathbb{N}$, we acquire

$$0 < \phi(\delta(\epsilon)) \leq V(a+T, x(a+T,a,x_a)) \leq \phi(\delta_0) - \frac{\pi(\delta)}{\Gamma(\alpha+1)}(T-n_0)^{(\alpha)} \leq 0, \tag{2.63}$$

This leads to a contradiction. Consequently, there exists a $t \in [a, a+T] \cap \mathbb{N}$ such that $|x(t,a,x_a)| < \delta(\epsilon)$. Given the uniform stability of the zero solution and the arbitrary nature of t, it follows that $|x(t,a,x_a)| < \epsilon$ for all $t \geq a+T$ whenever $|x_a| < \delta_0$.

□

Theorem 2.10 ([229]). *Suppose a function* $V(t,x) \in C([\mathbb{N}_a) \times \mathbb{R}^n, \mathbb{R}+)$ *exists, satisfying*

$$\begin{aligned} &\phi(\|x(t)\|) \leq V(t,x) \leq \psi(\|x(t)\|), \quad \forall (t,x) \in \mathbb{N}_a \times \mathbb{R}^n, \\ &{}^C\Delta_a^{\alpha} V(t,x(t)) \leq -\psi(\|x(t+a-1)\|), \quad \forall a \in \mathbb{N}_a, (t,x) \in \mathbb{N}_0 \times \mathbb{R}^n. \end{aligned} \tag{2.64}$$

If ϕ *and* ψ *are elements of* $\mathcal{K}$*, valid for all* $(t,x) \in \mathbb{N}_a \times \mathbb{R}^n$*, then the zero solution of* (2.57) *achieves a state of global uniform asymptotic stability.*

Proof. Having satisfied the conditions of Theorem 3.27, the trivial solution of (2.57) attains uniform asymptotic stability. The task now is to demonstrate that the domain of attraction for $x \to 0$ spans the entirety of $\mathbb{R}^n$. Since $\lim_{r\to\infty} \phi(r) \to \infty$, the value of δ_0 in the proof of Theorem 3.27 may be arbitrarily large, and ϵ can be chosen such that $\psi(\delta_0) < \phi(\epsilon)$. Hence, the globally uniform asymptotic stability of $x \to 0$ is confirmed. □

2. **Incommensurate Caputo nonlinear fractional discrete system**
In this section, we present novel findings pertaining to the stability analysis of the nonlinear incommensurate Fractional-order Discrete Systems, characterized by the following expression:

$$\begin{cases} {}^C\Delta_0^{\alpha_1} x_1(t) = g_1(t+\alpha_1-1, x_1(t+\alpha_1-1)), \\ {}^C\Delta_0^{\alpha_2} x_2(t) = g_2(t+\alpha_2-1, x_2(t+\alpha_2-1)), \\ \ldots \\ {}^C\Delta_0^{\alpha_n} x_n(t) = g_n(t+\alpha_n-1, x_n(t+\alpha_n-1)), \end{cases} \tag{2.65}$$

here, $x(t) = (x_1(t); x_2(t); ...; x_n(t))^T \in \mathbb{R}^n$, ${}^C\Delta_0^{\alpha_i}$ denotes the Caputo operator of order α_i where $0 < \alpha_i \leq 1$ for $i = 1, 2, ..., n$.
Additionally, $g(t, x(t)) = (g_1(t, x_1(t)), g_2(t, x_2(t)), ..., g_n(t, X_n(t)) : \mathbb{R}^n \to \mathbb{R}^n$ represents a continuous differentiable function. In this context, we assume $g(0) = 0$ corresponds to the zero equilibrium point.

Theorem 2.11 ([234]). *Should all roots of the characteristic equation (2.66)*

$$det\left(diag\left(w\left(1-\frac{1}{w}\right)^{\alpha_1}, w\left(1-\frac{1}{w}\right)^{\alpha_2}, ..., w\left(1-\frac{1}{w}\right)^{\alpha_n}\right) - J\right) = 0, \tag{2.66}$$

are situated inside the unit disk, then the trivial solution of system (2.65) associated with the initial condition $x(0) = x_0 \in \mathbb{R}^n$ *achieves local asymptotic stability, where* J *represents the Jacobian matrix of* g *evaluated at* 0.

To facilitate the computations, we present Theorem 2.12 below.

Theorem 2.12 ([234]). *Let's assume that* $0 < \alpha_i < 1$ *for* $i = 1, 2, ..., n$*, and* M *represents the Lowest Common Multiple of the denominators* μ_i *of* α_i*'s, where* $\alpha_i = \frac{v_i}{\mu_i}$ *with* $(v_i, \mu_i) = 1$*,* $v_i, \mu_i \in \mathbb{Z}_+$ *for* $i = 1, 2, ..., n$*. Let* $\sigma = \frac{1}{M}$*. If at least one root of the subsequent equation*

$$det\left(diag\left(\mu^{M\sigma_1}, \mu^{M\sigma_2}, ..., \mu^{M\sigma_n}\right) - (1-\mu^M)J\right) = 0, \tag{2.67}$$

ies within the set $\mathbb{C}/K^{\sigma}$*, then the trivial solution of system (2.65) with the initial condition* $x(0) = x_0$ *achieves local asymptotic stability.*

(2.68)

Example 2.6. *Consider the subsequent nonlinear incommensurate fractional-order discrete system:*

$$\begin{cases} {}^{C}\Delta_0^{\frac{1}{2}} x_1(t) = -x_2(t)e^{-x_1(t)} - x_1(t)e^{-x_2(t)}, \\ {}^{C}\Delta_0^{\frac{1}{4}} x_2(t) = \dfrac{1}{2}x_2(t)e^{-x_1(t)} - \dfrac{9}{16}x_1(t)e^{-\frac{1}{2}x_2(t)}. \end{cases} \tag{2.69}$$

The Jacobian matrix J *is expressed as follows:*

$$J = \begin{pmatrix} -1 & 1 \\ -\dfrac{9}{16} & \dfrac{1}{2} \end{pmatrix}, \tag{2.70}$$

with $M = 4$*, we have the characteristic equation (2.71)*

$$\frac{1}{16}\mu^8 + \frac{1}{2}\mu^6 - \mu^5 - \frac{1}{8}\mu^4 + \mu^3 - \frac{1}{2}\mu^2 + \mu + \frac{1}{16} = 0, \tag{2.71}$$

its solutions are as follows:

$$\mu = \begin{pmatrix} -1.1634 \\ -6.0451X10^{-2} \\ -0.78732 + 3.1894i \\ -0.78732 - 3.1894i \\ 1.3269 - 0.4875i \\ 1.3269 + 0.4875i \\ 7.2415X10^{-2} - 0.80874i \\ 7.2415X10^{-2} + 0.80874i \end{pmatrix}. \tag{2.72}$$

Since $\mu_i \in \mathbb{C}/K^{\frac{1}{4}}$*, the solution of system (2.69) exhibits local asymptotic stability. Figure 2.4 illustrates the stability situation considering the initial condition* $x_0 = (0.1, 0.1)^T$*.*

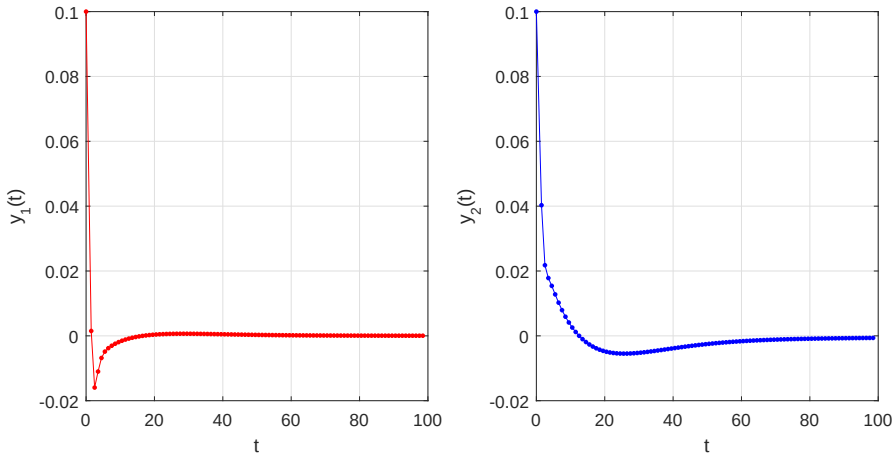

Figure 2.4: Temporal Dynamics of System States (2.69) with Initial Condition $x_0 = (0.1, 0.1)^T$ and Order $\alpha = (\frac{1}{2}, \frac{1}{4})^T$.

2.5 Stability of Nabla Discrete Fractiona-Order Systems

Lyapunov stability is employed to guarantee the stability of equilibrium points, while class K functions are utilized for analyzing the fractional Lyapunov direct approach. The essential definitions and lemmas presented in this section are based on key insights from the prominent reference [230]. In this section, we extend the Lyapunov function approach to investigate the stability of solutions to nabla Caputo commensurate fractional difference systems:

$$\begin{cases} {}^{C}\nabla_a^{\alpha} x(t) = g(t, x(t)), \\ x(a) = x_0, \quad t \in \mathbb{N}_{a+1}, \end{cases} \tag{2.73}$$

where $g : \mathbb{N}_a.\mathbb{R}^n \to \mathbb{R}^n$ is continuous and $0 < \alpha < 1$, it's essential to note that a Lyapunov function V for system (2.73) must be contingent on both t and x. For every $t \in \mathbb{N}_a$, we permit $g(t, 0) = 0$, ensuring that system (2.73) possesses the trivial solution. Below, we present the theorems addressing the stability of solutions for (2.73).

Lemme 2.1 ([230]). *Consider $x : \mathbb{N}_{a+1} \to \mathbb{R}$ and $x(t)$ satisfying the following inequality:*

$${}_a^{C}\nabla^{\alpha} x^2(t) \leq 2x(t)\, {}_a^{C}\nabla^{\alpha} x(t). \tag{2.74}$$

Theorem 2.13 ([230]). *Suppose a positive definite and decreasing scalar function $V(t, x(t)) \in C(\mathbb{N}_a.S^v, \mathbb{R}^+)$ exists such that:*

$${}^{C}\nabla_a^{\alpha} V(t, x(t)) \leq 0, \tag{2.75}$$

for all $a \in \mathbb{N}a$ and $(t, x) \in \mathbb{N}a.S^v$, then the zero solution of (2.73) exhibits uniform stability.

Theorem 2.14 ([230]). *Considering the Caputo discrete fractional-order system (2.73), the origin serves as an equilibrium point. Assuming the existence of a positive definite*

and monotonically decreasing Lyapunov function $V(t, x(t))$ *satisfying*

$$\begin{aligned} &\gamma_1(\|x(t)\|) \leq V(t, x(t)) \leq \gamma_2(\|x(t)\|), \\ &{}^{C}\nabla_a^{\alpha} V(t, x(t)) \leq -\gamma_3(\|x(t)\|), \end{aligned} \tag{2.76}$$

where $\alpha \in (0, 1)$ *and* $\gamma_1, \gamma_2, \gamma_3$ *belong to the class of discrete* κ *functions. Consequently, system (2.73) exhibits asymptotic stability.*

Definition 2.6 ([230]). *The equilibrium point* x_e *of system (2.73) is said to be Mittag–Leffler stable if there exist parameters* κ, $\sigma \in (0, 1)$, $\nu \in [\sigma, \sigma + 1)$, $b > 0$ *and a weighting function* $w : \mathbb{D} \to \mathbb{R}_0$ *satisfying*

$$\|x(t)\| \leq (w(x(a))E_{\sigma,\nu}(\kappa, t, a)), \tag{2.77}$$

where $w(x(t))$ *exhibits Lipschitz continuity with respect to* $x(t)$, $w(0) = 0$, $t \in \mathbb{N}_{a+1}$, $a \in \mathbb{R}$, $\mathbb{D} \subset \mathbb{R}^n$, $\mathbb{R}_0 = \{w \in \mathbb{R} : w \geq 0\}$

Theorem 2.15 ([230]). *For system (2.73), assuming the presence of parameters* $\alpha \in (0, 1)$, b, c, q_1, q_2, $q_3 > 0$, *and a Lyapunov function* $V(t, x(t)) : \mathbb{N}_{a+1} \times D \to \mathbb{R}_0$ *satisfying:*

$$\begin{aligned} &q_1\|x(t)\|^b \leq V(t, x(t)) \leq q_2\|x(t)\|^{bc}, \\ &{}^{C}\nabla_a^{\alpha} V(t, x(t)) \leq -q_3\|x(t)\|^{bc}, \end{aligned} \tag{2.78}$$

given $x(t) \in D$, $t \in \mathbb{N}_{a+1}$, $a \in \mathbb{R}$, *and* $V(t, x(t))$ *is Lipschitz continuous with respect to* $x(t)$, *then system (2.73) is Mittag–Leffler stable at* $x_e = 0$.

Remarque 2.2. *The convergence behavior of Mittag–Leffler functions indicates that Mittag–Leffler stability is a particular case of asymptotic stability.*

In the presence of inevitable uncertainties or disturbances, fulfilling condition (2.78) becomes a formidable task. Consequently, a novel stability criterion is formulated herein.

Theorem 2.16 ([230]). *In the context of system (2.73), provided that parameters* $\alpha \in (0, 1)$, b, c, q_1, q_2, q_3, $q_4 > 0$ *are present, along with a Lyapunov function* $V(t, x(t)) : \mathbb{N}_{a+1} \times D \to \mathbb{R}$ *that satisfies:*

$$q_1\|x(t)\|^b \leq V(t, x(t)) \leq q_2\|x(t)\|^{bc}, \tag{2.79}$$

$${}^{C}\nabla_a^{\alpha} V(t, x(t)) \leq -q_3\|x(t)\|^{bc} + q_4, \tag{2.80}$$

in situations where $x(t) \in D$, $t \in \mathbb{N}_{a+1}$, $a \in \mathbb{R}$, $V(t, x(t))$ *exhibits Lipschitz continuity concerning* $x(t)$, *system (2.73) attains uniform ultimate boundedness at* $x_e = 0$. *Furthermore, for any*$\varepsilon > 0$, *there exists* $T \in \mathbb{N}_{a+1}$ *such that:*

$$\|x(t)\| \leq \left(\frac{q_2 q_4}{q_1 q_3} + \frac{\epsilon}{q_1}\right)^{\frac{1}{b}}, \quad t \geq T, \quad k \ni \mathbb{N}_{a+1}. \tag{2.81}$$

Proof. By merging (2.79) and (2.80), we derive:

$${}^{C}\nabla_a^{\alpha} V(t, x(t)) \leq -q_3 q_2^{-1} V(t, x(t)) + q_4. \tag{2.82}$$

To satisfy inequality (2.82), it is imperative for there to be a nonnegative compensation sequence $c(t)$, such that:

$$ {}^{C}\nabla_{a}^{\alpha} V(t, x(t)) + c(t) = -q_3 q_2^{-1} V(t, x(t)) + q_4. \tag{2.83} $$

Defining $z(t) := V(t, x(t)) - \frac{q_2 q_3}{4}$, $t \in \mathbb{N}_a$ results in:

$$ {}^{C}\nabla^{\alpha} z(t) + c(t) = -q_3 q_2^{-1} z(t). \tag{2.84} $$

Upon applying the nabla Laplace transform to (2.84), we obtain:

$$ s^{\alpha} X(s) - s^{\alpha-1} z(a) + A(s) = -q_3 q_2^{-1} X(s), \tag{2.85} $$

where $X(s) := \mathcal{N}_a\{z(t)\}$, and $A(s) := \mathcal{N}_a\{c(t)\}$. From this, $X(s)$ can be reformulated as:

$$ X(s) = \frac{z(a) s^{\alpha-1} - A(s)}{s^{\alpha} + q_3 q_2^{-1}}. \tag{2.86} $$

By introducing $\kappa := -q_3 q_2^{-1}$ and accounting for the existence and uniqueness of the nabla Laplace transform, the sole solution of (2.84) can be represented as:

$$ z(t) = z(a) E_{\alpha,1}(\kappa, t, a) - c(t) * E_{\alpha,\alpha}(\kappa, t, a). \tag{2.87} $$

Given the non-negativity of $\mathcal{E}_{\alpha,\alpha}(\kappa, t, a)$ and $c(t)$ (refer to [15]), it follows that:

$$ z(t) \leq z(a) E_{\alpha,1}(\kappa, t, a). \tag{2.88} $$

Utilizing $\lim_{t \to +\infty} \mathcal{E}_{\alpha,1}(\kappa, t, a) = 0$, for any $\varepsilon > 0$, there exists $T \in \mathbb{N}_{a+1}$ such that

$$ z(t) = V(t, x(t)) - \frac{q_2 q_4}{q_3} \leq \varepsilon, \tag{2.89} $$

for all $t \geq T, t \in \mathbb{N}_{a+1}$.

Employing (2.79) and (2.89), we deduce:

$$ \|x(t)\| \leq \left(\frac{q_2 q_4}{q_1 q_3} + \frac{\varepsilon}{q_1} \right)^{\frac{1}{b}}, \quad \text{for all } t \geq T, t \in \mathbb{N}_{a+1}. \tag{2.90} $$

This affirms the sought-after outcome as stated in Theorem 3.9.

□

To enhance the versatility of the Lyapunov method, $m(t)$ is introduced in place of q_4 in Theorem 3.9, thereby reinforcing boundedness to enhance attractiveness.

Theorem 2.17 ([230]). *For system (2.73), assuming the presence of parameters $\alpha, \gamma \in (0, 1)$, and $b, c, q_1, q_2, q_3, \sigma > 0$, also a Lyapunov function $V(t, x(t)) : \mathbb{N}_{a+1} \times D \to \mathbb{R}_0$ that fulfills:*

$$ q_1 \|x(t)\|^b \leq V(t, x(t)) \leq q_2 \|x(t)\|^{bc}, \tag{2.91} $$

$$ {}^{C}\nabla^{\alpha} V(t, x(t)) \leq -q_3 \|x(t)\|^{bc} + m(t), \tag{2.92} $$

$$ \sum_{j=a+1}^{\infty} \left| {}^{G}\nabla_{j}^{\gamma} m(j) \right| = \sigma < +\infty, \tag{2.93} $$

$$\lim_{t\to+\infty} m(t) = 0, \tag{2.94}$$

where $x(t) \in D$, $t \in \mathbb{N}_{a+1}$, $a \in \mathbb{R}$, $V(t, x(t))$*displays Lipschitz continuity concerning* $x(t)$, *ystem* (4.11) *exhibits uniform attractiveness at* $x_e = 0$, *In other words, for any* $x(a) \in D$, *the following holds:*

$$\lim_{t\to+\infty} x(t) = 0. \tag{2.95}$$

Proof. Through the amalgamation of (2.91) and (2.92), we derive:

$${}^{C}\nabla_a^{\alpha} V(t, x(t)) \leq -q_3 q_2^{-1} V(t, x(t)) + m(t). \tag{2.96}$$

Consequently, there must exist a nonnegative compensation sequence $c(t)$ such that

$${}^{C}\nabla_a^{\alpha} V(t, x(t)) + c(t) = -q_3 q_2^{-1} V(t, x(t)) + m(t). \tag{2.97}$$

In accordance with (2.94), the nabla Laplace transform of $h(t)$ exists. Performing the nabla Laplace transform on (2.97) results in:

$$s^{\alpha} V_f(s) - s^{\alpha-1} V(a, x(a)) + A(s) = -q_3 q_2^{-1} V_f(s) + M(s), \tag{2.98}$$

where $V_f(s) := \mathcal{N}_a\{V(t, x(t))\}$, $A(s) := \mathcal{N}_a\{c(t)\}$, $M(s) := \mathcal{N}_a\{h(t)\}$. Thus $V_f(s)$ can be represented as:

$$V_f(s) = \frac{V(a, x(a)) s^{\alpha-1} - A(s) + M(s)}{s^{\alpha} + q_3 q_2^{-1}}. \tag{2.99}$$

By defining $\kappa := -q_3 q_2^{-1}$ and considering once more the existence and uniqueness of the nabla Laplace transform, the exclusive solution of (2.97) can be represented as:

$$V(t, x(t)) = V(a, x(a)) E_{\alpha,1}(\kappa, t, a) + [m(t) - c(t)] * E_{\alpha,\alpha}(\kappa, t, a). \tag{2.100}$$

Given the non-negativity of $c(t)$ and $E_{\alpha,\alpha}(\kappa, t, a)$, it follows that:

$$V(t, x(t)) \leq V(a, x(a)) E_{\alpha,1}(\kappa, t, a) + m(t) * E_{\alpha,\alpha}(\kappa, t, a). \tag{2.101}$$

The initial term on the right side of (2.101) fulfills:

$$\lim_{t\to+\infty} V(a, x(a)) E_{\alpha,1}(\kappa, t, a) = 0, \tag{2.102}$$

Consequently, it is essential to establish:

$$\lim_{t\to+\infty} m(t) \times E_{\alpha,\alpha}(\kappa, t, a) = 0. \tag{2.103}$$

By employing the elementary property of the nabla convolution operation, we obtain:

$$\begin{aligned} m(t) * E_{\alpha,\alpha}(\kappa, t, a) &= m(t) * \left((t-a)^{-\gamma-1} * (t-a)^{\gamma-1} * E_{\alpha,\alpha}(\kappa, t, a)\right), \\ &= {}^{G}\nabla^{\gamma} m(t) * {}^{G}\nabla^{-\gamma} E_{\alpha,\alpha}(\kappa, t, a), \\ &= {}^{G}\nabla^{\gamma} m(t) * E_{\alpha,\alpha+\gamma}(\kappa, t, a). \end{aligned} \tag{2.104}$$

By defining $g(t) := {}^{G}\nabla^{\gamma} m(t)$, $\phi(t) := E_{\alpha,\alpha+\gamma}(\kappa, t, a)$, verifying $\lim_{t\to+\infty} \phi(t) = 0$ is straightforward. Consequently, for everyh $2\epsilon\sigma > 0$, there exists $T_1 \in \mathbb{N}_{a+1}$, such that

$$0 \leq \phi(t) < \frac{\epsilon}{2\sigma}, \tag{2.105}$$

is satisfied for $t \geq T_1, t \in \mathbb{N}_{a+1}$. Employing (2.93), one have

$$|g(t)\times\phi(t)| = \left|\sum_{j=a+1}^{t} g(t-j+a+1)\phi(j)\right| = \sum_{j=a+1}^{T_1-1} |g(t-j+a+1)|\phi(j)+\sum_{j=T_1}^{+\infty} |g(t-j+a+1)|\phi(j). \tag{2.106}$$

Given

$$\sum_{j=a+1}^{T_1-1} |g(t-j+a+1)|\phi(j) + \frac{\epsilon}{2\sigma}\sum_{j=T_1}^{t} |g(t-j+a+1)|$$

, once more

$$\begin{aligned} |g(t) \times \phi(t)| &= \sum_{j=a+1}^{T_1-1} |g(t-j+a+1)|\phi(j) + \frac{\epsilon}{2\sigma}\sum_{a+1}^{t-T_1+a+1} |g(j)|, \\ &\leq \sum_{j=a+1}^{T_1-1} |g(t-j+a+1)|\phi(j) + \frac{\epsilon}{2}. \end{aligned} \tag{2.107}$$

Drawing from (2.94), $\lim_{t\to+\infty} g(t) = 0$ follows immediately.
Consequently, for every $\frac{\epsilon}{2\sum_{j=a+1}^{T_1-1}\phi(j)} > 0$, there exists $T_2 \in \mathbb{N}_{a+1}$ in a manner that

$$|h(t)| < \frac{\epsilon}{2\sum_{j=a+1}^{T_1-1}\phi(j)}, \tag{2.108}$$

holds for $t \geq T_2, t \in \mathbb{N}_{a+1}$.

By replacing (2.107) into (2.108), we obtain:

$$|g(t) * \phi(t)| < \frac{\epsilon}{2P\sum_{j=a+1}^{T-1}\phi(j)} T_1 - 1 \sum_{j=a+1} \phi(j) + \frac{\epsilon}{2} = \epsilon, \tag{2.109}$$

for $t \geq \max\{T_1, T_1 + T_2 - a - 2\}$, establishing (31).

In accordance with (2.91) and (2.101)-(2.103), we obtain:

$$\lim_{t\to+\infty} q_1\|x(t)\|^b \leq \lim_{t\to+\infty} V(t, x(t)) = 0. \tag{2.110}$$

This concludes the proof.

□

Example 2.7. *Consider the following system*

$$\begin{cases} {}^C\nabla_a^\alpha x_1(t) = -x_1^3(t) - 2x_1(t)x_2^2(t), \\ {}^C\nabla_a^\alpha x_2(t) = -2x_2(t). \end{cases} \tag{2.111}$$

where $0 < \alpha < 1$, $t \in \mathbb{N}_{a+1}$, $a \in \mathbb{R}$.
Choosing Lyapunov function as $V(t, x(t)) = x_1^2(t) + x_2^2(t)$ *and according to Theorem 2.13 one can have*

$$\begin{aligned} {}^C\nabla_a^\alpha V(t, x(t)) &\leq 2x_1(t)\,{}^C\nabla_a^\alpha x_1(t) + 2x_2(t)\,{}^C\nabla_a^\alpha x_2(t), \\ &\leq -2x_1^4(t) - 4x_2^2(t) - 4x_1^2(t)x_2^2(t) < 0. \end{aligned} \tag{2.112}$$

Consequently, system (2.111) is asymptoticly stable. Setting $\alpha = 0.8$, $x_1(0) = 0.1$, $x_2(0) = 0.2$, *the evolution of* $x(t)$ *is shown as Figure 2.5.*

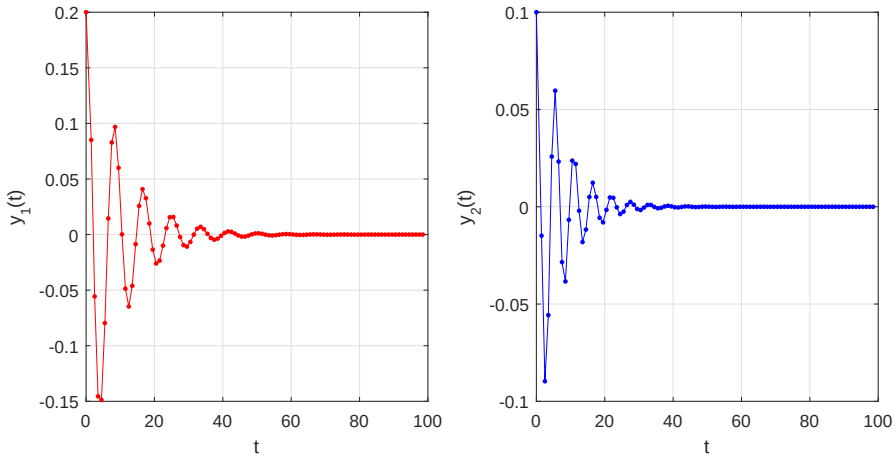

Figure 2.5: The stability of the trivial solution of system (2.111) with $x_1(0) = 0.1$, $x_2(0) = 0.2$ and $\alpha = 0.8$.

2.6 Stability of h-Discrete Fractional-order systems

All theoretical constructs, such as definitions and lemmas, presented in this section are directly taken from the significant sources referenced in [231] and [235].

2.6.1 Stability of Delta h-Discrete Fractional-Order Systems

Next, we will explore the stability of Caputo fractional-order h-difference systems using the discrete fractional Lyapunov direct method. Let's examine the following nonlinear commensurate fractional-order h-difference equations.

$$\begin{cases} {}^{C}_{h}\Delta^{\alpha}_{a}x(t) = g(t+\alpha h, x(t+\alpha h)), & 0 < \alpha \leq 1, \\ x(a) = x_a, \end{cases} \tag{2.113}$$

here, g is continuous with respect to x.
Now, we introduce Theorem 2.18 employing a discrete fractional Lyapunov direct method for system (2.113):

Theorem 2.18 ([231]). *Suppose $x = 0$ serves as an equilibrium point for system (2.113). If there exists a positive definite and decrescent scalar function $V(t, x(t))$, as well as discrete class-$\mathbb{K}$ functions $\gamma_1, \gamma_2, \gamma_3$, such that:*

$$\gamma_1(\|x(t)\|) \leq V(t, x(t)) \leq \gamma_2(\|x(t)\|), \quad t \in (h\mathbb{N})_a, \tag{2.114}$$
$${}^{C}_{h}\Delta^{\alpha}_{a}V(t, x(t)) \leq -\gamma_3(\|x(t+\alpha h\|), \quad t \in \mathbb{N}_{a+1-\alpha}. \tag{2.115}$$

Then, system (2.113) demonstrates asymptotic stability.

To utilize Theorem 2.18, we introduce the following crucial Lemmas:

Lemme 2.2 ([231]). *For $\alpha \in (0, 1]$, if*

$${}^{C}_{h}\Delta^{\alpha}_{a}y(t) \geq {}^{C}_{h}\Delta^{\alpha}_{a}x(t), \quad t \in \mathbb{N}_{a+1-\alpha}, \tag{2.116}$$

and $x(a) = y(a)$. Then

$$y(t+\alpha h) \geq x(t+\alpha h). \tag{2.117}$$

Lemme 2.3 ([231]). *For any discrete time instant $t \in \mathbb{N}_{a+1-\alpha}$, the following inequality is valid:*

$${}^{C}_{h}\Delta^{\alpha}_{a}x^2(t) \leq 2x(t+\alpha h)\,{}^{C}_{h}\Delta^{\alpha}_{a}x(t), \quad 0 < \alpha \leq 1. \tag{2.118}$$

Remarque 2.3. *For $x = (x_1(t), ..., x_n(t))^T$, with $t \in \mathbb{N}_{a+1-\alpha}$, Lemma 2.3 remains applicable. For instance, it could be formulated as:*

$${}^{C}_{h}\Delta^{\alpha}_{a}(x^T(t)x(t)) \leq 2x^T(t+\alpha h)\,{}^{C}_{h}\Delta^{\alpha}_{a}x(t), \quad 0 < \alpha \leq 1. \tag{2.119}$$

Example 2.8. *Let's examine the following nonlinear commensurate fractional difference system:*

$$\begin{cases} {}^{C}_{h}\Delta^{\alpha}_{0}x_1(t) = x_1(t+\alpha h) + x_2^3(t+\alpha h), \\ {}^{C}_{h}\Delta^{\alpha}_{0}x_2(t) = x_1(t+\alpha h) - x_2(t+\alpha h). \end{cases} \tag{2.120}$$

given the initial conditions $x_1(0) = 0.4$ *and* $x_2(0) = 0.8$. *We utilize the Lyapunov function*

$$V(t, x(t)) = \frac{1}{2}x_1^2(t) + \frac{1}{2}x_2^4(t). \tag{2.121}$$

As per Lemma 2.2, we find that

$$\begin{aligned} {}_h^C\Delta_0^\alpha V(t, x(t)) \leq & x_1(t+\alpha h)\, {}_h^C\Delta_0^\alpha x_1(t+\alpha h) + \frac{1}{2}x_2^2(t+\alpha h)\, {}_h^C\Delta_0^\alpha x_2^2(t+\alpha h), \\ & \leq x_1(t+\alpha h)\, {}_h^C\Delta_0^\alpha x_1(t+\alpha h) + x_2^3(t+\alpha h)\, {}_h^C\Delta_0^\alpha x_2(t+\alpha h), \\ & \leq x_1^2(t+\alpha h) - x_2^4(t+\alpha h) < 0. \end{aligned} \tag{2.122}$$

Consequently, by virtue of Theorem 2.18, the system achieves asymptotic stability. We can construct a numerical formulation of a fractional nonlinear system utilizing the h-fractional sum operator detailed in Chapter 1. Figure 2.6 illustrates the outcomes, corroborating the theoretical results for $h = 0.1$ *and* $\alpha = 0.7$.

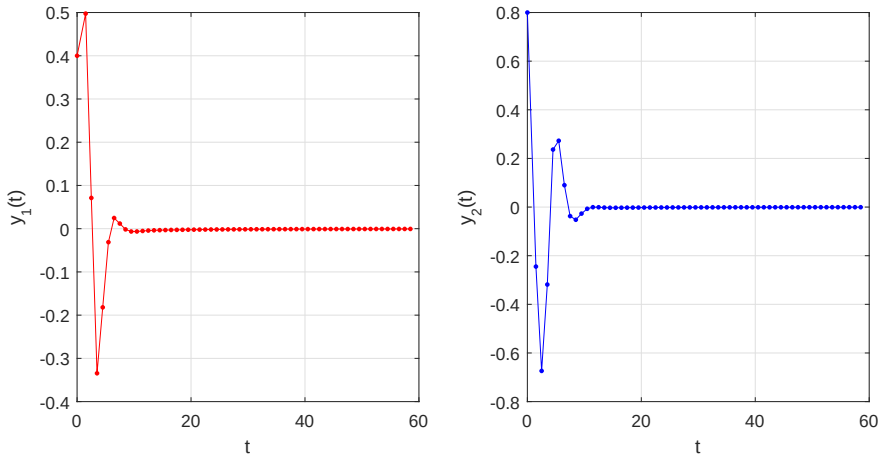

Figure 2.6: The progression of the solution x of system 2.8 with $\alpha = 0.7$ and $h = 0.1$ is depicted.

2.6.2 Stability of Nabla h-Discrete Fractional-Order Systems

1. **Commensurate nonlinear Nabla h-discrete systems**
   Let's examine the following fractional difference equation:

$$ {}_a^C\nabla_h^\alpha x(t) = f(t, x(t)), \quad x(a) = x_a, \quad \alpha \in (0, 1], \quad t \in \mathbb{N}_{a,h}, \tag{2.123}$$

   where f belongs to the set $\mathbb{N}_{a,h}$ and $x(t)$ is a positive definite and decreasing function. It is straightforward to establish that this equation has a unique solution.

   Theorem 2.19 ([231]). *Suppose* $x = 0$ *serves as an equilibrium point of equation* (2.123). *If there exists a positive definite and decreasing scalar function* $V(t, x)$, *along with class-*$\mathcal{K}$ *functions* γ_1, γ_2, *and* γ_3, *satisfying:*

$$\gamma_1(\|x(t)\|) \leq V(t, x(t)) \leq \gamma_2(\|x(t)\|), \quad t \in \mathbb{N}_{a,h}, \tag{2.124}$$

   and

$$ {}_a^C\nabla_h^\alpha V(t, x(t)) \leq -\gamma_3(\|x(t)\|), \quad t \in \mathbb{N}_{a,h}. \tag{2.125}$$

   Then, equation (2.123) *exhibits asymptotic stability.*

Proof. From inequalities (2.124) and (2.125), we obtain:

$$({}_a^C\nabla_h^\alpha V)(t,x(t)) \leq -\gamma_3(\gamma_2^{-1}(V(t,x(t)))), \quad t \in \mathbb{N}_{a,h}. \tag{2.126}$$

Let's consider the fractional difference equation:

$$({}_a^C\nabla_h^\alpha U)(t,x(t)) = -\gamma_3(\gamma_2^{-1}(U(t,x(t)))), \quad t \in \mathbb{N}_{a,h}. \tag{2.127}$$

When $V(a,x(a)) \leq U(a,x(a))$, we have

$$V(t,x(t)) \leq U(t,x(t)), \quad t \in \mathbb{N}_{a,h}. \tag{2.128}$$

Consequently, $U(t,x(t)) \leq U(a,x(a))$ for $t \in \mathbb{N}a,h$. Utilizing (2.124), we obtain

$$\|x(t)\| \leq \gamma_1^{-1}(V(t,x(t))). \tag{2.129}$$

Which leads us to,

$$\|x(t)\| \leq \gamma_1^{-1}(U(a,x(a))). \tag{2.130}$$

It then follows from the definition of stability that equation (2.123) is stable. Moreover, we have $\lim_{t\to\infty} V(t,x(t)) = 0$. Since $\gamma_1 \in \mathcal{K}$ and

$$\gamma_1(\|x(t)\|) \leq V(t,x(t)), \tag{2.131}$$

we conclude that $\lim_{t\to\infty} x(t) = 0$. Hence, equation (2.123) is asymptotically stable. This concludes the proof. □

Lemme 2.4 ([231]). *Assume $\alpha \in (0,1]$, $x(t) \geq 0$, $t \in \mathbb{N}_{a,h}$. Then the following inequality holds*

$$({}_a^C\nabla_h^\alpha x^2)(t) \leq 2x(t)({}_a^C\nabla_h^\alpha x)(t), \quad t \in \mathbb{N}_{a,h}. \tag{2.132}$$

Example 2.9. *Let's examine the following nabla h-fractional difference equation:*

$$({}_a^C\nabla_h^\alpha x)(t) = -x^3(t), \tag{2.133}$$

in the context of the nabla h-fractional difference equation, with parameters $\alpha = 0.9$, $a = 0$, $h = 1$, and $x \in \mathbb{R}$, where $t \in \mathbb{N}_{a,h}$, the equation yields the trivial solution $x(t) = 0$. It can be observed that:

$$x^{(\alpha-1)}(t)({}_a^C\nabla_h^\alpha x)(t) = x^{(\alpha-1)}(t)(-x^3(t)) = -x^{12/5}(t) \leq 0, \tag{2.134}$$

for $\alpha = \frac{2}{5}$. Hence, according to Theorem 3.12, equation (2.133) exhibits stability, as evidenced by Figure 3.13.

2. **Incommensurate nonlinear Nabla h-discrete systems**
Taking into account the foolowing incommensurate h-Nabla fractional-order context difference system

$$\begin{cases} {}_h^C\nabla_a^{\alpha_1} x_1(t) = g_1(t,x_1(t)), \\ {}_h^C\nabla_a^{\alpha_2} x_2(t) = g_2(t,y_2(t)), \\ \ldots \\ {}_h^C\nabla_a^{\alpha_n} x_n(t) = g_n(t,x_n(t)), \end{cases} \tag{2.135}$$

In this framework, we have $x(t) = (x_1(t), x_2(t), ..., x_n(t))^T \in \mathbb{R}^n$, with $0 < \alpha_i < 1$ for $i = 1, 2, ..., n$. The function $g = (g_1, g_2, ..., g_n)^T : \mathbb{R}^n \to \mathbb{R}^n$ is continuously differentiable. For simplicity, we set $a = 0$.

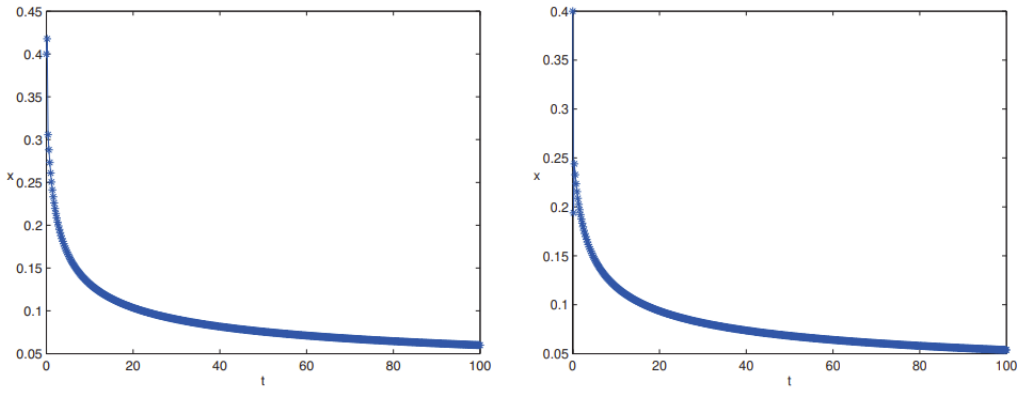

Figure 2.7: The Dynamics of Solution x of 2.133 with $\alpha = 0.4$, $h = 1$, $x_a = 0.1$, and $x_a = 0.4$.

Theorem 2.20 ([234]). *Suppose* 0 *stands as an equilibrium point for system (2.135). If all roots of the characteristic equation:*

$$det\left(diag\left(\left(1-\frac{1}{w}\right)^{\alpha_1},\left(1-\frac{1}{w}\right)^{\alpha_2},...,(\left(1-\frac{1}{w}\right)^{\alpha_n}\right)-HJ\right)=0, \tag{2.136}$$

lie within the unit disk, then system (2.135) possesses a unique solution for all initial vectors sufficiently close to 0. *Furthermore,* 0 *is asymptotically stable, where* J *denotes the Jacobian matrix of* g *at* 0 *and* $H = diag(h^{\alpha_1}, h^{\alpha_2}, ..., h^{\alpha_n})$.

Theorem 2.21 ([234]). *Consider rational numbers* α_i *between* 0 *and* 1, *for* $i = 1, 2, ..., n$. *Let* M *be the lowest common multiple of* u_i *and* v_i, *such that* $\alpha_i = \frac{v_i}{u_i}$, *where* $gcd(u_i, v_i) = 1$ *and* $u_i, v_i \in \mathbb{Z}_+$, *for* $i = 1, 2, ..., n$. *Set* $\sigma = \frac{1}{M}$. *Then, the zero solution of system (2.135) with initial value* $x_0 = x(0)$ *is locally asymptotically stable if any zero solution of the polynomial equation:*

$$det\left(diag\left(\mu^{M\alpha_1},\mu^{M\alpha_2},...,\mu^{M\alpha_n}\right)-HJ\right)=0, \tag{2.137}$$

are contained within the region $\mathbb{C}/K^\sigma$, *where* K^σ *represents the set of complex numbers* w *satisfying*

$$|w| \leq \left(2\cos\left(\frac{arg(w)}{\sigma}\right)^\sigma\right), \quad and, \quad |arg(w)| \leq \frac{\sigma\pi}{2}, \tag{2.138}$$

and J *denotes the Jacobian matrix of* g *evaluated at* 0, *then the zero solution of system (2.135) with initial value* $x_0 = x(0)$ *is locally asymptotically stable.*

Example 2.10. *In relation to system (2.135), the following system can be expressed:*

$$\begin{cases} {}_1^C\nabla_0^{\frac{1}{2}} = -1.01\sin(x_1(t)) + 0.98\sin(x_2(t)), \\ {}_1^C\nabla_0^{\frac{1}{4}} = 0.48x_2(t)\cos(x_1(t)) - 0.56x_1(t)\cos(x_2(t)). \end{cases} \tag{2.139}$$

The origin serves as an equilibrium point for the system under consideration. Furthermore, the Jacobian matrix J *of this system can be derived as follows:*

$$J = \begin{pmatrix} -1.01 & 0.98 \\ -0.56 & 0.48 \end{pmatrix}. \tag{2.140}$$

Given that $M = 4$, equation (2.141) is obtained:

$$\mu^3 - 0.48\mu^2 + 1.01\mu + 0.064 = 0. \tag{2.141}$$

The solutions to this equation are as follows:

$$\mu = \begin{pmatrix} -6.1349X10^{-2} \\ 0.27067 - 0.98486i \\ 0.27067 + 0.98486i \end{pmatrix}. \tag{2.142}$$

We can conclude from Theorem 2.21 that the zero solution of system (2.139) is locally asymptotically stable, as $\mathbb{C}/K$. To verify the accuracy of this result, Figure 2.8 demonstrates that the states of the solution of system (2.139) indeed converge to the origin.

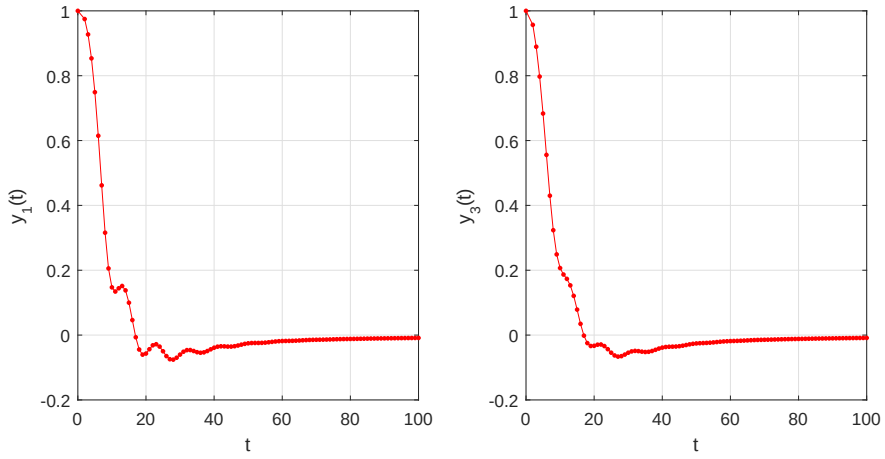

Figure 2.8: Convergence Behavior of States x_1 and x_2 in System (2.139) with $\alpha_1 = \frac{1}{2}$ and $\alpha_2 = \frac{1}{4}$.

2.7 Conclusion

This chapter has explored the critical importance of system stability within the domain of dynamic system analysis and strategic design, particularly highlighting the advancements in discrete fractional-order systems. The development of methodologies, such as the discrete generalized Gronwall inequality, and the exploration of positivity and Mittag–Leffler stabilities, have collectively expanded the toolkit available for assessing the stability of these complex systems.

An important advancement in this area has been the identification of positive definite quadratic forms as optimal candidates for Lyapunov functions in discrete fractional-order systems. This breakthrough has facilitated the widespread use of the second Lyapunov method, especially in commensurate systems, although challenges remain in its application to incommensurate systems.

This chapter focused on a specific class of discrete fractional-order systems that encompass both commensurate and incommensurate scenarios. These systems are characterized by a combination of linear and nonlinear components, ensuring a comprehensive and methodologically sound investigation. This dual approach allows for a nuanced understanding of stability across diverse and real-world applications.

Moreover, this chapter serves as a significant overview of the evolving topic of stability analysis in discrete fractional-order systems. By providing valuable insights and robust methodologies, it aims to advance the state-of-the-art in this critical field.

Chapter 3

An Overview on Fractional-Order Neural Networks

3.1 Introduction

The intricate topic of fractional-order neural networks sits at the intersection of biology and computational science, marking a significant area of study over the past two decades. This fusion of fractional calculus with neural networks has led to efficiency gains and substantial advancements. Unlike traditional integer-order neural networks, fractional-order neural networks excel in capturing subtle memory and hereditary traits inherent in various neuroscience processes.

Moreover, they possess fundamental capabilities for information processing, stimulus anticipation, and facilitating frequency-independent phase shifts in oscillatory neuronal firing. These characteristics make fractional-order neural networks versatile tools with vast potential applications in neural networks, promising advancements in understanding and modeling complex biological systems.

To comprehensively explore this topic, we start with a foundational introduction to neural networks. Neurons, the fundamental units of the nervous system, have been studied for millennia as part of the quest to understand the human brain. The concept of artificial neural networks began to take shape in 1943 with Warren McCulloch and Walter Pitts proposing a theoretical model of neuron function.

Despite initial skepticism, pioneering researchers like Teuvo Kohonen, Stephen Grossberg, James Anderson, and Kunihiko Fukushima persevered in their work, laying the groundwork for the renewed interest in neural network research. The introduction of the Hopfield neural network in the early 1980s by John Hopfield marked a significant turning point, offering a revolutionary approach to associative memory.

Neural networks have since gained widespread attention across various fields, including image processing, optimization, pattern recognition, and more. Achieving stable equilibria, especially in optimization tasks, has become a key focus, highlighting the importance of neural networks in modern research.

This chapter emphasizes the critical role of fractional-order neural networks, exploring

their diverse applications and contributions to neural network research. As exploration continues, the integration of fractional calculus with neural networks holds promise for further insights and advancements, shaping the future of computational neuroscience and problem-solving methodologies. The intersection of these disciplines offers opportunities to unravel the complexities of biological systems and inspire innovative computational approaches.

3.2 Biological Neural Networks

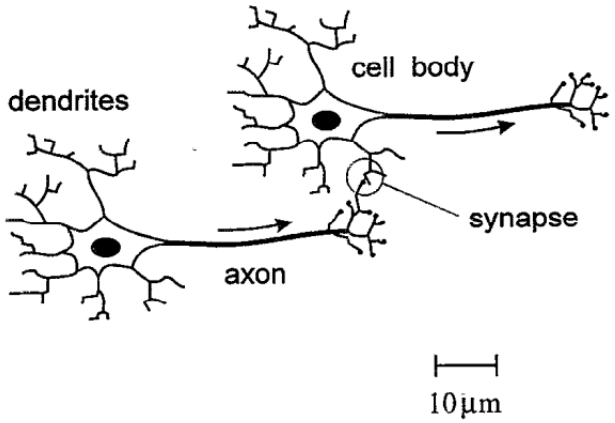

Figure 3.1: Illustration: Two biological neurons showing dendrites receiving inputs, axons transmitting action potentials, and synapses facilitating neuronal interactions.

Understanding the intricacies of the human brain is both a daunting and captivating scientific challenge. Scientists are particularly interested in biological neural networks, which are crucial for advancing pattern recognition and information processing systems, including the development of artificial network models. Here, we provide a condensed overview of biological neural networks for a holistic understanding.

The human brain consists of approximately 100 billion electrically active cells called neurons. These neurons vary in shape and size, but they share common features. Neurons receive signals through dendritic branching and transmit them via axons. Communication between neurons occurs at synapses, the junctions between them. Remarkably, a single neuron can form connections with thousands of others, resulting in over 100 trillion synapses in the brain. Despite each neuron operating on a relatively slow timescale (around 1 millisecond), the parallel processing of information across numerous synapses grants the brain effective processing power surpassing even current supercomputers. This parallelism also confers a high level of fault tolerance, as the loss of neurons minimally affects performance.

Neurons exhibit an all-or-nothing response, emitting an electrical impulse when they ”fire.” This impulse travels along the axon and triggers the release of chemical neurotransmitters upon reaching a synapse. These neurotransmitters influence the subsequent

neuron, either increasing (excitatory synapse) or decreasing (inhibitory synapse) the likelihood of firing. Each synapse possesses an associated strength (or weight), dictating the impact of the impulse on the post-synaptic neuron. Neurons perform computations by weighing the inputs they receive, and if the cumulative stimulation exceeds a certain threshold, the neuron fires. Networks of such neurons demonstrate versatile information processing capabilities.

The study of biological neural networks provides valuable insights into the functioning of the human brain. By understanding these networks, scientists aim to develop artificial neural networks that mimic their behavior, leading to advancements in various fields such as artificial intelligence and neuroscience.

3.3 Artificial Neural Networks

3.3.1 The Neuron Models

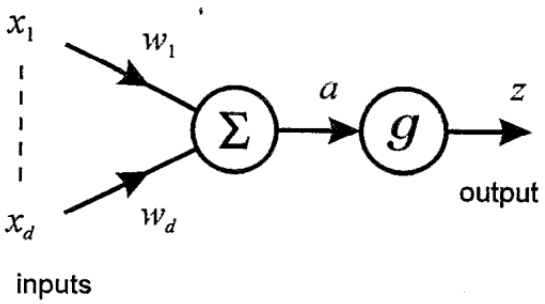

Figure 3.2: Representation of a Single Neuron in the McCulloch-Pitts Model: Weighted Sum and Non-linear Activation .

In a groundbreaking paper by McCulloch and Pitts in 1943, they introduced a fundamental mathematical model of a single neuron, as depicted in Figure 3.2. This model acts as a non-linear transformation, converting a set of input variables (where $i = 1, ..., d$) into an output variable z. From now on, we'll call this artificial neuron model a "processing unit" or simply a "unit" to differentiate it from its biological counterpart.

The McCulloch-Pitts model describes a process where the signal x_i at input i is multiplied by a parameter w_i (similar to synaptic strength in a biological network). This product is then added to all other weighted input signals, resulting in a total input to the unit represented by the equation:

$$a = \sum_{i=1}^{d} w_i x_i + w_0. \tag{3.1}$$

Here, the offset parameter w_0 is the bias (similar to the firing threshold in a biological neuron). Formally, the bias can be seen as a special case of a weight, treating an extra

th!

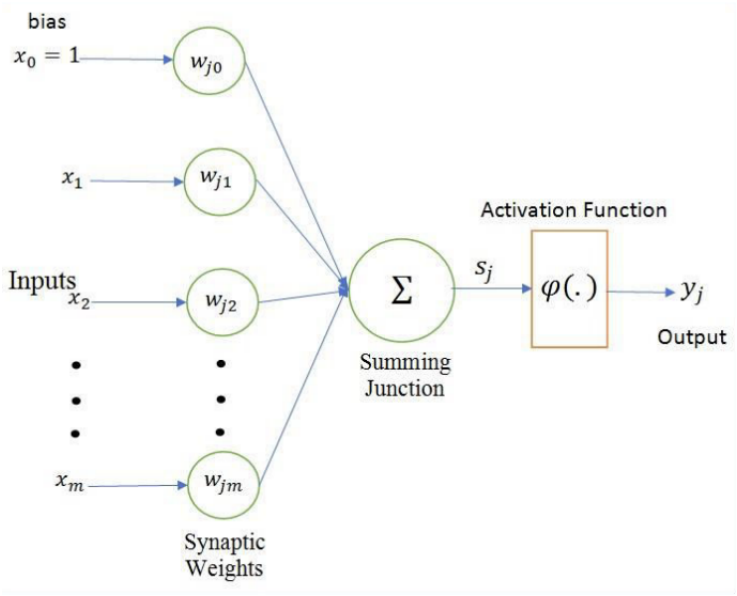

Figure 3.3: An Alternative Nonlinear Representation of a Neuron.

input with a permanently set value $x_0 = 1$. Consequently, the equation can be expressed as:

$$a = \sum_{i=0}^{d} w_i x_i. \tag{3.2}$$

It's important to note that weights (and the bias) can be positive or negative, representing excitatory or inhibitory synapses. The unit's output z, loosely analogous to a neuron's average firing rate, is determined by applying a non-linear activation function $g()$, such that:

$$z = g(a). \tag{3.3}$$

There are various forms of the activation function $g()$, which we'll elaborate on in the upcoming sections.

This simple neuron model serves as the foundational mathematical component in numerous artificial neural network models. Connecting multiple such processing elements allows the construction of a versatile class of non-linear mappings applicable to a broad spectrum of practical problems. Weight values can be adjusted through an appropriate training algorithm, enabling networks to learn from external data.

3.3.2 Activation Function

Activation functions, represented by $g(s)$, play a pivotal role in the functionality of neural networks. Their primary purpose is to introduce non-linearity into the network, enabling the model to learn intricate patterns and relationships within the data. The choice of activation function significantly influences the network's capacity to capture complex features and make accurate predictions.

- **Sigmoid Activation Function**

  The sigmoid function, often denoted by $\sigma(x)$, is a fundamental component in machine learning algorithms, particularly in logistic regression models. It serves a critical role in transforming input values into a bounded range between 0 and 1. This mathematical operation is particularly advantageous in scenarios necessitating binary classification, where the objective is to categorize inputs into two distinct classes.

  Mathematically, the sigmoid function is expressed as follows:

$$\sigma(x) = \frac{1}{1 + e^{-x}}. \tag{3.4}$$

  he sigmoid function finds widespread application in logistic regression, a statistical technique extensively employed in machine learning tasks. In logistic regression models, the sigmoid function is employed to map the linear combination of input features to a probability score. This probability score indicates the likelihood of a specific input belonging to a particular class.

  For instance, in the domain of spam email detection, logistic regression models leverage the sigmoid function to estimate the probability that an email is spam. The sigmoid-transformed output assigns values ranging from 0 to 1, where a value closer to 1 suggests high confidence that the email is spam, while a value nearer to 0 indicates a lower likelihood of it being spam.

- **Hyperbolic Tangent** (tanh) **Activation Function**

  The hyperbolic tangent function, denoted as $\tanh(x)$, is similar to the sigmoid function but expands its output range to include values between -1 and 1. This function is particularly useful when dealing with inputs that have both negative and positive values, providing a centered output range.

  Mathematically, the hyperbolic tangent function is given by:

$$\tanh(x) = \frac{e^{x} - e^{-x}}{e^{x} + e^{-x}}. \tag{3.5}$$

  The $\tanh(x)$ function finds frequent application in machine learning, especially in recurrent neural networks. recurrent neural networks are specialized for modeling sequential dependencies in data, making them ideal for tasks involving time-series data or any data with inherent temporal relationships.

  The advantage of using the hyperbolic tangent function lies in its ability to map input values to a range spanning from -1 to 1. This centered range proves advantageous in scenarios where input data exhibits both positive and negative patterns. For example, in natural language processing tasks employing recurrent neural networks, the $\tanh(x)$ function assists in capturing and processing sequences of words, ensuring that both positive and negative sentiments are adequately represented.

- **Rectified Linear Unit (ReLU) Activation Function**

The Rectified Linear Unit (ReLU) activation function holds a pivotal role in neural networks, prized for its simplicity and effectiveness in training deep models.

Mathematically, the ReLU function is represented by the equation:

$$f(x) = \max(0, x). \tag{3.6}$$

What sets ReLU apart is its straightforward behavior: it replaces all negative input values with zero while leaving positive values unchanged. This inherent non-linearity introduces a beneficial sparsity property, allowing the network to focus on relevant features and efficiently learn intricate patterns.

ReLU has garnered widespread adoption, particularly in tasks like image classification and within convolutional neural networks. Its effectiveness in image-related applications stems from its capability to capture and emphasize significant features while disregarding less relevant information. This renders ReLU especially well-suited for scenarios where extracting meaningful features from images is critical, such as in the initial layers of convolutional neural networks.

- **Leaky ReLU Activation Function**

  The Leaky Rectified Linear Unit (Leaky ReLU) activation function serves as a solution to the "dying ReLU" problem, where neurons can become inactive during training. It introduces a small, non-zero gradient for negative inputs, preventing neurons from completely shutting down.

  The functional form of Leaky ReLU is expressed by the equation:

$$f(x) = \max(\alpha x, x). \tag{3.7}$$

  Unlike standard ReLU, which sets negative values to zero, Leaky ReLU allows a fraction α of the negative input to pass through, adding a mild slope to the negative side. This controlled leakage of information addresses the issue of neurons becoming "dead" or inactive during training, a problem encountered when ReLU sets all negative values to zero.

  Leaky ReLU is beneficial in various scenarios, especially in architectures like generative adversarial networks (GANs), where the risk of dead neurons can hinder learning. By incorporating this controlled leakiness, Leaky ReLU ensures continuous flow of information through neurons, facilitating more effective training and preventing premature saturation.

- **Swish Activation Function**

  The Swish activation function emerges as a self-gated alternative that has shown effectiveness across various tasks.

  The mathematical representation of the Swish function is given by:

$$f(x) = x \cdot \frac{1}{1 + e^{-\beta x}}. \tag{3.8}$$

  Swish exhibits a self-gating property, where the input x is modulated by the sigmoid of βx. This self-gating mechanism adds smoothness to the function, enabling it to

capture complex data relationships. The choice of the β parameter allows control over the shape and characteristics of the Swish function.

Swish has found notable application in natural language processing and image classification tasks. Its success in these areas is attributed to its ability to capture subtle patterns and relationships in data, making it well-suited for tasks that demand a deeper understanding of input features. ⋱

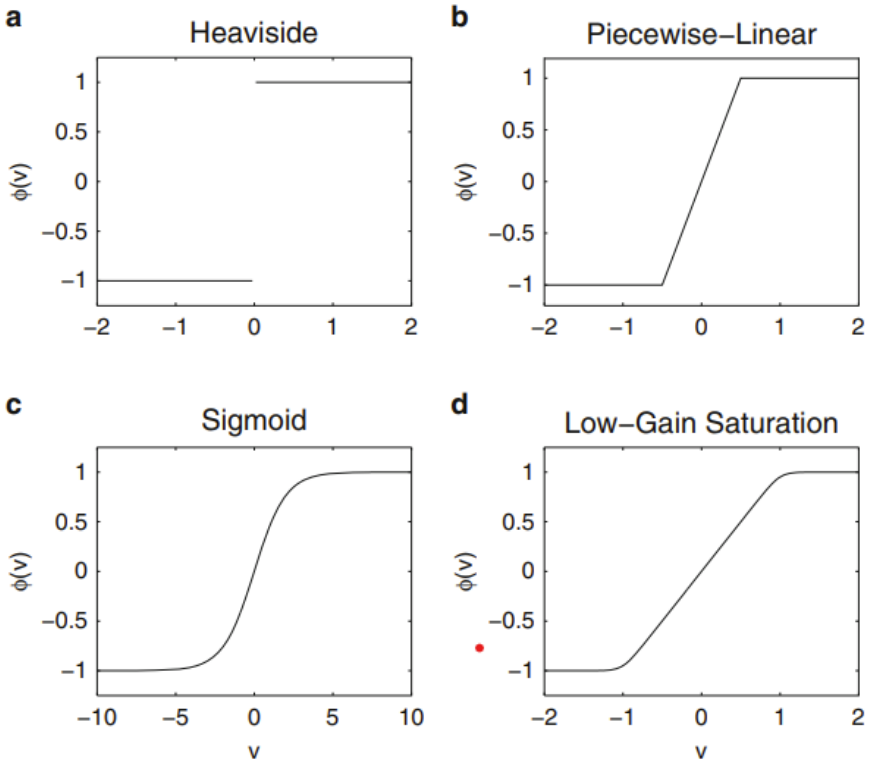

Figure 3.4: A variety of standard activation functions.

3.3.3 General Properties of The Neural Networks

Neural Networks, characterized by their intricate architecture and adaptive learning capabilities, have proven to be indispensable tools across a diverse spectrum of applications. The multifaceted advantages that Neural Networks bring to various domains are multifarious and can be expounded upon as follows:

1. **Non-linear Systems Mastery:**
   Neural networks, renowned for their formidable capacity to unravel the intricacies embedded in non-linear systems [236][237], emerge as pivotal instruments in the exploration and understanding of complex relationships within dynamic frameworks. These sophisticated networks play a crucial role in deciphering and modeling patterns, making them indispensable across a diverse array of applications. Their ability to adapt and learn dynamically positions neural networks as powerful tools in the quest for insights into complex, real-world phenomena.

2. **Adaptive Flexibility:**
Neural networks stand out with their remarkable capacity for adaptation, endowing them with the ability to dynamically fine-tune network parameters in the face of ever-changing environments. This unique adaptability not only sets neural networks apart but also equips them to expertly handle challenges associated with imprecision, fuzziness, noise, and probabilistic information [237]. It is this versatility that makes neural networks invaluable across a wide spectrum of applications, where their ability to navigate and make sense of complex, non-linear systems is a key asset [236].

3. **Computational Empowerment:**
Neural networks harness their computational prowess through a massively parallel distributed structure and a capacity for learning and generalization. Empirical evidence supports the assertion that neural networks can adeptly approximate any complex function—whether large-scale, linear, or non-linear—when provided with suitable training data [236]-[238]. This characteristic positions Neural Networks as versatile tools capable of tackling a wide spectrum of tasks, from pattern recognition to complex decision-making processes.

4. **Rich Properties and Capabilities:**
Going beyond their computational might, Neural Networks exhibit a suite of advantageous properties, encompassing nonlinearity, adept input–output mapping, adaptivity, and proficiency in function approximation and generalization [236]. These characteristics endow neural networks with the versatility and resilience to tackle complex tasks across various domains. Their ability to capture patterns, adapt to dynamic environments, and generalize from training data makes neural networks invaluable in applications ranging from image recognition and natural language processing to control systems and decision support.

5. **Universality Spectrum:**
Neural networks manifest a universality spectrum [239], showcasing their proficiency in approximating smooth batch data that includes input, output, and potentially gradient information of a function [240]. Moreover, neural networks demonstrate adeptness in approximating derivatives of a function [241]. This broad range of capabilities positions neural networks as versatile tools capable of handling diverse types of data and functions, making them applicable across a myriad of domains and problem-solving scenarios.

6. **Integral Role in Dynamic Systems and Fault Detection:** Neural networks play a pivotal role not only in identifying dynamic systems but also in the realm of fault detection. Going beyond mere fault detection, neural networks contribute to providing a post-fault model for robotic manipulators. This model proves invaluable for effectively isolating and identifying faults and, where feasible, accommodating failures [242]. The adaptability and learning capabilities of Neural Networks empower them to navigate the intricacies of dynamic systems, offering practical solutions for fault detection and post-fault modeling in robotic applications.

3.4 Fractional-Order Neural Networks

In the past twenty years, the fusion of fractional calculus with neural networks has given rise to a significant field called fractional-order neural networks. This integration has been pivotal in both biology and computational science. Fractional-order neural networks show improved efficiency and notable advancements compared to traditional integer-order neural networks. They are particularly adept at capturing memory and hereditary characteristics present in various neuroscience processes.

Furthermore, fractional-order neural networks possess versatile computational capabilities. They efficiently process information, anticipate stimuli, and facilitate frequency-independent phase shifts in oscillatory neuronal firing. As a result, these networks hold.

3.4.1 Dynamic Analysis of Fractional Order Neural Networks

Due to the broad applications of fractional-order neural networks, significant efforts have been dedicated to advancing their theoretical foundations. In particular, there's been notable attention on the dynamic analysis of continuous fractional-order neural networks. A substantial body of literature has emerged, categorizing the dynamics of these networks into chaos, limit cycles, bifurcation, and stability aspects.

Numerous scholarly works have explored the dynamic properties of fractional-order neural networks, providing insights into various dynamical outcomes. This section offers a concise survey, summarizing the findings from different papers. The focus is on chaos, limit cycles, bifurcation phenomena, and the stability of fractional-order neural networks, contributing to a comprehensive understanding of their complex dynamics.

Chaos of Fractional Order Neural Networks

Chaos, characterized by its nonlinear and seemingly random behavior, plays a significant role in various fields such as biology, physiology, mathematics, physics, electronics, information sciences, and economics. The emergence of fractional-order neural networks has unveiled the occurrence of chaos within this framework, particularly evident in fractional-order cellular neural networks as demonstrated in [244]. This discovery has sparked scholarly interest, leading to extensive research on chaotic fractional-order neural networks [245, 246]. In these studies, researchers have adopted a common analytical approach,

manipulating the fractional order and observing resulting dynamics through numerical simulations. This method enables the identification of specific fractional order intervals, allowing differentiation of diverse dynamics within the studied systems. Such endeavors contribute to a nuanced understanding of chaotic phenomena within fractional-order neural networks, providing insights into their intricate behaviors under various parameter conditions.

To illustrate this methodology, consider a concrete example from a seminal work [245], where the dynamics of a ring neural network with 3 neurons were meticulously analyzed as follows:

$$\begin{cases} {}_0^C D_t^\alpha x_1(t) = -a x_1(t) + T_0 \sin x_1(t) + T_1 \sin x_2(t) + T_2 \sin x_3(t), \\ {}_0^C D_t^\alpha x_2(t) = -a x_2(t) + T_2 \sin x_1(t) + T_0 \sin x_2(t) + T_1 \sin x_3(t), \\ {}_0^C D_t^\alpha x_3(t) = -a x_3(t) + T_1 \sin x_1(t) + T_2 \sin x_2(t) + T_0 \sin x_3(t). \end{cases} \tag{3.9}$$

To explore the connection between the dynamics of the system described by equation (3.9) and its fractional order α, we utilize the parameters provided in [247], specifically $\alpha = 1$, $\Theta_0 = 2$, $\Theta_1 = 1$, and $\Theta_2 = -9$. By incrementing α from 0.65 to 1, system (3.9) exhibits diverse dynamics around the initial point $(0, 0, 0)^T$, including asymptotic stability, limit cycles, and chaos.

For $\alpha \in [0.65, \frac{2}{3})$, the null solution of system (3.9) demonstrates asymptotic stability. In Fig. 3.6, the trajectory of system (3.9) with $\alpha = 0.65$ converges asymptotically to the zero solution. As α increases to $\frac{2}{3} \approx 0.667$, a Hopf bifurcation occurs, resulting in the emergence of an asymptotically stable limit cycle in a neighborhood of the origin for $\alpha \in (\frac{2}{3}, 0.78]$. Within the interval $(0.78, 0.8)$, two symmetrical asymptotically stable limit cycles are observed. Eventually, the system transitions into a chaotic regime for $\alpha \in [0.8, 1)$.

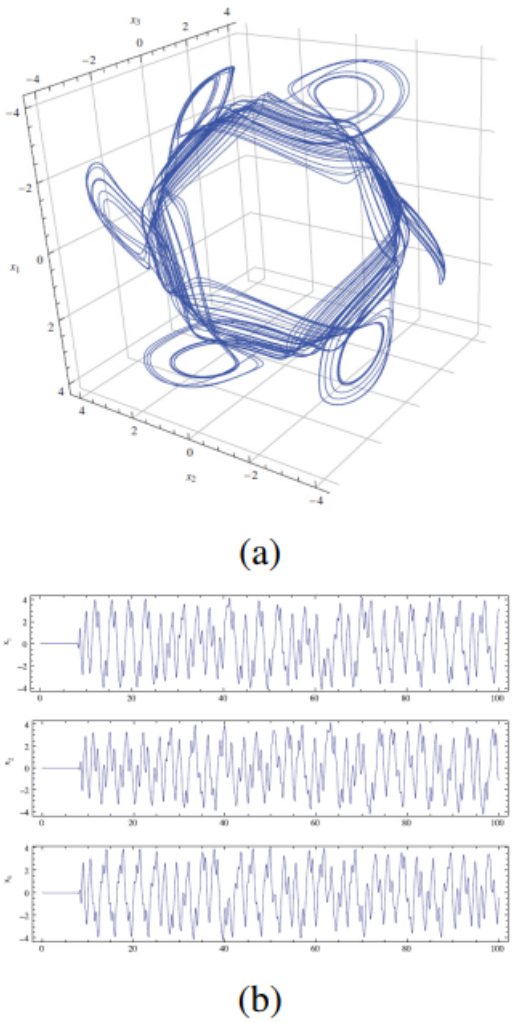

Figure 3.5: Dynamic Behavior of System (3.9) with $\alpha = 0.9$ (Chaotic).

Limit Cycle and Hopf Bifurcation of Fractional Order Neural Networks

A limit cycle, representing a distinct periodic solution within dynamic systems, holds significant implications in neuroscience and biology [248] due to its accurate depiction of

stable periodic variations. With the acknowledgment of fractional calculus in various systems such as biological, economic, social, and neural systems, discussions concerning the limit cycle of fractional-order neural networks have become common, often supported by numerical evidence [245, 249].This investigation is exemplified by visual representations in Figs. 3.7 and 7.10 in the previous subsection.

In 2009, H.A. El-Saka and colleagues proposed a condition for Hopf bifurcation in a fractional-order system [250]. This condition is particularly relevant when dealing with an n-dimensional fractional-order system:

$$ {}_0^C D_t^\alpha = f(x; a). \tag{3.10} $$

The Hopf bifurcation criterion is met when a attains the critical value $a = a^*$

$$ \begin{cases} arg[\kappa(a^*)] = \dfrac{\alpha\pi}{2}, \\ |\kappa(a^*)| = 1, \\ \dfrac{d\kappa(a^*)}{da} \neq 0. \end{cases} \tag{3.11} $$

Expanding on the aforementioned criterion, researchers have delved into Hopf bifurcation analysis for fractional neural networks in [**?**, 251].This approach has been a standard method for discussing Hopf bifurcation in fractional neural networks, both in theoretical exploration and simulation, until a groundbreaking reference [252] emerged in 2012, challenging and revising the established findings.

In the seminal work by E. Kaslik and S. Sivasundaram [252], it was emphasized that fractional-order autonomous dynamical systems lack periodic solutions. This critical observation suggests that fractional-order neural networks, conceptualized as such systems, theoretically cannot possess a limit cycle and Hopf bifurcation. Consequently, previous simulation results indicating the presence of a limit cycle in fractional-order neural networks may not hold validity. As a result, research focus has shifted, with fewer efforts directed towards exploring limit cycles and Hopf bifurcations. Instead, more scholars have shifted their attention towards understanding the stability or chaotic behavior of fractional-order neural networks.

Stability of Fractional Order Neural Networks

In the absence of comprehensive theoretical findings, there has been a surge in works related to fractional-order neural networks aiming to explore chaos and limit cycles through numerical simulations. However, with the assertion of the non-existence of a limit cycle in fractional-order neural networks as established in [252], the research landscape has undergone a shift. More recent investigations are now steering back towards theoretical innovations, particularly focusing on advancing the understanding of stability in fractional-order neural networks [253, 254, 255].

To enhance comprehension in the exploration of the stability of fractional-order neural networks, let's consider the model characterized by:

$$ {}_0^C D_t^\alpha x_i(t) = -c_i x_i(t) + \sum_{j=1}^{n} a_{ij} f_j(x_j(t)) + I_i, \tag{3.12} $$

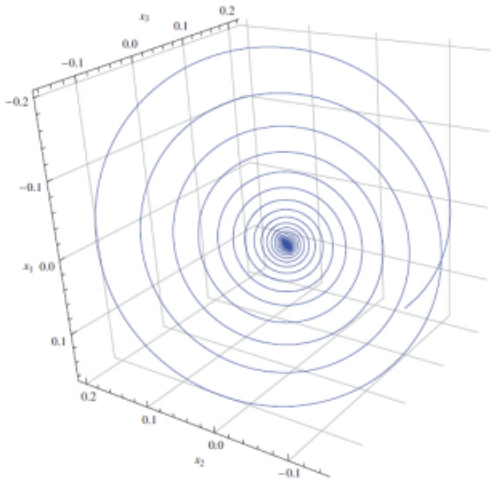

Figure 3.6: Asymptotically Stability of system (3.9) for $\alpha = 0.65$.

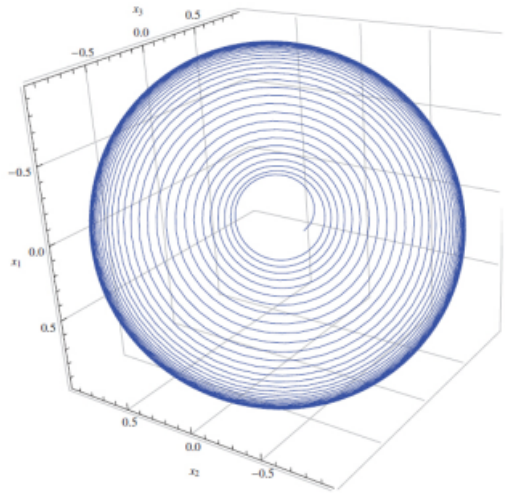

Figure 3.7: Asymptotically stable limit cycle of neural networks (3.9) for $\alpha = 0.67$.

here, $i = 1, 2, \ldots, n$, where n signifies the number of units within the neural network. The state of the i-th unit at time t is denoted by $x_i(t)$, and f_j represents the activation function of the j-th neuron. The parameter $c_i > 0$ determines the rate at which the i-th neuron resets its potential to the resting state when disconnected from the network. Additionally, a_{ij} stands for the constant connection weight of the j-th neuron on the i-th neuron, and I_i corresponds to the constant external inputs.

Subsequently, we can represent the system described by equation (3.12) in a vectorized form as follows:

$$ {}_0^C D_t^\alpha x(t) = -Ax(t) + Df(x(t)) + I, \tag{3.13} $$

where $A = \text{diag}\{c_1, c_2, \ldots, c_n\}$, $D = (a_{ij})_{n\times n}$, $f(x) = (f_1(x_1), f_2(x_2), \ldots, f_n(x_n))^T$, $I = (I_1, I_2, \ldots, I_n)^T$. Examining the stability of fractional-order neural networks typically entails linearizing system (3.13) and deducing its local stability conditions. However, it's

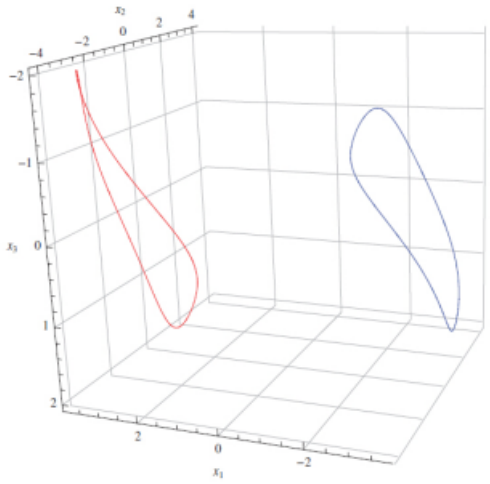

Figure 3.8: The Evolution of System (3.9) with $\alpha = 0.79$ (Featuring Two Asymptotically Stable Limit Cycles).

crucial to recognize that the linearized stability method primarily offers insights into local stability. In the quest for global stability conditions, the Mittag-Leffler stability method, also referred to as the Lyapunov direct method, has garnered prominence and provided more extensive stability outcomes. Furthermore, recent years have seen the emergence of alternative methods. To elaborate, a detailed enumeration of these methods is presented below.

- **Linearized stability method** Let us commence by presenting the widely acknowledged necessary and sufficient condition for the stability of linear fractional-order systems. Consider an n-dimensional linear fractional-order system:

$$ {}_0^C D_t^q x = Dx, \tag{3.14}$$

here, $0 < q < 2$ denotes the fractional order, and $D \in \mathbb{R}^{n\times n}$ is a constant matrix. The linear autonomous fractional-order system described above achieves asymptotic stability if and only if:

$$ |\arg(\kappa)| > \frac{q\pi}{2}, \quad \forall \kappa \in \sigma(D), \tag{3.15}$$

here, $\sigma(D)$ represents the set of all eigenvalues of the matrix D. For the case when $0 < q < 1$, an equivalent necessary and sufficient condition for the aforementioned inequality is:

$$ |\Im(\kappa)| > \Re(\kappa) \tan\left(\frac{q\pi}{2}\right), \quad \forall \kappa \in \sigma(D). \tag{3.16}$$

In the context of fractional-order neural networks described by (3.13), the linearized stability method can be articulated as follows:

1. Determine the steady states $\bar{x}_s$ of fractional-order neural networks described by (3.13), which are solutions to:

$$ -A\bar{x} + Df(\bar{x}) + I = 0. \tag{3.17}$$

2. For a given $\bar{x}$, compute its Jacobian matrix using the expression:
$$J(\bar{x}) = -A + DDf(\bar{x}), \tag{3.18}$$
where $Df(\bar{x}) = diag\{f_1'(\bar{x}_1), f_2'(\bar{x}_2), \ldots, f_n'(\bar{x}_n)\}$.
3. If all eigenvalues κ_s of the Jacobian matrix $J(\bar{x})$ adhere to:
$$|\arg(\kappa_s)| > \frac{q\pi}{2}, \quad \forall \kappa_s \in \sigma(J(\bar{x})), \tag{3.19}$$
the steady state $\bar{x}$ achieves local asymptotic stability.

While the linearized stability method proves straightforward and effective for assessing local stability at a steady state, it falls short of providing insights into global stability due to the inherent nonlinearity of fractional-order neural networks described by (3.13).

- **Mittag-Leffler stability method** To establish the global stability of fractional-order neural networks described by (3.13), one of the commonly employed methods is the Mittag-Leffler stability method, also known as the Lyapunov direct method. When dealing with a nonlinear fractional-order system:
$${}_0^C D_t^\alpha x(t) = f(t, x(t)). \tag{3.20}$$
If a steady state $\bar{x} = 0$ is present in the solution of the nonlinear fractional-order system, it is deemed Mittag-Leffler stable if:
$$\|x(t)\| \leq [m(x_0)E_a(-\kappa(t)^\alpha)]^b, \tag{3.21}$$
here, $\kappa > 0$, $b > 0$, $\|\cdot\|$ denotes an arbitrary norm, and $m(x) \geq 0$ ($m(0) = 0$) adheres to the locally Lipschitz condition on $x \in \mathbb{R}^n$ with Lipschitz constant m_0, $E_a(\cdot)$ is a Mittag-Leffler function. Mittag-Leffler stability implies asymptotic stability for fractional-order systems, i.e., $\lim_{t\to+\infty} \|x(t)\| = 0$. To establish Mittag-Leffler stability, Y. Li, Y.Q. Chen, and I. Podlubny proposed a significant sufficient condition known as the Lyapunov direct method, outlined as follows:

- **(Fractional-order) Lyapunov direct approach [256]:** The equilibrium $\bar{x} = 0$ for the previously mentioned nonlinear fractional-order system achieves Mittag-Leffler stability under the presence of positive constants $\alpha_1, \alpha_2, \alpha_3, a, b$ and a continuously differentiable function $V(t; x(t))$ that complies with the following conditions:
$$\begin{aligned} &\alpha_1\|x\|^a \leq V(t; x(t)) \leq \alpha_2\|x\|^{ab}, \\ &{}_0^C D_t^q V(t; x(t)) \leq -\alpha_3\|x\|^{ab}, \end{aligned} \tag{3.22}$$
Here, $t \geq 0$, $q \in (0, 1)$, $V(t; x(t)) : [0, +\infty) \times D \to \mathbb{R}$ adheres to the locally Lipschitz condition on x, where $D \subset \mathbb{R}^n$ is a domain containing the origin. IIf these assumptions are valid universally across $\mathbb{R}^n$, the equilibrium $\bar{x} = 0$ achieves global Mittag-Leffler stability.

In 2014, a pair of inequalities were introduced, offering a potent tool for selecting suitable Lyapunov functions. The two inequalities [257, 258]are formulated as follows:
$$\begin{aligned} &{}_0D_t^q|x(t^+)| \leq \mathrm{sgn}(x(t))\,{}_0D_t^q|x(t)|, \quad \forall q \in (0, 1), \\ &\frac{1}{2}\,{}_0D_t^q x^2(t) \leq x(t)\,{}_0D_t^q x(t), \quad \forall q \in (0, 1), \end{aligned} \tag{3.23}$$

Here, $x(t) \in \mathbb{R}$ represents a continuous and differentiable function. Utilizing these two inequalities, $\|x\|_1$ (or $\sum_{i=1}^{n} \beta_i |x_i|$, $\beta_i > 0$) and $\|x\|_2^2$ (or $x^T P x$, P is positive definite) emerge as effective Lyapunov functions for scrutinizing the global stability of fractional-order neural networks (3.13). The corresponding stability outcomes are delineated in [257, 259]. These studies consistently provided conditions ensuring the existence and uniqueness of steady states in fractional-order neural networks (3.13) through the contraction mapping theorem. Subsequently, they derived global stability conditions using the Lyapunov direct method.

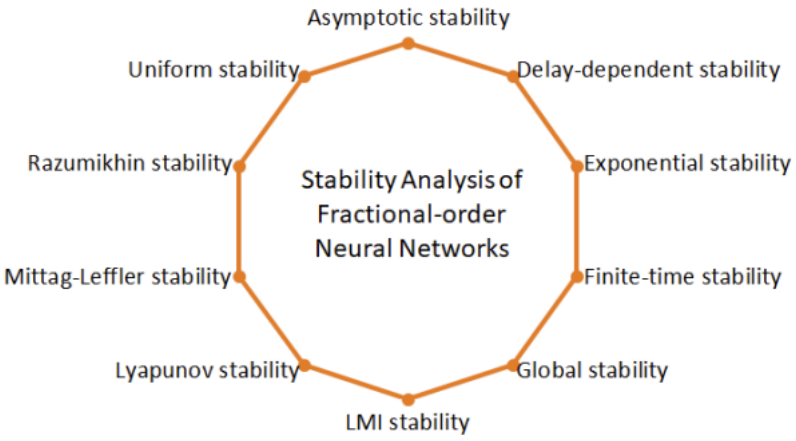

Figure 3.9: Diverse Stability Analysis Methods Employed in Fractional-Order Neural Networks.

3.4.2 Application of Fractional Neural Networks

Neural networks integrated with fractional calculus have been extensively employed in various domains such as function approximation, chaos characterization, estimation, global dissipativity, periodicity, and heat transfer modeling. Researchs have extended across diverse fields including medicine, image processing, encryption, robotics, and beyond. This section the primary applications of fractional neural networks are explored, comprising two main areas where fractional calculus plays a pivotal role.

Digital Image Processing

In the topic of digital imagery, which manifests in two-dimensional form, an array of digital picture elements constitutes the visual landscape. To refine and manipulate this visual data for a multitude of applications, digital image processing emerges as a requisite. Figure 3.10 delineates the sequential procedures integral to image processing [260]. The integration of fractional calculus with supplementary parameters introduces an additional layer of flexibility to optimization processes. Consequently, fractional calculus assumes a principle role across various stages of digital image manipulation. Within scholarly literature, Fractional Neural Networks have emerged as formidable tools for an array of

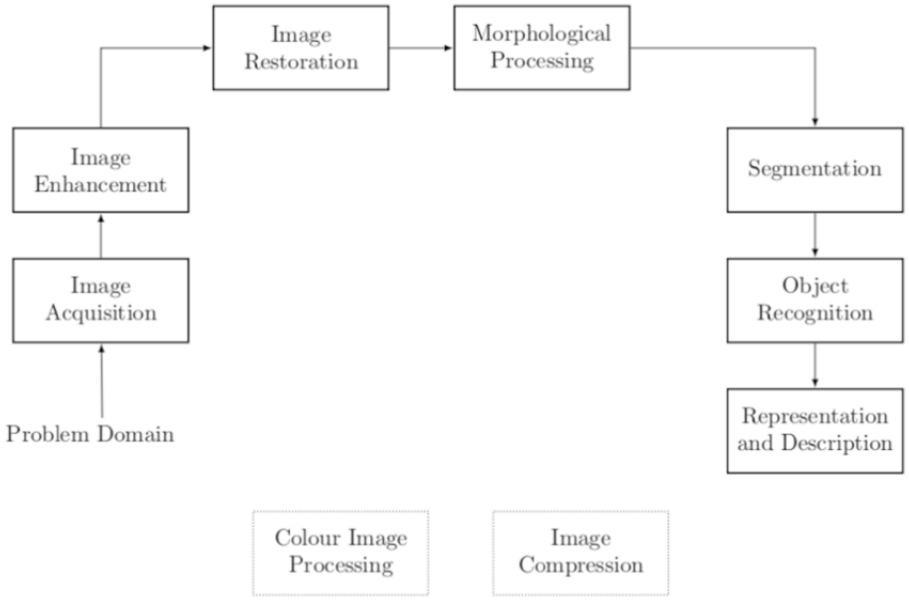

Figure 3.10: Image processing steps Gonzalez and Woods (2009).

image processing tasks, including but not limited to noise mitigation, image encryption, and image refinement facilitated by diverse fractional derivatives.

Biomedical Engineering

In the study [261], a novel approach employing a deep-convolution long-short term memory network was developed to mitigate artifacts in EEG signals. To optimize weight selection and updating processes, the researchers utilized a hybrid algorithm called Optimum Cat Swarm Fractional Calculus Optimization, which integrates fractional calculus with cat swarm optimization. This innovative algorithm harnesses the strengths of both fractional calculus and cat swarm optimization to enhance the efficacy of artifact removal in EEG signals.

Finance

In [262], a novel approach involving Neural Networks was introduced to model financial systems. Leveraging the distinctive characteristics and adaptability of fractional order differences, this method accommodated the inherent complexities of financial data. To address the influence of noise disturbances on financial assets, a stochastic term was incorporated into the model. Additionally, impulsive perturbations and a time delay parameter were introduced to regulate the dynamic behavior of the model, with stability analysis conducted using the fractional Lyapunov method.

Conventional forecasting methods often fall short in accurately predicting stock market prices. However, in [263], a groundbreaking solution emerged. They proposed an innovative approach that combines a Long Short-Term Memory network with fractional calculus to forecast fluctuations in financial markets effectively. By integrating the Autoregressive Fractional Integrated Moving Average model with Long Short-Term Memory, they developed a robust recurrent network capable of mitigating volatility and prevent-

ing overfitting. Performance evaluation metrics such as mean absolute error, root mean squared error, and mean absolute percentage error were utilized to assess the model's accuracy, revealing an impressive 80 percent improvement over traditional methods.

[264] introduced a synchronization scheme aimed at achieving design and antiphase synchronization between two fractional order Cellular Neural Networks and the financial system. Meanwhile, [265] proposed an innovative hybrid model that combines Principal Component Analysis with Artificial Neural Network techniques. By incorporating fractional calculus, this model demonstrated remarkable efficacy in predicting stock market indexes and foreign exchange rates. Furthermore, the utilization of ANN expedited predictions, while the application of the wavelet transform ensured consistent frequency tracking.

Controller

A controller plays a crucial role in ensuring stability and synchronization within Fractional-order Artificial Neural Networks. Managing nonlinear systems also demands effective controllers, and designing one for fractional-order systems presents a significant challenge. In the literature, various types of controllers have been proposed, among which Sliding Mode Controller holds prominence.

Sliding Mode Controller stands out as a widely used controller for nonlinear systems due to its ability to address two critical challenges: stability and robustness. It has found applications in diverse fields such as robotic manipulators, process control, defense, and power electronics. The structure and implementation of Sliding Mode Controller can be tailored to the system dynamics, rendering it less sensitive to disturbances. Numerous designs integrating neural networks with sliding mode controllers have been proposed by researchers, leveraging the benefits of fractional calculus to enhance controller design freedom and accuracy compared to integer-order systems.

Fractional-order Sliding Mode Controller, coupled with adaptation laws, has been proposed to synchronize Fractional-order Neural Networks utilizing the Lyapunov theorem. Fractional-order adaptation laws facilitate online system parameter estimation for unknown parameters. Stable Fractional-order Neural Networks of the Hopfield type have been developed using optimal discontinuous control techniques, leveraging properties and theorems such as the Mittag-Leffler function for system stability. In various studies, Sliding Mode Controlle have been effectively employed to achieve projective synchronization of Fractional-order Neural Networks.

Furthermore, in the pursuit of Global Projective synchronization of two non-identical Fractional-order Neural Networks within finite time, researchers have adopted a sliding mode controller with fractional calculus. These studies demonstrate the properties of global asymptotic stability over finite time and calculate the synchronization time required for achieving this objective.

System Identification

In [266] and [267], the fusion of Fractional Calculus and Neural Networks has been explored as a powerful tool for system identification. [266] introduced an algorithm combining Least Mean Square with a newly developed variant to enhance the accuracy of

nonlinear system identification, exemplified by the Van der Pol-Dung oscillator. They employed a Functional Link Artificial Neural Network filter to generate input samples with varying time shifts and investigated the computational timing of different algorithms.

[267] proposed an Neural Networks learning algorithm based on G-L as a fractional operator for system identification. They modified the Gradient Descent algorithm to identify three distinct systems and compared the model's performance in terms of Root Mean Square Error and goodness of fit against other system identification models. Their model requires fewer parameters and achieves higher accuracy.

[268] introduced a hybrid model of Radial Basis Function Neural Network and fractional-order system for nonlinear dynamic system identification. The identification process involves two stages: the first stage identifies the structural parameters of FOS in the frequency domain, while the second stage computes the Radial Basis Function Neural Network weights and fractional-order system parameters. Lyapunov stability theory is employed to ensure system stability.

In [269], a novel Neural Network methodology for system identification is proposed, utilizing optimal parameters to mitigate uncertainties between the real system and the proposed model. A three-layered neuronal compensation scheme is employed to uncover the relationship between derivative fractality and the Caputo fractional derivative.

3.4.3 Recent Advances in Different Fractional Neural Network Models

In recent years, significant strides have been made in the development and exploration of various fractional neural network models. These advancements have ushered in a new era of research, pushing the boundaries of traditional neural network architectures. From novel formulations to innovative applications, researchers have been actively engaged in enhancing our understanding and leveraging the capabilities of fractional neural networks.

In [270], researchers delve into discrete fractional-order neural networks using a Fuzzy Lyapunov synthesis approach, specifically applied to model heat transfer dynamics. Moving on to [271], a unique class of fractional-order neural networks is investigated, focusing on α-exponential stability and introducing a novel fractional-order method for analyzing network stability, including chaotic synchronization.

Moreover, [272] tackles fractional-order neural networks with delays, establishing conditions for their uniform stability, while [273] explores finite-time stability using Caputo fractional derivatives, Gronwall theorem, Laplace transforms, and Mittag-Leffler approximation approaches.

In parallel, [274] scrutinizes fractional-order neural networks with delayed systems, with a particular focus on finite-time stability and novel delay-dependent conditions. Transitioning to [275], researchers analyze fractional-order neural networks based on Riemann-Liouville with discrete and distributed delays, rigorously examining asymptotic stability.

Expanding the scope, [276] contributes to stability analysis of fractional-order neural networks with and without delay using fractional approaches such as Lyapunov and Razumikhin. Conversely, [277] zooms in on fractional-order neural networks with double

leakage delays, conducting a thorough analysis of their stability and bifurcation, including Hopf bifurcation.

Moving to [278], the paper tackles parameter synchronization and identification in fractional-order neural networks with time delays, employing analytical techniques and adaptive control methods. Furthermore, [279] investigates global projective synchronization of fractional-order neural networks, utilizing a combination of open-loop and adaptive control strategies.

In contrast, [280] focuses on non-identical fractional-order neural networks, employing sliding mode control for global projective synchronization and considering uncertainty parameters for memristor-based neural networks with fractional-order multiple time-delays.

Delving into adaptive projective synchronization, [281] analyzes time-delayed fractional-order neural networks, utilizing efficient hybrid control strategies. Transitioning, [282] studies the synchronization dynamics of uncertain fractional-order neural networks with disturbed parameters, introducing an adaptive synchronization controller based on the fractional-order extension of the Lyapunov stability criterion.

In [283], Global Mittag-Leffler's synchronization is investigated in fractional-order neural networks with discontinuous activation functions, providing insights into studying such networks and establishing requirements for asymptotic stability.

Continuing exploration, [284] delves into a class of neural networks with fractional-order derivatives, introducing conditions based on Krasnoselskii's fixed point theorem and inequality techniques. In [285], researchers present LMI stability conditions for linear and non-linear fractional-order systems, conducting a global stability analysis of fractional-order neural networks.

Lastly, [286] focuses on the parameter estimation problem of fractional-order neural networks, employing identification based on the synchronization method, introducing parameter update laws, and adaptive control for simultaneous parameter identification and synchronization.

Fractional-Order Hopfield Neural Networks

Depicted in Fig. 3.11, the design of the Hopfield network model integrates both linear and nonlinear components, forming a network with a size denoted by N. In this architecture, 'Block A' replicates the synaptic and nonlinear traits observed in biological neurons, while 'Block B' specifically mimics the time-delay aspects intrinsic to biological neurons. The equations governing the model, as outlined in [287], are expressed as follows:

$$\begin{aligned} A_i \frac{dP_i}{dt} &= \sum_{j=1}^{N} \left(\frac{1}{R_{ij}}\right) V_j - P_i \left(\frac{1}{R_{i0}} + \sum_{j=1}^{N} \frac{1}{R_{ij}}\right) + I_i, \\ P_i &= \left(\frac{1}{\kappa}\right) \phi_i^{-1} V_i, \end{aligned} \tag{3.24}$$

here, P_i represents the input of the operational amplifier at the $i-$th neuron, V_i signifies the output of the operational amplifier at the $i-$th neuron, and κ denotes the learning rate.

The governing equations for the fractional-order manifestation of the Hopfield network model, derived from Eqs. (3.24), are expressed as:

$$\begin{aligned} A_i D^{\alpha} &= \sum_{j=1}^{N} \left(\frac{1}{R_{ij}}\right) V_j - P_i \left(\frac{1}{R_{i0}} + \sum_{j=1}^{N} \frac{1}{R_{ij}}\right) + I_i, \\ P_i &= \left(\frac{1}{\kappa}\right) \phi_i^{-1} V_i, \end{aligned} \tag{3.25}$$

here, $d^{\alpha} dt^{\alpha}$ represents the fractional-order derivative of order $\alpha \in (0, 1)$

The exploration of Hopf bifurcation in Fractional-Order Neural Networks (FONNs) began in 2011 [288]. Researchers introduced a new type of neural network model, called the Fractional-Order Hopfield Neural Network, by modifying the standard capacitor in Hopfield neural networks. They aimed to understand how changing the fractional order affects the network's behavior. In 2012, another study focused on stability in these networks, looking at specific parameters that influence their behavior [289]. This research revealed that as the fractional order increases, the dynamics of the networks become more complex, sometimes leading to chaotic behavior.

Another study in 2012 proposed using a mathematical function called the Mittag-Leffler function to synchronize certain types of chaotic neural networks, including the Fractional-Order Hopfield Neural Network [290]. Around the same time, researchers were exploring different dynamical behaviors in these networks, finding a wide range of interesting phenomena. In 2014, researchers looked specifically at stability in Fractional-Order Hopfield Neural Networks with time delays [291]. They introduced two new types of network structures and derived conditions for when these networks remain stable.

In 2015, researchers investigated the existence of solutions and stability conditions using a mathematical framework called Filippov solutions [292]. They found that under certain conditions, the equilibrium points of the networks may not be unique. Then, in 2016, researchers developed a new method using linear matrix inequalities to analyze the stability of these networks [293]. This method provided a comprehensive understanding of how different factors influence the stability of Fractional-Order Hopfield Neural Networks. Overall, these studies highlight the complex dynamics and stability of these networks, shedding light on their behavior under different conditions.

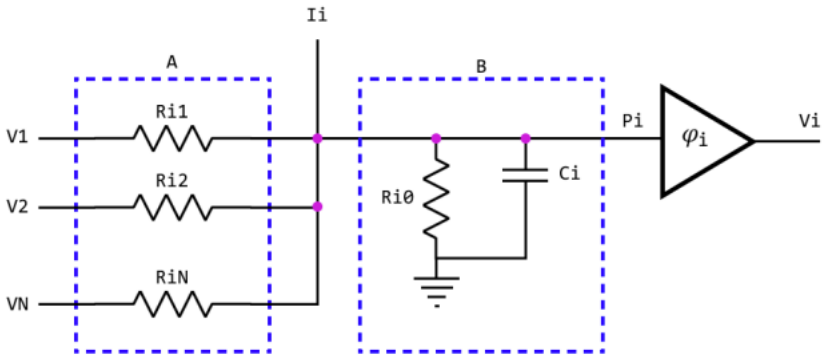

Figure 3.11: Design of the Hopfield Network Model.

Fractional-Order Cellular Neural Network

In Cellular Neural Networks, the cell serves as the fundamental building block, as depicted in Fig. 3.12. It's essential to note that each cell in a Cellular Neural Networks only connects with its neighboring cells. The equations governing the dynamics of the circuit, including input, state, and output equations, are detailed as follows [294]:

$$\begin{aligned} u_{ij}(t) &= E_{ij}, \\ C\frac{dx_{ij}(t)}{dt} &= -\frac{1}{Rx}x_{ij}(t) + \sum_{A(k,l)\in Nr(i,j)} D(i,j;k,)y_k(t) \\ &\quad + \sum_{A(k,)\in Nr(i,j)} B(i,j;k,)u_k(t) + A(i,j;k,)x_k(t) + I, \\ y_{ij}(t) &= \frac{1}{2}(|x_{ij}(t)+1| - |x_{ij}(t)-1|), \end{aligned} \tag{3.26}$$

here, $A(i,j)$ denotes the cell at the $i-$th row and $j-$th column. The variables u_{ij}, x_{ij}, and y_{ij} represent the input, state, and output voltages, respectively, of each neighboring cell $A(k,)$. The voltage-controlled current sources are defined as:

$$I_{xy}(i,j;k,) = D(i,j;k,)y_k, \tag{3.27}$$

$$I_{xu}(i,j;k,) = B(i,j;k,)u_k, \tag{3.28}$$

$$I_{xx}(i,j;k,) = A(i,j;k,)x_k, \tag{3.29}$$

In equations (3.27), (3.28), and (3.29), D, B, and A serve as coefficients, known as cloning templates. The neighborhood $Nr(i,j)$ of cell $A(i,j)$ is defined as:

$$Nr(i,j) = \{A(k,) : \max(|k-i| - |-j|) \le r\}, \tag{3.30}$$

From the depicted circuit in Fig. 2, the governing equations for the fractional-order form of CNN are given by:

$$\begin{aligned} u_{ij}(t) &= E_{ij}, \\ {}^{C}D^{\alpha}x_{ij}(t) &= -\frac{1}{Rx}x_{ij}(t) + \sum_{A(k,)\in Nr(i,j)} D(i,j;k,)y_k(t), \\ &\quad + \sum_{A(k,)\in Nr(i,j)} B(i,j;k,)u_k(t) + A(i,j;k,)x_k(t) + I \\ y_{ij}(t) &= \frac{1}{2}(|x_{ij}(t)+1| - |x_{ij}(t)-1|), \end{aligned} \tag{3.31}$$

here, D^{α} represents the fractional-order derivative of order $\alpha \in (0,1)$.

In recent years, fractional-order cellular neural networks have seen notable advancements, offering practical solutions through innovative techniques and learning algorithms. For instance, in 2012, researchers introduced a fractional-order four-cell cellular neural networks architecture aimed at enhancing the security of chaotic communication systems [295]. Building on this, subsequent studies in 2014 utilized the fractional Lyapunov method and Mittag-Leffler functions to extend fractional-order cellular neural networks to accommodate time-varying delays [296].

In 2018, fractional-order adaptive laws were applied to address multiple-time delays and fractional-order linear delayed systems, paving the way for a deeper understanding

of stability theory in controlling fractional-order cellular neural networks, regardless of sector nonlinearities [297]. Advancements continued in 2020, where researchers explored a fractional-order differential inequality with time delays, leveraging feedback control to analyze the complex structure and robust synchronization of fractional-order cellular neural networks under linear coupling delays [298].

Moving forward, in 2021, the contraction mapping principle was employed alongside fractional-order cellular neural networks to investigate asymptotically w-periodic oscillations in these networks [299]. By partitioning the system and exploring synchronization and stability issues, researchers uncovered novel insights using simplified inequalities with quadratic terms [300]. This approach, coupled with the development of Lyapunov-Krasovskii functionals, promises to further enhance our understanding of fractional-order cellular neural networks dynamics.

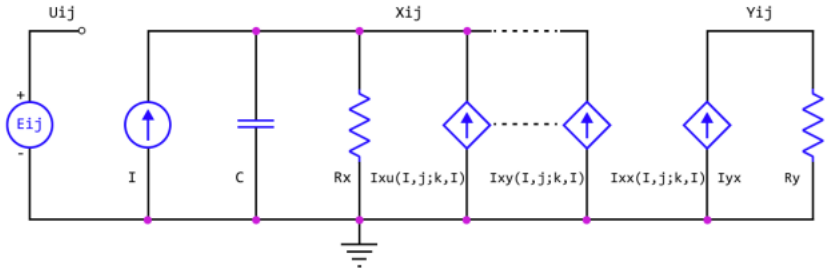

Figure 3.12: Structure of the Cellular Network Model.

Fractional-Order Memristor-Based Neural Networks

Memristors, remarkable electronic devices mimicking resistors while retaining charge memory, have transformed intricate neuromorphic setups like cellular neural networks. As nano solid-state switches, memristors mitigate memory and communication hurdles associated with traditional CMOS technology.

Their non-volatile nature spurred the advent of memristor crossbar arrays, offering dense, parallel computing useful in MVM, search tasks, and bitwise operations. Particularly in cellular neural networks, memristors expedite neural network layers, mitigating concerns regarding memory constraints and communication inefficiencies [301, 302].

In 2014, stability conditions were devised for memristor-based fractional-order neural networks, probing dynamic behaviors, equilibrium uniqueness, and network synchronization [303]. Progress in synchronization and stability criteria, along with global boundedness, employed techniques like Gronwall inequality and Laplace transforms.

Advancements extended to attractivity, global boundedness, synchronization conditions, and parameter uncertainty in memristor-based fractional-order neural networks. Innovations in 2020 tackled synchronization challenges, introducing methods to counter fixed-time synchronization, manage reaction-diffusion and time delay, and ensure Mittag-

Leffler synchronization [311].

Furthermore, new theorems enhanced comprehension of fractional-order stability in quaternion-valued systems. Utilizing techniques such as Filippov solutions, Laplace transforms, Mittag-Leffler functions, and Generalized Gronwall inequality, insights into dynamic behaviors, stability, and passivity of memristor-based systems were gained, fostering adaptability and reducing conservatism [312, 313].,

Fractional-Order Complex Valued Neural Networks

Exploring stability in fractional-order complex-valued neural networks has garnered attention in recent years. In 2014, a groundbreaking study introduced a novel fractional-order complex-valued neural network, leveraging fractional-order differential equations to assess stability. This approach integrated memristor-based neural networks, offering insights into network stability [314].

In parallel, another research initiative [315] delved into complex-valued recurrent neural networks, unveiling a model that identified appropriate activation functions for diverse complex processes. This model, featuring continuous fractional-order complex-valued neural networks with a time-delay algorithm, enriched the understanding of network dynamics.

Moreover, a study in [316] investigated the dissipativity of neural networks incorporating time delays, employing a fractional-order complex-valued neural network framework. This analysis utilized Lyapunov functions and fractional Halanay inequality, alongside Caputo fractional-order differential equations. Such a holistic approach facilitated stability exploration in both linear and non-linear systems, extending its applicability to economic systems.

3.5 Discrete Fractional-Order Neural Networks

In recent years, the study of Discrete Fractional Neural Networks has gained significant traction due to their potential to model and understand complex real-world phenomena. The motivation behind delving into Discrete Fractional Neural Networks lies in their ability to capture the intricate dynamics and non-linear behaviors exhibited by various systems in fields such as biology, physics, economics, and engineering.

At their core, Discrete Fractional Neural Networks are characterized by their discrete-time nature, where system dynamics evolve in distinct time steps. This discrete formulation enables the modeling of systems with inherent time lags and discrete events, making Discrete Fractional Neural Networks particularly well-suited for capturing real-world phenomena exhibiting temporal dependencies.

The mathematical representation of Discrete Fractional Neural Networks involves formulating discrete-time dynamical equations that describe the evolution of the network states over time. These equations often incorporate fractional-order operators such as: Delta fractional-order operator, Nabla fractional-order operator and h-discrete fractional operators, allowing for the modeling of memory and long-range dependencies inherent in

many real-world systems.

One of the primary motivations for studying Discrete Fractional Neural Networks is their capability to provide a more accurate representation of dynamic systems with memory and long-range dependencies. Traditional neural networks often struggle to capture such phenomena adequately, especially in systems where past states significantly influence current behavior. Discrete Fractional Neural Networks , with their ability to incorporate fractional-order dynamics, offer a promising avenue to address this limitation by enabling the modeling of memory effects and complex temporal dependencies more effectively.

Moreover, Discrete Fractional Neural Networks hold relevance in modeling real-world phenomena due to their ability to simulate systems exhibiting chaotic behavior. Chaotic systems are prevalent in nature and can be found in weather patterns, population dynamics, and financial markets, among others. Understanding and predicting the behavior of chaotic systems is crucial for various applications, ranging from weather forecasting to stock market analysis. Discrete Fractional Neural Networks provide a powerful tool for modeling and analyzing chaotic systems, offering insights into their underlying dynamics and aiding in prediction and control tasks.

Furthermore, Discrete Fractional Neural Networks offer practical applications in synchronization phenomena observed in coupled systems. Synchronization plays a vital role in various natural and artificial systems, including neuronal networks, power grids, and communication networks. By studying Discrete Fractional Neural Networks, researchers can gain insights into the mechanisms underlying synchronization phenomena and develop techniques for controlling and optimizing synchronized behavior in complex systems.

3.5.1 Stability in Discrete Fractional-Order Neural Networks

In the topic of discrete fractional neural networks, issues like oscillation, divergence, or instability often arise due to time lags. Moreover, dynamic systems grapple with stability challenges. Examining the existence, uniqueness, and global asymptotic stability of equilibrium points stands as a focal point in nonlinear circuit theory. A discrete fractional neural networks with global asymptotic stability ensures the computation of the global optimal solution, regardless of initial conditions, mitigating the risk of erroneous suboptimal responses. However, the presence of multiple stable equilibrium points poses a drawback, potentially leading to inaccurate suboptimal outcomes. To mitigate such risks and ensure convergence towards the global optimum solution, a singular globally asymptotically stable equilibrium point is imperative.

Extensive literature explores stability analysis for discrete fractional neural networks, particularly considering time lags and fractional-order-based neural networks. This section presents research on stability in discrete fractional neural networks. Various stability methodologies, including the discrete fractional Lyapunov method, Razumikhin-type theorem, Barbalat lemma, Matrix measure approach, extended impulsive difference inequality, Cauchy–Schiwartz inequality, and others, are employed to achieve stability in discrete fractional neural networks.

These stability methodologies are applied across different types of neural networks, employing various fractional order differences. Most analyses utilize Caputo, R-L, and G-

L differences in fractional orders. The stability achieved in these diverse types of discrete fractional neural networks may be robust, globally robust, asymptotic, uniform, exponential, finite-time, or Mittag-Leffler. The methodologies employed to attain stability in discrete fractional neural networks are elucidated as follows:

Stability via Mittag–Leffler Functions

Upon reviewing the literature, it becomes apparent that the combination of Mittag–Leffler functions (either one or two-sided) and various inequality theorems or properties, such as the discrete fractional Lyapunov method, can effectively ensure stability. As demonstrated in [317], Mittag–Leffler stability exhibits faster convergence compared to exponential stability, particularly near the origin.

Uniform Stability

The concept of uniform stability for discrete fractional-order complex valued neural networks has been proposed in [318]. This study explores two distinct forms of activation functions and leverages the Banach fixed point theorem to establish stability for neural networks.

Asymptotic Stability

Asymptotic stability indicates that solutions starting sufficiently close to the equilibrium not only remain proximate but also eventually converge to the equilibrium, as outlined in [319].

Stability within Finite Time

[320] introduce finite-time stability, characterized by faster convergence, enhanced robustness, and effective disturbance rejection properties.

Exponential Stability

[321] propose a novel fractional-order difference inequality, enabling the attainment of exponential stability. The convergence rate of the network is determined by the order of the differential equation.

3.5.2 Chaos in Discrete Fractional-Order Neural Networks

Chaos in discrete fractional neural networks often manifests as complex, irregular behavior in the network dynamics, challenging conventional methods of analysis. Numerical methods play a pivotal role in detecting and understanding chaos in discrete fractional neural networks, offering insights into the underlying dynamics and system behavior.

Lyapunov exponents, a fundamental tool in chaos theory, provide a quantitative measure of the divergence of nearby trajectories in the network phase space. By calculating the Lyapunov exponents of discrete fractional neural networks, researchers can assess the system's sensitivity to initial conditions and identify regions of chaotic behavior.

Bifurcation diagrams offer another powerful technique for characterizing chaos in discrete fractional neural networks. These diagrams visualize changes in the network

dynamics as system parameters are varied, revealing the emergence of complex behavior such as periodic orbits, bifurcations, and chaotic attractors. By systematically analyzing bifurcation diagrams, researchers can elucidate the underlying mechanisms driving chaos in discrete fractional neural networks and gain insights into the system's behavior across different parameter regimes.

Combining these numerical methods enables a comprehensive understanding of chaos in discrete fractional neural networks. Lyapunov exponents provide quantitative measures of chaos, while bifurcation diagrams offer qualitative insights into the system's behavior. Together, these tools facilitate the identification and characterization of chaos in discrete fractional neural networks, paving the way for further exploration and application in various domains.

3.5.3 Synchronization in Discrete Fractional-Order Neural Networks

Synchronization in neural networks refers to the phenomenon where individual neurons or groups of neurons exhibit coordinated behavior over time. It signifies the emergence of ordered patterns of activity, characterized by the alignment of phase or frequency among network components. Synchronization is of paramount importance in neural systems as it underlies essential cognitive functions such as information processing, memory formation, and sensory perception. Moreover, synchronization facilitates communication and signal propagation within the brain, enabling efficient coordination of neuronal activity across different brain regions.

Achieving synchronization in discrete fractional neural networks involves employing various techniques to ensure coordinated behavior among network elements. Adaptive control techniques offer a dynamic approach to synchronization by continuously adjusting network parameters in response to changing conditions. These techniques leverage feedback mechanisms to regulate the network's dynamics and promote synchronization among interconnected neurons. By adapting to external stimuli and internal states, adaptive control techniques enable discrete fractional neural networks to maintain stable synchronization in the presence of disturbances or uncertainties.

Feedback techniques, on the other hand, utilize the information from network states to modulate the strength of connections or adjust the network's structure to promote synchronization. By providing feedback signals based on the deviation from desired synchronization patterns, these techniques enable discrete fractional neural networks to self-organize and achieve desired coordination among neurons. Feedback mechanisms play a crucial role in regulating network dynamics and ensuring robust synchronization in discrete fractional neural networks under varying conditions.

These synchronization techniques have been applied across various types of discrete fractional-order neural networks. Notably, the majority of research endeavors have focused on discrete Caputo and R-L-based fractional defference neural networks. Synchronization achievements in these discrete fractional neural networks encompass quasi, asymptotic, Mittag-Leffler, finite-time, exponential, and projective synchronization. Several methods for achieving synchronization of discrete fractional neural networks are delineated as follows:

Projective Synchronization

Projective synchronization facilitates rapid communication and possesses a proportional characteristic, making it a favored method over others ([322]).

Global Mittag-Leffler Synchronization

Utilizing the global Mittag-Leffler function contributes to achieving synchronization in discrete fractional neural networks ([323][324]).

Adaptive Synchronization

discrete fractional neural networks adaptive synchronization is achieved through adaptive and feedback control mechanisms ([325]).

Exponential Synchronization

[326] achieve exponential synchronization of discrete fractional-order memristive neural networks incorporating time delay. An exponential function is employed to study the fractional-order difference system, considering various cases post-impulsive effects implementation.

Global Synchronization

[327] implement two types of output feedback controllers to achieve Global synchronization of discrete fractional-order neural networks.

Chaos Synchronization

When a chaotic system generates a signal, that signal cannot be synchronized with another system. [328] determine the chaos synchronization of discrete fractional-order neural networks.

3.6 Conclusion

This chapter offers a comprehensive overview of modeling systems integrating fractional neural networks, exploring their challenges, issues, and applications across diverse domains. It outlines various equations utilized for computing fractional derivatives and differences within different types of fractional-order neural networks and discrete fractional-order neural networks. Fractional derivatives and differences emerge as potent tools for capturing the memory and hereditary characteristics of processes, enhancing the accuracy of systems employing fractional-order neural networks compared to their integer-order counterparts.

In the quest for stability criteria for fractional-order neural networks and discrete fractional-order neural networks, the chapter conducts a thorough examination of various methodologies, encompassing the fixed-point theorem, fractional-order differential equations theory, the Lyapunov direct method, and the linear matrix inequality approach. Additionally, it synthesizes several synchronization criteria, such as the fractional Lyapunov

method, Mittag-Leffler function, matrix eigenvalue theory. Furthermore, it explores the utilization of controllers like sliding mode control, among others.

The chapter further delves into reviews on the hardware implementations of fractional-order neural networks and their diverse application areas. Overall, the chapter underscores the community's dedication to advancing the field of fractional calculus and discrete fractional calculus theory within neural networks, fostering the development of efficient and accurate systems leveraging optimal resources.

Part II

Applications

Chapter 4

Asymptotic Behavior in Discrete Fractional and Variable-Order Neural Networks

4.1 Introduction

Fractional calculus, a powerful extension of traditional calculus, enables the modeling and control of systems with complex dynamics, self-similarity, and inverse power law behavior, transcending various domains from physics to economics [329, 330, 331, 332, 333]. While fractional-order continuous systems have been extensively studied, their discrete counterparts have received less attention despite their increasing significance in recent years [334, 335]. Notably, discrete fractional calculus introduces challenges and opportunities distinct from its continuous counterpart [336, 337, 340]. Stability analyses for discrete fractional systems, including neural networks, have been explored, albeit with a focus primarily on commensurate systems [341, 342, 344, 345]. However, the stability of systems with incommensurate orders remains relatively uncharted territory, highlighting a gap in existing literature [346, 347, 348].

The stability assessment of discrete fractional neural networks, crucial for their practical applicability, has predominantly revolved around commensurate systems [348, 349, 350]. In contrast, incommensurate systems, where the orders of neurons vary, offer a more realistic representation of neural dynamics but pose unique challenges in stability analysis. Despite advancements in stability analysis methodologies for commensurate systems, such as Lyapunov methods and Mittag-Leffler stability, these approaches are not directly applicable to incommensurate systems [351, 352, 353]. Consequently, there is a pressing need for tailored stability analysis techniques for incommensurate discrete fractional neural networks, addressing the complexities arising from variable orders and non-commensurability.

This chapter addresses this gap by introducing novel stability criteria and comparison theorems tailored for incommensurate discrete fractional systems. Specifically, we propose a fractional difference comparison theorem employing the Caputo nabla definition with incommensurate fractional orders, establishing stability criteria for non-commensurate Caputo nabla fractional-order systems. Furthermore, we present a stability criterion for incommensurate systems with variable orders, extending our analysis to discrete incommensurate fractional-order neural networks. The contributions of this

paper include: Introduction of a novel fractional difference comparison theorem employing the Caputo nabla definition with incommensurate fractional orders. Establishment of stability criteria for commensurate and non-commensurate Caputo nabla fractional-order systems and incommensurate systems with variable order. Application of these stability results to discrete incommensurate fractional-order neural networks.

4.2 Asymptotic Stability of Commensurate Discrete Fractional-Order Neural Networks

In this part we investigate the stability conditions unique to commensurate discrete fractional-order neural networks, employing specialized techniques to assess their asymptotic stability.
We commence this section by presenting essential results derived from our investigation into key inequalities related to discrete fractional calculus. These foundational results are crucial for understanding the theoretical framework that underpins our stability analysis.

Theorem 4.1. *Let* $-1 < \kappa < 0$, *then* ${}_hE_{\overline{\alpha}}(\kappa, t)$ *is monotinically decreasing and* $0 < {}_hE_{\overline{\alpha}}(\kappa, t) \leq 1$ *for* $t \in \mathbb{N}_{0,h}$.

Proof. As per the definition of the discrete Mittag-Leffler function with nabla-h, when $t = 0$

$$ {}_hE_{\overline{\alpha}}(\kappa, 0) = 1 + \sum_{k=1}^{\infty} \kappa^k \frac{t_h^{\overline{k\alpha}}}{\Gamma(\alpha k + 1)} = 1 > 0. $$

When $t = 1$, we aim to demonstrate that for $h > 0$ and $-1 < \kappa < 0$, ${}_hE_{\overline{\alpha}}(\kappa, 1) > 0$. Assuming the opposite, let's suppose that when $t = 1$, $h > 0$, and $-1 < \kappa < 0$, ${}_hE_{\overline{\alpha}}(\kappa, 1) \leq 0$. For $h = 1$:

$$ {}_hE_{\overline{\alpha}}(\kappa, 1) = \sum_{k=0}^{\infty} \kappa^k = \frac{1}{1-\kappa} > 0 $$

For $-1 < \kappa < 0$, when $t \in \mathbb{N}_{2,h}$, leveraging the relationship between the Beta function and the Gamma function $B(p, q) = \dfrac{\Gamma(p)\Gamma(q)}{\Gamma(p+q)}$, we can obtain:

$$ \begin{aligned} {}_hE_{\overline{\alpha}}(\kappa, t) &= \sum_{k=0}^{\infty} \kappa^k \frac{t_h^{\overline{k\alpha}}}{\Gamma(\alpha k + 1)} = \sum_{k=0}^{\infty} \kappa^k h^{k\alpha} \frac{\Gamma\left(\frac{t}{h} + k\alpha\right)}{\Gamma\left(\frac{t}{h}\right)\Gamma(\alpha k + 1)}, \\ &= \sum_{k=0}^{\infty} \kappa^k h^{k\alpha} \frac{\Gamma\left(\frac{t}{h} - 1 + k\alpha + 1\right)}{\left(\frac{t}{h} - 1\right)\Gamma\left(\frac{t}{h} - 1\right)\Gamma(\alpha k + 1)}, \\ &= \sum_{k=0}^{\infty} \frac{\kappa^k h^{k\alpha}}{\left(\frac{t}{h} - 1\right) B\left(\frac{t}{h} - 1, \alpha k + 1\right)}. \end{aligned} $$

The Stirling's formula asserts that for a fixed value of q and sufficiently large p, the asymptotic relationship $B(p,q) - \Gamma(q)p^{-q}$ holds true. This formula is invaluable in approximating the behavior of the Beta function for large values of its parameters, aiding in various mathematical analyses and computations. Hence,

$$\sum_{k=0}^{\infty} \frac{\kappa^k h^{k\alpha}}{\left(\frac{t}{h}-1\right) B\left(\frac{t}{h}-1, \alpha k+1\right)} \sim \sum_{k=0}^{\infty} \frac{\left[\kappa h^{\alpha}\left(\frac{t}{h}-1\right)^{\alpha}\right]^k}{\Gamma(\alpha k+1)}, \; t-1 \to +\infty.$$

It's evident that the approximation results align with the continuous-time findings of the Mittag-Leffler function. Specifically, when $0 < \alpha < 1$, we have the following expression:

$$ {}_hE_{\alpha}(t) = \sum_{k=0}^{\infty} \frac{(-t^{\alpha})^k}{\Gamma\left(\alpha k+1\right)} \sim \frac{t^{-\alpha}}{\Gamma(1-\alpha)},$$

for $0 < \alpha < 1$, $0 < \kappa < 1$ and as $t - h \to +\infty$ we obtain

$$ {}_hE_{\overline{\alpha}}(\kappa, t) \sim -\frac{(t-h)^{-\alpha}}{\kappa\Gamma(1-\alpha)},$$

so ${}_hE_{\overline{\alpha}}(\kappa, t) > 0$ for $t \in \mathbb{N}_{2,h}$.
Drawing from the aforementioned analysis, we can conclude that:${}_hE_{\overline{\alpha}}(\kappa, t) > 0$ for $t \in \mathbb{N}_{0,h}$, $0 < \kappa \leq 1$, $0 < \alpha \leq 1$ and $h > 0$. Expanding upon the aforementioned analysis, it becomes evident that: ${}_hE_{\overline{\alpha,\alpha}}(\kappa, t) > 0$.
To establish the monotonicity of ${}_hE\overline{\alpha}(\kappa, t)$ as a decreasing function, it suffices to demonstrate that $\nabla_{h,h} E\overline{\alpha}(\kappa, t) \leq 0$. Referring to (1.32), we derive the following:

$$\begin{aligned}
\nabla_h \, {}_hE_{\overline{\alpha}}(\kappa, t) &= \frac{{}_hE_{\overline{\alpha}}(\kappa, t) - {}_hE_{\overline{\alpha}}(\kappa, t-h)}{h}, \\
&= \frac{\sum_{k=0}^{\infty} \kappa^k \frac{t_h^{\overline{k\alpha}}}{\Gamma(\alpha k+1)} - \sum_{k=0}^{\infty} \kappa^k \frac{(t-h)_h^{\overline{k\alpha}}}{\Gamma(\alpha k+1)}}{h}, \\
&= \sum_{k=0}^{\infty} \frac{\kappa^k}{\Gamma(\alpha k+1)} \nabla_h t_h^{\overline{k\alpha}}, \\
&= \sum_{k=0}^{\infty} \frac{\kappa^k}{\Gamma(\alpha k+1)} k\alpha t_h^{\overline{k\alpha-1}}, \\
&= \sum_{k=1}^{\infty} \frac{\kappa^k}{\Gamma(\alpha k)} t_h^{\overline{\alpha-1}}, \\
&= \sum_{k=0}^{\infty} \frac{\kappa^{(k+1)}}{\Gamma(\alpha(k+1))} t_h^{\overline{(k+1)\alpha-1}}, \\
&= \kappa \, {}_hE_{\overline{\alpha,\alpha}}(\kappa, t) < 0.
\end{aligned}$$

Hence, we conclude that $0 < {}_hE\overline{\alpha}(\kappa, t) \leq {}_hE\overline{\alpha}(\kappa, 0) = 1$ for $t \in \mathbb{N}_{0,h}$ and $0 < \kappa \leq 1$. This completes the proof. □

Consider the nonhomogeneous equation represented by:

$$\begin{cases} {}_a^C\nabla_h^\alpha x(t) = wx(t) + \beta f(t, x(t)), \\ x(a) = x_a, \end{cases} \tag{4.1}$$

where w, c are constants,$|w| < \alpha$, $0 < \alpha \leq 1$, $t \in \mathbb{N}_{a,h}$ and g a continous function on $C(\mathbb{N}_{a,h}, \mathbb{R})$.
In the following, we'll assume $a = 0$.

Lemme 4.1. *The exact solution for problem (4.1) is given by*

$$x(t) = {}_hE_{\overline{\alpha}}(w, t-a)x_a + h\beta \sum_{k=\frac{a}{h}+1}^{\frac{t}{h}} {}_{h;}E_{\overline{\alpha,\alpha}}(w, t-\rho(kh))f(x(kh)). \tag{4.2}$$

Proof. By applying the Laplace transform to both sides of equation (4.1), we get:

$$N_{a,h}[{}_a^C\nabla_h^\alpha x(t)](s) = wN_{a,h}[x(t)](s) + \beta N_{a,h}[f(t, x(t))](s),$$

it is clear that

$$s^\alpha N_{a,h}[x(t)](s) - s^{\alpha-1}x_a = wN_{a,h}[x(t)](s) + \beta N_{a,h}[f(t, x(t))](s),$$

then, we have

$$N_{a,h}[x(t)](s) = \frac{s^{\alpha-1}}{s^\alpha - w}x_a + \frac{\beta}{s^\alpha - w}N_{a,h}[f(t, x(t))](s). \tag{4.3}$$

By performing the Laplace inverse transform on both sides, and referencing equations (1.176), (1.177), and (1.182), we obtain the following results:

$$x(t) = {}_hE_{\overline{\alpha}}(w, t-a)x_a + h\beta \sum_{k=\frac{a}{h}+1}^{\frac{t}{h}} {}_hE_{\overline{\alpha,\alpha}}(w, t-\rho(kh))f(x(kh)), \tag{4.4}$$

that is the expression for the Caputo nonhomogeneous difference equation (4.1). In fact, applying the Laplace transform to both sides of (4.4) yields the following result:

$$\begin{aligned} N_{a,h}[x(t)](s) &= N_{a,h}[{}_hE_{\overline{\alpha}}(w, t-a)x_a](s) + N_{a,h}[h\beta \sum_{k=\frac{a}{h}+1}^{\frac{t}{h}} {}_hE_{\overline{\alpha,\alpha}}(w, t-\rho(kh))f(x(kh))](s), \\ &= \frac{s^{\alpha-1}}{s^\alpha - w}x_a + \frac{\beta}{s^\alpha - w}N_{a,h}[f(t, x(t))](s). \end{aligned}$$

Through this process, we consequently arrive at the right-hand side of equation (4.3). □

Lemme 4.2. *Let $x : \mathbb{N}_{a,h} \to \mathbb{R}$ denote a function defined on the discrete set $\mathbb{N}_{a,h}$ and $x(t)$ be the solution that satisfies the following inequality:*

$$x(t) \leq {}_hE_{\overline{\alpha}}(w, t-a)x_a + h\beta \sum_{k=\frac{a}{h}+1}^{\frac{t}{h}} {}_hE_{\overline{\alpha,\alpha}}(w, t-\rho(kh))x(kh).$$

then

$$x(t) \leq x_a\, {}_hE_{\overline{\alpha}}(w+\beta, t-a), \tag{4.5}$$

where $|w| < v$ and $|w + c| < v$.

Proof. Suppose $K : \mathbb{N}_{a,h} \to \mathbb{R}^+$ is a function defined on the discrete set $\mathbb{N}_{a,h}$, where $\mathbb{R}^+$ denotes the set of positive real numbers. Let us further consider

$$x(t) = {}_hE_{\overline{\alpha}}(w, t-a)x_a + h\beta \sum_{k=\frac{a}{h}+1}^{\frac{t}{h}} {}_hE_{\overline{\alpha,\alpha}}(w, t-\rho(kh))x(kh) - K(t).$$

Upon applying the Laplace transform to both sides of the equation and subsequently utilizing convolution, we obtain

$$N_{a,h}[x(t)](s) = \frac{s^{\alpha-1}}{s^\alpha - w}x_a + \frac{\beta}{s^\alpha - w}N_{a,h}[x(t)](s) - N_{a,h}[K(t)](s),$$

$$N_{a,h}[x(t)](s) = \frac{s^{\alpha-1}}{s^\alpha - w - \beta}x_a - N_{a,h}[K(t)](s) - \frac{\beta}{s^\alpha - w - \beta}N_{a,h}[g(t)](s).$$

Now, by employing the inverse Laplace transform, it follows that

$$x(t) = x_a\, {}_hE_{\overline{\alpha}}(w+\beta, t-a) - h\beta \sum_{k=\frac{a}{h}+1}^{\frac{t}{h}} {}_hE_{\overline{\alpha,\alpha}}(w+\beta, t-\rho(kh))K(kh) - g(t).$$

Given that $g(t)$ and ${}_hE_{\overline{\alpha,\alpha}}(w+\beta, t-a)$ are both positive functions, we can establish the following inequality:

$$-hc \sum_{k=\frac{a}{h}+1}^{\frac{t}{h}} {}_hE_{\overline{\alpha,\alpha}}(w+\beta, t-\rho(kh))K(kh) - K(t) \leq 0,$$

hence,

$$x(t) \leq x_a\, {}_hE_{\overline{\alpha}}(w+\beta, t-a).$$

This inequality completes the proof.

□

4.2.1 Mittag-Leffler Stability Analysis of Discrete Fractional Neural Networks

Now, we delve into the Mittag-Leffler stability analysis of fractional discrete neural networks. By examining the stability properties of these networks using the Mittag-Leffler function, we aim to provide a comprehensive understanding of their dynamic behavior. We propose a novel class of neural networks designed for fractional discrete-time systems.

$$ {}^C_a\nabla^\alpha_h x(t) = -Bx(t) + Dg(t, x(t)). \tag{4.6}$$

In the context of our proposed fractional discrete-time neural networks, the state vector $x(t) = (x_1(t), x_2(t), ..., x_n(t))^T \in \mathbb{R}^n$ comprises the individual components of the system's state. The matrix $B = \text{diag}(b_1, b_2, ..., b_n) \in \mathbb{R}^{n\times n}$ denotes the self-feedback connection weight matrix, with $b_i > 0$ for each i. Additionally, $D = (d_{ij})_{n\times n} \in \mathbb{R}^{n\times n}$ represents the connection weight matrix governing interactions between different components of the state vector.
The activation function $g(x(t)) = (g_1(x(t)), g_2(x(t)), ..., g_n(x(t)))^T : C(\mathbb{N}_{a,h} \to \mathbb{R}^n)$ maps

the state vector to its corresponding output vector. Here, $C(\mathbb{N}_{a,h} \to \mathbb{R}^n)$ denotes the space of continuous functions mapping the discrete set $\mathbb{N}_{a,h}$ to $\mathbb{R}^n$.
Next, we present the exact solution of the system described by Equation (4.6). By solving this system analytically, we gain deeper insights into the behavior and properties of the fractional discrete neural networks under consideration.

Theorem 4.2. *Equation (4.6) is equivalent to the fractional sum equation*

$$x(t) = {}_hE_{\overline{\alpha}}(-B, t-a)x_a + h\sum_{k=\frac{a}{h}+1}^{\frac{t}{h}} {}_hE_{\overline{\alpha,\alpha}}(-B, t-\rho(kh))Dg(x(kh)),\ t \in \mathbb{N}_{a,h}, \tag{4.7}$$

where

$${}_hE_{\overline{\alpha}}(-B, t-a) = \begin{bmatrix} {}_hE_{\overline{\alpha}}(-b_1, t-a) & \dots & 0 \\ & & \\ 0 & \dots & {}_hE_{\overline{\alpha}}(-b_n, t-a) \end{bmatrix},$$

and $0 < b_i < \alpha,\ i = \{1, ..., n\}$

Proof. The system described by Equation (4.6) is equivalent to

$$\begin{cases} {}_a^C\nabla_h^\alpha x_1(t) = -b_1x_1(t) + \sum_{j=1}^n d_{1j}g_j(t, x_j(t)), \\ {}_a^C\nabla_h^\alpha x_2(t) = -b_2x_2(t) + \sum_{j=1}^n d_{2j}g_j(t, x_j(t)), \\ \dots \\ {}_a^C\nabla_h^\alpha x_n(t) = -b_nx_n(t) + \sum_{j=1}^n d_{nj}g_j(t, x_j(t)). \end{cases}$$

Utilizing Equation (4.5) and for $t \in \mathbb{N}_{a,h}$, we can demonstrate that this system is equivalent to

$$\begin{cases} x_1(t) = {}_hE_{\overline{\alpha}}(-b_1, t-a)x_1(a) + h\sum_{k=\frac{a}{h}+1}^{\frac{t}{h}} {}_hE_{\overline{\alpha,\alpha}}(-b_1, t-\rho(kh))\sum_{j=1}^n d_{1j}g_j(kh, x_j(kh)), \\ x_2(t) = {}_hE_{\overline{\alpha}}(-b_1, t-a)x_2(a) + h\sum_{k=\frac{a}{h}+1}^{\frac{t}{h}} {}_hE_{\overline{\alpha,\alpha}}(-b_2, t-\rho(kh))\sum_{j=1}^n d_{2j}g_j(kh, x_j(kh)), \\ \dots \\ x_n(t) = {}_hE_{\overline{\alpha}}(-b_n, t-a)x_1(a) + h\sum_{k=\frac{a}{h}+1}^{\frac{t}{h}} {}_hE_{\overline{\alpha,\alpha}}(-b_n, t-\rho(kh))\sum_{j=1}^n d_{nj}g_j(kh, x_j(kh)). \end{cases}$$

This equivalence can be expressed as

$$x(t) = \begin{bmatrix} {}_hE_{\overline{\alpha}}(-b_1, t-a) & \dots & 0 \\ & & \\ 0 & \dots & {}_hE_{\overline{\alpha}}(-b_n, t-a) \end{bmatrix} x(a) + {}^h\sum_{k=\frac{a}{h}+1}^{\frac{t}{h}} \begin{bmatrix} {}_hE_{\overline{\alpha,\alpha}}(-b_1, t-\rho(kh)) & \dots & 0 \\ & & \\ 0 & \dots & {}_hE_{\overline{\alpha,\alpha}}(-b_n, t-\rho(kh)) \end{bmatrix} Dg(x(kh)).$$

This step concludes the proof. □

Now, we proceed by introducing the following assumptions:

(H_1) For every t belonging to $\mathbb{N}_{a,h}$, $g(t,x)$ denotes a continuous function with respect to x, and there exists a positive constant from $\mathbb{R}^+$ such that the following inequality holds:

$$\|g(t,x) - g(t,y)\| \leq \|x - y\|$$

for all x, y in $C(\mathbb{N}_{a,h}, \mathbb{R}^n)$.

(H_2) For every t in $\mathbb{N}_{a,h}$, there exists a positive constant γ less than 1, satisfying the condition:

$$h \sum_{k=\frac{a}{h}+1}^{\frac{t}{h}} {}_hE_{\overline{\alpha,\alpha}}(-B, t - \rho(kh))\|D\| < \gamma.$$

Theorem 4.3. *Under the assumptions* (H_1) *and* (H_2)*, it can be concluded that system (4.6) possesses a unique solution.*

Proof. Define the space

$$C_m = \{x, x \in C(\mathbb{N}_{a,h}, \mathbb{R}^n), \ \lim_{t\to+\infty} x(t) = 0\}, \ \|x(t)\| \leq m\}$$

We assume that $\|x_a\| \leq \delta$, $\gamma = \max\limits_{i=1,\ldots,n} \sum\limits_{j=1}^{n} |d_{ij}|$

we define the operator $Q : C_m \to C_m$

$$Qx(t) = {}_hE_{\overline{\alpha}}(-B, t-a)x_a + h \sum_{k=\frac{a}{h}+1}^{\frac{t}{h}} {}_hE_{\overline{\alpha,\alpha}}(-B, t - \rho(kh))Dg(x(kh)).$$

It is evident that Q is well-defined on C_m. Indeed,
if $\dfrac{\delta}{1-\gamma} < m$ and $\|x(t)\| \leq m$, then it follows that $\|Qx(t)\| \leq m$.

$$\begin{aligned}
\|Qx(t)\| &\leq {}_hE_{\overline{\alpha}}(-B, t-a)\|x_a\| + \|h \sum_{k=\frac{a}{h}+1}^{\frac{t}{h}} {}_hE_{\overline{\alpha,\alpha}}(-B, t - \rho(kh))Dg((x(kh))\|, \\
&\leq {}_hE_{\overline{\alpha}}(-B, t-a)\|x_a\| + h\|D\| \sum_{k=\frac{a}{h}+1}^{\frac{t}{h}} {}_hE_{\overline{\alpha,\alpha}}(-B, t - \rho(kh))\|(x(t)\|, \\
&\leq \delta + \gamma m \leq m.
\end{aligned}$$

Furthermore, by utilizing Lemma 4.2 and the properties of the h-discrete Mittag-Leffler function, we can deduce that $\lim\limits_{t\to+\infty} Qx(t) = 0$ as both ${}_hE_{\overline{\alpha}}(-B, t-a)$ and ${}_hE_{\overline{\alpha,\alpha}}(-B, t-a)$ are positive, non-increasing functions.

Finally, considering two arbitrary solutions $x(t)$ and $y(t)$ of (4.6), we obtain

$$\begin{aligned}\|Qx(t) - Qy(t)\| &= \|h \sum_{k=\frac{a}{h}+1}^{\frac{t}{h}} {}_hE_{\overline{\alpha,\alpha}}(-B, t-\rho(kh))D[g(x(kh)) - g(y(kh))]\|,\\ &\leq h \sum_{k=\frac{a}{h}+1}^{\frac{t}{h}} {}_hE_{\overline{\alpha,\alpha}}(-B, t-\rho(kh))\|D\|\|x(t) - y(t)\|,\\ &< \gamma\|x(t) - y(t)\|,\\ &< \|x(t) - y(t)\|.\end{aligned}$$

Q is a contraction mapping. By the Banach fixed-point theorem, Q possesses a unique fixed point $x(t)$ in C_m, which also serves as the unique solution of (4.6). Furthermore, $\lim_{t\to+\infty} x(t) = 0$ implies that the zero solution is attractive. □

Theorem 4.4. *If assumptions (H_1) and (H_2) hold, and if $-\alpha < v + l\gamma < 0$, then system (4.6) exhibits Mittag-Leffler stability, where $v = \max_{i=1,\dots,n}\{-b_i\}$.*

Proof. From the summation equation, we derive:

$$\begin{aligned}|x_i(t)| &= |\,{}_hE_{\overline{\alpha}}(-b_i, t-a)x_i(a) + h \sum_{k=\frac{a}{h}+1}^{\frac{t}{h}} {}_hE_{\overline{\alpha,\alpha}}(-b_i, t-\rho(kh)) \sum_{j=1}^{n} d_{ij}h_i(x_j(kh))|,\\ &\leq |x_i(a)|\,{}_hE_{\overline{\alpha}}(-b_i, t-a) + h\sum_{j=1}^{n}|d_{ij}| \sum_{k=\frac{a}{h}+1}^{\frac{t}{h}} {}_hE_{\overline{\alpha,\alpha}}(-b_i, t-\rho(kh))|x_j(kh)|,\\ &\leq |x_i(a)|\,{}_hE_{\overline{\alpha}}(v, t-a) + h\gamma \sum_{k=\frac{a}{h}+1}^{\frac{t}{h}} {}_hE_{\overline{\alpha,\alpha}}(v, t-\rho(kh))|x_j(kh)|.\end{aligned}$$

By utilizing (4.5) and applying the norm operator to both sides of the inequality, we obtain:

$$\begin{aligned}\|x(t)\| &\leq \|x_a\|\,{}_hE_{\overline{\alpha}}(v, t-a) + h\gamma \sum_{k=\frac{a}{h}+1}^{\frac{t}{h}} {}_hE_{\overline{\alpha,\alpha}}(v, t-\rho(kh))\|x(t)\|,\\ &\leq \|x_a\|\,{}_hE_{\overline{\alpha}}(v+\gamma, t-a).\end{aligned}$$

Given that $-\alpha < v+l\gamma < 0$ the neural network described by (4.6) exhibits Mittag-Leffler stability. □

4.2.2 Stability Analysis of Multiple-Order Discrete Fractional Neural Networks

We conduct a comprehensive examination of the multiple-order discrete-time fractional neural networks, detailing their structure, behavior, and underlying mathematical formulations. These networks are defined by the following equations:

$$\begin{aligned}{}^{C}_{t_k}\nabla_h^{\alpha_k} x(t) = -Bx(t) + Dg(t, x(t)),\ t \in \{t_{kl} + h, ..., t_{(k+1)l}\},\end{aligned} \tag{4.8}$$

where $0 < \alpha_k \leq 1,\ k = 0, ..., m-1,\ m$ is the number of the intervals.
This expression can be simplified as:

$$\begin{cases} {}_{t_0}^{C}\nabla_h^{\alpha_0} x(t) = -Bx(t) + Dg(t, x(t)),\ t \in \{t_0 + h, ..., t_l\}, \\ {}_{t_l}^{C}\nabla_h^{\alpha_1} x(t) = -Bx(t) + Dg(t, x(t)),\ t \in \{t_l + h, ..., t_{2l}\}, \\ ... \\ {}_{t_{(m-1)l}}^{C}\nabla_h^{\alpha_{(m-1)}} x(t) = -Bx(t) + Dg(t, x(t)),\ t \in \{t_{(m-1)l} + h, ..., t_{ml}\}. \end{cases}$$

Theorem 4.5. *Under asumptions $(H_1), (H_2)$, if $\alpha < v + l\gamma < 0$ then system (4.8) is asymptoticly stable, where $\alpha = \min_{k=0,...,m-1}\{\alpha_k\}$*

Proof. Equation (4.8) can be represented as:

$$\begin{cases} x(t) = {}_hE_{\alpha_0}(-B, t - t_0)x_{t_0} + h\sum\limits_{k=\frac{t_0}{h}+1}^{\frac{t}{h}} {}_hE_{\alpha_0,\alpha_0}(-B, t - \rho(kh))Dg(x(kh)),\ t \in \{t_0 + h, ..., t_l\}, \\ x(t) = {}_hE_{\alpha_1}(-B, t - t_l)x_{t_l} + h\sum\limits_{k=\frac{t_l}{h}+1}^{\frac{t}{h}} {}_hE_{\alpha_1,\alpha_1}(-B, t - \rho(kh))Dg(x(kh)),\ t \in \{t_l + h, ..., t_{2l}\}, \\ ... \\ x(t) = {}_hE_{\alpha_{m-1}}(-B, t - t_{(m-1)l})x_{t_{(m-1)l}} + h\sum\limits_{k=\frac{t_{(m-1)l}}{h}+1}^{\frac{t}{h}} {}_hE_{\alpha_{m-1},\alpha_{m-1}}(-B, t - \rho(kh))Dg(x(kh)), \\ \qquad\qquad t \in \{t_{(m-1)l} + h, ..., t_{ml}\}. \end{cases}$$

Utilizing (4.5), it ensues:

$$\begin{cases} \|x(t)\| \leq \|x_{t_0}\|\, {}_hE_{\alpha_0}(v + l\gamma, t - t_0),\ \text{with}\ -\alpha_0 < v + l\gamma < 0\ \text{and}\ t \in \{t_0 + h, ..., t_l\}, \\ \|x(t)\| \leq \|x_{t_l}\|\, {}_hE_{\alpha_1}(v + l\gamma, t - t_l),\ \text{with}\ -\alpha_1 < v + l\gamma < 0\ \text{and}\ t \in \{t_l + h, ..., t_{2l}\}, \\ ... \\ \|x(t)\| \leq \|x_{t_{(m-1)l}}\|\, {}_hE_{\alpha_{m-1}}(v + l\gamma, t - t_{(m-1)l}),\ \text{with}\ -\alpha_{m-1} < v + l\gamma < 0 \\ \qquad \text{and}\ t \in \{t_{(m-1)l} + h, ..., t_{ml}\}. \end{cases}$$

$x(t)$ achieves asymptotic stability over the interval $t_0 + h, ..., t_{ml}$ if and only if $\alpha < v + l\gamma < 0$, where α is chosen as the minimum among $\alpha_k{}_{k=0}^{m-1}$. In this scenario, we have:

$$\begin{cases} \|x(t_l)\| \leq \|x_{t_0}\|\, {}_hE_{\alpha_0}(v + l\gamma, t_l - t_0), \\ \|x(t_{2l})\| \leq \|x_{t_l}\|\, {}_hE_{\alpha_1}(v + l\gamma, t_{2l} - t_l), \\ ... \\ \|x(t)\| \leq \|x_{t_{(m-1)l}}\|\, {}_hE_{\alpha_{m-1}}(v + l\gamma, t - t_{(m-1)l}). \end{cases}$$

Therefore, we obtain:

$$\|x(t)\| \leq m(x(t_0))\, {}_hE_{\alpha_{m-1}}(v + l\gamma, t - t_{(m-1)l}),$$

where

$$m(x(t_0)) = \|x_{t_0}\| \prod_{k=0}^{m-2} {}_hE_{\alpha_k}(v + l\gamma, t_{(k+1)l} - t_{kl})$$

where $m(x(t_0)) > 0,\ m(0) = 0$, and given that the Mittag-Leffler function is positive. □

4.2.3 Numerical Examples

We demonstrate the practical application of stability theory in the context of fractional discrete-time neural networks through the detailed examination of the following illustrative examples.

Example 4.1. *Let's examine the following neural networks operating in the domain of fractional discrete time.*

$$\begin{cases} {}_a^C\nabla_h^\alpha x_1(t) = -b_1 x_1(t) + d_{11}\sin(x_1(t)) + d_{12}\sin(x_2(t)) + d_{13}\sin(x_3(t)), \\ {}_a^C\nabla_h^\alpha x_2(t) = -b_2 x_2(t) + d_{21}\sin(x_1(t)) + d_{22}\sin(x_2(t)) + d_{23}\sin(x_3(t)), \\ {}_a^C\nabla_h^\alpha x_3(t) = -b_3 x_3(t) + d_{31}\sin(x_1(t)) + d_{32}\sin(x_2(t)) + d_{33}\sin(x_3(t)). \end{cases} \tag{4.9}$$

Below, we present the numerical formula for the solution of equation (4.9):

$$x(i) = x_0 + \frac{h^\alpha}{\Gamma(\alpha)} \sum_{j=a+1}^{i} \frac{\Gamma(i-j+\alpha)}{\Gamma(i-j+1)} \left(-Bx(j) + D\sin(x(j))\right).$$

We employ the parameters outlined below:

$$B = \begin{bmatrix} 0.8 & 0 & 0 \\ 0 & 0.8 & 0 \\ 0 & 0 & 0.8 \end{bmatrix}, \quad D = \begin{bmatrix} 0.1 & -0.3 & 0.15 \\ -0.2 & 0.5 & -0.1 \\ 0.25 & 0.15 & 0.3 \end{bmatrix}, \quad x(0) = \begin{bmatrix} 1 \\ 1 \\ 1 \end{bmatrix}, \quad \alpha = 0.7, \quad h = 0.9.$$

We can verify that these parameters satisfy assumptions (H_1) and (H_2), as well as the conditions outlined in Theorem 4.3 and Theorem 4.7. Figure 6.5 provides a visual representation of the behavior of $x_1(t)$ and $x_2(t)$ over time. It can be observed that both tend to zero as t approaches positive infinity, indicating asymptotic stability of the solution.

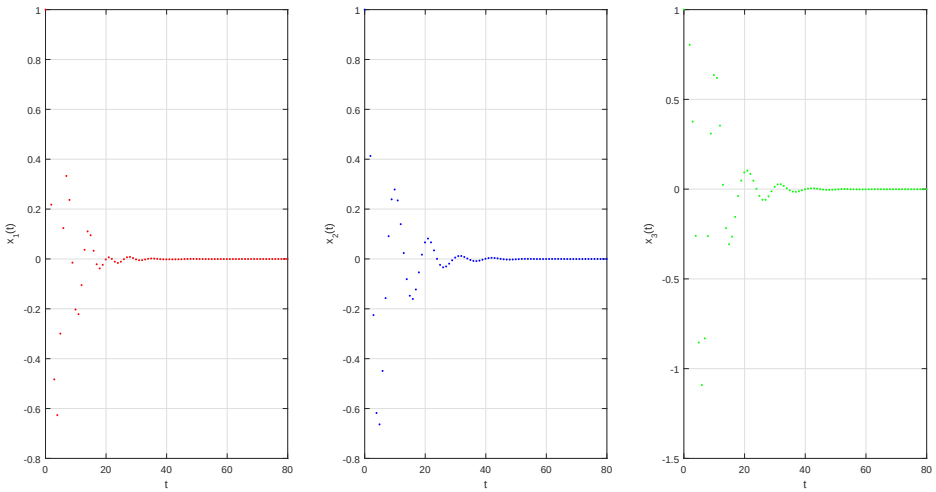

Figure 4.1: Numerical solution of neural networks (4.9).

Example 4.2. *We suggest the following variable-order fractional discrete-time neural networks:*

$$\begin{cases} {}_{t_{kl}}^C\nabla_h^{\alpha_k} x_1(t) = -b_1 x(t) + d_{11}\tanh(x_1(t)) + d_{12}\tanh(x_2(t)), \\ {}_{t_{kl}}^C\nabla_h^{\alpha_k} x_2(t) = -b_2 x(t) + d_{21}\tanh(x_1(t)) + d_{22}\tanh(x_2(t)). \end{cases} \tag{4.10}$$

Let's define the parameters as follows: $b_1 = 0.95,\ b_2 = 0.95,\ d_{11} = 0.2,\ d_{12} = 0.4,\ d_{21} = -0.1,\ d_{22} = 0.5,\ m = 6,\ k = \{0, 1, 2, 3, 4, 5\}$ *and* $x_1(0) = 1, x_2(0) = -1$.

case 1. *we consider*

$(\alpha_0, \alpha_1, \alpha_2, \alpha_3, \alpha_4, \alpha_5) = (0.7, 0.65, 0.6, 0.55, 0.5, 0.45),\ h = 1.5$ *and* $t \in [0, 150]$

case 2. *we have*

$(\alpha_0, \alpha_1, \alpha_2, \alpha_3, \alpha_4, \alpha_5) = (0.56, 0.51, 0.46, 0.41, 0.36, 0.31),\ h = 0.8$ *and* $t \in [0, 60]$.

The numerical solution to equation (4.10) can be expressed as:

$$\begin{cases} x_1(i) = x_0 + \dfrac{h^{\alpha_0}}{\Gamma(\alpha_0)} \displaystyle\sum_{j=1}^{i} \frac{\Gamma(i-j+\alpha_0)}{\Gamma(i-j+1)} \left(-b_1 x(j) + d_{11} \tanh(x_1(j)) + d_{12} \tanh(x_2(j))\right), \\ x_2(i) = x_0 + \dfrac{h^{\alpha_0}}{\Gamma(\alpha_0)} \displaystyle\sum_{j=1}^{i} \frac{\Gamma(i-j+\alpha_0)}{\Gamma(i-j+1)} \left(-b_2 x(j) + d_{21} \tanh(x_1(j)) + d_{22} \tanh(x_2(j))\right), \\ \quad i = \{0, 1, ..., l\}, \\ \\ x_1(i) = x(l) + \dfrac{h^{\alpha_1}}{\Gamma(\alpha_1)} \displaystyle\sum_{j=l+1}^{i} \frac{\Gamma(i-j+\alpha_1)}{\Gamma(i-j+1)} \left(-b_1 x(j) + d_{11} \tanh(x_1(j)) + d_{12} \tanh(x_2(j))\right), \\ x_2(i) = x(l) + \dfrac{h^{\alpha_1}}{\Gamma(\alpha_1)} \displaystyle\sum_{j=l+1}^{i} \frac{\Gamma(i-j+\alpha_1)}{\Gamma(i-j+1)} \left(-b_2 x(j) + d_{21} \tanh(x_1(j)) + d_{22} \tanh(x_2(j))\right), \\ \quad i = \{l+1, l+2, ..., 2l\}, \\ ... \end{cases}$$

$$\begin{cases} x_1(i) = x((m-1)l) + \dfrac{h^{\alpha_{m-1}}}{\Gamma(\alpha_{m-1})} \displaystyle\sum_{j=(m-1)l+1}^{i} \frac{\Gamma(i-j+\alpha_{m-1})}{\Gamma(i-j+1)} \left(-b_1 x(j) + d_{11} \tanh(x_1(j)),\right. \\ \left. + d_{12} \tanh(x_2(j)),\right. \\ x_2(i) = x((m-1)l) + \dfrac{h^{\alpha_{m-1}}}{\Gamma(\alpha_{m-1})} \displaystyle\sum_{j=(m-1)l+1}^{i} \frac{\Gamma(i-j+\alpha_{m-1})}{\Gamma(i-j+1)} \left(-b_2 x(j) + d_{21} \tanh(x_1(j)),\right. \\ \left. + d_{22} \tanh(x_2(j)) \quad i = \{(m-1)l+1, (m-1)l+2, ..., ml\}.\right. \end{cases}$$

The stability of system (4.10) is ensured as the parameters satisfy the required assumptions and conditions. The asymptotic stability of the variable-order neural network is demonstrated in Figure 4.2 and Figure 4.3.

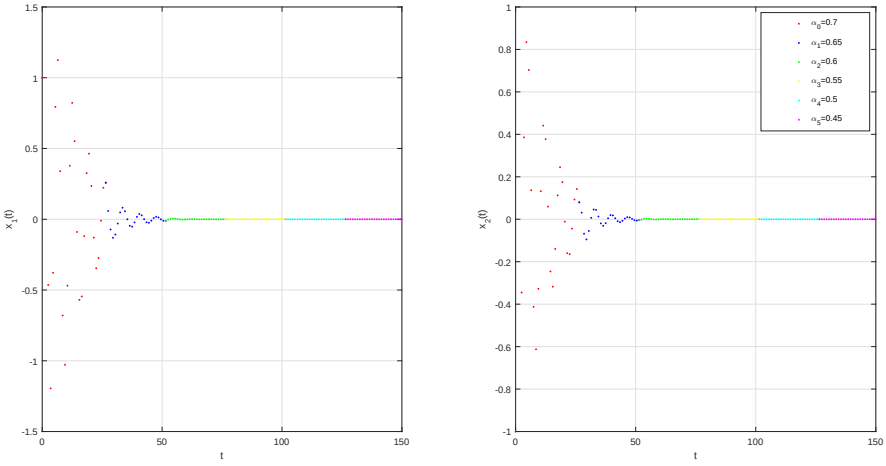

Figure 4.2: Numerical solution of variable-order Neural network (4.10) **case 1**.

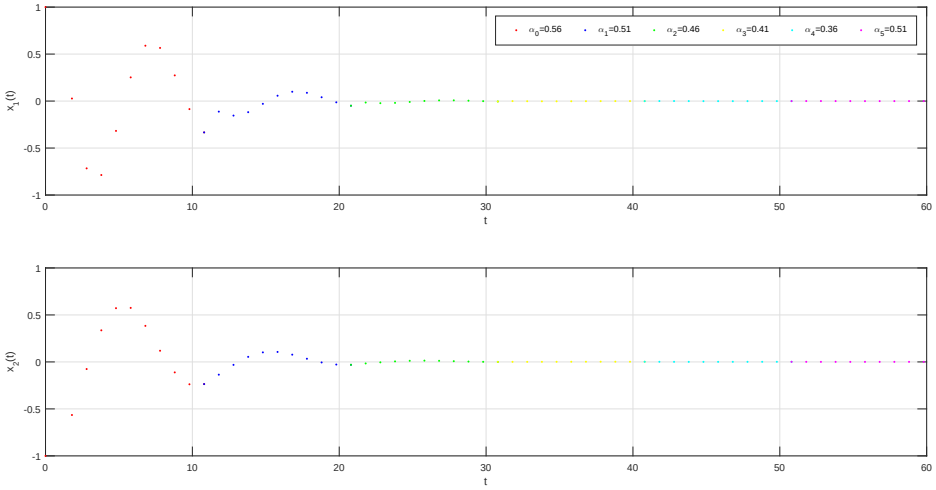

Figure 4.3: Numerical solution of variable-order Neural network (4.10) **case 2**.

4.3 Asymptotic Stability of Incommensurate Discrete Fractional-order Neural Networks

In this subsection, we investigate the stability criteria pertinent to incommensurate discrete fractional-order neural networks, utilizing techniques to evaluate their asymptotic stability. Our investigation begins with the exposition of crucial stability results for a general nonlinear incommensurate discrete fractional-order system. These foundational results will subsequently be applied to the neural network model under consideration, providing a robust framework for analyzing its stability.

4.3.1 General Discrete Fractional Model

Let's take a closer look at the initial value problem involving incommensurate order:

$$ {}^{C}\nabla^{\alpha}x(t) = f(t, x(t)), \quad x(0) = x_0, \tag{4.11} $$

where $x(t) = (x_1(t), x_2(t), \ldots, x_n(t))^T \in \mathbb{R}^n$, ${}^C\nabla^\alpha x(t) = ({}^C\nabla^{\alpha_1} x_1(t), {}^C\nabla^{\alpha_2} x_2(t), \ldots, {}^C\nabla^{\alpha_n} x_n(t))^T$, the non-commensurate orders $\alpha_i \in (0, 1]$, and $f(t, x(t))$ is a continuously differentiable function.

To delve into the stability analysis of these systems, we introduce a tailored comparison principle specifically designed for fractional-order difference systems characterized by incommensurate orders. Subsequently, we apply this principle to fractional-order neural networks featuring incommensurate orders.

Under the assumption of $f(.)$ being continuous and satisfying the Lipschitz condition, we establish that the system described by equation (4.11) possesses an equilibrium point residing within the space $C([0, T], C_d)$ irrespective of the initial condition $x_0 = (x_{01}, x_{02}, \ldots, x_{0n})$.

Now, let's thoroughly examine the subsequent fractional-order discrete inequality:

$$ {}_a^C\nabla^\alpha V(t, x(t)) \leq g(t, V_1(t, x_1(t)), V_2(t, x_2(t)), \ldots, V_n(t, x_n(t))), \tag{4.12} $$

where

$$ {}_a^C\nabla^\alpha V(t, x(t)) = ({}_a^C\nabla^{\alpha_1} V_1(t, x_1(t)), {}_a^C\nabla^{\alpha_2} V_2(t, x_2(t)), \ldots, {}_a^C\nabla^{\alpha_n} V_n(t, x_n(t)). $$

Furthermore,

$$ {}_a^C\nabla^\alpha W_1(t, x(t)) = g(t, W_1(t, x_1(t)), W_2(t, x_2(t)), \ldots, W_n(t, x_n(t))), \tag{4.13} $$

where ${}_a^C\nabla^\alpha W(t, x(t)) = ({}_a^C\nabla^{\alpha_1} W_1(t, x_1(t)), {}_a^C\nabla^{\alpha_2} W_2(t, x_2(t)), \ldots, {}_a^C\nabla^{\alpha_n} W_n(t, x_n(t))$ and $W_i(t, x_i(t))$. Equations (4.12) and (4.13) represent the compared and comparison systems, respectively. By analyzing the asymptotic behavior of $W(t, x(t))$, we can subsequently employ the comparison principle to scrutinize the asymptotic stability of $V(t, x(t))$.

Lemme 4.3. *Let's scrutinize the subsequent fractional-order difference inequalities along with their accompanying initial conditions:* $0 \leq V_i(0, x_i(0)) \leq W_i(0, y_i(0)), i = 1, 2, \ldots,$

$$ \begin{aligned} {}_a^C\nabla^{\alpha_1} V_1(t, x_1(t)) &\leq {}_a^C\nabla^{\alpha_1} W_1(t, y_1(t)), \\ {}_a^C\nabla^{\alpha_2} V_2(t, x_2(t)) &\leq {}_a^C\nabla^{\alpha_2} W_2(t, y_2(t)), \\ &\vdots \\ {}_a^C\nabla^{\alpha_n} V_n(t, x_n(t)) &\leq {}_a^C\nabla^{\alpha_n} W_n(t, y_n(t)). \end{aligned} $$

The following inequalities are valid:

$$ V_i(t, x_i(t)) \leq W_i(t, y_i(t)), \quad \forall t > 0, \quad i = 1, 2, \ldots, n, \tag{4.14} $$

where $V_i(t, x_i(t))$ *and* $W_i(t, x_i(t)) : [0, \infty) \times \mathbb{N}_a \to [0, \infty)$.

Proof. For every $i = 1, 2, \ldots$, in the scenario where ${}_a^C\nabla^{\alpha_i} W_i(t, x_i(t)) \leq {}_a^C\nabla^{\alpha_i} W_i(t, y_i(t))$, there exists a non-negative function $m_i(t)$ satisfying :

$$ {}_a^C\nabla^{\alpha_i} V_i(t, x_i(t)) + m_i(t) = {}_a^C\nabla^{\alpha_i} W_i(t, y_i(t)). \tag{4.15} $$

Upon applying the Laplace transformation to equation (4.15), we obtain:

$$ s^{\alpha_i}\mathfrak{L}(V_i)(s) - s^{\alpha_i - 1} V_i(0, x_i(0)) + \mathfrak{L}(m_i)(s) = s^{\alpha_i}\mathfrak{L}(W_i)(s) - s^{\alpha_i - 1} W_i(0, y_i(0)). \tag{4.16} $$

We can represent equation (4.16) as:

$$s^{\alpha_i}(N(V_i)(s) - N(W_i)(s)) = s^{\alpha_i - 1}(V_i(0, x_i(0)) - W_i(0, y_i(0))) - \mathfrak{L}(m_i)(s). \tag{4.17}$$

Put differently,

$$N(V_i)(s) - N(W_i)(s) = s^{-1}(V_i(0, x_i(0)) - W_i(0, y_i(0))) - s^{-\alpha_i} N(m_i)(s). \tag{4.18}$$

When expressed in the time domain, we obtain

$$V_i(t, x_i(t)) - W_i(t, y_i(t)) = V_i(0, x_i(0)) - W_i(0, y_i(0)) - \sum_{k=a+1}^{t} (t - \rho(k) + a)^{\alpha_i - 1} m_i(\tau). \tag{4.19}$$

Furthermore, given $V_i(0, x_i(0)) \leq W_i(0, y_i(0))$ and $m_i(t) \geq 0$ we have:

$$V_i(t, x_i(t)) \leq W_i(t, y_i(t)). \tag{4.20}$$

Consequently,

$$V(t, x(t)) \leq W(t, y(t)), \quad \forall t > 0. \tag{4.21}$$

□

4.3.2 Stability of Incommensurate Discsrete Fractional Neural Networks

The evolution of a discrete fractional-order neural network is governed by the subsequent fractional-order difference equation, which delineates the interplay of network components over discrete time intervals.

$${}_a^C\nabla^{\alpha_i} x_i(t) = -c_i x_i(t) + \sum_{j=1}^{n} d_{ij} g_j(t, x_j(t)) + I_i. \tag{4.22}$$

To put it succinctly:

$${}_a^C\nabla^{\overline{\alpha}} x(t) = -Ax(t) + Dg(t, x(t)) + I. \tag{4.23}$$

In the subsequent formulation, where i is an element of the set of natural numbers, t is a non-negative real number, and $\overline{\alpha} = [\alpha_1, \alpha_2, ..., \alpha_n]$, wherein n denotes the total count of units within the neural network.

Following this, we put forth the subsequent assumptions:

(A_1) The activation functions g_j within the neural network demonstrate Lipschitz continuity, ensuring the existence of positive constants L_j, where $j = 1, 2, \ldots, n$. These constants are characterized such that $|g_j(u) - g_j(v)| < L_j|u - v|$, $\forall u, v \in \mathbb{R}$.

(A_2) The parameters c_i, d_{ij}, and g_j are subject to the condition that all roots of

$$\det\left(\operatorname{diag}\left(\left(1 - \frac{1}{s}\right)^{\alpha_1}, \left(1 - \frac{1}{s}\right)^{\alpha_2}, \ldots, \left(1 - \frac{1}{s}\right)^{\alpha_n}\right) - \mathbf{A}^{\alpha}\right) = 0, \tag{4.24}$$

possess negative real components, with $\mathbf{A}^{\boldsymbol{\alpha}}$ being defined as:

$$\mathbf{A}^{\alpha} = \begin{bmatrix} \sum_{j=1}^{n} |d_{1j}|L_j + |d_{11}|L_1 - 2c_1 & |d_{12}|L_2 & \dots & |d_{1n}|L_n, \\ |d_{21}|L_1 & \sum_{j=1}^{n} |d_{2j}|L_j + |d_{22}|L_2 - 2c_2 & \dots & |d_{2n}|L_n, \\ \vdots & \vdots & \ddots & \vdots, \\ |d_{n1}|L_1 & |d_{n2}|L_2 & \dots & \sum_{j=1}^{n} |d_{nj}|L_j + |d_{nn}|L_n - 2c_n. \end{bmatrix}$$

Theorem 4.6. *AGiven the fulfillment of conditions* (A_1) *and* (A_2)*, the discrete fractional-order neural network delineated by* (4.78)*, featuring incommensurate order, demonstrates global asymptotic stability.*

Proof. Let $x^* = (x_1^*, x_2^*, ..., x_n^*)^T$ denote an equilibrium point of (4.23), and let $x(t)$ represent any solution of (4.23). Introduce $y_i(t) = x_i(t) - x_i^*$, which yields:

$$ {}_a^C\nabla^{\alpha_i} y_i(t) = -c_i y_i(t) + \sum_{j=1}^{n} (d_{ij} g_j(t, x_j(t)) - d_{ij} g_j(x_j^*)), \quad i = 1, 2, \dots, n. \tag{4.25}$$

Alternatively, expressed compactly:

$$ {}_a^C\nabla^{\alpha} y(t) = -Ay(t) + D(g(x(t)) - g(x^*)). \tag{4.26}$$

Let's construct the function $V(t)$ as follows:

$$V(t) = \sum_{i=1}^{n} V_i(t) = \sum_{i=1}^{n} y_i^2(t). \tag{4.27}$$

Determining the α_i-th order defferences of $V_i(t)$ as the solution trajectory of equation (4.79) progresses results in:

$$ {}_a^C\nabla^{\alpha_i} V_i(t) \le 2y_i(t)\, {}_a^C\nabla^{\alpha_i} y_i(t) = 2y_i(t) \left(-c_i y_i(t) + \sum_{j=1}^{n} (d_{ij} g_j(x_j(t)) - d_{ij} g_j(x_j^*)) \right). \tag{4.28}$$

Upon further simplification of (4.28), we obtain:

$$\begin{aligned} {}_a^C\nabla^{\alpha_i} V_i(t) &\le -2c_i y_i^2(t) + \sum_{j=1}^{n} 2|y_i(t)||d_{ij}|L_j|y_j(t)| \\ &\le \left(\sum_{j=1}^{n} |d_{ij}|L_j + |d_{ii}|L_i - 2c_i \right) V_i(t) + \sum_{j=1, i\neq j}^{n} |d_{ij}|L_j V_j(t). \end{aligned} \tag{4.29}$$

Representing (4.29) as a set of inequalities for each i yields:

$$\begin{aligned} {}_a^C\nabla^{\alpha_1} V_1(t) &\le \left(\sum_{j=1}^{n} |d_{1j}|L_j + |d_{11}|L_1 - 2c_1 \right) V_1(t) + \sum_{j=2}^{n} |d_{1j}|L_j V_j(t), \\ {}_a^C\nabla^{\alpha_2} V_2(t) &\le \left(\sum_{j=1}^{n} |d_{2j}|L_j + |d_{22}|L_2 - 2c_2 \right) V_2(t) + \sum_{j=1, j\neq 2}^{n} |d_{2j}|L_j V_j(t), \\ &\vdots \\ {}_a^C\nabla^{\alpha_n} V_n(t) &\le \left(\sum_{j=1}^{n} |d_{nj}|L_j + |d_{nn}|L_n - 2c_n \right) V_n(t) + \sum_{j=1}^{n-1} |d_{nj}|L_j V_j(t). \end{aligned} \tag{4.30}$$

Utilizing the system (4.30), we can formulate the non-commensurate fractional-order linear comparison system as follows:

$$\begin{aligned}
{}_a^C\nabla^{\alpha_1} W_1(t) &= \left(\sum_{j=1}^{n} |d_{1j}|L_j + |d_{11}|L_1 - 2c_1\right) W_1(t) + \sum_{j=2}^{n} |d_{1j}|L_j W_j(t),\\
{}_a^C\nabla^{\alpha_2} W_2(t) &= \left(\sum_{j=1}^{n} |d_{2j}|L_j + |d_{22}|L_2 - 2c_2\right) W_2(t) + \sum_{j=1, j\neq 2}^{n} |d_{2j}|L_j W_j(t),\\
&\vdots\\
{}_a^C\nabla^{\alpha_n} W_n(t) &= \left(\sum_{j=1}^{n} |d_{nj}|L_j + |d_{nn}|L_n - 2c_n\right) W_n(t) + \sum_{j=1}^{n-1} |d_{nj}|L_j W_j(t).
\end{aligned} \tag{4.31}$$

In an alternative representation, we can express it in vector-matrix form as:

$$\begin{bmatrix} {}_a^C\nabla^{\alpha_1} W_1(t) \\ {}_a^C\nabla^{\alpha_2} W_2(t) \\ \vdots \\ {}_a^C\nabla^{\alpha_n} W_n(t) \end{bmatrix} =$$
$$\begin{bmatrix} \sum_{j=1}^{n} |d_{1j}|L_j + |d_{11}|L_1 - 2c_1 & |d_{12}|L_2 & \dots & |d_{1n}|L_n \\ |d_{21}|L_1 & \sum_{j=1}^{n} |d_{2j}|L_j + |d_{22}|L_2 - 2c_2 & \dots & |d_{2n}|L_n \\ \vdots & \vdots & \ddots & \vdots \\ |d_{n1}|L_1 & |d_{n2}|L_2 & \dots & \sum_{j=1}^{n} |d_{nj}|L_j + |d_{nn}|L_n - 2c_n \end{bmatrix}$$
$$\times \begin{bmatrix} W_1(t) \\ W_2(t) \\ \vdots \\ W_n(t) \end{bmatrix}. \tag{4.32}$$

By leveraging the insights provided by Lemma 4.3, we establish a relationship where $V_i(t)$ is bounded by $W_i(t)$, $t \geq 0$ and $i = 1, 2, \dots, n$. This relationship, guided by Assumption 2, leads to the global asymptotic stability of the zero solution in the incommensurate fractional-order linear comparison system (4.32). Essentially, it indicates that as t converges to zero. Building upon the foundation laid by Lemma 4.3 and the expression (2.39), we deduce that $V_i(t)$ also converges to zero, subsequently implying the convergence of $y_i(t)$ to zero as t tends to infinity. Consequently, we establish the global asymptotic stability of the incommensurate fractional-order neural networks (4.23). This concludes the proof.

□

4.3.3 Examples and Simulations

To underscore the practicality and precision of the proposed formulation, we present two comprehensive numerical demonstrations. These demonstrations serve to validate the effectiveness and applicability of our approach in real-world scenarios, offering insights into its performance and robustness across various settings and conditions.

Example 4.3. *Let's consider the incommensurate discrete fractional-order Network model :*

$$\begin{cases} {}_a^C\nabla^{\alpha_1} x_1(t) &= -0.3x_1(t) + 0.01\sin(x_1(t)) - 0.02\sin(x_2(t)), \\ {}_a^C\nabla^{\alpha_2} x_2(t) &= -0.1x_2(t) - 0.03\sin(x_1(t)) + 0.04\sin(x_2(t)), \end{cases} \tag{4.33}$$

where $\alpha_1 = \frac{1}{3}$ *and* $\alpha_2 = \frac{1}{4}$. *Notably,* $L_i = 1$. *Through straightforward calculations, we determine that the unique equilibrium value* x^* *for* (4.33) *are found to be* $(0, 0)$, *and the matrix* $\hat{A}$ *is given by:*

$$\mathbf{A} = \begin{bmatrix} 0.01 & -0.02 \\ -0.03 & 0.04 \end{bmatrix}. \tag{4.34}$$

As a result, the characteristic equation $det(s^\alpha I - \mathbf{A}) = 0$ *simplifies to* $s^{9/5} - 4s^{3/5} - 2s^{7/10} - 4 = 0$. *Introducing new variables* $s_1 = s^{1/2}$ *and* $s_2 = s^{1/5}$, *we obtain the bivariate polynomial:*

$$a(s_1, s_2) = s_2^4 - 2s_1s_2 - 4s_2^3 - 4 = 0. \tag{4.35}$$

Using elementary operations, we compute the companion matrix as follows:

$$\mathbf{A} = \begin{bmatrix} 0.34 & 0.02 \\ 0.03 & 0.14 \end{bmatrix}. \tag{4.36}$$

Leveraging Matlab's Linear Matrix Inequality (LMI) control toolbox, we verify the practical applicability of the LMI outlined in Theorem 4.6. This validation corroborates the conclusion, as asserted by Theorem 4.6, that the equilibrium point x^* *is characterized by asymptotic stability. Figure 4.4 visually illustrates the convergence of the solution trajectory for system* (4.33) *towards the asymptotically stable equilibrium point* x^*.

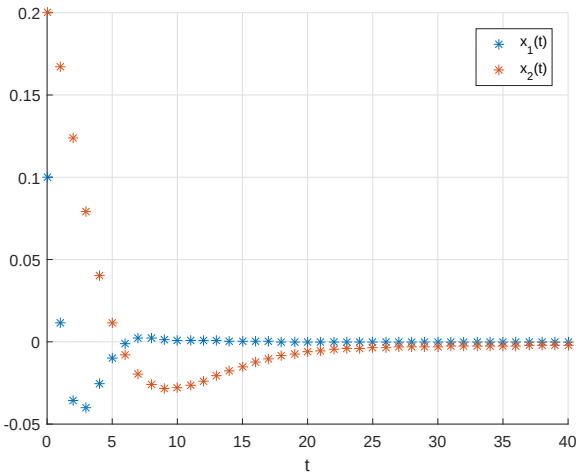

Figure 4.4: Solution Convergence to Equilibrium Point x^* in System (4.33).

4.4 Asymptotic Stability of Commensurate Discrete Variable-Order Neural Networks

This part acces the development of stability criteria uniquely suited to commensurate networks, aiming to elucidate their asymptotic stability properties. By exploring the

stability nuances of commensurate discrete variable-order neural networks, this subsection contributes valuable insights to enhance our understanding of their dynamic behavior, thereby facilitating their application across various domains.

4.4.1 Stability of Variable-Order Systems with Discrete Nabla Operator

We commence by presenting fundamental stability results regarding to general discrete variable-order system. These results are crucial for establishing the asymptotic stability of the specific neural network model under investigation. By applying these theoretical insights, we aim to rigorously determine the stability properties of the neural networks in question.

Lemme 4.4. *Consider $x : \mathbb{N}_{a+1} \to \mathbb{R}$ and $x(t)$ satisfying the following inequality:*

$$ {}_a^C\nabla^{\alpha(t)} x^2(t) \leq 2x(t)\, {}_a^C\nabla^{\alpha(t)} x(t). \tag{4.37}$$

Proof. It is necessary to demonstrate equivalently.

$$ {}_a^C\nabla^{\alpha(t)} x^2(t) - 2x(t)\, {}_a^C\nabla^{\alpha(t)} x(t) \leq 0. \tag{4.38}$$

Alternatively, we have:

$$\begin{aligned}
{}_a^C\nabla^{\alpha(t)} x^2(t) - 2x(t)\, {}_a^C\nabla^{\alpha(t)} x(t) &= \frac{1}{\Gamma(1-\alpha(t))} \sum_{s=a+1}^{t} (t-\rho(s))^{\overline{-\alpha(t)}} [(x(s) - x(s-1)) \\
&\quad - 2(x(t)x(s) - x(t)x(s-1))], \\
&= \frac{1}{\Gamma(1-\alpha(t))} \sum_{s=a+1}^{t} (t-\rho(s))^{\overline{-\alpha(t)}} [(x^2(s) - x^2(s-1)) \\
&\quad - 2(x(t)x(s) - x(t)x(s-1))], \\
&= \frac{1}{\Gamma(1-\alpha(t))} \sum_{s=a+1}^{t} (t-\rho(s))^{\overline{-\alpha(t)}} [(x(t) - x(s))^2 \\
&\quad - (x(t) - x(s-1))^2], \\
&= \frac{1}{\Gamma(1-\alpha(t))} \sum_{s=a+1}^{t} (t-\rho(s))^{\overline{-\alpha(t)}} \nabla_s (x(t) - x(s))^2.
\end{aligned}$$

Employing summation by parts as described in equation (5.80), let $g(s-1) = (t - \rho(s))^{\overline{-\alpha(t)}}$ and $f(s) = (x(s) - x(t))^2$.
Since

$$ \nabla_s (t-\rho(s))^{\overline{-\alpha(t)}} = -\alpha(t)(t-\rho(s))^{\overline{-\alpha(t)-1}}. \tag{4.39}$$

The resulting expression is:

$$\begin{aligned}
{}_a^C\nabla^{\alpha(t)}x^2(t) - 2x(t)\,{}_a^C\nabla^{\alpha(t)}x(t) &= \frac{-1}{\Gamma(1-\alpha(t))}\sum_{s=a+1}^{t}\nabla_s(t-\rho(s))^{\overline{-\alpha(t)}}(x(s)-x(t))^2 \\
&\quad + (t-\rho(s))^{\overline{-\alpha(t)}}(x(s)-x(t))^2|_a^t, \\
&= \frac{-\alpha(t)}{\Gamma(1-\alpha(t))}\sum_{s=a+1}^{t}(t-\rho(s)+1)^{\overline{-\alpha(t)-1}}(x(s)-x(t))^2 \\
&\quad - (t-\rho(a))^{\overline{-\alpha(t)}}(x(a)-x(t))^2 \le 0.
\end{aligned}$$

With that, the proof is concluded. □

In our comprehensive exploration, we delve into the dynamics of a discrete variable fractional-order system, described by the following formulation:

$$\begin{cases} {}_a^C\nabla^{\alpha(t)}x(t) = f(t,x(t)), \quad t \in \mathbb{N}_{a+1}, \\ x(a) = x_0, \end{cases} \tag{4.40}$$

where $0 < \alpha_1 \le \alpha(t) \le \alpha_2 < 1$.

The ensuing theorem extends the Lyapunov direct method into a variable-order framework, laying the groundwork for the asymptotic stability analysis of discrete variable-order systems.

Theorem 4.7. *Let's assume that there exists a positive definite and monotonically decreasing Lyapunov functionV$(t,x(t))$ satisfying:*

$$\gamma_1(\|x(t)\|) \le V(t,x(t)) \le \gamma_2(\|x(k)\|), \tag{4.41}$$

$${}_a^C\nabla^{\alpha(t)}V(t,x(t)) \le -\gamma_3(\|x(k)\|), \tag{4.42}$$

here, $\alpha(t) \in (0,1)$ and $\gamma_1,\gamma_2,\gamma_3$ are discrete class–κfunctions. Consequently, system (4.40) is asymptotically stable.

Proof. for $T \in \mathbb{N}_{a+1}$ we have

$$T^{-\alpha(t)} = \frac{\Gamma(T-\alpha(t))}{\Gamma(T)} \le \begin{cases} T^{-\alpha_1}, & 0 \le T \le 1, \\ T^{-\alpha_2}, & T > 1. \end{cases} \tag{4.43}$$

Let's examine $T = t-a$, and $Y = \max\{T^{-\alpha_1}, T^{-\alpha_2}\}$. Utilizing the property of $\Gamma(t)$ on $(0,1)$, we establish $\Gamma(1-\alpha_1) \le \Gamma(1-\alpha(t)) \le \Gamma(1-\alpha_2)$, This, in conjunction with the

definitions outlined in (1.203), yields:

$$\begin{aligned}
{}_a^C\nabla^{\alpha(t)}V(t,x(t)) &= \frac{1}{\Gamma(1-\alpha(t))}\sum_{s=a+1}^{t}(t-\rho(s))^{\overline{-\alpha(t)}}\nabla_s V(s,x(s)),\\
&\geq \frac{1}{\Gamma(1-\alpha_2)}\sum_{s=a+1}^{t}(t-\rho(s))^{\overline{-\alpha(t)}}\nabla_s V(s,x(s)),\\
&\geq \frac{Y}{\Gamma(1-\alpha_2)}\sum_{s=a+1}^{t}(\frac{t-\rho(s)}{T})^{\overline{-\alpha(t)}}\nabla_s V(s,x(s)),\\
&\geq \frac{Y}{\Gamma(1-\alpha_2)}\sum_{s=a+1}^{t}(\frac{t-\rho(s)}{T})^{\overline{-\alpha_1}}\nabla_s V(s,x(s)),\\
&\geq \frac{1}{\kappa}\,{}_a^C\nabla^{\alpha_1}V(t,x(t)),
\end{aligned}$$

where $\kappa = \dfrac{\Gamma(1-\alpha_1)}{\Gamma(1-\alpha_2)T^{\alpha_1}Y} > 0$.
Therefore,

$${}_a^C\nabla^{\alpha_1}V(t,x(t)) \leq \kappa\,{}_a^C\nabla^{\alpha(t)}V(t,x(t)). \tag{4.44}$$

As a result, we deduce that:

$${}_a^C\nabla^{\alpha_1}V(t,x(t)) \leq -\kappa\gamma_3(\gamma_2^{-1}(V(t,x(t))). \tag{4.45}$$

Given that $V(t,x(t))$ is positive definite and monotonically decreasing, we can infer that $V(a,x(a)) \geq 0$. Thus, naturally:

$$V(t,x(t)) \leq V(a,x(a)), \tag{4.46}$$

this leads to

$$\|x(t)\| \leq -\kappa\gamma_3(\gamma_2^{-1}(\|x(a)\|)). \tag{4.47}$$

Considering the relationship between the nature of $V(t,x(t))$ and the class κ of functions , and referring to Theorem 2.15, we conclude that system (4.40) is asymptotically stable. □

Theorem 4.8. *Suppose that $x = 0$ serves as an equilibrium point of system (4.40). If there exists a positive continuous function $V(t,x(t))$ such that, for arbitrary positive constants q_1, q_2q_3, a, b the following inequality holds true:*

$$q_1\|x(t)\|^b \leq V(t,x(t)) \leq q_2\|x(k)\|^{bc}, \tag{4.48}$$

$${}_a^C\nabla^{\alpha(t)}V(t,x(t)) \leq -q_3\|x(k)\|^{bc}. \tag{4.49}$$

Then, the equilibrium point of (4.40) is asymptoticly stable.

Proof. From (4.44) and (4.48), we have:

$${}_a^C\nabla^{\alpha_1}V(t,x(t)) \leq -\kappa q_3q_2^{-1}(V(t,x(t)). \tag{4.50}$$

Then, there exists a nonnegative function $m(t)$ exists such that

$$\_a{}^C\nabla^{\alpha_1}V(t,x(t)) = -\kappa q_3q_2^{-1}V(t,x(t)) - m(t). \tag{4.51}$$

Taking the Laplace transform of equation (4.51) and considering the initial condition $V(0) = V(0, x(0))$, we obtain

$$s_1^{\alpha} V_f(s) - s^{\alpha_1 - 1} V(a, x(a)) = -\kappa q_3 q_2^{-1} V_f(s) - M(s). \tag{4.52}$$

Consequently, the Laplace transform denoted as $V_f(s)$ can be formulated as:

$$V_f(s) = \frac{V(a, x(a)) s^{\alpha_1 - 1} - M(s)}{s_1^{\alpha} + \kappa q_3 q_2^{-1}}, \tag{4.53}$$

where $M(s) = N[m(t)](s)$ and $V_f(s) = N[V(t, x(t)](s)$.
Defining $\kappa = \kappa q_3 q_2^{-1}$ and considering the properties of existence and uniqueness of the nabla Laplace transform, the unique solution of (4.52) is given by:

$$V(t, x(t)) = V(a, x(a)) E_{\overline{\alpha_1,1}}(\kappa, t - a) - m(t) * E_{\overline{\alpha_1,\alpha_1}}(\kappa, t, a), \tag{4.54}$$

from the nonnegativity of $m(t)$ and $E_{\overline{\alpha_1,\alpha_1}}(\kappa, t-a)$one can deduce the following inequality:

$$V(t, x(t)) \leq V(a, x(a)) E_{\overline{\alpha_1,1}}(\kappa, t - a), \tag{4.55}$$

which leads to the conclusion that

$$\lim_{t \to +\infty} V(a, x(a)) E_{\overline{\alpha_1,1}}(\kappa, t - a) = 0. \tag{4.56}$$

Plugging in equation (2.78) into equation (2.76) yields

$$\|x(t)\| \leq [\frac{\|x(a)\|}{q_1} E_{\overline{\alpha_1,1}}(\kappa, t - a)]^{\frac{1}{b}}. \tag{4.57}$$

Suppose $m = V(a, x(a))$ and $q_1 \geq 0$. It follows that $m = 0$ if and only if $x(a) = 0$. Since $V(t, x(t))$ is positive definite and monotonically decreasing, $m(0) = 0$ and m is Lipschitz. Therefore, system (4.40) is Mittag-Leffler stable, concluding the proof.

□

4.4.2 Stablity of Discrete Variable-Order Neural Networks

We introduce the subsequent variable fractional discrete-time neural network model:

$${}_a^C \nabla^{\alpha(t)} x(t) = -Ax(t) + Dg(t, x(t)) + I, \tag{4.58}$$

We introduce first the following assumptions

Assumption 1 (A_1) At every time point $t \in \mathbb{N}_{a+1}$, $g(t, x)$ signifies a continuous function concerning x, and there exists a set of positive constants $G_i \in \mathbb{R}_*^+, i = 1, ..., n$ satisfying

$$|g_i(t, x) - g_i(t, y)| \leq G_i |x - y|, \tag{4.59}$$

for every $x, y \in \mathbb{R}$.

Assumption 2 (A_2) There exist a constant $k \in \mathbb{R}$ such that

$$k = \max_{\left\{ i=1,...,n \{ -c_i + \sum_{j=1}^{n} \frac{|d_{ij}| G_j + |d_{ji}| G_i}{2} \right\} < 0.} \tag{4.60}$$

Theorem 4.9. *If conditions* $(A_1), (A_2)$ *are satisfied, then system* (4.58) *is asymptotically stable.*

Proof. Suppose the equilibrium point of (6.9) is denoted by $x(t) = x^*$. By introducing the change of variable $e_i(t) = x_i(t) - x^*$, we can express the equilibrium point as the origin, yielding:

$$ {}_a^C\nabla_t^{\alpha(t)} e_i(t) = -c_i e_i(t) + \sum_{j=1}^{n} d_{ij}[g_j(t, x_j(t)) - g_j(t, x_j^*)]. \tag{4.61} $$

Let's select the Lyapunov function as:

$$ V(t, x(t)) = \frac{1}{2}\sum_{i=1}^{n} e_i^2(t). \tag{4.62} $$

Taking the discrete nabla variable-order derivative with order $\alpha(t)$ of the Lyapunov function with respect to time, and considering (A_1) and (A_2), we derive the following:

$$
\begin{aligned}
{}_a^C\nabla^{\alpha(t)} V(t, e(t)) =& \frac{1}{2}\sum_{i=1}^{n} {}_a^C\nabla^{\alpha(t)} e_i^2(t), \\
&\leq \sum_{i=1}^{n} e_i(t)\, {}_a^C\nabla^{\alpha(t)} e_i(t), \\
&= \sum_{i=1}^{n} e_i(t)(-c_i e_i(t) + \sum_{j=1}^{n} d_{ij}[g_j(t, x_j(t)) - g_j(t, x_j^*)]), \\
&\leq \sum_{i=1}^{n} e_i(t)[-c_i e_i(t) + \sum_{j=1}^{n} |d_{ij}| G_j |e_j(t)|], \\
&\leq \sum_{i=1}^{n} -c_i e_i^2(t) + \sum_{j=1}^{n} |d_{ij}| G_j e_j(t) e_i(t)], \\
&\leq \sum_{i=1}^{n}{}_n - c_i e_i^2(t) + \sum_{j=1}^{n} |d_{ij}| G_j \frac{e_j^2(t) + e_i^2(t)}{2}, \\
&\leq \sum_{i=1}^{n} -c_i e_i^2(t) + e_i^2(t) \sum_{j=1}^{n} \frac{|d_{ij}| G_j + |d_{ji}| G_i}{2}, \\
&\leq \sum_{i=1}^{n} e_i^2(t)[-c_i + \sum_{j=1}^{n} \frac{|d_{ij}| G_j + |d_{ji}| G_i}{2}] \leq k\|e\|,
\end{aligned}
$$

where $k = \max\limits_{i=1,\ldots,n} \left\{ -c_i + \sum\limits_{j=1}^{n} \dfrac{|d_{ij}| G_j + |d_{ji}| G_i}{2} \right\} < 0.$

This implies ${}_a^C\nabla^{\alpha(t)} V(t, x(t)) \leq 0$. Therefore, according to Theorems 4.7 and 4.8, system (4.58) is asymptotically stable. □

4.4.3 Numerical Simulations

We will now present several examples accompanied by simulations to substantiate the theoretical results previously discussed. These examples will serve to illustrate the practical

application and effectiveness of the proposed methodologies, providing concrete evidence of their validity through detailed numerical experiments.

Example 4.4. *Let's examine the given system:*

$$\begin{cases} {}_a^C\nabla^{\alpha(t)}x_1(t) = -0.3x_1(t) + x_2^3(t), \\ {}_a^C\nabla^{\alpha(t)}x_2(t) = -0.3x_1(t) - x_2(t). \end{cases} \tag{4.63}$$

We can choose the Lyapunov candidate function as follows:

$$V(t, x(t)) = \frac{1}{2}x_1^2(t) + \frac{1}{4}x_2^4(t). \tag{4.64}$$

Utilizing (4.37), we derive:

$$\begin{aligned} {}_a^C\nabla^{\alpha(t)}V(t, x(t)) &= {}_a^C\nabla^{\alpha(t)}(\frac{1}{2}x_1^2(t) + \frac{1}{4}x_2^4(t)), \\ &\leq x_1(t)\,{}_a^C\nabla^{\alpha(t)}x_1(t) + x_2^3(t)\,{}_a^C\nabla^{\alpha(t)}x_2(t)), \\ &= x_1(t)[-0.3x_1(t) + x_2^3(t)] + x_2^3(t)[-0.3x_1(t) - x_2(t)], \\ &= -x_1^2(t) - x_2^4(t) \leq 0. \end{aligned}$$

The Lyapunov function's variable fractional difference is negative definite. Utilizing Theorem 4.3, we conclude that system (4.63) is asymptotically stable, with the origin being the equilibrium point.

Figure 4.5 illustrates the evolution of system (4.63). The plot clearly demonstrates the asymptotic stability of the solution for the initial condition $x(0) = (-1, 1)$ and the variable-order function $\alpha(t) = \dfrac{|\ln \dfrac{1}{t+1}|}{6}$ with $t \in \{0, ..., 80\}$.

The numerical solution of system (4.63) is as follows:

$$\begin{cases} x_1(i) = x_1(0) + \dfrac{1}{\Gamma\left(\dfrac{|\ln \frac{1}{i+1}|}{6}\right)} \displaystyle\sum_{j=1}^{i} \dfrac{\Gamma\left(i - j + \dfrac{|\ln \frac{1}{i+1}|}{6}\right)}{\Gamma(i - j + 1)} \left(-0.3x_1(j) + x_2^3(j)\right), \\ x_2(i) = x_2(0) + \dfrac{1}{\Gamma\left(\dfrac{|\ln \frac{1}{i+1}|}{6}\right)} \displaystyle\sum_{j=1}^{i} \dfrac{\Gamma\left(i - j + \dfrac{|\ln \frac{1}{i+1}|}{6}\right)}{\Gamma(i - j + 1)} \left(-0.3x_1(j) - x_2(j)\right). \end{cases} \tag{4.65}$$

Example 4.5. *Consider the following discrete-time neural networks of variable fractional-order*

$$\begin{cases} {}_a^C\nabla^{\alpha(t)}x_1(t) = -c_1x_1(t) + d_{11}\sin(x_1(t)) + d_{12}\sin(x_2(t)) + I_1, \\ {}_a^C\nabla^{\alpha(t)}x_2(t) = -c_2x_2(t) + d_{21}\sin(x_1(t)) + d_{22}\sin(x_2(t)) + I_2. \end{cases} \tag{4.66}$$

Consider the following parameters:$c_1 = 1.7$, $c_2 = 2$, $d_{11} = 0.1$, $d_{12} = -0.8$, $d_{21} = 0.5$, $d_{22} = -0.4$, $I_1 = 0.1, I_2 = -0.1$ $\alpha(t) = |\frac{1}{6} - e^{-\frac{t}{4}}|$ *and the initial condition* $x_1(0) = 0.4, x_2(0) = 0.3$ *with* $t \in \{0, ..., 80\}$

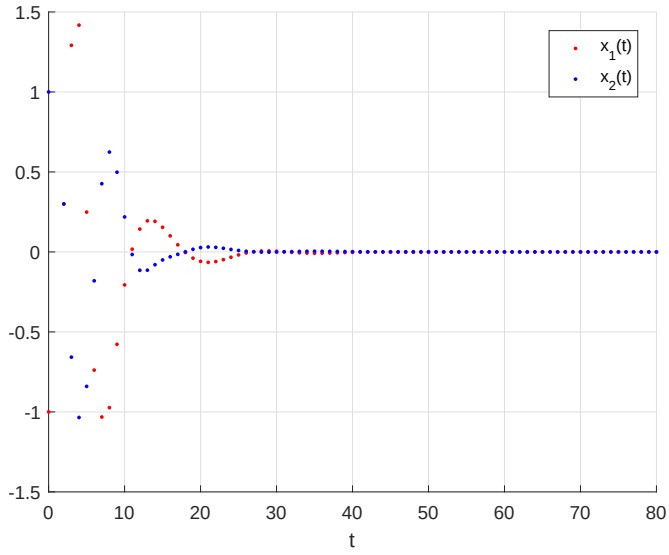

Figure 4.5: Numerical solution of system (4.63).

The numerical solution of (4.66) *is provided as follows:*

$$\begin{cases} x_1(i) = x_1(0) + \dfrac{1}{\Gamma\left(|\frac{1}{6} - e^{-\frac{i}{4}}|\right)} \displaystyle\sum_{j=1}^{i} \frac{\Gamma\left(i-j+|\frac{1}{6} - e^{-\frac{i}{4}}|\right)}{\Gamma(i-j+1)}(-a_1 x(j) + b_{11}\sin(x_1(j)) \\ \qquad +b_{12}\sin(x_2(j)) + I_1), \\ x_2(i) = x_2(0) + \dfrac{1}{\Gamma\left(|\frac{1}{6} - e^{-\frac{i}{4}}|\right)} \displaystyle\sum_{j=1}^{i} \frac{\Gamma\left(i-j+|\frac{1}{6} - e^{-\frac{i}{4}}|\right)}{\Gamma(i-j+1)}(-a_2 x(j) + b_{21}\sin(x_1(j)) \\ \qquad +b_{22}\sin(x_2(j)) + I_2), \end{cases} \tag{4.67}$$

We can verify that these parameters satisfy assumptions (A_1), (A_2), *and the condition in Theorem 4.9. Figure 4.6 depicts the behavior of* $x_1(t)$ *and* $x_2(t)$, *respectively. Both tend to zero as* $t \to +\infty$, *indicating asymptotic stability of the solution.*

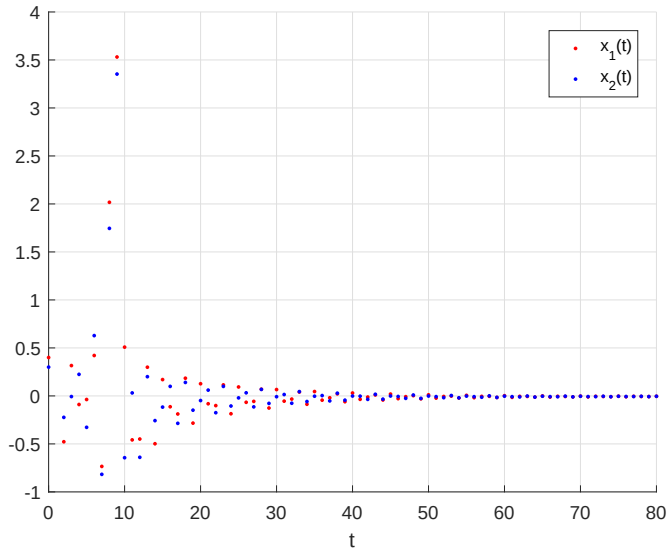

Figure 4.6: Numerical solution of neural networks (4.66).

4.5 Asymptotic Stability of Incommensurate Discrete Variable-Order Neural Networks

This section is dedicated to unraveling the stability characteristics unique to incommensurate discrete variable-order networks, which exhibit diverse fractional variable-orders across neurons. By delving into the of these networks, we aim to uncover the stability criteria and behaviors that distinguish them from commensurate systems. The analysis will focus on the Mittag-Leffler stability of these neural networks, providing a comprehensive understanding of their dynamic properties and stability conditions.

4.5.1 General Result

In this part, we delve into an investigation of the stability properties of variable-order fractional systems distinguished by incommensurate orders. Our methodology involves employing the robust Lyapunov method to analyze the system dynamics. Let's shift our attention to the examination of the following nonlinear discrete system with variable orders:

$$ {}^{C}\nabla^{\overline{\alpha(t)}}x(t) = f(t, x(t)), \quad x(0) = x_0, \tag{4.68} $$

where $x(t) = (x_1(t), x_2(t), \ldots, x_n(t))^T \in \mathbb{R}^n$,
${}^{C}\nabla^{\alpha(t)}x(t) = ({}^{C}\nabla^{\alpha_1(t)}x_1(t), {}^{C}\nabla^{\alpha_2(t)}x_2(t), \ldots, {}^{C}\nabla^{\alpha_n(t)}x_n(t))^T$, the incommensurate-orders $\alpha_i(t) \in (0, 1]$, and $f(t, x(t))$ is a continuously differentiable function.

Theorem 4.10. *If we contemplate system (4.68) following the Caputo definition, the conditions for asymptotic stability can be identified through the existence of class K functions γ_1, γ_2, γ_3, parameters $\beta \in (0, \min\{\alpha_i(t)\}$, $p_i > 0$, and Lyapunov functions $V_i(t, x_i(t)) : \mathbb{N}_a \times D \to \mathbb{R}$ for each $i = 1, 2, \ldots, n$, satisfying:*

$$\gamma_1(||x(t)||) \leq \sum_{i=1}^{n} p_i \, {}^{C}\nabla^{\alpha_i(t)-\beta} V_i(t, x_i(t)) \leq \gamma_2(\|x(t)\|) \tag{4.69}$$

$$\sum_{i=1}^{n} p_i \frac{\partial V_i(t, x_i(t))}{\partial x_i(t)} f_i(t, x(t)) \leq -\gamma_3(\|x(t)\|) \tag{4.70}$$

In the scenario where $x(t) \in D$, $t \in \mathbb{N}_{a+1}$, $a \in \mathbb{R}$, and $V_i(t, x_i(t))$ is a differentiable and convex function regarding $x_i(t)$, the system (4.68) is considered to be uniformly asymptotically stable at $x_e = 0$.

Proof. For the global Lyapunov function, let's select

$$V(t, x(t)) := \sum_{i=1}^{n} p_i \, {}^{C}\nabla^{\alpha_i(t)-\beta} V_i(t, x_i(t)). \tag{4.71}$$

Equivalently, equation (4.69) can be expressed as:

$$\gamma_1(\|x(t)\|) \leq V(t, x(t)) \leq \gamma_2(\|x(t)\|). \tag{4.72}$$

By utilizing Lemma 2.3 and equation (4.70), we obtain:

$$\begin{aligned}
{}^{C}\nabla^{\beta} \sum_{i=1}^{n} p_i \, {}^{C}\nabla^{\alpha_i(t)-\beta} V_i(t, x_i(t)) &= \sum_{i=1}^{n} p_i \, {}^{C}\nabla^{\beta} \, {}^{C}\nabla^{\alpha_i(t)-\beta} \nabla V_i(t, x_i(t)), && (4.73)\\
&= \sum_{i=1}^{n} p_i \, {}^{C}\nabla^{\alpha_i(t)} V_i(t, x_i(t)), && (4.74)\\
&\leq \sum_{i=1}^{n} p_i \frac{\partial V_i(t, x(t))}{\partial x_i(t)} \, {}^{C}\nabla^{\alpha_i(t)} x_i(t), && (4.75)\\
&= \sum_{i=1}^{n} p_i \frac{\partial V_i(t, x(t))}{\partial x_i(t)} f_i(t, x(t)) \leq -\gamma_3(\|x(t)\|). && (4.76)
\end{aligned}$$

Utilizing Equations (4.73) through (4.76) along with Lemma 2.1, we find:

$${}^{C}\nabla^{\alpha_i(t)} V(t, x(t)) \leq -\gamma_3(\|x(t)\|).$$

Thus, the proof is concluded. □

4.5.2 Application to Incommensurate Discrete Variable-Order Neural Networks

We investigate the discrete fractional variable-order neural network outlined as follows:

$${}_{a}^{C}\nabla^{\alpha_i(t)} x_i(t) = -c_i x_i(t) + \sum_{j=1}^{n} d_{ij} g_j(t, x_j(t)) + I_i. \tag{4.77}$$

In short:

$${}_{a}^{C}\nabla^{\alpha(t)} x(t) = -Ax(t) + Dg(t, x(t)) + I. \tag{4.78}$$

We rely on the following assumptions to guide our exploration into the asymptotic stability of the incommensurate discrete-time variable-order neural networks (4.78):

(A_3) The following condition is satisfied:

$$\max_{i=1,\dots,n}\left(-c_i+\frac{\sum_{j=1}^{n}|d_{ij}|G_j+|d_{ji}|L_i}{2}\right)<0.$$

Theorem 4.11. *When conditions (A_1) and (A_3) are fulfilled, the incommensurate variable-order neural network specified by equation (4.78) achieves asymptotic stability.*

Proof. We'll proceed with a comparable approach as previously outlined. Introduce $y_i(t)=x_i(t)-x_i^*$, yielding

$${}_a^C\nabla^{\alpha_i(t)}y_i(t)=-c_iy_i(t)+\sum_{j=1}^{n}(d_{ij}g_j(t,x_j(t))-d_{ij}g_j(x_j^*)),\quad i=1,2,\dots,n. \tag{4.79}$$

Now, let's construct the auxiliary function $V(t)$ as follows:

$$V(t)=\frac{1}{2}\sum_{i=1}^{n}{}_a^C\nabla^{\alpha_i(t)-\beta}y_i^2(t), \tag{4.80}$$

where $\beta\in(0,\min\alpha_i(t))$. Calculating the $\alpha_i(t)$-order differences of $V(t)$ along the trajectory of (4.79) yields

$$\begin{aligned}{}_a^C\nabla^{\beta}V(t)&=\frac{1}{2}\sum_{i=1}^{n}{}_a^C\nabla^{\alpha_i(t)}y_i^2(t),\\&\le\sum_{i=1}^{n}y_i(t)\,{}_a^C\nabla^{\alpha_i(t)}y_i(t),\\&=y_i(t)\left(-c_iy_i(t)+\sum_{j=1}^{n}(d_{ij}g_j(x_j(t))-d_{ij}g_j(x_j^*))\right).\end{aligned} \tag{4.81}$$

Further simplification of (4.81) leads to

$$\begin{aligned}{}_a^C\nabla^{\alpha_i}V_i(t)&\le\sum_{i=1}^{n}y_i(t)\left[-c_iy_i(t)+\sum_{j=1}^{n}|d_{ij}|L_j|y_j(t)|\right],\\&\le\sum_{i=1}^{n}-c_iy_i^2(t)+\sum_{j=1}^{n}|d_{ij}|L_jy_j(t)y_i(t),\\&\le\sum_{i=1}^{n}-c_iy_i^2(t)+\sum_{j=1}^{n}|d_{ij}|L_j\frac{y_j^2(t)+y_i^2(t)}{2},\\&\le\sum_{i=1}^{n}-c_iy_i^2(t)+y_i^2(t)\sum_{j=1}^{n}\frac{|d_{ij}|L_j+|d_{ji}|L_i}{2},\\&\le\sum_{i=1}^{n}y_i^2(t)\left[-c_i+\frac{\sum_{j=1}^{n}|d_{ij}|L_j+|d_{ji}|L_i}{2}\right],\\&\le k\|e\|.\end{aligned} \tag{4.82}$$

Since $\max_{i=1,\dots,n}\left(-c_i+\dfrac{\sum_{j=1}^{n}|d_{ij}|L_j+|d_{ji}|L_i}{2}\right)<0$, then, ${}_a^C\nabla^{\beta}V(t,x(t))\leq 0$. Hence, in accordance with Theorems 4.10, the system represented by equation (4.78) attains asymptotic stability. □

4.5.3 Numerical Applications

To demonstrate the practicality and accuracy of the proposed formulation, we will provide two numerical simulations. In these simulations, we will apply the variable fractional discrete-time neural network model to solve specific problems. By examining these examples, we aim to showcase not only the theoretical soundness of the model but also its effectiveness in practical scenarios.

Example 4.6. *Let's explore the system governed by the following incommensurate variable-order difference equations:*

$$\begin{cases} {}_a^C\nabla^{\alpha_1(t)}x_1(t) &= -0.3x_1(t)+0.01\tanh(x_1(t))-0.02\tanh(x_2(t))+\tanh(x_3(t)),\\ {}_a^C\nabla^{\alpha_2(t)}x_2(t) &= -0.3x_1(t)+0.01\tanh(x_1(t))-0.02\tanh(x_2(t))+\tanh(x_3(t)),\\ {}_a^C\nabla^{\alpha_3(t)}x_3(t) &= -0.3x_1(t)+0.01\tanh(x_1(t))-0.02\tanh(x_2(t))+\tanh(x_3(t)), \end{cases} \tag{4.83}$$

where

$$\begin{cases} \alpha_1(t)=\left|\dfrac{1}{2}-e^{-4(t+1)}\right|,\\ \alpha_2(t)=\dfrac{1}{5}|\log(t+3)|,\\ \alpha_3(t)=\dfrac{1}{2}-\dfrac{e^{\frac{-10}{t+1}}}{t+1}, \end{cases} \tag{4.84}$$

heren, $0<\alpha_1(t),\alpha_2(t),\alpha_3(t)<1$, $t\in\mathbb{N}_{a+1}$, *and* $a\in\mathbb{R}$. *Let's define the Lyapunov function as:*

$$V(t,x(t)):=\sum_{i=1}^{3}{}_a^C\nabla^{\alpha_i(t)-\beta}x_i^2(t), \tag{4.85}$$

for $\beta\in(0,\min\{\alpha_1(t),\alpha_2(t),\alpha_3(t)\})$, *the derivative of* V *concerning* ∇^{β} *is expressed as:*

$${}_a^C\nabla^{\beta}V(t,x(t))\leq\sum_{i=1}^{3}{}_a^C\nabla^{\beta}\,{}_a^C\nabla^{\alpha_i(t)-\beta}x_i^2(t)=\sum_{i=1}^{3}{}_a^C\nabla^{\alpha_i(t)}x_i^2(t). \tag{4.86}$$

Ensuring the non-negativity of $V(t,x(t))$, *the system* (4.83) *according to the Caputo definition exhibits asymptotic stability around the equilibrium point* $x_e=0$, *This behavior is visually depicted in Figure 4.7.*

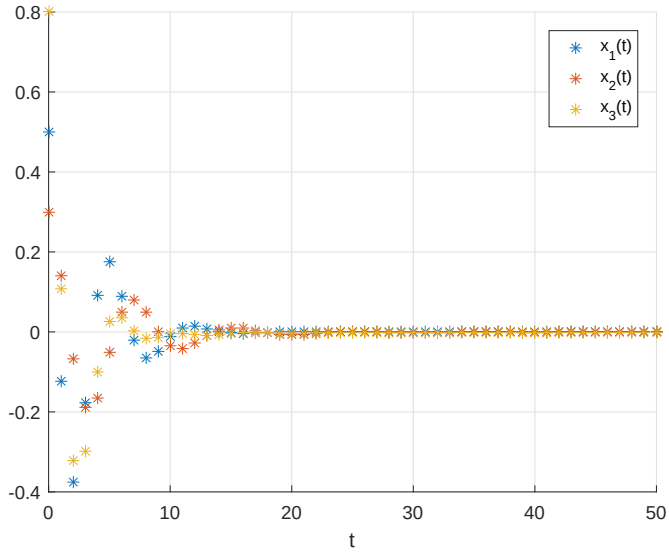

Figure 4.7: Convergence of the Solution Trajectory for System (4.83) Towards the Equilibrium Point x^*.

4.6 Conclusion

In summary, this chapter makes a significant contribution to the field by addressing a noticeable gap in the current literature concerning the stability analysis of incommensurate discrete fractional systems, with a particular emphasis on their application to neural networks. While commensurate systems have been extensively studied, the stability characteristics of incommensurate systems with variable orders have largely remained uncharted territory. Through the development of novel stability criteria and comparison theorems specifically tailored for incommensurate systems, this paper not only sheds light on their asymptotic stability properties but also opens up avenues for further exploration and application in diverse domains.

The key contributions of this chapter extend beyond mere theoretical advancements; they encompass the practical implications of these stability analysis techniques, especially in the realm of discrete fractional-order neural networks. By introducing a fractional difference comparison theorem and establishing stability criteria applicable to non-commensurate systems, this research lays the groundwork for a more nuanced understanding of stability in complex systems characterized by variable orders. Moreover, the application of these findings to discrete incommensurate fractional-order neural networks offers promising insights into their behavior and potential applications in real-world scenarios.

Furthermore, this chapter not only identifies the challenges posed by incommensurate systems but also provides innovative solutions to address them. Through meticulous theoretical developments and rigorous analysis, the authors present a comprehensive framework for studying the stability of incommensurate discrete fractional systems, thereby advancing the state-of-the-art in this burgeoning field. This multidimensional approach, integrating theoretical rigor with practical relevance, underscores the significance of this research in shaping future investigations and applications in the realm of discrete frac-

tional calculus and neural network dynamics.

Chapter 5

Finite-Time Dynamics in Discrete Fractional and Variable-Order Neural Networks

5.1 Introduction

In recent years, the concept of finite-time stability has emerged as a critical aspect of system analysis, particularly in the topic of fractional calculus. Unlike traditional Lyapunov stability, finite-time stability provides insights into system convergence within a defined timeframe, offering practical relevance across various domains [354, 355]. Despite its significance, finite-time stability in fractional systems, especially discrete fractional systems, remains relatively underexplored.

Finite-time stability considerations have led to the investigation of discrete fractional calculus, offering a pathway to integrate memory effects into time discretization models. Notable efforts have been made to develop fractional backward or nabla difference operators [356, 357, 358], such as the discrete left Caputo type with Mittag-Leffler kernels. However, there's a notable gap in understanding the h-fractional nabla discrete ABC type difference and its applications in the context of finite-time stability.

Recent studies have explored finite-time stability in various fractional systems, including Caputo delta fractional difference equations and nonlinear fractional delay systems [361, 362, 363, 364]. However, there's a scarcity of research focusing on finite-time stability in discrete fractional neural networks, where stability analysis is crucial for practical applicability.

This chapter aims to address this gap by delving deeper into the finite-time stability analysis of discrete fractional systems, particularly focusing on neural networks. We introduce novel stability criteria and comparison theorems tailored for finite-time stability analysis, providing valuable insights into the convergence behavior of these systems within finite timeframes.

5.2 Finite-Time Stability of Commensurate Discrete ABC type h-Fractional-Order Neural Networks

This subsection investigates the finite-time stability analysis of commensurate discrete ABC type h-fractional-order neural networks. Adopting a straightforward methodology, we aim to elucidate the stability properties of these networks over finite time intervals. By focusing on commensurate systems and employing accessible techniques, we endeavor to provide practical insights into the finite-time behavior of ABC type h-fractional-order neural networks.

We start by providing an important inequality, known as a discrete generalized Gronwall inequality. This inequality is crucial for establishing the stability and boundedness of solutions to discrete fractional-order systems. By leveraging this fundamental tool, we can derive essential stability results that will be applied to the analysis of fractional-order discrete-time fractional neural networks. The discrete generalized Gronwall inequality plays a pivotal role in the subsequent stability proofs and is a cornerstone of our theoretical framework.

5.2.1 Generalized Discrete Fractional ABC Gronwal Inequality

Lemme 5.1 ([365]). *Let $\phi(t)$ and $\psi(t)$ be non-negative, non-decreasing discrete functions, and suppose the condition $0 < \psi(t) \leq M < 1$ holds for all $t \in \mathbb{N}_a$. Additionally, $x(t)$ is a non-negative function that satisfies the following inequality:*

$$x(t) \leq \phi(t) + \psi(t)\, {}_a\nabla_h^{-\alpha} x(t), \tag{5.1}$$

then

$$x(t) \leq \phi(t)\, r_h E_{\overline{\alpha}}(\psi(t), t-a). \tag{5.2}$$

Theorem 5.1. *Assume that $0 < \alpha < \frac{1}{2}$, and consider the function*

$$\frac{H(\alpha,h)(1-\alpha+\alpha h)}{H(\alpha,h)(1-\alpha+\alpha h)-(1-\alpha)v(t)}u(t),$$

which is nonnegative and nondecreasing. Additionally,

$$\frac{\alpha v(t)}{H(\alpha,h)(1-\alpha+\alpha h)-(1-\alpha)v(t)},$$

is nondecreasing and satisfies

$$0 < \frac{\alpha v(t)}{H(\alpha,h)(1-\alpha+\alpha h)-(1-\alpha)v(t)} \leq 1.$$

For any $t \in \mathbb{N}_{a,h}$, where $x(t)$ is nonnegative, the following inequality holds:

$$x(t) \leq u(t) + v(t)\, {}_a^{AB}\nabla_h^{-\alpha} x(t), \tag{5.3}$$

then,

$$\begin{aligned} x(t) \leq{}& \frac{H(\alpha,h)(1-\alpha+\alpha h)}{H(\alpha,h)(1-\alpha+\alpha h)-(1-\alpha)v(t)}u(t)\, {}_h \\ &\times E_{\overline{\alpha}}\left(\frac{\alpha v(t)}{H(\alpha,h)(1-\alpha+\alpha h)-(1-\alpha)v(t)}, t-a\right). \end{aligned}$$

Proof. We have

$$x(t) \leq u(t) + v(t)_a^{AB}\nabla_h^{-\alpha}x(t). \tag{5.4}$$

This results in

$$x(t) \leq u(t) + v(t)(\frac{1-\alpha}{H(\alpha,h)(1-\alpha+\alpha h)}x(t) + \frac{\alpha}{H(\alpha,h)(1-\alpha+\alpha h)}\,{}_a\nabla_h^{-\alpha}x(t)).$$

Consequently, the subsequent inequality holds:

$$\begin{aligned} x(t) &\leq \left(1 - \frac{(1-\alpha)v(t)}{H(\alpha,h)(1-\alpha+\alpha h)}\right)^{-1}(u(t) + \frac{\alpha v(t)}{H(\alpha,h)(1-\alpha+\alpha h)}\,{}_a\nabla_h^{-\alpha}x(t)), \\ &= \frac{H(\alpha,h)(1-\alpha+\alpha h)}{H(\alpha,h)(1-\alpha+\alpha h)-(1-\alpha)v(t)}u(t) + \frac{\alpha v(t)}{H(\alpha,h)(1-\alpha+\alpha h)-(1-\alpha)v(t)}\,{}_a\nabla_h^{-\alpha}x(t). \end{aligned}$$

Presently, consider the following scenario:

$$\begin{aligned} \phi(t) &= \frac{H(\alpha,h)(1-\alpha+\alpha h)}{H(\alpha,h)(1-\alpha+\alpha h)-(1-\alpha)v(t)}u(t), \\ \psi(t) &= \frac{\alpha v(t)}{H(\alpha,h)(1-\alpha+\alpha h)-(1-\alpha)v(t)}. \end{aligned}$$

By applying Lemma 5.1, we reach the following conclusion:

$$x(t) \leq \frac{H(\alpha,h)(1-\alpha+\alpha h)}{H(\alpha,h)(1-\alpha+\alpha h)-(1-\alpha)v(t)}u(t)\,{}_hE_{\overline{\alpha}}\left(\frac{\alpha v(t)}{H(\alpha,h)(1-\alpha+\alpha h)-(1-\alpha)v(t)}, t-a\right).$$

The proof is now complete. □

5.2.2 Applications to ABC Type h-Fractional Discrete Neural Networks

This section is concerned with the finite time stability of $\hbar$-fractional nabla ABC neural networks. First, we introduce the following fractional-order discrete-time neural network.

$${}_a^{ABC}\nabla_h^{\alpha}x_i(t) = -c_ix_i(t) + \sum_{j=1}^{n} d_{ij}g_j(t,x_j(t)) + I_i. \tag{5.5}$$

Let $x(t) = (x_1(t), x_2(t), ..., x_n(t))^T \in \mathbb{R}^n$ be the state vector, $A = diag(c_1, A_2, ..., A_n) \in \mathbb{R}^{nn}$ is the self-feedback connection weight with $c_i > 0$, $D = (d_{ij})_{nn} \in \mathbb{R}^{n*n}$ is the connection weight matrix, $g(t,x(t)) = (g_1(t,x_1(t)), g_2(t,x(t)), ..., g_n(t,x(t)))^T : C(\mathbb{N}_{a,h} \to \mathbb{R}^n)$ is the activation function, and $I = (I_1, ..., I_n)^T$ is the vector of external inputs. Before delving into the investigation, let's establish a few assumptions.

(A_1) Let's denote $g(t,x(t))$ as a continuous function that meets the Lipschitz criterion concerning $\varkappa$, meaning that

$$|g_i(t,x_i(t)) - g_i(t,\mathfrak{z}_i(t))| \leq l_i|x_i(t) - \mathfrak{z}_i(t)|, \quad t \in \mathbb{N}_{a,h}. \tag{5.6}$$

(A_2) Suppose there exists a positive constant γ such that the following condition holds:

$$0 < \frac{\alpha\gamma}{H(\alpha,h)(1-\alpha+\alpha h)-(1-\alpha)\gamma} \leq 1, \tag{5.7}$$

where $\gamma = \max\limits_{i=1,...,n}\left\{c_i + \sum\limits_{n}^{j=1}|d_{ij}|l_j\right\}$ and $\sigma = \max\limits_{i=1,...,n} I_i$.

Definition 5.1. *[365] For positive numbers δ, ϵ, and p, we define system (6.9) as finite-time stable with respect to δ, ϵ, T if and only if the following condition holds:*

$$\|\phi\| \leq \delta \quad and \quad \|I\| \leq p, \tag{5.8}$$

then,

$$\|x(t)\| \leq \epsilon, \quad t \in \mathbb{N}_{a,h}. \tag{5.9}$$

Let's now delve into examining the uniqueness of the solution to system (6.9) utilizing the h-fractional generalized Gronwall inequality.

Theorem 5.2. *Supposing that (A_1) and (A_2) hold, the solution of (6.9) is guaranteed to be unique.*

Proof. Consider two solutions of (6.9), denoted by x and $\mathfrak{z}$. Let o be defined as $o(t) = x(t) - \mathfrak{z}(t)$ for $t \in \mathbb{N}a, h$. Given that $x(a) = \mathfrak{z}(a)$, we aim to show that $o(t) = 0$ for $t \in \mathbb{N}a, h$. We have

$$ {}_{a}^{ABC}\nabla_{h}^{\alpha} o_i(t) = -c_i o_i(t) + \sum_{j=1}^{n} d_{ij}(g_j(t, x_j(t)) - g_j(t, \mathfrak{z}_j(t))).$$

This is equivalent to the expression:

$$\begin{aligned} |o_i(t)| &= |\, {}_{a}^{AB}\nabla_{h}^{-\alpha} \left(-c_i o_i(t) + \sum_{j=1}^{n} d_{ij}(g_j(t, x_j(t)) - g_j(t, \mathfrak{z}_j(t))) \right) |, \\ &\leq {}_{a}^{AB}\nabla_{h}^{-\alpha} \left(c_i |o_i(t)| + \sum_{j=1}^{n} |d_{ij}| l_j |x_j(t) - \mathfrak{z}_j(t)| \right), \\ &\leq {}_{a}^{AB}\nabla_{h}^{-\alpha} \left((c_i + \sum_{j=1}^{n} |d_{ij}| l_j) |o_i(t)| \right). \end{aligned}$$

Hence, it is possible that

$$\|o(t)\| \leq \gamma \, {}^{AB}\nabla_{h}^{-\alpha} (\|o(t)\|).$$

It's evident from Theorem 5.1 that

$$\|o(t)\| \leq \frac{H(\alpha, h)(1 - \alpha + \alpha h)}{H(\alpha, h)(1 - \alpha + \alpha h) - (1 - \alpha)\alpha} 0 \, {}_{h}E_{\alpha} \left(\frac{\alpha\gamma}{H(\alpha, h)(1 - \alpha + \alpha h) - (1 - \alpha)\alpha}, t - a \right).$$

This implies that $|o(t)| = 0$, hence $o(t) = 0$. By strong induction, we conclude that the solution to (6.9) is unique. Thus, the proof is completed. □

Continuing our exploration of the finite-time stability of system (6.9), we arrive at the following theorem.

Theorem 5.3. *Assuming that conditions (A_1) and (A_2) are satisfied, system (6.9) exhibits finite-time stability if and only if $|\Phi| < \delta$ and if*

$$\frac{H(\alpha, h)(1 - \alpha + \alpha h)}{H(\alpha, h)(1 - \alpha + \alpha h) - (1 - \alpha)\gamma} \kappa \times \, {}_{h}E_{\overline{\alpha}} \left(\frac{\alpha\gamma}{H(\alpha, h)(1 - \alpha + \alpha h) - (1 - \alpha)\gamma}, t - a \right) \leq \frac{\delta}{\epsilon}.$$

where

$$\kappa = \|\Phi\| + \frac{\sigma(1 - \alpha)}{H(\alpha, h)(1 - \alpha + \alpha h)} + \frac{\sigma\alpha(t - a)_{h}^{\overline{\alpha}}}{H(\alpha, h)(1 - \alpha + \alpha h)\Gamma(\alpha + 1))},$$

Proof. Suppose that $x(a) = \Phi$. It is evident that equation (6.9) can be reformulated as a fractional-order integral equation.

$$x_i(t) = x_i(a) + {}_{a}^{AB}\nabla_{h}^{-\alpha}\left(-c_i x_i(t) + \sum_{j=1}^{n} d_{ij} g_j(t, x_j(t)) + I_i\right). \tag{5.10}$$

which brings us to

$$|x_i(t)| \leq |x_i(a)| + {}_{a}^{AB}\nabla_{h}^{-\alpha}\left(c_i|x_i(t)| + \sum_{j=1}^{n} |d_{ij}|l_j|x_j(t)| + |I_i|\right),$$

$$\leq |x_i(a)| + (c_i + \sum_{j=1}^{n} |d_{ij}|l_j|)\, {}_{a}^{AB}\nabla_{h}^{-\alpha}|x_j(t)| + {}_{a}^{ABC}\nabla_{h}^{\alpha}\sigma.$$

Hence, as a result of Theorem 5.1, we obtain

$$\|\varkappa(t)\| \leq \|\Phi\| + \frac{\sigma(1-\varsigma)}{H(\varsigma,\hbar)(1-\varsigma+\varsigma\hbar)} + \frac{\sigma\varsigma(t-a)_{\hbar}^{\overline{\varsigma}}}{H(\varsigma,\hbar)(1-\varsigma+\varsigma\hbar)\Gamma(\varsigma+1))} + \gamma\, {}_{a}^{AB}\nabla_{\hbar}^{-\varsigma}\|\varkappa(t)\|.$$

Next, by utilizing Lemma **??**, we derive

$$\|x(t)\| \leq \frac{H(\alpha,h)(1-\alpha+\alpha h)}{H(\alpha,h)(1-\alpha+\alpha h)-(1-\alpha)v(t)} u(t)\, {}_{h}E_{\overline{\alpha}}\left(\frac{\alpha v(t)}{H(\alpha,h)(1-\alpha+\alpha h)-(1-\alpha)v(t)}, t-a\right),$$

where

$$u(t) = \|\Phi\| + \frac{\sigma(1-\alpha)}{H(\alpha,h)(1-\alpha+\alpha h)} + \frac{\sigma\alpha(t-a)_{h}^{\overline{\alpha}}}{H(\alpha,h)(1-\alpha+\alpha h)\Gamma(\alpha+1))},$$

and

$$v(t) = \gamma,$$

with

$$0 < \frac{\alpha\gamma}{H(\alpha,h)(1-\alpha+\alpha h)-(1-\alpha)v(t)} \leq 1.$$

Given Definition 5.2, we can infer that system (6.9) is stable within a finite time, thus concluding the proof. □

5.2.3 Numerical Examples

We now present examples to illustrate the theoretical findings. These examples will serve to demonstrate the practical applicability and effectiveness of the proposed methodologies. By conducting detailed numerical simulations, we aim to provide a clear understanding of how the theoretical results can be applied to real-world scenarios. Each example will highlight different aspects of the theory, showcasing the robustness and versatility of the proposed finite-time stability criteria for discrete fractional-order fractional neural networks.

Example 5.1. *We examine the following three-dimensional discrete-time ħ-fractional neural network:*

$$x(t) = -Ax(t) + D\sin(x(t)) + I, \tag{5.11}$$

where $\sin(x(t)) = (\sin(x_1(t), \sin(x_2(t), \sin(x_3(t))^T$ *for* $t \in \mathbb{N}_{0,h}$.
We present the numerical solution of the system under consideration (5.11) as follows:

$$\begin{cases} x_i(\ell) = x_i(0) + \dfrac{1-\alpha}{H(\alpha,h)(1-\alpha+\alpha h)}[-c_i x_i(\ell) + d_{i1}\sin(x_1(\ell)) + d_{i2}\sin(x_2(\ell)) + d_{i3}\sin(x_2(\ell)) + I_i] \\ \quad + \dfrac{\alpha h^\alpha}{H(\alpha,h)(1-\alpha+\alpha h)\Gamma(\alpha)} \displaystyle\sum_{j=1}^{\ell} \frac{\Gamma(\ell-j+\alpha)}{\Gamma(\ell-j+1)}(-c_i x_i(j) + d_{i1}\sin(x_1(j)) + d_{i2}\sin(x_2(j)) \\ +d_{i3}\sin(x_2(\ell)) + I_i), \quad i = 1, ..., 3. \end{cases} \tag{5.12}$$

Case.1 *We examine the parameters*

$$A = \begin{pmatrix} 0.3 & 0 & 0 \\ 0 & 0.5 & 0 \\ 0 & 0 & 0.1 \end{pmatrix}, \quad D = \begin{pmatrix} -0.4 & 0.5 & 0.1 \\ 0.3 & -0.4 & -0.3 \\ 0.2 & 0.6 & -0.3 \end{pmatrix}, \quad I = \begin{pmatrix} 0 \\ 0 \\ 0 \end{pmatrix}. \tag{5.13}$$

Moreover, we set $\alpha = 0.2$ *and* $h = 0.5$, *and the following parameters are computable:*

$$\gamma = 1.5, \quad \sigma = 0.$$

For $\delta = 3$, *the primary obstacle lies in determining the finite time* T. *We compute the value of*

$$\frac{\alpha\gamma}{H(\alpha,h)(1-\alpha+\alpha h) - (1-\alpha)\gamma} = 0.974100401595700 \leq 1$$

. Under certain conditions, finite-time behavior is observable. In Fig. 5.1, it is evident that at the finite time $T = 50$, *which aligns with the theoretical predictions.*

Case.2 *For the parameters provided* $c_{11} = 0.1$, $c_{22} = 0.1$, $c_{33} = 0.1$, $d_{11} = 0.3$, $d_{12} = -0.2$, $d_{13} = 0.2$, $d_{21} = 0.4$, $d_{22} = -0.1$,
$d_{23} = 0.2$, $d_{31} = 0$, $d_{32} = 0.1$, $d_{33} = 0.5$, $I_1 = 0.01$, $I_2 = 0$, *and* $I_3 = 0.01$,
Moreover, with $\alpha = 0.5$ *and* $h = 0.6$, *we obtain* $\sigma = 0.01$ *and* $\gamma = 1$. *The primary challenge lies in computing the finite time* T. *For* $\delta = 0.5$, *evaluating*

$$\frac{\alpha\gamma}{H(\alpha,h)(1-\alpha+\alpha h) - (1-\alpha)\gamma} = 0.949489737259976 \leq 1$$

, we observe finite-time behavior for $T = 40$. *The system with the specified parameters is evidently finite-time stable, as depicted in Fig. 5.2.*

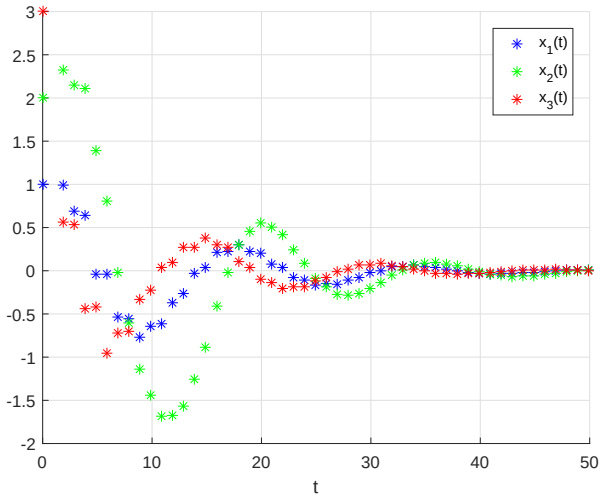

Figure 5.1: Numerical solution of discrete neural network (5.11) for the initial condition $(1, 2, 3)^T$.

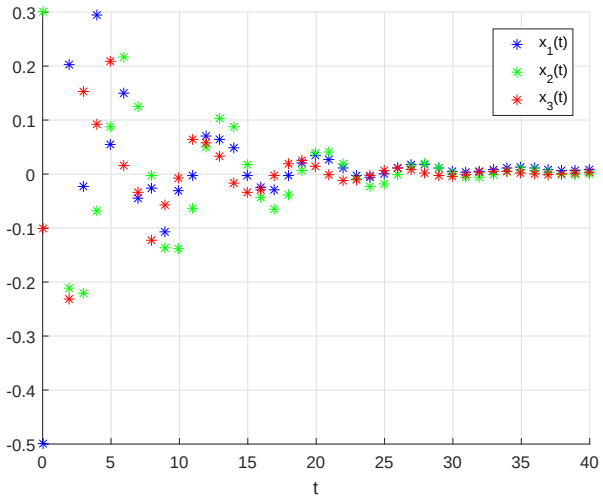

Figure 5.2: Numerical solution of discrete neural network (5.11) for the initial condition $(-0.5, 0.3, -0.1)^T$.

5.3 Finite-Time Stability of Incommensurate Discrete Fractional-Order Neural Networks

This part is devoted to examining the existence and stability over finite time periods of incommensurate discrete fractional neural networks.

To initiate, let's introduce a neural network model characterized by dynamics operating within a framework of fractional, incommensurate discrete time. This model represents a system where neural network dynamics evolve over time intervals that are

fractionally related and lack a common measure.

$$ {}_{a}^{C}\nabla^{\alpha_i} x_i(t) = -c_i x_i(t) + \sum_{j=1}^{n} d_{ij} g_j(t, x_j(t)) + I_i. \tag{5.14} $$

Where In this section, we delineate several assumptions to establish the foundation for our analysis of the system's dynamics.

(A_1) Let's assume that $g(t, x(t))$ is a continuous function that satisfies the Lipschitz condition with respect to x. This condition implies:

$$ |g_i(t, x_i(t)) - g_i(t, \mathfrak{z}_i(t))| \leq l_i |x_i(t) - \mathfrak{z}_i(t)|, \quad t \in \mathbb{N}_a. \tag{5.15} $$

(A_2) Let's assume the existence of a positive constant γ that satisfies the following condition:

$$ 0 < \gamma \leq 1, \quad \text{and} \quad \gamma = \max_{i=1,\ldots,n} \left\{ c_i + \sum_{n}^{j=1} \frac{d_{ijj} + d_{jii}}{2} \right\}. \tag{5.16} $$

5.3.1 Finite-Time Stability Analysis

Next, we will delve into the solvability of the system (5.14).

Theorem 5.4. *If conditions (A_1) and (A_2) hold, the solution of (5.14) is guaranteed to be unique.*

Proof. Consider x and y as solutions of (5.14) with identical initial conditions. Let's denote their difference by $o(t) = x(t) - y(t)$.

To start, we construct a simple Lyapunov function as follows:

$$ V(t) = \sum_{i=1}^{n} v_i(t), \quad \text{and} \quad v_i(t) = \frac{1}{2} o_i^2(t). \tag{5.17} $$

Then, we have:

$$ \begin{aligned} {}^{C}\nabla_a^{\alpha_i} v_i(t) &= \frac{1}{2} {}^{C}\nabla_a^{\alpha_i} o_i^2(t), \\ &\leq o_i(t) {}^{C}\nabla_a^{\alpha_i} o_i(t), \\ &= o_i(t) \left(-c_i o_i(t) + \sum_{j=1}^{n} d_{ij} \left(g_j(t, x_j(t)) - g_j(t, y_j(t)) \right) \right), \\ &\leq -c_i o_i^2(t) + \sum_{j=1}^{n} |d_{ij}|_j o_i(t) o_j(t), \\ &\leq -c_i o_i^2(t) + \sum_{j=1}^{n} |d_{ij}|_j \frac{o_j^2(t) + o_i^2(t)}{2}, \\ &\leq -c_i o_i^2(t) + o_i^2(t) \sum_{j=1}^{n} | \frac{|d_{ij}|_j + |d_{ji}|_i}{2}, \\ &\leq \gamma v_i(t), \end{aligned} \tag{5.18} $$

where

$$\gamma = \max_{i=1,\dots,n} \left(-c_i + \sum_{j=1}^{n} |\frac{|b_{ij}|_j + |b_{ji}|_i}{2} \right).$$

This leads to the following:

$${}^{C}\nabla_{a}^{\alpha_i} v_i(t) = \gamma v_i(t) - f_i(t), \tag{5.19}$$

here, $f(t) = (f_1(t), f_2(t), \dots, f_n(t))$ represents a function with positive values. Next, we employ the Nabla discrete Laplace transform to derive the following:

$$N_a \left[{}^{C}\nabla_{a}^{\alpha_i} v_i(t) \right](s) = \gamma N_a \left[v_i(t) \| \right](s) - N_a \left[f_i(t) \right](s), \tag{5.20}$$

thereby indicating

$$N_a \left[v_i(t) \right](s) = -\frac{1}{s^{\alpha_i} - \gamma} N_a \left[f_i(t) \right](s). \tag{5.21}$$

Continuing with the inverse Laplace transform, we obtain

$$\begin{cases} v_1(t) & = -\sum\limits_{k=a+1}^{t} E_{\alpha_1,\alpha_1}(\gamma, t-\rho(k)) f_1(k), \\ v_2(t) & = -\sum\limits_{k=a+1}^{t} E_{\alpha_2,\alpha_2}(\gamma, t-\rho(k)) f_2(k), \\ \dots & \\ v_n(t) & = -\sum\limits_{k=a+1}^{t} E_{\alpha_n,\alpha_n}(\gamma, t-\rho(k)) f_n(k). \end{cases} \tag{5.22}$$

This suggests that

$$v_i(t) \leq 0, \quad i = 1, \dots, n. \tag{5.23}$$

Following that, we obtain

$$\|o(t)\| = V(t) = \sum_{i=1}^{n} v_i(t) \leq 0. \tag{5.24}$$

Therefore, utilizing strong induction and confirming that $|x(t) - y(t)| = 0$ implies $x(t) - y(t) = 0$, we can assert the uniqueness of the solution to equation (5.14). This completes the proof.

□

Moving forward, we turn our attention to examining the finite-time stability of nabla neural networks with incommensurate fractional orders. To begin, let's introduce the following definition concerning finite-time stability.

Definition 5.2. *[365] A system (5.14) is considered finite-time stable with respect to the parameters δ, ϵ, T, where $\delta < \epsilon$, if and only if, for positive values of α and any system solution, there exists a finite time T such that, for all $t \geq T$, the following condition holds.*

$$\|\phi\| \leq \delta \quad \textit{and} \quad \|I\| \leq \alpha, \tag{5.25}$$

then,

$$\|x(t)\| \leq \epsilon, \quad t \in \mathbb{N}_a. \tag{5.26}$$

Theorem 5.5. *If conditions* (A_1) *and* (A_2) *are satisfied, then the system (5.14) exhibits finite-time stability if and only if* $|\Phi| < \delta$ *and:*

$$\sum_{i=1}^{n} E_{\alpha_i}(\gamma, t-a) \leq \frac{\epsilon}{\delta}.$$

Proof. Assume $x^* \in \mathbb{R}^n$ is the unique fixed point of system (5.14), then,

$$-c_i x_i^* + \sum_{j=1}^{n} d_{ij} g_j(x_i^*) + I_i = 0, \quad i = 1, \ldots, n. \tag{5.27}$$

In the following analysis, we will establish the finite-time stability of x^*. Assuming $x(t)$ as an arbitrary solution of system (5.14), we have:

$$\begin{cases} {}^{C}\nabla_a^{\alpha_1}(x_1(t) - x_1^*) & = -c_1(x_1(t) - x_1^*) + \sum_{j=1}^{n} d_{1j}\left(g_j(t, x_j(t)) - g_j(t, x_j^*(t))\right), \\ {}^{C}\nabla_a^{\alpha_2}(x_2(t) - x_2^*) & = -c_2(x_2(t) - x_2^*) + \sum_{j=1}^{n} d_{2j}\left(g_j(t, x_j(t)) - g_j(t, x_j^*(t))\right), \\ \ldots & \\ {}^{C}\nabla_a^{\alpha_n}(x_n(t) - x_n^*) & = -c_n(x_n(t) - x_n^*) + \sum_{j=1}^{n} d_{nj}\left(g_j(t, x_j(t)) - g_j(t, x_j^*(t))\right). \end{cases} \tag{5.28}$$

For the Lyapunov function defined as follows:

$$V(t) = \sum_{i=1}^{n} v_i(t), \quad \text{and} \quad v_i(t) = \frac{1}{2}(x_i(t) - x_i^*)^2(t). \tag{5.29}$$

Then, we have:

$$\begin{aligned} {}^{C}\nabla_a^{\alpha_i} v_i(t) &= \frac{1}{2}\, {}^{C}\nabla_a^{\alpha_i}(x_i(t) - x_i^*)^2(t), \\ &\leq (x_i(t) - x_i^*)\, {}^{C}\nabla_a^{\alpha_i}(x_i(t) - x_i^*), \\ &= (x_i(t) - x_i^*)\left(-c_i(x_i(t) - x_i^*) + \sum_{j=1}^{n} d_{ij}\left(g_j(t, x_j(t)) - g_j(x_j^*(t))\right)\right), \\ &\leq -c_i(x_i(t) - x_i^*)^2 + \sum_{j=1}^{n} |d_{ij}|_j (x_i(t) - x_i^*)(x_j(t) - x_j^*), \\ &\leq -c_i o_(x_i(t) - x_i^*)^2 + \sum_{j=1}^{n} |d_{ij}|_j \frac{(x_j(t) - x_j^*)^2 + (x_i(t) - x_i^*)^2}{2}, \\ &\leq -c_i(x_i(t) - x_i^*)^2 + (x_i(t) - x_i^*)^2 \sum_{j=1}^{n} |\frac{|d_{ij}|_j + |d_{ji}|_i}{2}, \\ &\leq \gamma v_i(t). \end{aligned} \tag{5.30}$$

Using the same approach as before, we derive:

$${}^{C}\nabla_a^{\alpha_i} v_i(t) = \gamma v_i(t) - f_i(t), \tag{5.31}$$

and

$$N_a\left[v_i(t)\right](s) = \frac{s^{\alpha_i-1}}{s^{\alpha_i}-\gamma}(x_{ai}-x_i^*) - \frac{1}{s^{\alpha_i}-\gamma}N_a\left[f_i(t)\right](s), \tag{5.32}$$

yielding the following system:

$$\begin{cases} v_1(t) &= (x_{a1}-x_1^*)E_{\alpha_1}(\gamma,t-a) - \sum\limits_{k=a+1}^{t} E_{\alpha_1,\alpha_1}(\gamma,t-\rho(k))f_1(k), \\ v_2(t) &= (x_{a2}-x_1^*)E_{\alpha_2}(\gamma,t-a) - \sum\limits_{k=a+1}^{t} E_{\alpha_2,\alpha_2}(\gamma,t-\rho(k))f_2(k), \\ \ldots & \\ v_n(t) &= (x_{an}-x_n^*)E_{\alpha_n}(\gamma,t-a) - \sum\limits_{k=a+1}^{t} E_{\alpha_n,\alpha_n}(\gamma,t-\rho(k))f_n(k), \end{cases} \tag{5.33}$$

this implies that

$$v_i(t) \le \|x_a - x^*\|E_{\alpha_i}(\gamma,t-a), \quad i=1,\ldots,n. \tag{5.34}$$

Thus, we have

$$\|(x(t)-x^*)\| = V(t) = \sum_{i=1}^{n} v_i(t) \le \|x_a - x^*\| \sum_{i=1}^{n} E_{\alpha_i}(\gamma,t-a). \tag{5.35}$$

Therefore, for

$$\sum_{i=1}^{n} E_{\alpha_i}(\gamma,t-a) \le \frac{\epsilon}{\delta}. \tag{5.36}$$

Consequently, we have

$$\|(x(t)-x^*)\| \le \epsilon. \tag{5.37}$$

□

5.3.2 Numerical Examples and Computer Simulations

In this section, we present two numerical examples encompassing various scenarios and simulations to showcase the practicality and effectiveness of our theoretical findings.

Example 5.2. *We examine a three-dimensional discrete-time incommensurate fractional neural network, described as follows:*

$$\begin{smallmatrix} C \\ a \end{smallmatrix}\nabla^{\overline{\alpha}} x(t) = -Ax(t) + D\sin(x(t)) + I. \tag{5.38}$$

Below are the numerical results for system (5.38):

$$\begin{cases} x_i(\ell) = x_i(0) \\ +\dfrac{1}{\Gamma(\alpha_i)}\displaystyle\sum_{k=1}^{i}\frac{\Gamma(i-k+\alpha_i)}{\Gamma(i-k+1)}\left(-c_i x_i(j) + d_{i1}\sin(x_1(j)) + d_{i2}\sin(x_2(j)) + d_{i3}\sin(x_2(\ell)) + I_i\right), \\ \quad i=1,\ldots,3. \end{cases} \tag{5.39}$$

Case.1 *Now, let's analyze the parameters:*

$$A = \begin{pmatrix} 0.2 & 0 & 0 \\ 0 & 0.2 & 0 \\ 0 & 0 & 0.2 \end{pmatrix}, \quad D = \begin{pmatrix} 0.04 & 0 & 0.02 \\ 0.03 & 0.04 & 0.01 \\ 0.04 & 0.01 & 0.02 \end{pmatrix}, \quad I = \begin{pmatrix} 0 \\ 0 \\ 0 \end{pmatrix}, \tag{5.40}$$

Additionally, considering $\alpha = (\frac{1}{4}, \frac{1}{7}, \frac{1}{3})$, *we can compute the subsequent parameters:* $\gamma = 1.5, \quad \sigma = 0$ *When* $\delta = 0.2$, *the primary challenge in determining the finite-time* T *arises from assessing the value of* $\gamma = 0.974100401595700$, *which is less than 1. Under specific prerequisites, finite-time dynamics can be observed. As portrayed in Figure 5.3, it is conspicuous that at* $T = 8$, *providing numerical confirmation of the theoretical predictions.*

Case.2 *Regarding the specified parameters:* $c_{11} = 0.4$, $c_{22} = 0.3$, $c_{33} = 0.3$, $d_{11} = -0.04$, $d_{12} = 0$, $d_{13} = -0.2$, $d_{21} = 0.1$, $d_{22} = -0.04$, $d_{23} = 0.01$, $d_{31} = -0.04$, $d_{32} = 0.01$, $d_{33} = -0.2$, $I_1 = 0$, $I_2 = 0$, *and* $I_3 = 0$, *In addition, for* $\alpha_1 =, \alpha_2 =, \alpha_3 =$, *we have* $\sigma = 0.01$ *and* $\gamma = 1$.

The main challenge is determining the finite-time value T. *With* $\delta = 2$, *calculating the value* $\gamma = 0.949489737259976$, *where* $\gamma \leq 1$, *we observe finite-time behavior for* $T = 10$. *It is evident from Figure 5.4 that the system, with the specified parameters, exhibits finite-time stability.*

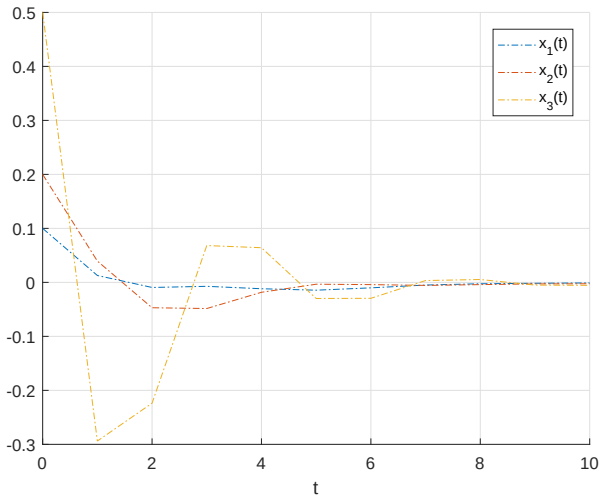

Figure 5.3: Evolution of system (5.38) with $x(0) = (0.1, 0.2, -0.1)^T$.

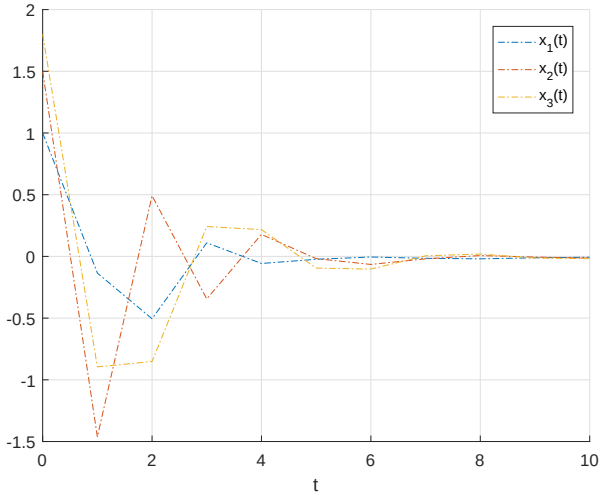

Figure 5.4: Evolution of system (5.38) with $with x(0) = (1, 1.5, 2)^T$.

5.4 Finite-Time Stability of Nabla Variable-Order Neural Networks

In this subsection, we present a straightforward exploration of the finite-time stability of nabla variable-order neural networks. Our approach prioritizes simplicity and clarity, aiming to provide accessible insights into how these networks behave within finite timeframes. By employing practical methodologies, we seek to uncover the stability properties of nabla variable-order neural networks, offering valuable understandings for their real-world applications.

5.4.1 A Gronwall Inequality

In a recent study, [365] introduced a Gronwall inequality associated with the Nabla fractional operator for fractional difference equations. Additionally, [366] derived a discrete Gronwall inequality for the discrete Atangana Baleanu fractional operator. Motivated by these works, in this section, we outline and demonstrate a novel variable-order discrete version of the generalized Gronwall's inequality.

Theorem 5.6. *Let $u(t)$ and $v(t)$ be discrete nonnegative, non-decreasing functions, with $0 \leq v(t) \leq L < 1$. For each $t \in \mathbb{N}_{a+1}$, $x(t)$ is nonnegative and satisfies the following:*

$$x(t) \leq u(t) + v(t)\nabla_t^{-\alpha(t)} x(t), \tag{5.41}$$

then,

$$x(t) \leq u(t) E_{\overline{\alpha_1}}(Kv(t), t-a), \tag{5.42}$$

where

$$\alpha_1 \leq \alpha(t) \leq \alpha_2, \quad S = \max\{(t-a)^{\alpha_1 - 1}, (t-a)^{\alpha_2 - 1}\} \quad \text{and} \quad K = \frac{S\Gamma(\alpha_1)}{(t-a)^{\overline{\alpha_1 - 1}}\Gamma(\alpha_2)}.$$

Proof. Referring to [367], it can be observed that for $T \in \mathbb{N}_{a+1}$ we have

$$T^{\alpha(t)-1} = \frac{\Gamma(T\alpha(t)-1)}{\Gamma(T)} \leq \begin{cases} T^{\alpha_1-1}, & 0 \leq T \leq 1, \\ T^{\alpha_2-1}, & T > 1. \end{cases} \tag{5.43}$$

With $T = t - a$ and $S = \max\{T^{\alpha_1-1}, T^{\delta_2-1}\}$, employing the properties of $\Gamma(t)$ on $(0,1)$, we deduce $\Gamma(\alpha_2) \leq \Gamma(\alpha(t)) \leq \Gamma(\alpha_1)$, which, combined with definitions 1.50, yields:

$$\begin{aligned} x(t) &\leq u(t) + v(t)\frac{1}{\Gamma(\alpha(t))}\sum_{s=a+1}^{t}(t-\rho(s))^{\overline{\alpha(t)-1}}x(s), \\ &\leq u(t) + v(t)\frac{S}{\Gamma(\alpha_2)}\sum_{s=a+1}^{t}\frac{(t-\rho(s))^{\overline{\alpha(t)-1}}}{T^{\overline{\alpha(t)-1}}}x(s), \\ &\leq u(t) + v(t)\frac{S}{\Gamma(\alpha_2)}\sum_{s=a+1}^{t}\left(\frac{(t-\rho(s))}{T}\right)^{\overline{\alpha_1-1}}x(s), \\ &\leq u(t) + Kv(t)\,{}_a\nabla_t^{-\alpha_1}x(t), \end{aligned}$$

where $K = \dfrac{S\Gamma(\alpha_1)}{T^{\overline{\alpha_1-1}}\Gamma(\alpha_2)}$.
Consider the operator $\psi x(t) = Kv(t)\,{}_a\nabla_t^{-\alpha_1}x(t)$, then,

$$x(t) \leq u(t) + \psi x(t). \tag{5.44}$$

Since the operator ψ is monotonic, we obtain

$$\psi x(t) \leq \psi u(t) + \psi^2 x(t). \tag{5.45}$$

Continuing with the above process yields

$$x(t) \leq \sum_{p=0}^{n-1}\psi^p u(t) + \psi^n x(t). \tag{5.46}$$

Next, we will demonstrate that

$$\psi^n x(t) \leq v^n(t)\,{}_a\nabla_t^{-n\alpha_1}x(t), \tag{5.47}$$

$$\lim_{n\to\infty}\psi^n = 0. \tag{5.48}$$

Certainly, inequality (5.47) evidently holds true for $n = 1$. Employing mathematical induction, for $n = p$, we obtain

$$\psi^p x(t) \leq v^p(t)\,{}_a\nabla_t^{-p\alpha_1}x(t). \tag{5.49}$$

Since $v(t)$ is a discrete non-decreasing function on $\mathbb{N}_{a+1}$, we obtain

$$\begin{aligned} \psi^{p+1}x(t) &= \psi(\psi^p x(t)), \\ &= Kv(t)\,{}_a\nabla_t^{-\alpha_1}\psi^p x(t)), \\ &\leq Kv(t)\,{}_a\nabla_t^{-\alpha_1}\left(v^p(s)\,{}_a\nabla_s^{-p\alpha_1}x(s)\right), \\ &= v(t)\frac{K}{\Gamma(\alpha_1)}\sum_{s=a+1}^{t}(t-\rho(s))^{\overline{\alpha_1-1}}\left(v^p(s)\frac{1}{\Gamma(p\alpha_1)}\sum_{s'=a+1}^{s}(s-\rho(s'))^{\overline{p\alpha_1-1}}x(s')\right), \\ &\leq Kv^{p+1}(t)\,{}_a\nabla_t^{-(p+1)\alpha_1}x(t), \end{aligned}$$

where the method for composing two fractional sums was utilized. Consequently, we may deduce that the inequality (5.47) holds for any $n \in \mathbb{N}_{a+1}$. Given $v(t) \leq L$, we can infer from inequality (5.47) that

$$\begin{aligned}\psi^n x(t) &\leq L^n \frac{K}{\Gamma(n\alpha_1)} \sum_{s=a+1}^{t} (t-\rho(s))^{\overline{n\alpha_1-1}} x(s),\\ &\leq KL^n X \frac{1}{\Gamma(n\alpha_1)} \sum_{s=a+1}^{t} (t-\rho(s))^{\overline{n\alpha_1-1}},\\ &= KXL^n \frac{(t-a)^{\overline{n\alpha_1}}}{\Gamma(n\alpha+1)}, \end{aligned} \tag{5.50}$$

where $X = \max_{t\in\mathbb{N}_{a+1}} \{x(t)\}$. As a result, relation (5.50) is derived. Furthermore, one can deduce that

$$\psi^n x(t) \leq KL^n X \frac{(t-a)^{\overline{n\alpha_1}}}{\Gamma(n\alpha_1+1)} \to 0 \quad \text{as} \quad n \to +\infty, \quad t \in \mathbb{N}_{a+1,}, \tag{5.51}$$

and we have $\lim_{n\to\infty} \psi^n x(t) = 0$. Therefore:

$$x(t) \leq \sum_{p=0}^{n-1} \psi^p u(t) = u(t) + \sum_{p=1}^{n-1} \psi^p u(t) \leq u(t) + \sum_{p=1}^{+\infty} \psi^p u(t) \leq u(t) + \sum_{p=1}^{+\infty} K^p v^p(t)\, {}_a\nabla_t^{-p\alpha_1} u(t). \tag{5.52}$$

From (5.47) and the hypothesis that $u(t)$ is a non-decreasing function for $t \in \mathbb{N}_{a+1}^T$, we can deduce that

$$\begin{aligned} x(t) &\leq u(t) + \sum_{p=1}^{+\infty} K^p v^p(t)\, {}_a\nabla_t^{-p\alpha_1} u(t),\\ &\leq u(t) + \sum_{p=1}^{+\infty} K^p v^p(t) \frac{1}{\Gamma(p\alpha_1)} \sum_{s=a+1}^{t} (t-\rho(s))^{\overline{p\alpha_1-1}} u(s),\\ &\leq u(t) + \sum_{p=1}^{+\infty} K^p v^p(t) u(t) \frac{1}{\Gamma(p\alpha_1)} \sum_{s=a+1}^{t} (t-\rho(s))^{\overline{p\alpha_1-1}},\\ &\leq u(t) + \sum_{p=1}^{+\infty} K^p v^p(t) u(t) \frac{(t-a)^{\overline{p\alpha_1}}}{\Gamma(p\alpha_1+1)},\\ &= u(t) \sum_{p=0}^{+\infty} (Kv(t))^p \frac{(t-a)^{\overline{p\alpha_1}}}{\Gamma(p\alpha_1+1)}\\ &= u(t) E_{\overline{\alpha_1}}(Kv(t), t-a). \end{aligned}$$

Like the conventional Gronwall inequality, the significance of (5.42) lies in its establishment of a bound for $x(t)$ in terms of $u(t)$, $v(t)$, and $\alpha(t)$. This concludes the proof. □

5.4.2 Finite–Time Stability of Nabla Variable-Order Neural Networks

To demonstrate the application of the essential results, we prove the uniqueness and limited time stability of nabla variable-order neural networks using the results from the prior section.
We investigate a discrete variable-ordre neural network:

$$ {}^{C}_{a}\nabla^{\delta(t)}x(t) = -A\varkappa(t) + Dg(t, x(t)) + I. \tag{5.53} $$

To begin, we make several assumptions before proceeding with the investigation of this study.

(H_1) Assume that $h(t, \varkappa(t))$ is a continuous function that satisfies the Lipschitz condition with respect to $\varkappa$. That is,

$$ |g_i(t, x_i(t)) - g_i(t, y_i(t))| \leq l_i|x_i(t) - y_i(t)|, \quad t \in \mathbb{N}_{a+1}. \tag{5.54} $$

(H_2) For c_i, d_{ij}, and l_j, the following conditions hold:

$$ 0 < -\min_{i=1,\dots,n} c_i + \sum_{i=1}^{n} \max_{j=1,\dots,n} |d_{ij}|l_j \leq 1. \tag{5.55} $$

(H_3) For γ and ϵ as defined in Definition **??**, the following holds:

$$ E_{\overline{\alpha_1}}\left(-\min_{i=1,\dots,n} c_i + \sum_{i=1}^{n} \max_{j=1,\dots,n} |d_{ij}|l_j, t-a\right) < \frac{\epsilon}{\gamma}. \tag{5.56} $$

Theorem 5.7. *Assuming that condition (H_1) is satisfied, if $x(t)$ and $y(t)$ are different solutions of system (5.53), then $x(t)$ equals $y(t)$.*

Proof. If x and y are distinct solutions to (5.53), both starting from the same initial conditions, we denote their difference as o, defined as $o(t) = x(t) - y(t)$. Then, for $t \in \mathbb{N}_{a+1}$, we have:

$$ o_i(t) = \frac{1}{\Gamma(\alpha(t))} \sum_{s=a+1}^{t} (t - \rho(s))^{\overline{\alpha(t)-1}} \left(-c_i o_i(s) + \sum_{j=1}^{n} d_{ij}(g_j(s, x_j(s)) - g_j(s, y_j(s)))\right), \quad i = 1, ..., n. \tag{5.57} $$

Consequently,

$$ |o_i(t)| \leq \frac{1}{\Gamma(\alpha(t))} \sum_{s=a+1}^{t} (t - \rho(s))^{\overline{\alpha(t)-1}} \left(c_i|o_i(s)| + \sum_{j=1}^{n} |d_{ij}||g_j(s, x_j(s)) - g_j(s, y_j(s))|\right), \tag{5.58} $$

$$ \leq \frac{1}{\Gamma(\alpha(t))} \sum_{s=a+1}^{t} (t - \rho(s))^{\overline{\alpha(t)-1}} \left(c_i|o_i(s)| + \sum_{j=1}^{n} |d_{ij}|l_j|o_j(s)|\right). \tag{5.59} $$

$$ \tag{5.60} $$

This results in

$$\begin{aligned}
\|o(t)\| &= \sum_{i=1}^{n} |o_i(t)|, \\
&\leq \frac{1}{\Gamma(\alpha(t))} \sum_{s=a+1}^{t} (t-\rho(s))^{\overline{\alpha(t)-1}} \left(p \sum_{i=1}^{n} |o_i(s)| + \sum_{i=1}^{n} \sum_{j=1}^{n} |d_{ij}| l_j |o_j(s)| \right), \\
&\leq \frac{1}{\Gamma(\alpha(t))} \sum_{s=a+1}^{t} (t-\rho(s))^{\overline{\alpha(t)-1}} \left(p\|o(s)\| + \beta \sum_{i=1}^{n} |o_i(s)| \right), \\
&\leq (p+\beta) \frac{1}{\Gamma(\alpha(t))} \sum_{s=a+1}^{t} (t-\rho(s))^{\overline{\alpha(t)-1}} \|o(t)\|, \\
&= (p+\beta)\, {}_a\nabla^{-\alpha(t)} \|o(t)\|,
\end{aligned}$$

where $p = \max\limits_{i=1,\dots,n} \{c_i\}$ and $\beta = \max\limits_{i=1,\dots,n} \sum\limits_{j=1}^{n} |d_{ji}| l_i$. Given that $\alpha + \beta$ and $|o(t)|$ are positive, employing the result of Theorem 5.6, we obtain:

$$\|o(t)\| \leq 0 \times E_{\overline{\alpha_1}}(p! + \beta, t-a). \tag{5.61}$$

Consequently, $|x(t) - y(t)| = 0$, thus, $x(t) = y(t)$ for $t \in \mathbb{N}_{a+1}^{T}$. This concludes the proof. □

Theorem 5.8. *Given that $(H_1) - (H_3)$ hold, the unique fixed point of system (5.53) is finite-time stable with respect to $t \in \mathbb{N}_{a+1}^{T}$.*

Proof. Let $x^* \in \mathbb{R}n$ be the unique fixed point of system (5.53), then

$$-c_i x_i^* + \sum_{j=1}^{n} d_{ij} g_j(t, x_j^*) + I_i = 0, \quad i = 1, \dots, n. \tag{5.62}$$

In the following, we will prove that x^* is finite-time stable. Let $x(t)$ be any solution of system (5.53), then:

$${}_a^C\nabla^{\alpha(t)}(x_i(t) - x_i^*) = -c_i(x_i(t) - x_i^*) + \sum_{j=1}^{n} d_{ij}(g_j(t, x_j(t)) - g_j(t, x_j^*)). \tag{5.63}$$

However, based on Definition 1.49, we have:

$$\begin{aligned}
{}_a^C\nabla^{\alpha(t)}|x_i(t) - x_i^*| &= \frac{1}{\Gamma(\alpha(t))} \sum_{s=a+1}^{t} (t-\rho(s))^{\overline{\alpha(t)-1}} |x_i(s) - x_i^*)| && (5.64) \\
&= \begin{cases} {}_a^C\nabla^{\alpha(t)}(x_i(t) - x_i^*), & \text{if } x_i(t) - x_i^* > 0, \\ 0, & \text{if } x_i(t) - x_i^* = 0, \\ -{}_a^C\nabla^{\alpha(t)}(x_i(t) - x_i^*), & \text{if } x_i(t) - x_i^* < 0, \end{cases} && (5.65) \\
&= sgn(x_i(t) - x_i^*)\, {}_a^C\nabla^{\alpha(t)}(x_i(t) - x_i^*). && (5.66)
\end{aligned}$$

Thus,

$$\begin{aligned}
{}_a^C\nabla^{\alpha(t)}|x_i(t)-x_i^*| &= sgn(x_i(t)-x_i^*)\,{}_a^C\nabla^{\alpha(t)}(x_i(t)-x_i^*),\\
&= sgn(x_i(t)-x_i^*)(-c_i(x_i(t)-x_i^*)+\sum_{j=1}^{n} d_{ij}(g_j(t,x_j(t))-g_j(t,x_j^*))),\\
&= -c_i|x_i(t)-x_i^*| + sgn(x_i(t)-x_i^*)\sum_{j=1}^{n} c_{ij}(g_j(t,x_j(t))-g_j(t,x_j^*)),\\
&\leq -c_i|x_i(t)-x_i^*| + \sum_{j=1}^{n}|d_{ij}|l_j|x_j(t)-x_j^*|.
\end{aligned}$$

Utilizing the fractional variable-order sum, we can conclude that

$$|\varkappa_i(t)-\varkappa_i^*| \leq -d_i\,{}_a\nabla^{-\delta(t)}|\varkappa_i(t)-\varkappa_i^*| + \sum_{j=1}^{n}|c_{ij}|l_j\,{}_a\nabla^{-\delta(t)}|\varkappa_j(t)-\varkappa_j^*| + |\varkappa_i(a)-\varkappa_i^*|. \tag{5.67}$$

We can directly obtain

$$\begin{aligned}
\|x(t)-x^*\| &= \sum_{i=1}^{n}|x_i(t)-x_i^*|,\\
&\leq -c_i\sum_{i=1}^{n}{}_a\nabla^{-\alpha(t)}|x_i(t)-x_i*| + \sum_{i=1}^{n}\sum_{j=1}^{n}|d_{ij}|l_j\,{}_a\nabla^{-\alpha(t)}|x_j(t)-x_j^*| + \sum_{i=1}^{n}|x_i(a)-x_i^*|,\\
&\leq -\min_{i=1,\dots,n} c_i\,{}_a\nabla^{-\alpha(t)}\|x(t)-x^*\| + \sum_{i=1}^{n}\max_{j=1,\dots,n}|d_{ij}|l_j\,{}_a\nabla^{-\alpha(t)}\sum_{j=1}^{n}|x_j(t)-x_j^*|\\
&\quad + \|\phi-x*\|,\\
&= \|\phi-x*\| + \left(-\min_{i=1,\dots,n} c_i + \sum_{i=1}^{n}\max_{j=1,\dots,n}|d_{ij}|l_j\right){}_a\nabla^{-\alpha(t)}\|x(t)-x^*\|.
\end{aligned}$$

Since $|\phi-x^*|$, $-\min_{i=1,\dots,n} c_i+\sum_{i=1}^{n}\max_{j=1,\dots,n}|d_{ij}|l_j$, and $|x(t)-x^*|$ are all positive, we can deduce from Theorem 5.6 and (H_3) that (5.68) holds.

$$\|x(t)-x^*\| \leq \|\phi-x^*\|F_{\overline{\delta_1}}\left(-\min_{i=1,\dots,n} c_i + \sum_{i=1}^{n}\max_{j=1,\dots,n}|d_{ij}|l_j, t-a\right) < \frac{\epsilon}{\gamma}. \tag{5.68}$$

In accordance with Definition 1.49, this immediately demonstrates that the fixed point x^* of system (5.53) is finite-time stable with respect to $t \in \mathbb{N}_{a+1}^{T}$. This concludes the proof. □

5.4.3 Numerical Simulations

Now, let's apply the theoretical stability conclusions to two numerical examples related to variable-order discrete neural networks. As demonstrated below, we've established

explicit numerical formulations for the nabla variable-order neural networks.

$$\begin{cases} x_1(i) = x_1(a) + \dfrac{1}{\Gamma(\alpha(i))} \displaystyle\sum_{j=1}^{i} \frac{\Gamma(i-j+\alpha(i))}{\Gamma(i-j+1)} \left(-c_1 x_1(i) + \sum_{j=1}^{n} d_{1j} g_j(i, x_j(j)) + I_1 \right), \\ \cdots \\ x_n(i) = x_n(a) + \dfrac{1}{\Gamma(\alpha(i))} \displaystyle\sum_{j=1}^{i} \frac{\Gamma(i-j+\alpha(i))}{\Gamma(i-j+1)} \left(-c_n x_n(i) + \sum_{j=1}^{n} d_{nj} g_j(i, x_j(i)) + I_n \right). \end{cases} \tag{5.69}$$

Example 5.3. *We investigate the following variable-order discrete neural networks:*

$$\begin{cases} {}_0^C\nabla^{\alpha(t)} x_1(t) = -c_1 x_1(t) + d_{11} \sin(x_1(t)) + d_{12} \sin(x_2(t)) + I_1, \\ {}_0^C\nabla^{\alpha(t)} x_2(t) = -c_2 x_2(t) + d_{21} \sin(x_1(t)) + d_{22} \sin(x_2(t)) + I_2. \end{cases} \tag{5.70}$$

Consider the following parameters:

$$A = \begin{pmatrix} 1.1 & 0 \\ 0 & 0.9 \end{pmatrix}, \quad D = \begin{pmatrix} 0.7 & 0.5 \\ 0.5 & -0.6 \end{pmatrix}, \quad I = \begin{pmatrix} 0 \\ 0 \end{pmatrix}, \tag{5.71}$$

and the variable-order function

$$\alpha(t) = \frac{|\ln\left(\dfrac{1}{t+1}\right) + 1|}{10}, \quad \alpha_1 = 0.1, \quad \alpha_2 = 0.2433987. \tag{5.72}$$

Finite-time dynamics are evident within the specified parameters. Specifically, for

$$-\min_{j=1,\ldots,n} c_j + \sum_{i=1}^{n} \max_{j=1,\ldots,n} l_j |d_{ij}| = 0.4, \tag{5.73}$$

$$E_{\overline{\alpha_1}}\left(-\min_{i=1,\ldots,n} c_i + \sum_{i=1}^{n} \max_{j=1,\ldots,n} |d_{ij}| l_j, 30 \right) \leq 1.172509622300451. \tag{5.74}$$

Opting for $\gamma = 0.4$ and $\epsilon = 0.469003848920180$ with $x(0) = (0.4, -0.4)^T$, we observe in Figure 5.5 that the solution is finite-time stable, corroborating the findings of Theorem 5.8.

Example 5.4. *Consider the discrete neural networks:*

$$\begin{cases} {}_0^C\nabla^{\alpha(t)} x_1(t) = -1.1 x_1(t) + 0.6 \tanh(x_1(t)) + 0.5 \tanh(x_2(t)) - 0.3 \tanh(x_3(t)), \\ {}_0^C\nabla^{\alpha(t)} x_2(t) = -1.2 x_2(t) + 0.2 \tanh(x_1(t)) - 0.6 \tanh(x_2(t)) + 0.5 \tanh(x_3(t)), \\ {}_0^C\nabla^{\alpha(t)} x_3(t) = -1.1 x_3(t) + 0.275 \tanh(x_1(t)) + 0.8 \tanh(x_2(t)) - 0.11 \tanh(x_3(t)), \end{cases} \tag{5.75}$$

with the variable-order function given by

$$\alpha(t) = |\frac{1}{6} - e^{-\frac{t}{4}}|, \quad \alpha_1 = 0.05646 \quad \text{and} \quad \alpha_2 = 0.83333. \tag{5.76}$$

It's evident that $l_j = 1$ for $j = 1, 2, 3$, and the activation functions satisfy (H_1). Additionally, $(H_2) - (H_3)$ are satisfied for $-\min_{j=1,\ldots,n} c_j + \sum_{i=1}^{n} \max_{j=1,\ldots,n} l_j |d_{ij}| = 0.9$,

$$E_{\overline{\alpha_1}}\left(-\min_{i=1,\ldots,n} c_i + \sum_{i=1}^{n} \max_{j=1,\ldots,n} |d_{ij}| l_j, 30 \right) \leq 1.142428052757200. \tag{5.77}$$

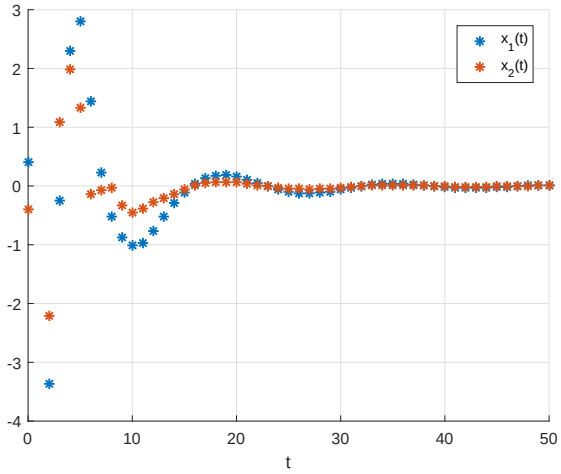

Figure 5.5: Numerical solution of neural networks (5.70).

Thus, according to Theorem 5.8, system (5.75) possesses a unique equilibrium point that is finite-time stable when $\gamma = 0.8$ *and* $\epsilon = 0.469003848920180$. *We examine the next three numerical simulation scenarios:*

Case 1: *Let* $x(0) = (0.8, 0.8, 0.8)^T$,

Case 2: *Let* $x(0) = (0.1, 0.5, 0.2)^T$,

Case 3: *Let* $x(0) = (1, -2, 5)^T$.

Figure 5.6, Figure 5.7, and Figure 5.8 depict the temporal responses of the neural network variables x_1, x_2, *and* x_3.

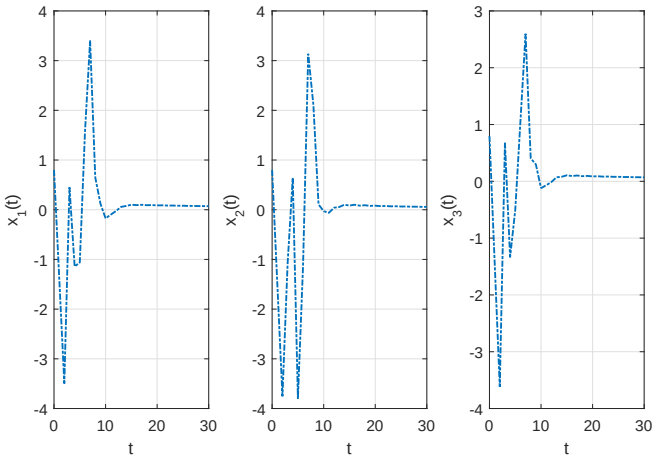

Figure 5.6: Numerical solution of neural networks (5.75).

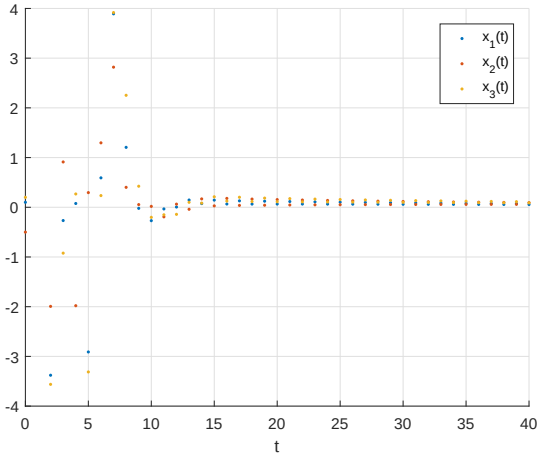

Figure 5.7: Numerical solution of neural networks (5.75).

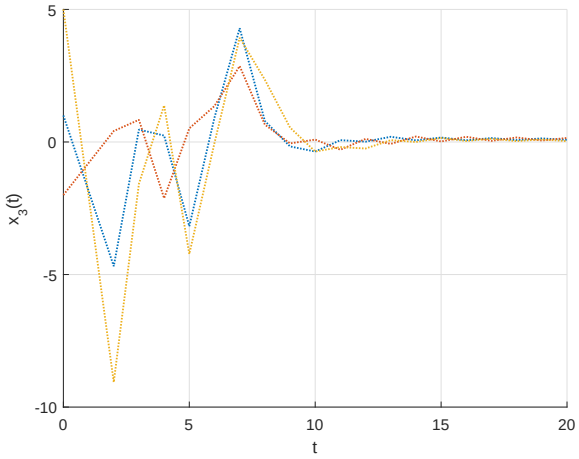

Figure 5.8: Numerical solution of neural networks (5.75).

5.5 Finite-Time Stability of Discrete ABC type Variable-Order Neural Networks

In this subsection, we embark on a straightforward examination of the finite-time stability of ABC type variable-order neural networks. Our approach emphasizes simplicity and directness, aiming to unravel the stability characteristics of these networks within finite time intervals. Through practical methodologies, we endeavor to elucidate the finite-time behavior of ABC type variable-order neural networks, offering practical insights for their application in diverse domains.

Lemme 5.2. *Let's consider a function x defined on the domain $\mathbb{N}_{a+1}$, such that $x(t)$ satisfies the following inequality:*

$$ {}^{ABC}_{a}\nabla^{\alpha} x^2(t) \leq 2x(t)\, {}^{ABC}_{a}\nabla^{\alpha} x(t). \tag{5.78}$$

Proof. We need to prove the equivalence of the following expression:

$$ {}_{a}^{ABC}\nabla^{\alpha}x^{2}(t) - 2x(t)\,{}_{a}^{ABC}\nabla^{\alpha}x(t) \leq 0. \tag{5.79}$$

Initially, we have

$$\begin{aligned}
{}_{a}^{ABC}\nabla^{\alpha}x^{2}(t) - 2x(t)\,{}_{a}^{ABC}\nabla^{\alpha}x(t) &= \frac{B(\alpha)}{1-\alpha}\sum_{s=a+1}^{t}[(x(s)-x(s-1)) - 2(x(t)x(s)-x(t)x(s-1))] \\
&\quad \times E_{\overline{\alpha}}\left(\frac{-\alpha}{1-\alpha}, t-\rho(s)\right), \\
&= \frac{B(\alpha)}{1-\alpha}\sum_{s=a+1}^{t}[(x^{2}(s)-x^{2}(s-1)) - 2(x(t)x(s)-x(t)x(s-1))] \\
&\quad \times E_{\overline{\alpha}}\left(\frac{-\alpha}{1-\alpha}, t-\rho(s)\right), \\
&= \frac{B(\alpha)}{1-\alpha}\sum_{s=a+1}^{t}[(x(t)-x(s))^{2} - (x(t)-x(s-1))^{2}]E_{\overline{\alpha}}\left(\frac{-\alpha}{1-\alpha}, t-\rho(s)\right), \\
&= \frac{B(\alpha)}{1-\alpha}\sum_{s=a+1}^{t}\nabla_{s}(x(t)-x(s))^{2}E_{\overline{\alpha}}\left(\frac{-\alpha}{1-\alpha}, t-\rho(s)\right).
\end{aligned}$$

By employing summation by parts as stated in equation (5.80),

$$\sum_{\jmath=a}^{b-1} g(\jmath+1)\nabla f(\jmath) = g(\jmath)f(\jmath)|_{a}^{b} - \sum_{\jmath=a}^{b-1} f(\jmath)\nabla g(\jmath), \tag{5.80}$$

for $g(s-1) = E_{\overline{\alpha}}(\kappa, t-(s-1))$ and $f(s) = (x(s)-x(t))^{2}$.
We can infer that:

$$\begin{aligned}
{}_{a}^{ABC}\nabla^{\alpha}x^{2}(t) - 2x(t)\,{}_{a}^{ABC}\nabla^{\alpha}x(t) &= -\frac{B(\alpha)}{1-\alpha}\sum_{s=a+1}^{t}(x(t)-x(s))^{2}\nabla_{s}E_{\overline{\alpha}}\left(\frac{-\alpha}{1-\alpha}, t-s\right) \\
&\quad + (x(t)-x(s))^{2}E_{\overline{\alpha}}\left(\frac{-\alpha}{1-\alpha}, t-s\right)|_{a}^{t}.
\end{aligned}$$

Conversely, we obtain:

$$\begin{aligned}
\nabla_{s}E_{\overline{\alpha}}(\kappa, t-s) &= E_{\overline{\alpha}}(\kappa, t-s) - E_{\overline{\alpha}}(\kappa, t-(s-1)), \\
&= \sum_{k=0}^{\infty}\kappa^{k}\frac{(t-s)^{\overline{k\alpha}}}{\Gamma(\alpha k+1)} - \sum_{k=0}^{\infty}\kappa^{k}\frac{(t-(s-1))^{\overline{k\alpha}}}{\Gamma(\alpha k+1)}, \\
&= \sum_{k=0}^{\infty}\frac{\kappa^{k}}{\Gamma(\alpha k+1)}\nabla_{s}(t-s)^{\overline{k\alpha}}.
\end{aligned}$$

Because

$$\nabla_{s}(t-\rho(s))^{\overline{\alpha}} = \alpha(t-\rho(s))^{\overline{\alpha-1}}, \tag{5.81}$$

this implies that:

$$\begin{aligned}\nabla_s E_{\overline{\alpha}}(\kappa, t-s) &= \sum_{k=0}^{\infty} \frac{\kappa^k}{\Gamma(\alpha k+1)} k\alpha (t-s)^{\overline{k\alpha-1}}, \\ &= \sum_{k=0}^{\infty} \frac{\kappa^k}{\Gamma(\alpha k)} (t-s)_h^{\overline{\alpha-1}}, \\ &= E_{\overline{\alpha},0}(\kappa, t-s),\end{aligned}$$

thus, we get:

$$\begin{aligned}{}_a^{ABC}\nabla^{\alpha} x^2(t) - 2x(t)\,{}_a^{ABC}\nabla^{\alpha} x(t) = -\frac{B(\alpha)}{1-\alpha} \sum_{s=a+1}^{t} (x(t)-x(s))^2 E_{\overline{\alpha},0}\left(\frac{-\alpha}{1-\alpha}, t-s\right) \\ - (x(t)-x(a))^2 E_{\overline{\alpha}}\left(\frac{-\alpha}{1-\alpha}, t-a\right).\end{aligned}$$

Since $\kappa \leq 0$, , we have

$${}_a^{ABC}\nabla^{\alpha} x^2(t) - 2x(t)\,{}_a^{ABC}\nabla^{\alpha} x(t) \leq 0,$$

this concludes the proof. □

5.5.1 Generalized Discrete Variable-Order ABC Gronwal Inequality

In this section, we introduce a novel variable-order discrete ABC-type Gronwall inequality, representing a pioneering contribution to the literature by extending existing inequalities of this kind.

Theorem 5.9. *Suppose* $0 < \alpha < \frac{1}{2}$ *and the functions* $\frac{B(\alpha)}{B(\alpha)-(1-\alpha)v(t)}u(t)$ *and* $\frac{\alpha v(t)}{B(\alpha)-(1-\alpha)v(t)}$ *are both non-negative and non-decreasing for all* $t \in \mathbb{N}_a$. *Additionally,* $x(t)$ *is non-negative, and the following inequality is satisfied:*

$$x(t) \leq u(t) + v(t)\,{}_a^{AB}\nabla^{-\alpha} x(t), \tag{5.82}$$

then,

$$x(t) \leq \frac{B(\alpha)}{B(\alpha)-(1-\alpha)v(t)} u(t) E_{\overline{\alpha}}\left(\frac{\alpha v(t)}{B(\alpha)-(1-\alpha)v(t)}, t-a\right).$$

Proof. First, let's establish the following:

$$x(t) \leq u(t) + v(t)\,{}_a^{AB}\nabla^{-\alpha} x(t), \tag{5.83}$$

leading to:

$$x(t) \leq u(t) + v(t)\left(\frac{1-\alpha}{B(\alpha)} x(t) + \frac{\alpha}{B(\alpha)}\,{}_a\nabla^{-\alpha} x(t)\right).$$

Thus, we can deduce that the following inequality is established:

$$\begin{aligned} x(t) &\leq \left(1 - \frac{(1-\alpha)v(t)}{B(\alpha)}\right)^{-1} \left(u(t) + \frac{\alpha v(t)}{B(\alpha)}\, {}_a\nabla^{-\alpha} x(t)\right) \\ &= \frac{B(\alpha)}{B(\alpha) - (1-\alpha)v(t)} u(t) + \frac{\alpha v(t)}{B(\alpha) - (1-\alpha)v(t)}\, {}_a\nabla^{-\alpha} x(t). \end{aligned}$$

Now, let's consider the following:

$$\begin{aligned} \phi(t) &= \frac{B(\alpha)}{B(\alpha) - (1-v)v(t)} u(t), \\ \psi(t) &= \frac{\alpha v(t)}{B(\alpha) - (1-\alpha)v(t)}. \end{aligned}$$

Utilizing Lemma 5.1, we can infer the following:

$$x(t) \leq \frac{B(\alpha)}{B(\alpha) - (1-\alpha)v(t)} u(t) E_{\alpha}\left(\frac{\alpha v(t)}{B(\alpha) - (1-\alpha)v(t)}, t - a\right).$$

This completes the proof. □

Remarque 5.1. *The uniqueness of the Gronwall inequality presented here sets it apart from existing literature. For instance, in [368], a generalized discrete fractional variable-order Gronwall inequality was introduced to analyze the finite-time stability of nonlinear Nabla fractional variable-order discrete neural networks. In [369], the Atangana-Baleanu h-fractional difference sum operator was utilized to explore a generalized h-Gronwall inequality, addressing the uniqueness theorem and finite-time stability criterion of nonlinear h-fractional neural networks. Notably, the Gronwall inequality proposed in this study represents a broader concept than those previously found, as evidenced by its application to the investigation of stability and synchronization within a specific class of discrete variable-order neural networks.*

5.5.2 Solvability Conditions

In this section, we delve into the exploration of a variable-order discrete ABC-type neural network. We accomplish this by utilizing the discrete generalized ABC-type Gronwall inequality.
To begin, we introduce the following neural network with dynamics operating in fractional variable-order discrete time.

$$ {}^{ABC}_{a}\nabla^{\alpha} x_i(t) = -c_i x_i(t) + \sum_{j=1}^{n} d_{ij} g_j(t, x_j(t)) + I_i. \tag{5.84}$$

Now, we introduce several assumptions to establish the groundwork for our analysis of the system's dynamics.

(A_1) Suppose $g(t, x(t))$ is a continuous function satisfying the Lipschitz condition with respect to $\varkappa$. This condition implies:

$$|g_i(t, x_i(t)) - g_i(t, \mathfrak{z}_i(t))| \leq l_i |x_i(t) - \mathfrak{z}_i(t)|, \quad t \in \mathbb{N}_a. \tag{5.85}$$

(A_2) Suppose there exists a positive constant γ satisfying the following condition:

$$0 < \frac{\alpha\gamma}{B(\alpha) - (1-\alpha)\gamma} \leq 1, \tag{5.86}$$

$$\text{where } \gamma = \max_{i=1,\dots,n} \left\{ c_i + \sum_{n}^{j=1} |d_{ij}| l_j \right\} \text{ and } \sigma = \max_{i=1,\dots,n} I_i$$

(A_3) Let's assume the existence of a positive constant ν such that:

$$0 < \frac{\alpha\nu}{B(\alpha) - (1-\alpha)\nu} \leq 1, \tag{5.87}$$

$$\text{here } \nu = \max_{i=1,\dots,n} \left\{ c_i + \sum_{n}^{j=1} \frac{d_{ijj} + d_{jii}}{2} \right\}.$$

Subsequently, we will investigate the solvability of equation (5.84) using the variable-order generalized ABC Gronwall inequality.

Theorem 5.10. *If conditions (A_1) and (A_2) are satisfied, the solution to equation (5.84) is guaranteed to be unique.*

Proof. Let x and $\mathfrak{z}$ both be solutions to equation (5.84). We define o as $o(t) = x(t) - \mathfrak{z}(t)$ for $t \in \mathbb{N}a$. Given $x(a) = \mathfrak{z}(a)$, we aim to demonstrate $o(t) = 0$ for $t \in \mathbb{N}a$. This results in the following conclusion:

$$ {}^{ABC}_{a}\nabla^{\alpha} o_i(t) = -c_i o_i(t) + \sum_{j=1}^{n} d_{ij}(g_j(t, x_j(t)) - g_j(t, \mathfrak{z}_j(t))).$$

This equivalence can be expressed as:

$$\begin{aligned} |o_i(t)| =& |\, {}^{AB}_{a}\nabla^{-\alpha} \left(-c_i o_i(t) + \sum_{j=1}^{n} d_{ij}(g_j(t, x_j(t)) - g_j(t, \mathfrak{z}_j(t))) \right)|, \\ \leq & \, {}^{AB}_{a}\nabla^{-\alpha} \left(c_i |o_i(t)| + \sum_{j=1}^{n} |d_{ij}| l_j |x_j(t) - \mathfrak{z}_j(t)| \right), \\ \leq & \, {}^{AB}_{a}\nabla^{-\alpha} \left((c_i + \sum_{j=1}^{n} |d_{ij}| l_j) |o_i(t)| \right). \end{aligned}$$

Thus, we can conclude that

$$\|o(t)\| \leq \gamma \, {}^{AB}a\nabla^{-\alpha} \left(\|o(t)\| \right).$$

As indicated in Theorem 5.9, it is apparent that

$$\|o(t)\| \leq \frac{B(\alpha)}{B(\alpha) - (1-\alpha)\alpha} 0 \times E_{\overline{\alpha}} \left(\frac{\alpha\gamma}{B(\alpha)(1-\alpha+\alpha) - (1-\alpha)\alpha}, t - a \right).$$

By utilizing strong induction and verifying that $|o(t)| = 0$ implies $o(t) = 0$, we affirm the uniqueness of the solution to equation (5.84). This concludes the proof. □

5.5.3 Finite-Time Stability Results

In this section, we delve into the investigation of finite-time stability in nabla ABC neural networks with variable order. To begin, we introduce the following definition related to finite-time stability.

Theorem 5.11. *If conditions* (A_1) *and* (A_2) *hold, then system (5.84) demonstrates finite-time stability if and only if* $|\Phi| < \delta$ *and:*

$$\frac{B(\alpha)}{B(\alpha)-(1-\alpha)\gamma}\kappa E_{\overline{\alpha}}\left(\frac{\alpha\gamma}{B(\alpha)-(1-\alpha)\gamma}, t-a\right) \leq \frac{\delta}{\epsilon},$$

here

$$\kappa = \|\Phi\| + \frac{\sigma(1-alpha)}{B(\alpha)} + \frac{\sigma\alpha(t-a)^{\overline{\alpha}}}{B(\alpha)\Gamma(\alpha+1))}.$$

Proof. Given that $x(a) = \Phi$, it's clear that equation (5.84) can be restated as a summation equation with variable order.

$$x_i(t) = x_i(a) + {}_a^{AB}\nabla^{-\alpha}\left(-c_i x_i(t) + \sum_{j=1}^{n} d_{ij} g_j(t, x_j(t)) + I_i\right). \tag{5.88}$$

This restatement leads us to the subsequent outcome.

$$|x_i(t)| \leq |x_i(a)| + {}_a^{AB}\nabla^{-\alpha}\left(c_i|x_i(t)| + \sum_{j=1}^{n}|d_{ij}|l_j|x_j(t)| + |I_i|\right),$$

$$\leq |x_i(a)| + (c_i + \sum_{j=1}^{n}|d_{ij}|l_j|)\,{}_a^{AB}\nabla^{-\alpha}|x_j(t)| + {}_a^{ABC}\nabla^{\alpha}\sigma.$$

Therefore, we can infer that

$$\|x(t)\| \leq \|\Phi\| + \frac{\sigma(1-\alpha)}{B(\alpha)} + \frac{\sigma\alpha(t-a)^{\overline{\alpha}}}{B(\alpha)\Gamma(\alpha+1))} + \gamma\,{}_a^{AB}\nabla^{-\alpha}\|x(t)\|.$$

Now, by utilizing Theorem 5.9, we derive.

$$\|x(t)\| \leq \frac{B\alpha)}{B(\alpha)-(1-\alpha)v(t)}u(t)E_{\overline{\alpha}}\left(\frac{\alpha v(t)}{B(\alpha)-(1-\alpha)v(t)}, t-a\right),$$

here

$$u(t) = \|\Phi\| + \frac{\sigma(1-\alpha)}{B(\alpha)} + \frac{\sigma\alpha(t-a)^{\overline{\alpha}}}{B(\alpha)\Gamma(\alpha+1))},$$

and

$$v(t) = \gamma,$$

while

$$0 < \frac{\alpha\gamma}{B(\alpha)-(1-\alpha)v(t)} \leq 1.$$

According to the conditions outlined in Definition 5.1, it can be deduced that system (5.84) exhibits finite-time stability. This completes the proof. □

5.5.4 Computer Simulation

In this section, to demonstrate the practicality and effectiveness of our theoretical findings, we present two numerical examples that cover a range of scenarios and simulations.

Example 5.5. *We analyze a discrete-time fractional neural network in a three-dimensional context, as follows:*

$$ {}^{ABC}_{a}\nabla^{\alpha}x(t) = -Ax(t) + D\sin(x(t)) + I. \tag{5.89}$$

The numerical results for system (5.89) are as follows:

$$\begin{cases} x_i(\ell) = x_i(0) + \dfrac{1-\alpha(i)}{B(\alpha(i))}[-c_i x_i(\ell) + d_{i1}\sin(x_1(\ell)) + d_{i2}\sin(x_2(\ell)) + d_{i3}\sin(x_2(\ell)) + I_i] \\ \quad + \dfrac{\alpha(i)}{B(\alpha(i)))}\displaystyle\sum_{k=1}^{i}\frac{\Gamma(i-k+\alpha(i))}{\Gamma(i-k+1)}(-c_i x_i(j) + d_{i1}\sin(x_1(j)) + d_{i2}\sin(x_2(j)) \\ \quad + d_{i3}\sin(x_2(\ell)) + I_{i)}, \quad i=1,\ldots,3. \end{cases} \tag{5.90}$$

Case.1 *Let's examine the parameters:*

$$A = \begin{pmatrix} 0.2 & 0 & 0 \\ 0 & 0.2 & 0 \\ 0 & 0 & 0.2 \end{pmatrix}, \quad D = \begin{pmatrix} 0.04 & 0 & 0.02 \\ 0.03 & 0.04 & 0.01 \\ 0.04 & 0.01 & 0.02 \end{pmatrix}, \quad I = \begin{pmatrix} 0 \\ 0 \\ 0 \end{pmatrix}; \tag{5.91}$$

Additionally, given $\alpha = \dfrac{|\ln\left(\frac{1}{t+1}\right)|}{t+20}$ *we can determine the parameters as follows:*

$$\gamma = 1.5, \quad \sigma = 0.$$

With $\delta = 0.2$*, the main difficulty in identifying the finite-time* T *lies in calculating*

$$\frac{\alpha\gamma}{B(\alpha) - (1-\alpha)\gamma} = 0.974100401595700$$

, which is less than or equal to 1.

Given certain conditions, finite-time behavior can be observed. Figure 5.9 illustrates that at finite-time $T = 10$*, the numerical results validate the theoretical predictions, confirming our findings.*

Case.2 *Regarding the parameters provided:*

$c_{11} = 0.4,\ c_{22} = 0.3,\ c_{33} = 0.3,\ d_{11} = 0.3,\ d_{11} = -0.04,\ d_{12} = 0,\ d_{13} = -0.2,\ d_{21} = 0.1,\ d_{22} = -0.04,$
$d_{23} = 0.01,\ d_{31} = -0.04,\ d_{32} = 0.01,\ d_{33} = -0.2,\ I_1 = 0,\ I_2 = 0,$ *and* $I_3 = 0.$

Moreover, with the selection $\alpha = \dfrac{1}{2} - \dfrac{\exp\left(\frac{-1}{t+1}\right)}{t+1}$*, we obtain* $\sigma = 0.01$ *and* $\gamma = 1.$

The main challenge lies in establishing the finite-time value T*. When* $\delta = 2$*, evaluating the expression*

$$\frac{\alpha\gamma}{B(\alpha) - (1-\alpha)\gamma} = 0.949489737259976$$

, which is less than or equal to 1, indicates finite-time behavior for $T = 15$*. The system with the given parameters is evidently stable in finite-time, as shown in Figure 5.10.*

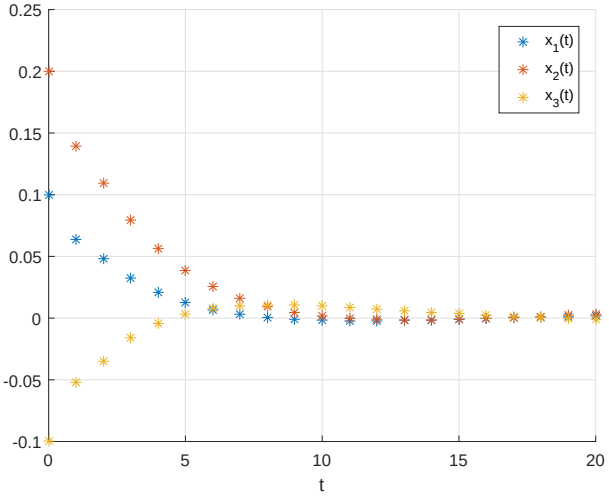

Figure 5.9: Evolution of system (5.89) with $x(0) = (0.1, 0.2, -0.1)^T$.

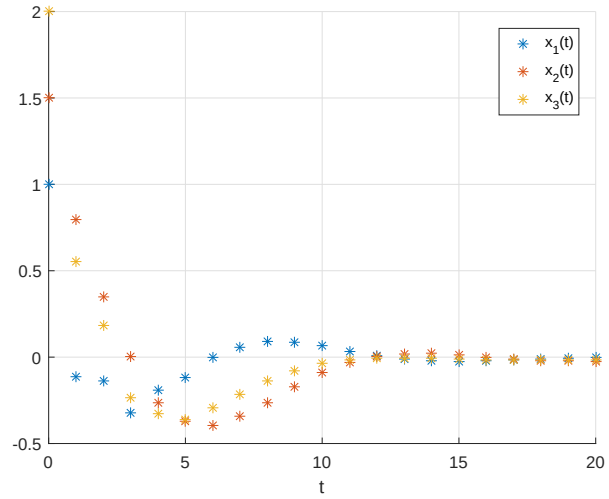

Figure 5.10: Evolution of system (5.89) with with $x(0) = (1, 1.5, 2)^T$.

5.6 Conclusion

In conclusion, this chapter has contributed to advancing the understanding of finite-time stability in discrete fractional systems, particularly within the domain of neural networks. By addressing the notable gap in research concerning finite-time stability analysis, we have introduced novel methodologies tailored for analyzing the convergence behavior of discrete fractional neural networks within finite timeframes.

Our exploration has shed light on the complexities involved in ensuring stability over finite time periods, highlighting the need for specialized techniques in the analysis of discrete fractional systems. Through the introduction of novel stability criteria and comparison theorems, we have provided valuable insights into the behavior of these systems

under finite-time dynamics.

The findings presented in this paper offer practical implications for the design and implementation of discrete fractional neural networks, particularly in applications where stability within finite timeframes is paramount. By bridging the gap between theoretical analysis and practical application, our work contributes to the broader understanding of fractional systems and their role in real-world scenarios.

Moving forward, further research is warranted to explore additional aspects of finite-time stability in discrete fractional systems, including more complex network architectures and diverse applications. Additionally, efforts to validate the proposed methodologies through extensive numerical simulations and experimental validations will be crucial in enhancing the reliability and robustness of finite-time stability analysis techniques.

Overall, the insights provided in this chapter pave the way for future advancements in the field of discrete fractional systems, offering new avenues for exploring the dynamics and stability properties of these systems within finite timeframes.

Chapter 6

Other Stability Type for Discrete Fractional-Order Neural Networks

6.1 Introduction

Ulam-Hyers stability, a relatively underexplored aspect, holds significant implications for the robustness and predictability of discrete systems. Although the literature on this topic is sparse [370, 371, 372], recent efforts have illuminated its importance, particularly within the context of discrete-time fractional variable-order neural networks [373]. These networks, characterized by their discrete nature and variable orders, present unique challenges in stability analysis.

Similarly, uniform stability has garnered attention due to its relevance in ensuring system behavior consistency across various scenarios [374, 375, 376]. The pursuit of adequate criteria for studying uniform stability in discrete-time fractional variable-order neural networks remains an active area of research [377], driven by the need for reliable and efficient models in engineering and scientific applications.

This chapter contributes to this evolving landscape by presenting novel criteria for Ulam-Hyers stability and uniform stability in discrete-time neural networks with variable orders. The proposed model, grounded in the Caputo h-difference operator, offers insights into the dynamics and stability of such networks, thereby advancing our understanding of their behavior.

The chapter is structured as follows: The first part Introduces the equations governing the proposed variable-order fractional discrete neural network, laying the groundwork for the subsequent stability analysis. This section also presents two novel theorems that address the existence of solutions and establish Ulam-Hyers stability, providing rigorous criteria for evaluating the stability of the system. Furthermore, it demonstrates the practical implications of the theoretical findings through numerical simulations, highlighting the importance of Ulam-Hyers and uniform stability in real-world applications. The second part Discusses several results on both the existence and uniqueness of the solutions of the considered discrete-time neural networks, utilizing the Banach fixed point technique. This section also presents our major conclusions, focusing on constraints related to the uniform stability of the addressed neural networks. Finally, the significance of the key findings is demonstrated using two numerical examples, which illustrate the practical

relevance and application of the theoretical results.

6.2 Ulam Hyers Stability for Discrete Fractional Multivariable Order Neural Networks

This section adresses the stability of discrete fractional-order neural networks, focusing on Ulam Hyers stability. It's a key concept that helps us understand how these networks respond to slight changes. By exploring this, we aim to shed light on how stable these networks are under different conditions.

The variable-order fractional discrete neural network that we propose can be mathematically described by the following formulation:

$$ {}^{C}_{h}\Delta^{\alpha_k}_{t_{kl}} x(t) = -Ax(t+\alpha_k h) + Dg(x(t+\alpha_k h)). \tag{6.1}$$

This equation can be simplified to a more manageable form, facilitating a deeper understanding and analysis of the system's dynamics and stability

$$\begin{cases} {}^{C}_{h}\Delta^{\alpha_0}_{t_0} x(t) = -Ax(t+\alpha_0 h) + Dg(x(t+\alpha_0 h)), & t \in \{t_0 + (1-\alpha_0)h, ..., t_l - \alpha_0 h\}, \\ {}^{C}_{h}\Delta^{\alpha_1}_{t_l} x(t) = -Ax(t+\alpha_1 h) + Dg(x(t+\alpha_1 h)), & t \in \{t_l + (1-\alpha_1)h, ..., t_{2l} - \alpha_1 h\}, \\ ... \\ {}^{C}_{h}\Delta^{\alpha_k}_{t_{kl}} x(t) = -Ax(t+\alpha_k h) + Dg(x(t+\alpha_k h)), & t \in \{t_{kl} + (1-\alpha_k)h, ..., t_{(k+1)l} - \alpha_k h\}. \end{cases} \tag{6.2}$$

$t \in (h\mathbb{N}_{t_{kl}+(1-\alpha_k)h}, \ \ 0 < \alpha_k \leq 1, \ \ k = 0, ..., m-1, \ \ m$ is the number of the intervals. Here, $x(t) = (x_1(t), ..., x_n(t))^T \in \mathbb{R}^n$ represents the state of the unit at time t, where n signifies the dimensionality. The matrix $A = diag(-a_1, ..., -a_p)$, with $c_i > 0$, serves the purpose of resetting the neurons' potential to the resting state upon disconnection from the network. Meanwhile, $D \in \mathbb{R}n * n$ corresponds to the connection weights within the neural network. Finally, $g(t, x(t)) \in C(h\mathbb{N})t_{kl} + (1-\alpha_k)h, \mathbb{R}^n)$ denotes the activation function, ensuring the continuity of g within the specified domain.

Lemme 6.1. *A function $x(t)$ is termed the solution of (6.1) if it adheres to the following conditions:*

$$x(t) = \begin{cases} x(t_0) + \dfrac{h}{\Gamma(\alpha_0)} \displaystyle\sum_{s=\frac{t_0}{h}+1-\alpha_0}^{\frac{t}{h}-\alpha_0} (t-\sigma(sh))^{\alpha_0-1}_{h}[-Ax(sh) + Dg(x(sh))], \quad t \in \{t_0 + h, ..., t_l\}, \\ x(t_0) + \displaystyle\sum_{n=1}^{m-1} \frac{h}{\Gamma(\alpha_{n-1})} \sum_{s=\frac{t_{(n-1)l}}{h}+1-\alpha_{n-1}}^{\frac{t}{h}-\alpha_{n-1}} (t-\sigma(sh))^{\alpha_{n-1}-1}_{h}[-Ax(sh) + Dg(x(sh))], \\ \quad + \dfrac{h}{\Gamma(\alpha_{m-1})} \displaystyle\sum_{s=\frac{t_{(m-1)l}}{h}+1-\alpha_{m-1}}^{\frac{t}{h}-\alpha_{m-1}} (t-\sigma(sh))^{\alpha_{m-1}-1}_{h}[-Ax(sh) + Df(x(sh))], \\ \quad t \in \{t_{(m-1)l} + h, ..., t_{ml}\}. \end{cases} \tag{6.3}$$

Proof. Equation (6.2) can be stated as equivalent to

$$\begin{cases} x(t) = x(t_0) + {}_h\Delta^{-\alpha_0}_{t_0+(1-\alpha_0)h}[-Ax(t) + Dg(x(t))], \quad t \in \{t_0 + h, ..., t_l\}, \\ x(t) = x(t_l) + {}_h\Delta^{-\alpha_1}_{t_l+(1-\alpha_1)h}[-Ax(t) + Dg(x(t))], \quad t \in \{t_l + h, ..., t_{2l}\}, \\ ... \\ x(t) = x(t_{(m-1)l}) + {}_h\Delta^{-\alpha_{(m-1)}}_{t_{(m-1)l}+(1-\alpha_{m-1})h}[-Ax(t) + Dg(x(t))], \quad t \in \{t_{(m-1)l} + h, ..., t_{ml}\}. \end{cases}$$

As for $k = 0$, t in the range $\{t_0 + (1 - \alpha_0)h, ..., t_l - v_0 h\}$, the solution of (6.1) can be formulated as:

$$x(t) = x(t_0) + {}_h\Delta^{-\alpha_0}_{t_0+(1-\alpha_0)h}[-Ax(t) + Dg(x(t))].$$

Further analysis yields:

$$x(t) = x(t_0) + \frac{h}{\Gamma(\alpha_0)} \sum_{s=\frac{t_0}{h}+1-\alpha_0}^{\frac{t}{h}-\alpha_0} (t - \sigma(sh))^{\alpha_0-1}_h[-Ax(sh) + Dg(x(sh))].$$

We can express $x(t_l) = x(t_0) + \frac{h}{\Gamma(\alpha_0)} \sum_{s=\frac{t_0}{h}+1-\alpha_0}^{\frac{t_l}{h}-\alpha_0} (t_l - \sigma(sh))^{\alpha_0-1}_h[-Ax(sh) + Dg(x(sh))]$ as an initial condition for:

$${}^C_h\Delta^{\alpha_1}_{t_l} x(t) = -Ax(t + \alpha_1 h) + Ag(x(t + \alpha_1 h)), \quad t \in \{t_l + (1 - \alpha_1)h, ..., t_{2l} - \alpha_1 h\}.$$

By employing a similar methodology, we can derive the expression of $x(t)$ for any t in the range $\{t_l + (1 - \alpha_1)h, ..., t_{2l} - \alpha_1 h\}$.

$$\begin{aligned} x(t) &= x(t_l) + \frac{h}{\Gamma(\alpha_1)} \sum_{s=\frac{t_0}{h}+1-\alpha_1}^{\frac{t}{h}-\alpha_1} (t - \sigma(sh))^{\alpha_1-1}_h[-Ax(sh) + Dg(x(sh))], \\ &= x(t_0) + \frac{h}{\Gamma(\alpha_0)} \sum_{s=\frac{t_0}{h}+1-\alpha_0}^{\frac{t_l}{h}-\alpha_0} (t_l - \sigma(sh))^{\alpha_0-1}_h[-Ax(sh) + Dg(x(sh))] \\ &\quad + \frac{h}{\Gamma(\alpha_1)} \sum_{s=\frac{t_l}{h}+1-\alpha_1}^{\frac{t}{h}-\alpha_1} (t - \sigma(sh))^{\alpha_1-1}_h[-Ax(sh) + Dg(x(sh))], \end{aligned}$$

for any t in the range $t \in \{t_{kl} + (1 - \alpha_k)h, ..., t_{(k+1)l-\alpha_k h}\}, k = 2, 3, ..., m - 1$ we can similarly derive $x(t)$ as follows

$$x(t) = \begin{cases} x(t_0) + \frac{h}{\Gamma(\alpha_0)} \sum_{s=\frac{t_0}{h}+1-\alpha_0}^{\frac{t}{h}-\alpha_0} (t - \sigma(sh))^{\alpha_0-1}_h[-Ax(sh) + Dg(x(sh))], \quad t \in \{t_0 + h, ..., t_l\}, \\ x(t_0) + \sum_{n=1}^{m-1} \frac{h}{\Gamma(\alpha_{n-1})} \sum_{s=\frac{t_{(n-1)l}}{h}+1-\alpha_{n-1}}^{\frac{t}{h}-\alpha_{n-1}} (t - \sigma(sh))^{\alpha_{n-1}-1}_h[-Ax(sh) + Dg(x(sh))] \\ \quad + \frac{h}{\Gamma(\alpha_{m-1})} \sum_{s=\frac{t_{(m-1)l}}{h}+1-\alpha_{m-1}}^{\frac{t}{h}-\alpha_{m-1}} (t - \sigma(sh))^{\alpha_{m-1}-1}_h[-Ax(sh) + Df(x(sh))], \\ \quad t \in \{t_{(m-1)l} + h, ..., t_{ml}\}, \end{cases}$$

and with that, the proof is completed. □

6.2.1 Existence of The Solution

The operator presented here is now defined:

$$Px(t) = x(t_0) + \sum_{n=1}^{m-1} \frac{h}{\Gamma(\alpha_{n-1})} \sum_{s=\frac{t_{(n-1)l}}{h}+1-\alpha_{n-1}}^{\frac{t}{h}-\alpha_{n-1}} (t-\sigma(sh))_h^{\alpha_{n-1}-1}[-Ax(sh)+Dg(x(sh))]$$

$$+ \frac{h}{\Gamma(\alpha_{m-1})} \sum_{s=\frac{t_{(m-1)l}}{h}+1-\alpha_{m-1}}^{\frac{t}{h}-\alpha_{m-1}} (t-\sigma(sh))_h^{\alpha_{m-1}-1}[-Ax(sh)+Dg(x(sh))], \quad t \in (h\mathbb{N})_{t_0+h}.$$

We can readily conclude that x is a solution of (6.1) if and only if x is a fixed point of the operator P. To establish existence results, we employ Kransnoselkii's fixed point theorem [378].

For any $t \in (h\mathbb{N})_{t_0+h}$, we define the operators

$$Tx(t) = \sum_{n=1}^{m-1} \frac{h}{\Gamma(\alpha_{n-1})} \sum_{s=\frac{t_{(n-1)l}}{h}+1-\alpha_{n-1}}^{\frac{t}{h}-\alpha_{n-1}} (t-\sigma(sh))_h^{\alpha_{n-1}-1}[-Ax(sh)+Dg(x(sh))],$$

and

$$Sx(t) = x(t_0) + \frac{h}{\Gamma(\alpha_{m-1})} \sum_{s=\frac{t_{(m-1)l}}{h}+1-\alpha_{m-1}}^{\frac{t}{h}-\alpha_{m-1}} (t-\sigma(sh))_h^{\alpha_{m-1}-1}[-Ax(sh)+Dg(x(sh))].$$

Next, we introduce the following assumptions.

(A_1) for all $t \in (h\mathbb{N}_{t_{(m-1)l}+(1-\alpha_{m-1})h}$, $g(t,x)$ represents a continuous function with respect to x, and there exists a constant $L \in \mathbb{R}^+$ such that

$$\|g(t,x) - g(t,y)\| \leq L\|x-y\|$$

(A_2) There exists a constant $M \in \mathbb{R}^+$ such that

$$M < 1$$

Where

$$M = [M_A + LM_D]\times$$
$$\left(\sum_{n=1}^{m-1} \frac{(t+(\alpha_{n-1}-1)h+t_{(n-1)l})_h^{(\alpha_{n-1})}}{\Gamma(1+\alpha_{n-1})} + \sup_{t\in\{t_{(m-1)l}+h,\ldots,t_{ml}\}} \frac{(t+(\alpha_{m-1}-1)h+t_{(m-1)l})_h^{(\alpha_{m-1})}}{\Gamma(1+\alpha_{m-1})} \right),$$

$$M_A = \|A\|_\infty, \quad M_D = \|D\|_\infty.$$

Now, a novel Theorem is illustrated, which proves the existence of the solution of the variable-order fractional discrete neural network (6.1).

Theorem 6.1. *Under Assumptions (A_1) and (A_2), for any $x \in \mathbb{R}^n$, there exists positive σ such that $\|x(t_0)\| \leq \sigma$. Then, system (6.1) has at least one bounded solution in $\Omega = \{x \in \mathbb{R}^n : \|x\| \leq r\}$ if the following condition hold*

$$r > \frac{\sigma}{1-M}.$$

Proof. It's clear that Ω constitutes a nonvoid, shut, delimited, and convex region within

Step 1. We demonstrate that S transforms Ω into itself. For any x belonging to Ω, we have:

$$\begin{aligned}\|Sx(t)\| &\leq \|x(t_0)\| + \frac{h}{\Gamma(\alpha_{m-1})} \sum_{s=\frac{t_{(m-1)l}}{h}+1-\alpha_{m-1}}^{\frac{t}{h}-\alpha_{m-1}} (t-\sigma(sh))_h^{\alpha_{m-1}-1} \| - Ax(sh) + Dg(x(sh))\|, \\ &\leq \sigma + [M_A + LM_D] \sup_{t\in\{t_{(m-1)l}+h,\ldots,t_{ml}\}} \frac{(t+(\alpha_{m-1}-1)h+t_{(m-1)l})_h^{(\alpha_{m-1})}}{\Gamma(1+\alpha_{m-1})}\|x\|, \\ &\leq \sigma + [M_A + LM_D] \sup_{t\in\{t_{(m-1)l}+h,\ldots,t_{ml}\}} \frac{(t+(\alpha_{m-1}-1)h+t_{(m-1)l})_h^{(\alpha_{m-1})}}{\Gamma(1+\alpha_{m-1})} r \leq r.\end{aligned}$$

This implies that $S\Omega$ is a subset of Ω.

Step 2. We need to demonstrate the continuity of S. Consider a sequence x_n in Ω such that x_n converges to x as n tends to infinity. Then, we can derive the following:

$$\begin{aligned}\|Sx_n(t) - Sx(t)\| &\leq \|x_n(t_0) - x(t_0)\| \\ &\quad + \|\frac{h}{\Gamma(\alpha_{m-1})} \sum_{s=\frac{t_{(m-1)l}}{h}+1-\alpha_{m-1}}^{\frac{t}{h}-\alpha_{m-1}} (t-\sigma(sh))_h^{\alpha_{m-1}-1}[-A(x_n(sh)-x(sh)) \\ &\quad + D(g(x_n(sh)) - g(x(sh)))]\|, \\ &\leq \|x_n(t_0) - x(t_0)\| \\ &\quad + [M_A + LM_D] \sup_{t\in\{t_{(m-1)l}+h,\ldots,t_{ml}\}} \frac{(t+(\alpha_{m-1}-1)h+t_{(m-1)l})_h^{(\alpha_{m-1})}}{\Gamma(1+\alpha_{m-1})}\|x_n(t) - x(t)\|.\end{aligned}$$

Thus, we can conclude that $|Sx_n(t) - Sx(t)| \to 0$ as $n \to +\infty$, indicating the continuity of S.

Step 3. We demonstrate that S is relatively compact. Selecting $t_1, t_2 \in \{t_{kl}+h, ..., t_{(k+1)l}\}$, $k =$

$1, 2, ...m-1$ and $t_1 < t_2$ we have

$$\|Sx(t_1) - Sx(t_2)\| \leq \frac{h}{\Gamma(\alpha_{m-1})}\| \sum_{s=\frac{t^{(m-1)l}}{h}+1-\alpha_{m-1}}^{\frac{t_1}{h}-\alpha_{m-1}} (t_1 - \sigma(sh))_h^{\alpha_{m-1}-1}[-Ax(sh) + Dg(x(sh))]$$

$$- \sum_{s=\frac{t^{(m-1)l}}{h}+1-\alpha_{m-1}}^{\frac{t_2}{h}-\alpha_{m-1}} (t_2 - \sigma(sh))_h^{\alpha_{m-1}-1}[-Ax(sh) + Dg(x(sh))]\|,$$

$$\leq \frac{h}{\Gamma(\alpha_{m-1})}\| \sum_{s=\frac{t^{(m-1)l}}{h}+1-\alpha_{m-1}}^{\frac{t_1}{h}-\alpha_{m-1}} (t_1 - \sigma(sh))_h^{\alpha_{m-1}-1}[-Ax(sh) + Dg(x(sh))]$$

$$- \sum_{s=\frac{t^{(m-1)l}}{h}+1-\alpha_{m-1}}^{\frac{t_1}{h}-\alpha_{m-1}} (t_2 - \sigma(sh))_h^{\alpha_{m-1}-1}[-Ax(sh) + Dg(x(sh))]$$

$$- \sum_{s=\frac{t_1}{h}+1-\alpha_{m-1}}^{\frac{t_2}{h}-\alpha_{m-1}} (t_2 - \sigma(sh))_h^{\alpha_{m-1}-1}[-Ax(sh) + Dg(x(sh))]\|,$$

$$\leq \frac{h}{\Gamma(\alpha_{m-1})}\| \sum_{s=\frac{t^{(m-1)l}}{h}+1-\alpha_{m-1}}^{\frac{t_1}{h}-\alpha_{m-1}} \left((t_1 - \sigma(sh))_h^{\alpha_{m-1}-1} - (t_2 - \sigma(sh))_h^{\alpha_k-1}\right)[-Ax(sh) + Dg(x(sh))]$$

$$- \sum_{s=\frac{t_1}{h}+1-\alpha_{m-1}}^{\frac{t_2}{h}-\alpha_{m-1}} (t_2 - \sigma(sh))_h^{\alpha_{m-1}-1}[-Ax(sh) + Dg(x(sh))]\|,$$

$$\leq \frac{h}{\Gamma(\alpha_{m-1})}[M_A + LM_D](\sum_{s=\frac{t^{(m-1)l}}{h}+1-\alpha_{m-1}}^{\frac{t_1}{h}-\alpha_{m-1}} |(t_1 - \sigma(sh))_h^{\alpha_{m-1}-1} - (t_2 - \sigma(sh))_h^{\alpha_k-1}|$$

$$+ \sum_{s=\frac{t_1}{h}+1-\alpha_{m-1}}^{\frac{t_2}{h}-\alpha_{m-1}} (t_2 - \sigma(sh))_h^{\alpha_{m-1}-1})r \quad \to 0, \quad \text{as } t_1 \to t_2.$$

This implies that $\{Sx : x \in \Omega\}$ s a bounded and uniformly Cauchy subset E. Utilizing Azela-Ascoli's Theorem [378], we conclude that $S\Omega$ is relatively compact.

Step 4. Selecting a fixed $y \in \Omega, \quad x = Tx + Sy$ for all $k = 0, 1, 2, ..., m-1$ and we have

$$\begin{aligned}
\|x\| &\leq \|Tx\| + \|Sy\|, \\
&\leq \sum_{n=1}^{m-1} \frac{h}{\Gamma(\alpha_{n-1})} \sum_{s=\frac{t_{(n-1)l}}{h}+1-\alpha_{n-1}}^{\frac{t}{h}-\alpha_{n-1}} (t-\sigma(sh))_h^{\alpha_{n-1}-1} \| - Ax(sh) + Dg(x(sh))\| \\
&\quad + \|y(t_0)\| + \frac{h}{\Gamma(\alpha_{m-1})} \sum_{s=\frac{t_{(m-1)l}}{h}+1-\alpha_{m-1}}^{\frac{t}{h}-\alpha_{m-1}} (t-\sigma(sh))_h^{\alpha_{m-1}-1} \| - Ay(sh) + Dg(y(sh))\|, \\
&\leq [M_A + LM_D] r \sum_{n=1}^{m-1} \frac{h}{\Gamma(\alpha_{n-1})} \sum_{s=\frac{t_{(n-1)l}}{h}+1-\alpha_{n-1}}^{\frac{t}{h}-\alpha_{n-1}} (t-\sigma(sh))_h^{\alpha_{n-1}-1} \\
&\quad + \sigma + [M_A + LM_D] r \frac{h}{\Gamma(\alpha_{m-1})} \sup_{t \in \{t_{(m-1)l}+h, ..., t_{ml}\}} \frac{(t + (\alpha_{m-1}-1)h + t_{(m-1)l})_h^{(\alpha_{m-1})}}{\Gamma(1+\alpha_{m-1})}, \\
&\leq \sigma + [M_A + LM_D] \Big(\sum_{n=1}^{m-1} \frac{(t + (\alpha_{n-1}-1)h + t_{(n-1)l})_h^{(\alpha_{n-1})}}{\Gamma(1+\alpha_{n-1})} \\
&\quad + \sup_{t \in \{t_{(m-1)l}+h, ..., t_{ml}\}} \frac{(t + (\alpha_{m-1}-1)h + t_{(m-1)l})_h^{(\alpha_{m-1})}}{\Gamma(1+\alpha_{m-1})} \Big) r \leq r.
\end{aligned}$$

Therefor, $\quad x \in \Omega.$

Ultimately, we establish that the operator T is a contraction mapping. Considering $x(t), y(t) \in \Omega$, the norm of $Tx(t) - Ty(t)$, is computed as follows:

$$\begin{aligned}
\|Tx(t) - Ty(t)\| = \| \sum_{n=1}^{m-1} \frac{h}{\Gamma(\alpha_{n-1})} \sum_{s=\frac{t_{(n-1)l}}{h}+1-\alpha_{k-n-1}}^{\frac{t}{h}-\alpha_{n-1}} (t-\sigma(sh))_h^{\alpha_{n-1}-1} [-A(x(sh) - y(sh)) \\
+ D(g(x(sh)) - g(yg(sh)))] \| \\
\leq [M_A + LM_D] \|x - y\| \sum_{n=1}^{m-1} \frac{(t + (\alpha_{n-1}-1)h + t_{(n-1)l})_h^{(\alpha_{n-1})}}{\Gamma(1+\alpha_{n-1})} < \|x - y\|.
\end{aligned}$$

Based on condition (A_2), it follows that the operator T behaves as a contraction mapping. By Krasnoselskii fixed-point Theorem [378], the composite operator $P = T + S$ possesses a fixed point within Ω, which constitutes a solution to (6.1).

□

6.2.2 Ulam-Hyers Stability of Discrete Fractional Multiple-Order Neural Network

Definition 6.1 (Ulam-Hyers stability [379]). *We define (6.1) to be Ulam-Hyers stable if there exists $c > 0$ such that for any $\epsilon > 0$, whenever $y \in \mathbb{R}$ satisfies*

$$\|{}_h^C \Delta_{t_{kl}}^{\alpha_k} x(t) + Ax(t + \alpha_k h) - Dg(x(t + \alpha_k h)\| \leq \epsilon, \tag{6.4}$$

for $t \in (h\mathbb{N})_{t_{kl}+(1-\alpha_k)h}, 0 < \alpha_k \leq 1, k = 0, ..., m-1.$
In this case, there exists a solution y *of (6.1) such that:*

$$\|x(t) - y(t)\| \leq c\epsilon.$$

Initially, we establish the following lemma.

Lemme 6.2. *Ifx solves Equation (6.4), then it satisfies the following.*

$$\|x(t)-x(t_0) + \sum_{n=1}^{m-1} \frac{h}{\Gamma(\alpha_{n-1})} \sum_{s=\frac{t_{(n-1)l}}{h}+1-\alpha_{n-1}}^{\frac{t}{h}-\alpha_{n-1}} (t-\sigma(sh))_h^{\alpha_{n-1}-1}[Ax(sh) - Dg(x(sh))]$$
$$+ \frac{h}{\Gamma(\alpha_{m-1})} \sum_{s=\frac{t_{(m-1)l}}{h}+1-\alpha_{m-1}}^{\frac{t}{h}-\alpha_{m-1}} (t-\sigma(sh))_h^{\alpha_{m-1}-1}[Ax(sh) - Dg(x(sh))]\| \leq d\epsilon,$$

where

$$d = \left(\sum_{n=1}^{m-1} \frac{(t + (\alpha_{n-1} - 1)h + t_{(n-1)l})_h^{(\alpha_{n-1})}}{\Gamma(1+\alpha_{n-1})} + \sup_{t \in \{t_{(m-1)l}+h, ..., t_{ml}\}} \frac{(t + (\alpha_{m-1} - 1)h + t_{(m-1)l})_h^{(\alpha_{m-1})}}{\Gamma(1+\alpha_{m-1})} \right)$$

.

Proof. Suppose $x(t)$ satisfies Equation (6.4). Then, there exists a function $f(t)$ such that and

$${}_h^C\Delta_{t_{kl}}^{\alpha_k} x(t) + Ax(t+\alpha_k h) - Dg(x(t+\alpha_k h) = f(t), \quad t \in \{t_{kl}+h, ..., t_{(k+1)l}\}, \quad k = 0, 1, 2, ..., m-1.$$

This implies that

$$\begin{cases} {}_h^C\Delta_{t_0}^{\alpha_0} x(t) + Ax(t+\alpha_0 h) - Dg(x(t+\alpha_0 h) = f(t), & t \in \{t_0 + h, ..., t_l\}, \\ {}_h^C\Delta_{t_l}^{\alpha_1} x(t) + Ax(t+\alpha_1 h) - Dg(x(t+\alpha_1 h) = f(t), & t \in \{t_l + h, ..., t_{2l}\}, \\ ... \\ {}_h^C\Delta_{t_{(m-1)l}}^{\alpha_{m-1}} x(t) + Ax(t+\alpha_{m-1} h) - Dg(x(t+\alpha_{m-1} h) = f(t), & t \in \{t_{(m-1)l} + h, ..., t_{ml}\}. \end{cases}$$

This is equivalent to stating that:

$$\begin{cases} x(t)-x(t_0)+\dfrac{h}{\Gamma(\alpha_0)}\displaystyle\sum_{s=\frac{t_0}{h}+1-\alpha_0}^{\frac{t}{h}-\alpha_0}(t-\sigma(sh))_h^{\alpha_0-1}[Ax(sh)-Dg(x(sh))] \\ \qquad =\dfrac{h}{\Gamma(\alpha_0)}\displaystyle\sum_{s=\frac{t_0}{h}+1-\alpha_0}^{\frac{t}{h}-\alpha_0}(t-\sigma(sh))_h^{\alpha_0-1}f(sh), \\ x(t)-x(t_l)+\dfrac{h}{\Gamma(\alpha_1)}\displaystyle\sum_{s=\frac{t_l}{h}+1-\alpha_1}^{\frac{t}{h}-\alpha_1}(t-\sigma(sh))_h^{\alpha_1-1}[Ax(sh)-Dg(x(sh))] \\ \qquad =\dfrac{h}{\Gamma(\alpha_1)}\displaystyle\sum_{s=\frac{t_1}{h}+1-\alpha_1}^{\frac{t}{h}-\alpha_1}(t-\sigma(sh))_h^{\alpha_1-1}f(sh), \\ \ldots \\ x(t)-x(t_{(m-1)l}+\dfrac{h}{\Gamma(\alpha_{m-1})}\displaystyle\sum_{s=\frac{t_{(m-1)l}}{h}+1-\alpha_{m-1}}^{\frac{t}{h}-\alpha_{m-1}}(t-\sigma(sh))_h^{\alpha_{m-1}-1}[Ax(sh)-Dg(x(sh))] \\ \qquad =\dfrac{h}{\Gamma(\alpha_{m-1})}\displaystyle\sum_{s=\frac{t_{(m-1)l}}{h}+1-\alpha_{m-1}}^{\frac{t}{h}-\alpha_{m-1}}(t-\sigma(sh))_h^{\alpha_{m-1}-1}f(sh). \end{cases}$$

Henceforth, we obtain:

$$\begin{cases} x(t_l)=x(t_0)+\dfrac{h}{\Gamma(\alpha_0)}\displaystyle\sum_{s=\frac{t_0}{h}+1-\alpha_0}^{\frac{t_l}{h}-\alpha_0}(t_l-\sigma(sh))_h^{\alpha_0-1}[-Ax(sh)+Dg(x(sh))] \\ \qquad +\dfrac{h}{\Gamma(\alpha_0)}\displaystyle\sum_{s=\frac{t_0}{h}+1-\alpha_0}^{\frac{t_l}{h}-\alpha_0}(t_l-\sigma(sh))_h^{\alpha_0-1}f(sh), \\ x(t_{2l})=x(t_l)+\dfrac{h}{\Gamma(\alpha_1)}\displaystyle\sum_{s=\frac{t_l}{h}+1-\alpha_1}^{\frac{t_{2l}}{h}-\alpha_1}(t_{2l}-\sigma(s))_h^{\alpha_1-1}[Ax(sh)-Dg(x(sh))] \\ \qquad +\dfrac{h}{\Gamma(\alpha_1)}\displaystyle\sum_{s=\frac{t_1}{h}+1-\alpha_1}^{\frac{t_{2l}}{h}-\alpha_1}(t_{2l}-\sigma(sh))_h^{\alpha_1-1}f(sh), \\ \ldots \\ x(t)-x(t_{(m-1)l}+\dfrac{h}{\Gamma(\alpha_{m-1})}\displaystyle\sum_{s=\frac{t_{(m-1)l}}{h}+1-\alpha_{m-1}}^{\frac{t}{h}-\alpha_{m-1}}(t-\sigma(sh))_h^{\alpha_{m-1}-1}[Ax(sh)-Dg(x(sh))] \\ \qquad =\dfrac{h}{\Gamma(\alpha_{m-1})}\displaystyle\sum_{s=\frac{t_{(m-1)l}}{h}+1-\alpha_{m-1}}^{\frac{t}{h}-\alpha_{m-1}}(t-\sigma(sh))_h^{\alpha_{m-1}-1}f(sh). \end{cases}$$

This subsequently results in the subsequent equality:

$$
\begin{aligned}
x(t)-x(t_0)+\sum_{n=1}^{m-1}\frac{h}{\Gamma(\alpha_{n-1})}&\sum_{s=\frac{t_{(n-1)l}}{h}+1-\alpha_{n-1}}^{\frac{t}{h}-\alpha_{n-1}}(t-\sigma(sh))_h^{\alpha_{n-1}-1}[Ax(sh)-Dg(x(sh))]\\
&+\frac{h}{\Gamma(\alpha_{m-1})}\sum_{s=\frac{t_{(m-1)l}}{h}+1-\alpha_{m-1}}^{\frac{t}{h}-\alpha_{m-1}}(t-\sigma(sh))_h^{\alpha_{m-1}-1}[Ax(sh)-Dg(x(sh))],\\
&=\sum_{n=1}^{m-1}\frac{h}{\Gamma(\alpha_{n-1})}\sum_{s=\frac{t_{(n-1)l}}{h}+1-\alpha_{n-1}}^{\frac{t}{h}-\alpha_{n-1}}(t-\sigma(sh))_h^{\alpha_{n-1}-1}f(sh)\\
&+\frac{h}{\Gamma(\alpha_{m-1})}\sum_{s=\frac{t_{(m-1)l}}{h}+1-\alpha_{m-1}}^{\frac{t}{h}-\alpha_{m-1}}(t-\sigma(sh))_h^{\alpha_{m-1}-1}f(sh).
\end{aligned}
$$

Now, by computing the norm of both sides, we obtain:

$$
\begin{aligned}
&\|x(t)-x(t_0)+\sum_{n=1}^{m-1}\frac{h}{\Gamma(\alpha_{n-1})}\sum_{s=\frac{t_{(n-1)l}}{h}+1-\alpha_{n-1}}^{\frac{t}{h}-\alpha_{n-1}}(t-\sigma(sh))_h^{\alpha_{n-1}-1}[Ax(sh)-Dg(x(sh))]\\
&+\frac{h}{\Gamma(\alpha_{m-1})}\sum_{s=\frac{t_{(m-1)l}}{h}+1-\alpha_{m-1}}^{\frac{t}{h}-\alpha_{m-1}}(t-\sigma(sh))_h^{\alpha_{m-1}-1}[Ax(sh)-Dg(x(sh))]\|,\\
&=\|\sum_{n=1}^{m-1}\frac{h}{\Gamma(\alpha_{n-1})}\sum_{s=\frac{t_{(n-1)l}}{h}+1-\alpha_{n-1}}^{\frac{t}{h}-\alpha_{n-1}}(t-\sigma(sh))_h^{\alpha_{n-1}-1}f(sh)\\
&+\frac{h}{\Gamma(\alpha_{m-1})}\sum_{s=\frac{t_{(m-1)l}}{h}+1-\alpha_{m-1}}^{\frac{t}{h}-v=\alpha_{m-1}}(t-\sigma(sh))_h^{\alpha_{m-1}-1}f(sh)\|,\\
&\leq\left(\sum_{n=1}^{m-1}\frac{(t+(\alpha_{n-1}-1)h+t_{(n-1)l})_h^{(\alpha_{n-1})}}{\Gamma(1+\alpha_{n-1})}+\sup_{t\in\{t_{(m-1)l}+h,\ldots,t_{ml}\}}\frac{(t+(\alpha_{m-1}-1)h+t_{(m-1)l})_h^{(\alpha_{m-1})}}{\Gamma(1+\alpha_{m-1})}\right)\|f\|,\\
&\leq\left(\sum_{n=1}^{m-1}\frac{(t+(\alpha_{n-1}-1)h+t_{(n-1)l})_h^{(\alpha_{n-1})}}{\Gamma(1+\alpha_{n-1})}+\sup_{t\in\{t_{(m-1)l}+h,\ldots,t_{ml}\}}\frac{(t+(\alpha_{m-1}-1)h+t_{(m-1)l})_h^{(\alpha_{m-1})}}{\Gamma(1+\alpha_{m-1})}\right)\epsilon.
\end{aligned}
$$

This concludes the proof. □

A novel theorem is presented, demonstrating the Ulam-Hyers stability of the variable-order fractional discrete neural network (6.1).

Theorem 6.2. *Under the assumptions* (A_1) *and* (A_2)*, it is established that system (6.1) exhibits Ulam-Hyers stability.*

Proof. It's evident that the solution y to (6.1) fulfills

$$\begin{aligned} y(t) =& x(t_0) + \sum_{n=1}^{m-1} \frac{h}{\Gamma(\alpha_{n-1})} \sum_{s=\frac{t_{(n-1)l}}{h}+1-\alpha_{n-1}}^{\frac{t}{h}-\alpha_{n-1}} (t-\sigma(sh))_h^{\alpha_{n-1}-1}[Ay(sh)-Dg(y(sh))] \\ &+ \frac{h}{\Gamma(\alpha_{m-1})} \sum_{s=\frac{t_{(m-1)l}}{h}+1-\alpha_{m-1}}^{\frac{t}{h}-\alpha_{m-1}} (t-\sigma(sh))_h^{\alpha_{m-1}-1}[Ay(sh)-Dg(y(sh))]. \end{aligned}$$

Therefore,

$$\begin{aligned} \|x(t)-y(t)\| =& \|x(t)-x(t_0) - \sum_{n=1}^{m-1} \frac{h}{\Gamma(\alpha_{n-1})} \sum_{s=\frac{t_{(n-1)l}}{h}+1-\alpha_{n-1}}^{\frac{t}{h}-\alpha_{n-1}} (t-\sigma(sh))_h^{\alpha_{n-1}-1}[-Ay(sh)+Dg(y(sh))] \\ &- \frac{h}{\Gamma(\alpha_{m-1})} \sum_{s=\frac{t_{(m-1)l}}{h}+1-\alpha_{m-1}}^{\frac{t}{h}-\alpha_{m-1}} (t-\sigma(sh))_h^{\alpha_{m-1}-1}[-Ay(sh)+Dg(y(sh))]\|, \\ =& \|x(t)-x(t_0) - \sum_{n=1}^{m-1} \frac{h}{\Gamma(\alpha_{n-1})} \sum_{s=\frac{t_{(n-1)l}}{h}+1-\alpha_{n-1}}^{\frac{t}{h}-\alpha_{n-1}} (t-\sigma(sh))_h^{\alpha_{n-1}-1}[-Ay(sh)+Dg(y(sh))] \\ &- \frac{h}{\Gamma(\alpha_{m-1})} \sum_{s=\frac{t_{(m-1)l}}{h}+1-\alpha_{m-1}}^{\frac{t}{h}-\alpha_{m-1}} (t-\sigma(sh))_h^{\alpha_{m-1}-1}[-Ay(sh)+Dg(y(sh))] \\ &- \sum_{n=1}^{m-1} \frac{h}{\Gamma(\alpha_{n-1})} \sum_{s=\frac{t_{(n-1)l}}{h}+1-\alpha_{n-1}}^{\frac{t}{h}-\alpha_{n-1}} (t-\sigma(sh))_h^{\alpha_{n-1}-1}[-Ax(sh)+Dg(x(sh))] \\ &- \frac{h}{\Gamma(\alpha_{m-1})} \sum_{s=\frac{t_{(m-1)l}}{h}+1-\alpha_{m-1}}^{\frac{t}{h}-\alpha_{m-1}} (t-\sigma(sh))_h^{\alpha_{m-1}-1}[-Ax(sh)+Dg(x(sh))] \\ &+ \sum_{n=1}^{m-1} \frac{h}{\Gamma(\alpha_{n-1})} \sum_{s=\frac{t_{(n-1)l}}{h}+1-\alpha_{n-1}}^{\frac{t}{h}-\alpha_{n-1}} (t-\sigma(sh))_h^{\alpha_{n-1}-1}[-Ax(sh)+Dg(x(sh))] \\ &+ \frac{h}{\Gamma(\alpha_{m-1})} \sum_{s=\frac{t_{(m-1)l}}{h}+1-\alpha_{m-1}}^{\frac{t}{h}-\alpha_{m-1}} (t-\sigma(sh))_h^{\alpha_{m-1}-1}[-Ax(sh)+Dg(x(sh))]\|, \\ \leq& \|x(t)-x(t_0) - \sum_{n=1}^{m-1} \frac{h}{\Gamma(\alpha_{n-1})} \sum_{s=\frac{t_{(n-1)l}}{h}+1-\alpha_{n-1}}^{\frac{t}{h}-\alpha_{n-1}} (t-\sigma(sh))_h^{\alpha_{n-1}-1}[-Ax(sh)+Dg(x(sh))] \end{aligned}$$

$$
\begin{aligned}
&- \frac{h}{\Gamma(\alpha_{m-1})} \sum_{s=\frac{t_{(m-1)l}}{h}+1-\alpha_{m-1}}^{\frac{t}{h}-\alpha_{m-1}} (t-\sigma(sh))_h^{\alpha_{m-1}-1}[-Ax(sh)+Dg(x(sh))]\| \\
&+ \| \sum_{n=1}^{m-1} \frac{h}{\Gamma(\alpha_{n-1})} \sum_{s=\frac{t_{(n-1)l}}{h}+1-\alpha_{n-1}}^{\frac{t}{h}-\alpha_{n-1}} (t-\sigma(sh))_h^{\alpha_{n-1}-1}[-A(x(sh)-y(sh)) \\
&+ D(g(x(sh))-g(y(sh)))]\| \\
&+ \| \frac{h}{\Gamma(\alpha_{m-1})} \sum_{s=\frac{t_{(m-1)l}}{h}+1-\alpha_{m-1}}^{\frac{t}{h}-\alpha_{m-1}} (t-\sigma(sh))_h^{\alpha_{m-1}-1}[-A(x(sh)-y(sh)) \\
&+ D(g(x(sh))-g(y(sh)))]\|, \\
\leq & \left(\sum_{n=1}^{m-1} \frac{(t+(\alpha_{n-1}-1)h+t_{(n-1)l})_h^{(\alpha_{n-1})}}{\Gamma(1+\alpha_{n-1})} + \sup_{t\in\{t_{(m-1)l}+h,\ldots,t_{ml}\}} \frac{(t+(\alpha_{m-1}-1)h+t_{(m-1)l})_h^{(\alpha_{m-1})}}{\Gamma(1+\alpha_{m-1})} \right) \epsilon \\
&+ [M_A + LM_D]\{ \sum_{n=1}^{m-1} \frac{(t+(\alpha_{n-1}-1)h+t_{(n-1)l})_h^{(\alpha_{n-1})}}{\Gamma(1+\alpha_{n-1})} \\
&+ \sup_{t\in\{t_{(m-1)l}+h,\ldots,t_{ml}\}} \frac{(t+(\alpha_{m-1}-1)h+t_{(m-1)l})_h^{(\alpha_{m-1})}}{\Gamma(1+v_{m-1})} \} \|x(t)-y(t)\|, \\
\leq & \frac{d}{1-M}\epsilon \leq c\epsilon,
\end{aligned}
$$

where

$$c = \frac{d}{1-M}.$$

This concludes the Ulam-Hyers stability of (6.1). □

6.2.3 Numerical Simulations

Example 6.1. *let's delve into the dynamics of the fractional variable-order neural network described by:*

$$
\begin{cases}
{}_h^C\Delta_{t_0}^{\alpha_0} x(t) = -Ax(t+\alpha_0 h) + D\tanh(x(t+\alpha_0 h)), & t \in \{t_0+(1-\alpha_0)h, \ldots, t_l-\alpha_0 h\}, \\
{}_h^C\Delta_{t_l}^{\alpha_1} x(t) = -Ax(t+\alpha_1 h) + D\tanh(x(t+\alpha_1 h)), & t \in \{t_l+(1-\alpha_l)h, \ldots, t_{2l}-\alpha_1 h\}, \\
{}_h^C\Delta_{t_{2l}}^{\alpha_2} x(t) = -Ax(t+\alpha_2 h) + D\tanh(x(t+\alpha_2 h)), & t \in \{t_{2l}+(1-\alpha_2)h, \ldots, t_{3l}-\alpha_2 h\}.
\end{cases} \tag{6.5}
$$

where $h = 0.5, \quad k = 0, 1, 2, \quad t \in (h\mathbb{N})_{t_{kl}-(1-\alpha_k)h}$ *and* $(\alpha_0, \alpha_1, \alpha_2) = (0.05, 0.1, 0.15)$. $\tanh(x(t)) = (\tanh x_1(t), \tanh(x_2(t))^T$,

$$
A = \begin{bmatrix} 0.2 & 0 & 0 \\ 0 & 0.2 & 0 \\ 0 & 0 & 0.2 \end{bmatrix}, \quad D = \begin{bmatrix} 0.002 & -0.004 & 0.0015 \\ -0.002 & 0.001 & -0.002 \\ -0.0025 & 0.0015 & -0.003 \end{bmatrix}, \quad x(0) = \begin{bmatrix} 0.9 \\ 0.6 \\ 0.3 \end{bmatrix}.
$$

Acknowledging that the conditions (A_1) *and* (A_2) *are met with* $M = 0.9866 < 1$, *we employ the subsequent numerical schemes to obtain the solution depicted in Figure 6.1. The initial condition* $x(0) = (0.9, 0.6, 0.3)^T$ *exemplifies the stability of the neural network*

under consideration.

$$\begin{cases} x(t) = x(t_0) + \dfrac{h^{\alpha_0}}{\Gamma(\alpha_0)} \displaystyle\sum_{t_0+1}^{t} \dfrac{\Gamma(t-j+\alpha_0)}{\Gamma(t-j+1)} \left(-Ax(j) + D\tanh(x(j))\right), \\ x(t) = x(t_l) + \dfrac{h^{\alpha_1}}{\Gamma(\alpha_1)} \displaystyle\sum_{t_l+1}^{t} \dfrac{\Gamma(t-j+\alpha_0)}{\Gamma(t-j+1)} \left(-Ax(j) + D\tanh(x(j))\right), \\ x(t) = x(t_{2l}) + \dfrac{h^{\alpha_2}}{\Gamma(\alpha_2)} \displaystyle\sum_{t_{2l}+1}^{t} \dfrac{\Gamma(t-j+\alpha_0)}{\Gamma(t-j+1)} \left(-Ax(j) + D\tanh(x(j))\right). \end{cases}$$

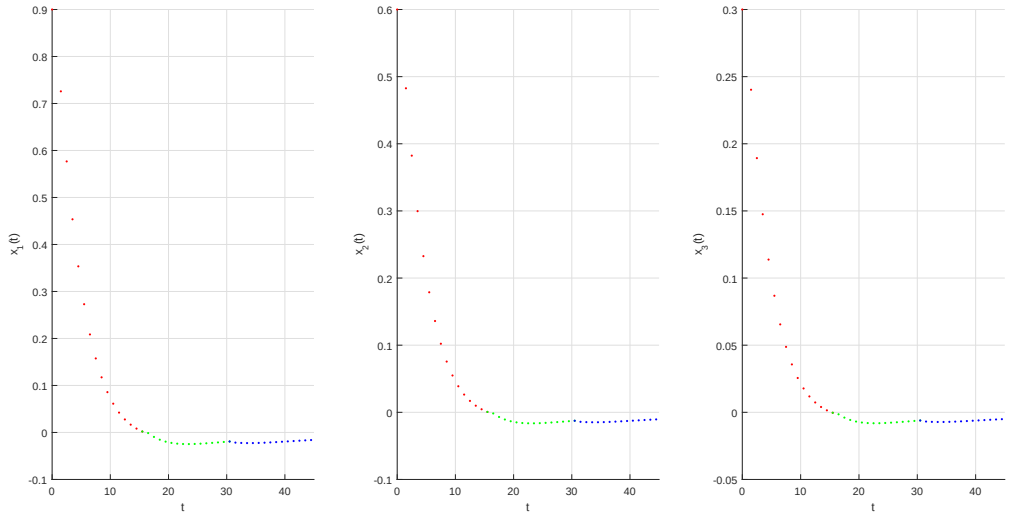

Figure 6.1: Numerical solution of the varibla-order neural network (6.5).

Example 6.2. *Let's explore a two-dimensional fractional discrete-time neural network given by:*

$$ {}^{C}_{h}\Delta^{\alpha_k}_{t_{kl}} x(t) = -Ax(t+\alpha_k h) + D\sin(x(t+\alpha_k h)), \quad 0 < \alpha_k \leq 1 \quad t \in (h\mathbb{N})_{kl+(1-\alpha_k)h} \quad k = 0,1,2,3. \tag{6.6}$$

where $sin(x(t)) = (sin(x_1(t)), sin(x_2(t)))^T$
suppose $x(0) = (1,-1)^T$, $(\alpha_0, \alpha_1, \alpha_2, \alpha_3) = (0.5, 0.4, 0.3, 0.2)$, $h = 1.3$ *and* $m = 4$

$$A = \begin{bmatrix} 0.046 & 0 \\ 0 & 0.046 \end{bmatrix}, \quad D = \begin{bmatrix} 0.0003 & 0 \\ -0.0004 & 0.0002 \end{bmatrix}.$$

We can delve into the stability analysis across various time domains, ensuring that the parameters meet all conditions outlined in Theorems (6.1) and (6.2). With $M = 0.9858 < 1$, *which satisfies the required conditions, we can examine the system's stability, as depicted in Figure 6.2.*

Example 6.3. *Consider the following neural network*

$$\begin{cases} {}^{C}_{h}\Delta^{\alpha_k}_{t_{kl}} x_1(t) = -c_1 x_1(t+\alpha_k h) + d_{11}\sin(x_1(t+\alpha_k h)) + d_{12}\sin(x_2(t+\alpha_k h)), \\ {}^{C}_{h}\Delta^{\alpha_k}_{t_{kl}} x_2(t) = -c_2 x_2(t+\alpha_1 h) + d_{21}\sin(x_1(t+\alpha_k h)) + d_{22}\sin(x_2(t+\alpha_k h)), \end{cases} \tag{6.7}$$

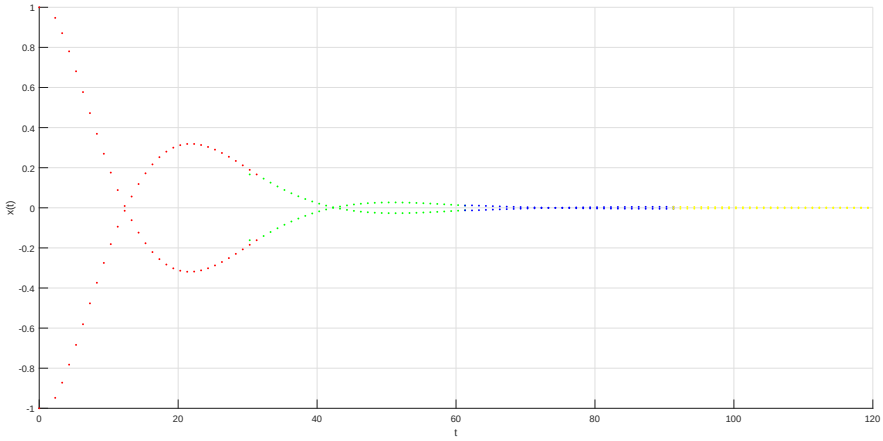

Figure 6.2: The numerical solution of neural network (6.6).

where $t \in (h\mathbb{N})_{t_{kl}+(1-\alpha_k)h}$, $\quad m = 4 \quad$ *and* $0 < \alpha_k \leq 1$.
In this example, we assess two distinct scenarios.

case 1 $t \in [0, 173], \quad h = 1.9, \quad (\alpha_0, \alpha_1, \alpha_2, \alpha_3) = (0.8, 0.6, 0.3, 0.4).$

$$\text{and} \quad A = \begin{bmatrix} 0.015 & 0 \\ 0 & 0.015 \end{bmatrix}, \quad BD = \begin{bmatrix} -0.0003 & 0 \\ -0.0004 & 0.0002 \end{bmatrix}, \quad x(0) = \begin{bmatrix} -0.001 \\ 0.0009 \end{bmatrix}$$

cases 2 $t \in [0, 120], \quad h = 1.25, \quad (\alpha_0, \alpha_1, \alpha_2, \alpha_3) = (0.05, 0.05, 0.05, 0.05).$

$$\text{and} \quad A = \begin{bmatrix} 0.1 & 0 \\ 0 & 0.1 \end{bmatrix}, \quad D = \begin{bmatrix} -0.03 & 0.02 \\ -0.01 & 0.06 \end{bmatrix}, \quad x(0) = \begin{bmatrix} -0.1 \\ 0.1 \end{bmatrix}$$

The conditions stipulated in theorems (6.1) and (6.2) are satisfied for $; M = 0.9212 < 1;$, *affirming stability. This assertion is supported by the numerical results depicted in Figure 6.3 and Figure 6.4, obtained using the prescribed computational algorithms.*

$$\begin{cases} x_1(t) = x_1(t_{kl}) + \dfrac{h^{\alpha_k}}{\Gamma(\alpha_k)} \displaystyle\sum_{t_k+1}^{i} \frac{\Gamma(t-j+\alpha_k)}{\Gamma(t-j+1)} \left(-c_1 x_1(j) + d_{11}\sin(x_1(j)) + d_{12}\sin(x_2(j))\right), \\ x_2(t) = x_2(t_{kl}) + \dfrac{h^{\alpha_k}}{\Gamma(\alpha_k)} \displaystyle\sum_{t_k+1}^{i} \frac{\Gamma(t-j+v_k)}{\Gamma(t-j+1)} \left(-c_2 x_2(j) + d_{21}\sin(x_1(j)) + d_{22}\sin(x_2(j)\right). \end{cases}$$

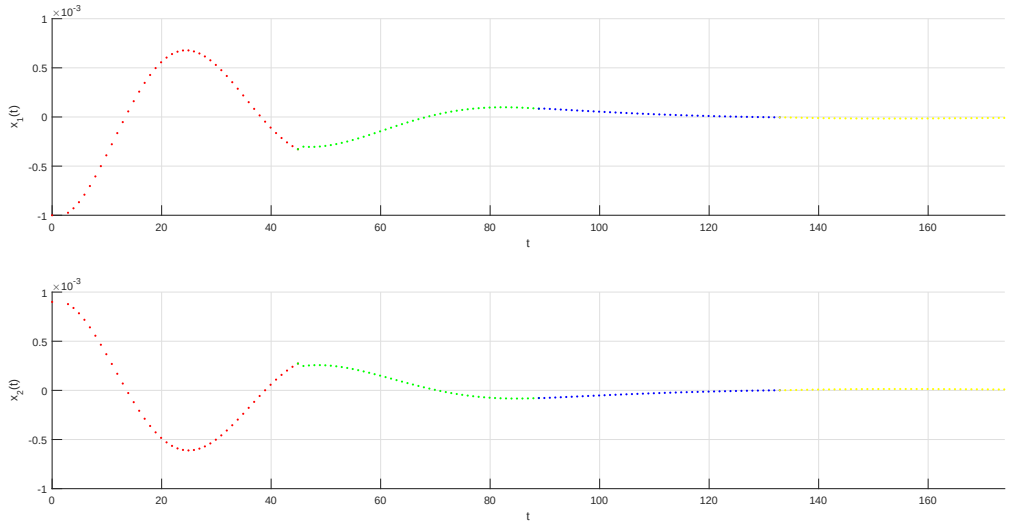

Figure 6.3: Numerical solution of neural network (6.7) **case 1**.

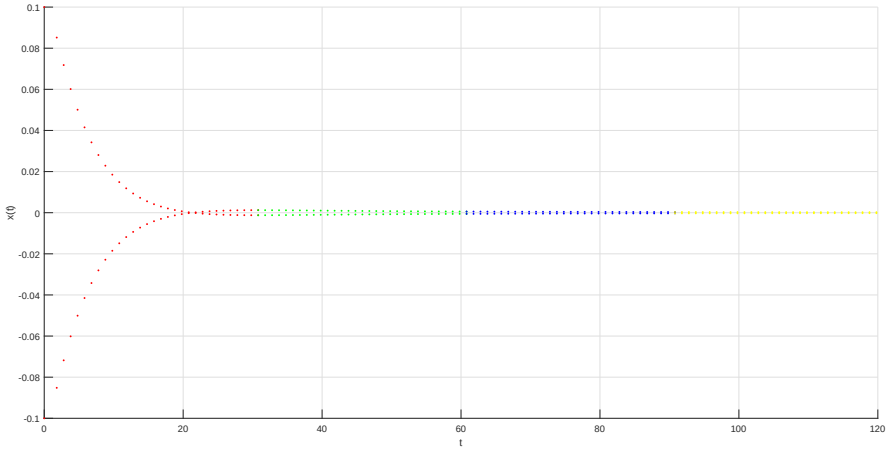

Figure 6.4: Neural network (6.7) **case 2**.

6.3 Uniform Stability for Discrete Variable-Order Neural Networks

In this section, we delve into the concept of uniform stability for discrete variable-order neural networks. Understanding uniform stability is crucial for assessing how these networks behave consistently across various scenarios. Through this exploration, we aim to provide insights into the robustness and reliability of such networks.

Lemme 6.3. *Let be* $t \in \mathbb{N}_{a+1}$ *the following hold*

$$\sum_{k=a+1}^{t} (t-\rho(k))^{\overline{\alpha(t)-1}} = \frac{(t-a)^{\alpha(t)}}{\alpha(t)}. \tag{6.8}$$

Proof. To start with, we have the following:

$$\sum_{k=a+1}^{t}(t-\rho(k))^{\overline{\alpha(t)-1}}=\sum_{k=a+1}^{t-1}(t-\rho(k))^{\overline{\alpha(t)-1}}+1^{\overline{\alpha(t)-1}}=\sum_{k=a+1}^{t-1}\frac{\Gamma(t-k+\alpha(t))}{\Gamma(t-k+1)}+\Gamma(\alpha(t)).$$

Since

$$\frac{\Gamma(k+1)}{\Gamma(k-\iota+1)}=\frac{1}{\iota+1}\left\{\frac{k+2}{k-\iota+1}-\frac{k+1}{k-\iota}\right\},$$

we set $k=t-k+\alpha(t)-1,\ \iota=\alpha(t)-1$, and we obtain

$$\frac{\Gamma(t-k+\alpha(t))}{\Gamma(t-k+1)}=\frac{1}{\alpha(t)}\left\{\frac{\Gamma(t-k+\alpha(t)+1)}{\Gamma(t-k+1)}-\frac{\Gamma(t-k+\alpha(t))}{\Gamma(t-k)}\right\}.$$

For all $k\in\{a+1,...,t-1\}$ we get

$$\begin{aligned}\sum_{k=a+1}^{t-1}\frac{\Gamma(t-k+\alpha(t))}{\Gamma(t-k+1)}=\frac{1}{k(t)}\{&\left(\frac{\Gamma(t-a+\alpha(t))}{\Gamma(t-a)}-\frac{\Gamma(t-a+\alpha(t)-1)}{\Gamma(t-a-1)}\right)\\&+\left(\frac{\Gamma(t-a+\alpha(t)-1)}{\Gamma(t-a-1)}-\frac{\Gamma(t-a+\alpha(t)-2)}{\Gamma(t-a-2)}\right)\\&+\left(\frac{\Gamma(t-a+\alpha(t)-2)}{\Gamma(t-a-2)}-\frac{\Gamma(t-a+\alpha(t)-3)}{\Gamma(t-a-3)}\right)\\&...\\&+\left(\frac{\Gamma(\alpha(t)+2)}{\Gamma(2)}-\frac{\Gamma(\alpha(t)+1)}{\Gamma(1)}\right)\},\end{aligned}$$

Hence, we obtain:

$$\begin{aligned}\sum_{k=a+1}^{t}(t-\rho(k))^{\overline{\alpha(t)-1}}&=\frac{1}{\alpha(t)}\left(\frac{\Gamma(t-a+\alpha(t))}{\Gamma(t-a)}-\Gamma(\alpha(t)+1)\right)+\Gamma(\alpha(t))\\&=\frac{1}{\alpha(t)}\frac{\Gamma(t-a+\alpha(t))}{\Gamma(t-a)},\\&=\frac{(t-a)^{\alpha(t)}}{\alpha(t)}.\end{aligned}$$

Thus, we conclude the proof. □

6.3.1 Existence and Uniqueness

The presented neural network operates in discrete time and incorporates variable-order fractional dynamics.

$$\begin{smallmatrix}ABC\\a\end{smallmatrix}\nabla_t^{\alpha(t)}x(t)=-Ax(t)+Dg(t,x(t))+I. \tag{6.9}$$

The system comprises several key components: $x(t)=(x_1(t),x_2(t),...,x_n(t))^T\in\mathbb{R}^n$ denotes the state vector of the system. $A=\mathrm{diag}(c_1,c_2,...,c_n)\in\mathbb{R}^{n\times n}$ stands for the self-feedback connection weight matrix, with $c_i>0$. $D=(d_{ij})_{n\times n}\in\mathbb{R}^{n\times n}$ represents the connection weight matrix. $g(x(t))=(g_1(x(t)),g_2(x(t)),...,g_n(x(t)))^T\in C(\mathbb{N}_{a+1},\mathbb{R}^n)$ is the activation function. $I=(I_1,...,I_n)^T$ symbolizes the vector of external inputs.

(A_1) for all $t \in \mathbb{N}_{a+1}$, $g_i(t,u)$ is a lipschitz continuous function with respect to u, ie

$$\exists l_i \in \mathbb{R}_+^* : \ |g_i(t,u) - g_i(t,v)| \leq l_i|u-v|; \ \forall u,v \in \mathbb{R}, \tag{6.10}$$

where $l = max_{i=1,\dots,n}\{l_i\}$.

(A_2) for all $t \in \mathbb{N}_{a+1}^T = \{a+1, a+2, ..., T\}$, there exists $Q \in \mathbb{R}_+^*$ and $Q < 1$ satisfying the condition:

$$Q = \frac{\Gamma(\gamma)(\gamma_1 + l\gamma_2)}{\Gamma(\gamma)(1-\beta)+\gamma} \left\{ (1-\gamma) + \frac{(T-a)^{\overline{\beta}}}{\Gamma(\beta)} \right\}, \tag{6.11}$$

where

$$\gamma_1 = \|A\|_\infty, \ \ \gamma_2 = \|D\|_\infty, \quad \gamma \leq \alpha(t) \leq \beta.$$

Theorem 6.3. *If conditions (A_1) and (A_2) are satisfied, the uniqueness of the solution to (6.9) is ensured.*

Proof. Per the properties of fractional discrete variable-order calculus, a solution to (6.9) can be expressed as:

$$x(t) = x_0 + \frac{1-\alpha(t)}{B(\alpha(t))}[-Ax(t) + Dg(t,x(t)) + I] + \frac{\alpha(t)}{B(\alpha(t))} {}_a\nabla_t^{-\alpha(t)}[-{}_C x(t) + Dg(t,x(t)) + I]. \tag{6.12}$$

By utilizing the following norm:

$$\|x\| = \sup_{t \in \mathbb{N}_{a+1}^T} \|x(t)\| \ \text{ and } \ \|x(t)\| = \max_{\{i=1,\dots,n\}} |x_i(t)|.$$

Problem (6.12) can be reformulated as a fixed-point problem. Let's define the following mapping:

$$\Phi x(t) = x_0 + \frac{1-\alpha(t)}{B(\alpha(t))}[-Ax(t) + Dg(t,x(t)) + I] \tag{6.13}$$

$$+ \frac{\alpha(t)}{B(\alpha(t))\Gamma(\alpha(t))} \sum_{k=a+1}^{t} (t-\rho(k))^{\overline{\alpha(t)-1}}[-Ax(k) + Dg(k,x(k)) + I], \tag{6.14}$$

where $\Phi x = (\Phi_1 x_1, \Phi_2 x_2, ..., \Phi_n x_n)$ and $\Phi_i x_i$ is described by:

$$\Phi_i x_i(t) = x_{i0} + \frac{1-\alpha(t)}{B(\alpha(t))}[-c_i x_i(t) + \sum_{j=1}^{n} d_{ij} g_j(t, x_j(t)) + I_i]$$

$$+ \frac{\alpha(t)}{B(\alpha(t))\Gamma(\alpha(t))} \sum_{k=a+1}^{t} (t-\rho(k))^{\overline{\alpha(t)-1}}[-c_i x_i(k) + \sum_{j=1}^{n} d_{ij} g_j(k, x_j(k)) + I_i].$$

For any two different functions $x, \mu \in \mathbb{R}^n$ we have

$$
\begin{aligned}
|\Phi_i x_i(t) - \Phi_i \mu_i(t)| &= |\frac{1-\alpha(t)}{B(\alpha(t))}[-c_i(x_i(t)-\mu_i(t)) + \sum_{j=1}^{n} d_{ij}(g_j(t,x_j(t)) - g_j(t,\mu_j(t)))] \\
&\quad + \frac{\alpha(t)}{B(\alpha(t))\Gamma(\alpha(t))} \sum_{k=a+1}^{t} (t-\rho(k))^{\overline{\alpha(t)-1}}[-c_i(x_i(k)-\mu_i(k)) \\
&\quad + \sum_{j=1}^{n} d_{ij}(g_j(k,x_j(k)) - g_j(k,\mu_j(k)))]|, \\
&\leq \frac{1-\alpha(t)}{B(\alpha(t))}[c_i|x_i(t)-\mu_i(t)| + \sum_{j=1}^{n} |d_{ij}|l_j|x_j(t)) - \mu_j(t)|] \\
&\quad + \frac{\alpha(t)}{B(\alpha(t))\Gamma(\alpha(t))} \sum_{k=a+1}^{t} (t-\rho(k))^{\overline{\alpha(t)-1}}[c_i|x_i(k)-\mu_i(k))| + \sum_{j=1}^{n} |d_{ij}|l_j|x_j(k)) - \mu_j(k)|], \\
&\leq \frac{1-\alpha(t)}{B(\alpha(t))\Gamma(\alpha(t))}[c_i|x_i(t)-\mu_i(t)| + \sum_{j=1}^{n} |d_{ij}|l_j|x_j(t)) - \mu_j(t)|] \\
&\quad + \frac{\alpha(t)}{B(\alpha(t))\Gamma(\alpha(t))} \sum_{k=a+1}^{t} (t-\rho(k))^{\overline{\alpha(t)-1}}[c_i|x_i(k)-\mu_i(k))| + \sum_{j=1}^{n} |d_{ij}|l_j v x_j(k)) - \mu_j(k)|].
\end{aligned}
$$

This leads us to:

$$
\begin{aligned}
\max_{\{i=1,\dots,n\}} |\Phi_i x_i(t) - \Phi_i \mu_i(t)| &\leq \frac{1-\alpha(t)}{B(\alpha(t))}[\gamma_1 \max_{\{i=1,\dots,n\}} |x_i(t)-\mu_i(t)| \\
&\quad + \gamma_2 l \max_{\{i=1,\dots,n\}} |x_i(t)) - \mu_i(t)|] \\
&\quad + \frac{\alpha(t)}{B(\alpha(t))\Gamma(\alpha(t))} \sum_{k=sa+1}^{t} (t-\rho(k))^{\overline{\alpha(t)-1}}[\gamma_1 \max_{\{i=1,\dots,n\}} |x_i(k)-\mu_i(k))| \\
&\quad + \gamma_2 l \max_{\{i=1,\dots,n\}} |x_j(k)) - \mu_j(k)|].
\end{aligned}
$$

Applying Lemma 6.3, we can conclude that

$$
\begin{aligned}
\|\Phi x - \Phi\mu\| &= \sup_{t\in\mathbb{N}_{a+1}^{T}} \left\{ \max_{\{i=1,\dots,n\}} |\Phi_i x_i(t) - \Phi_i \mu_i(t)| \right\}, \\
&\leq \left\{ \frac{(1-\gamma)\Gamma(\gamma)}{\Gamma(\gamma)(1-\beta)+\gamma} + \frac{\beta\Gamma(\gamma)}{\Gamma(\beta)(\Gamma(\gamma+1)(1-\beta)+\gamma)} \sup_{t\in\mathbb{N}_{a+1}^{T}} \sum_{k=a+1}^{t} (t-\rho(k))^{\overline{\alpha(t)-1}} \right\} \\
&\quad [\gamma_1 + l\gamma_2]\|x-\mu\|, \\
&\leq \{(1-\gamma) + \frac{1}{\Gamma(\beta)} \sup_{t\in\mathbb{N}_{a+1}^{T}} (t-a)^{\overline{\alpha(t)}} \frac{\Gamma(\gamma)[\gamma_1 + l\gamma_2]}{\Gamma(\gamma)(1-\beta)+\gamma} \|x-\mu\|, \\
&\leq \left\{ (1-\gamma) + \frac{(T-a)^{\overline{\beta}}}{\Gamma(\beta)} \right\} \frac{\Gamma(\gamma)[\gamma_1 + l\gamma_2]}{\Gamma(\gamma)(1-\beta)+\gamma} \|x-\mu\| = Q\|x-\mu\|.
\end{aligned}
$$

As per condition (A_2), we establish that $Q < 1$. Consequently, the mapping Φ acts as a contraction on $C(\mathbb{N}_{a+1}^{T}, \mathbb{R}^n)$. This implies that problem (6.13) possesses a unique fixed point by virtue of the Banach fixed point theorem, thus affirming the uniqueness of the solution to (6.9). This completes our demonstration. □

6.3.2 Stability Analysis

Definition 6.2. *[380] The discrete variable-order neural network system (6.9) with discrete Mittag-Leffler kernels, initialized at a, is considered uniformly stable if, for any $\epsilon > 0$, there exist two constants δ_ϵ and T, where $0 < \delta_\epsilon < \epsilon$ and $T > 0$. These constants are chosen such that for $s \in \mathbb{N}_{a+1}^{T} = a+1, a+2, ..., T$, and for any two solutions $x(t, a, \phi)$ and $\mu(t, a, \psi)$ with initial conditions $x_0 = \phi$ and $y_0 = \psi$, where $|\phi - \psi| < \delta_\epsilon$, it follows that $|x - \mu| < \epsilon$.*

Theorem 6.4. *Given the validity of (A_1) and (A_2), and if*

$$\frac{1}{1-Q} < \frac{\epsilon}{\delta}, \tag{6.15}$$

then, (6.9) exhibits uniform stability.

Proof. Consider two distinct solutions $x(t)$ and $\mu(t)$ of system (6.9), each with unique initial conditions x_0 and μ_0. Let $\phi = x_0$ and $\Phi = \mu_0$, which results in:

$$\begin{matrix}{}^{ABC}_{a}\nabla_{t}^{\alpha(t)}\end{matrix}(x(t) - \mu(t)) = \phi - \psi - A(x(t) - \mu(t)) + D(g(t, x(t) - g(t, \mu(t))). \tag{6.16}$$

This leads us to:

$$\begin{aligned} x(t) - \mu(t) = \phi - \psi &+ \frac{1-\alpha(t)}{B(\alpha(t))}[-A(x(t) - \mu(t)) + D(g(t, x(t) - g(t, \mu(t)))] \\ &+ \frac{\alpha(t)}{B(\alpha(t))\Gamma(\alpha(t))} \sum_{k=a+1}^{t} (-\rho(k)^{\overline{\alpha(t)-1}})[-A(x(k) - \mu(k)) \\ &+ D(g(k, x(k) - g(k, \mu(k)))]. \end{aligned}$$

Subsequently, applying (A_1) yields the following:

$$\begin{aligned} |x_i(t) - \mu_i(t)| = |\phi_i - \psi_i &+ \frac{1-\alpha(t)}{B(\alpha(t))}[-c_i(x_i(t) - \mu_i(t)) + \sum_{j=1}^{n} d_{ij}(g_j(t, x_j(t) - g_j(t, \mu_j(t)))] \\ &+ \frac{\alpha(t)}{B(\alpha(t))\Gamma(\alpha(t))} \sum_{k=a+1}^{t} (t - \rho(k)^{\overline{\alpha(t)-1}})[-c_i(x_i(k) - \mu_i(k)) \\ &+ \sum_{j=1}^{n} d_{ij}(g_j(k, x_j(k) - g_j(k, \mu_j(k)))]|, \\ &+ \frac{\alpha(t)}{B(\alpha(t))\Gamma(\alpha(t))} \sum_{k=a+1}^{t} (t - \rho(k))^{\overline{\alpha(t)-1}})| - c_i(x_i(k) - \mu_i(k)) \\ &+ \sum_{j=1}^{n} d_{ij}(g_j(k, x_j(k) - g_j(k, \mu_j(k)))]|, \\ &\leq |\phi_i - \psi_i| + \frac{1-\alpha(t)}{B(\alpha(t))}[c_i|x_i(t) - \mu_i(t)| + \sum_{j=1}^{n} l_j|d_{ij}||x_i(t) - \mu_i(t)|] \\ &+ \frac{\alpha(t)}{B(\alpha(t))\Gamma(\alpha(t))} \sum_{k=a+1}^{t} (t - \rho(k)^{\overline{\alpha(t)-1}})[c_i|(x_i(k) - \mu_i(k)| \\ &+ \sum_{j=1}^{n} l_j|d_{ij}||x_i(k) - \mu_i(k)|]. \end{aligned}$$

Hence, utilizing (A_2), we arrive at:

$$\begin{aligned}
\|x-\mu\| &\leq \|\phi-\psi\| + \sup_{t\in\mathbb{N}_{a+1}^{T}} \left\{\frac{1-\alpha(t)}{B(\alpha(t))}\right\}[\gamma_1+l\gamma_2]\|x-\mu\| \\
&+ \sup_{t\in\mathbb{N}_{a+1}^{T}} \left\{\frac{k(t)}{B(\alpha(t))\Gamma(\alpha(t))}\sum_{k=a+1}^{t}(t-\rho(k)^{\overline{\alpha(t)-1}})\right\}[\gamma_1+l\gamma_2]\|x-\mu\|, \\
&\leq \|\phi-\psi\| + \{\frac{(1-\gamma)\Gamma(\gamma)}{\Gamma(\gamma)(1-\beta+\gamma}[\gamma_1+l\gamma_2] \\
&+ \frac{\Gamma(\gamma)}{\Gamma(\beta)(\Gamma(\gamma+1)(1-\beta)+\gamma)}[\gamma_1+l\gamma_2]\sup_{t\in\mathbb{N}_{a+1}^{T}}(t-a)^{\Lambda(t)}\|x-\mu\|, \\
&= \|\phi-\psi\| + \frac{\Gamma(\gamma)(\gamma_1+l\gamma_2)}{\Gamma(\gamma)(1-\beta)+\gamma}\left\{(1-\gamma)+\frac{(T-a)^{\overline{\beta}}}{\Gamma(\beta)}\right\}\|x-\mu\|, \\
&< \frac{1}{1-\frac{\Gamma(\gamma)(\gamma_1+l\gamma_2)}{\Gamma(\gamma)(1-\beta)+\gamma}\left\{(1-\gamma)+\frac{(T-a)^{\overline{\beta}}}{\Gamma(\beta)}\right\}}\|\phi-\psi\|.
\end{aligned}$$

Thus, we establish that

$$\|x-\mu\| \leq \frac{1}{1-Q}\|\phi-\psi\|.$$

Consequently, for any $\epsilon > 0$, there exists $\delta_\epsilon = (1-Q)\epsilon$, such that if $|\phi-\psi| < \delta$, then $|x-\mu| < \epsilon$. In accordance with definition 6.2, (6.9) is uniformly stable, and the proof is complete. □

6.3.3 Numerical Simulations

Example 6.4. *Consider the two-dimensional neural network with discrete fractional variable order described by the following equations:*

$$\begin{cases}
{}_{a}^{ABC}\nabla_{t}^{\alpha(t)}x_1(t) = -c_1x_1(t) + d_{11}\sin(x_1(t)) + d_{12}\sin(x_2(d)) + I_1, \\
{}_{a}^{ABC}\nabla_{t}^{\alpha(t)}x_2(t) = -c_2x_2(t) + b_{21}\sin(x_1(t)) + d_{22}\sin(x_2(t)) + I_2.
\end{cases} \tag{6.17}$$

Consider the following parameters: $d_{11} = 0.2$, $d_{12} = -0.3$, $d_{21} = 0.4$, $d_{22} = -0.1$, $c_1 = 0.2$, $c_2 = 0.2$, $I_1 = 0.1, I_2 = 0.1$, $\alpha(t) = \dfrac{|\ln(\frac{3}{t+5})|}{3(t+1)}, t \in [0,50]$ *and the initial condition* $x_1(0) = -10, x_2(0) = -7$.

The numerical solution to (6.17) is provided as follows:

$$\begin{cases} x_1(i) = x_1(0) + \dfrac{1-\alpha(i)}{B(\alpha(i))}[-c_1x_1(i) + d_{11}\sin(x_1(i)) + d_{12}\sin(x_2(i)) + I_1] \\ \quad + \dfrac{\alpha(i)}{B(\alpha(i)))}\displaystyle\sum_{k=1}^{i}\frac{\Gamma(i-k+\Lambda(i))}{\Gamma(i-k+1)}\left(-c_1x_1(k) + d_{11}\sin(x_1(k)) + d_{12}\sin(x_2(k)) + I_1\right), \\ x_2(i) = x_2(0) + \dfrac{1-\alpha(i)}{B(\alpha(i))}[-c_2x_2(i) + d_{21}\sin(x_1(i)) + d_{22}\sin(x_2(i)) + I_2] \\ \quad + \dfrac{\alpha(i)}{B(\alpha(i)))}\displaystyle\sum_{k=1}^{i}\frac{\Gamma(i-k+\alpha(i))}{\Gamma(i-k+1)}\left(-c_2x_2(k) + d_{21}\sin(x_1(k)) + d_{22}\sin(x_2(k)) + I_2\right), \\ B(\alpha(i)) = 1-\alpha(i) + \dfrac{\alpha(i)}{\Gamma(\alpha(i))}, \qquad i \geq 1. \end{cases}$$

We can verify that these parameters satisfy assumptions (A_1) and (A_2), along with the condition in the theorem. The behavior of the solutions $x_1(t)$ and $x_2(t)$ is depicted in Figure 6.5. It's evident that each solution tends to zero as t approaches infinity, indicating the uniform stability of the solution.

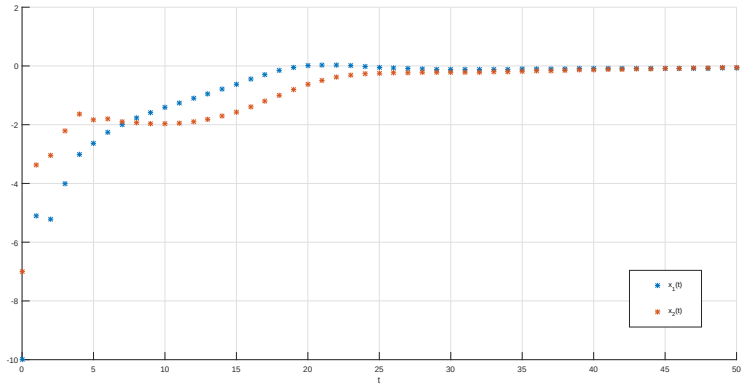

Figure 6.5: Numerical solution of neural networks (6.17).

Example 6.5. *Consider the discrete fractional variable-order neural network presented below:*

$$\begin{cases} {}_{a}^{ABC}\nabla_t^{\alpha(t)}x_1(t) = -c_1x_1(t) + d_{11}\tanh(x_1(t)) + d_{12}\tanh(x_2(t)) + d_{13}\tanh(x_3(t)) + I_1, \\ {}_{a}^{ABC}\nabla_t^{\alpha(t)}x_2(t) = -c_2x_2(t) + d_{21}\tanh(x_1(t)) + d_{22}\tanh(x_2(t)) + d_{23}\tanh(x_3(t)) + I_2, \\ {}_{a}^{ABC}\nabla_t^{\alpha(t)}x_3(t) = -c_3x_3(t) + d_{31}\tanh(x_1(t)) + d_{32}\tanh(x_2(t)) + d_{33}\tanh(x_3(t)) + I_3, \end{cases} \tag{6.18}$$

where

$$A = \begin{bmatrix} 0.1 & 0 & 0 \\ 0 & 0.1 & 0 \\ 0 & 0 & 0.1 \end{bmatrix}, \quad D = \begin{bmatrix} -0.4 & -0.1 & -0.2 \\ 0.1 & -0.4 & 0.1 \\ 0.4 & 0.1 & 0.2 \end{bmatrix}, \quad I = \begin{bmatrix} 0 \\ 0 \\ 0 \end{bmatrix}.$$

Given that assumptions (A_1) and (A_2) hold true, we can employ formulas (6.19) to obtain the numerical solution depicted in Figure 6.6, considering the initial condition

$x(0) = (0.1, 0.1, 0.1)^T$. *This illustration confirms the uniform stability of the analyzed neural network.*

$$\begin{cases} x(i) = x(0) + \dfrac{1-\alpha(i)}{B(\alpha(i))}[-Ax(i) + D\tanh(x(i))] \\ \qquad + \dfrac{\alpha(i)}{B(\alpha(i)))} \displaystyle\sum_{k=1}^{i} \dfrac{\Gamma(i-k+\alpha(i))}{\Gamma(i-k+1)} \left(-Ax(k) + D\tanh(x(k))\right), \\ B(\alpha(i)) = 1 - \alpha(i) + \dfrac{\alpha(i)}{\Gamma(\alpha(i))}, \qquad i \geq 1. \end{cases} \tag{6.19}$$

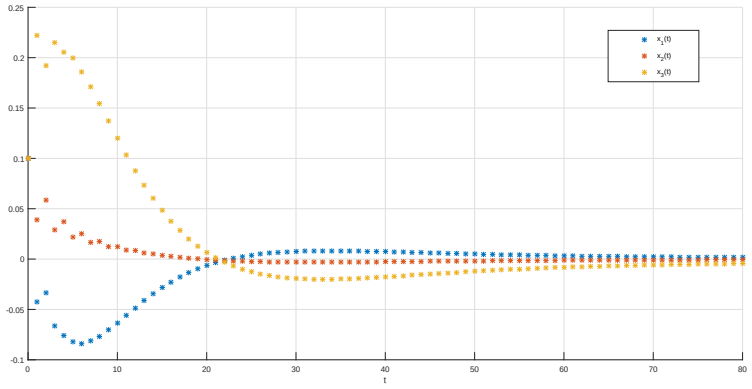

Figure 6.6: Numerical solution of discrete time variable-order neural networks (6.18).

6.4 Conclusion

In summary, the exploration of stability in discrete systems with non-integer orders, particularly Ulam–Hyers stability and uniform stability, represents a significant frontier within the topic of fractional calculus. While these areas have received less attention compared to their continuous counterparts, recent efforts have highlighted their significance, especially in the context of discrete-time fractional variable-order neural networks.

Ulam–Hyers stability offers insights into the reliability and predictability of discrete systems, particularly neural networks with variable orders. The ongoing pursuit of suitable criteria for studying uniform stability reflects the crucial need for dependable models in engineering and scientific applications.

This chapter contributes to this evolving field by presenting novel criteria for Ulam–Hyers stability and uniform stability in discrete-time neural networks with variable orders. Our proposed model, grounded in the Caputo h-difference operator, provides valuable insights into the dynamics and stability of such networks, advancing our understanding of their behavior.

Moving forward, more investigation is needed to explore stability in discrete systems with non-integer order more thoroughly. By continuing to explore Ulam–Hyers stability

and uniform stability, we can enhance the robustness and reliability of discrete-time fractional variable-order neural networks, paving the way for their broader applications in engineering and beyond.

Chapter 7

Synchronization in Discrete Fractional-Order Neural Networks

7.1 Introduction

Synchronization, a critical phenomenon in chaotic systems, has garnered significant attention within discrete fractional neural networks. Various synchronization paradigms, such as complete synchronization, projective synchronization, and lag synchronization, have deepened our understanding of complex system dynamics and opened avenues for innovative applications across diverse domains[381, 382, 383].

Complete synchronization stands as a fundamental concept, ensuring the convergence of all state variables in coupled systems to identical trajectories. This phenomenon has been extensively studied and applied in various contexts, ranging from secure communication systems to biomedical applications. Projective synchronization, on the other hand, allows for the coordination of specific state variables while preserving the independence of others. This flexibility has enabled tailored synchronization schemes to suit specific system requirements in engineering and control applications.

Recent research efforts have expanded beyond commensurate systems to explore synchronization in non-commensurate discrete fractional neural networks [384, 385, 386, 387]. These endeavors have underscored the importance of finite-time synchronization, offering improved robustness and interference suppression capabilities in practical engineering applications. Finite-time synchronization ensures that chaotic neural networks achieve synchronization within a defined time frame, enhancing the predictability and stability of interconnected systems [388, 389].

Motivated by these advancements, this chapter presents novel discrete incommensurate network models based on the Nabla Caputo difference operator. These models offer effective strategies to synchronize their dynamic behaviors, paving the way for innovative applications across diverse domains.

Structured as follows, The subsequent sections of this chapter unveil criteria and methodologies for achieving synchronization in discrete fractional neural networks, followed by numerical simulations to validate the proposed approaches. Finally, concluding remarks offer insights and reflections on the implications of the findings presented in this comprehensive investigation.

7.2 Synchronization in Commensurate Discrete Fractional-order neural networks

In the forthcoming analysis, we delve deeply into the synchronization phenomena of distinct discrete fractional-order neural networks. These networks are distinguished by :

$$ {}^{C}\nabla_{a}^{\alpha} x(t) = -Ax(t) + Dg(t, x(t)) + I; \tag{7.1} $$

In the equation provided, $t \geq 0$ represents the temporal parameter. The state vector at time t is denoted by $x(t) = (x_1(t), \ldots, x_n(t))^T \in \mathbb{R}^n$, where each $x_i(t)$ corresponds to the state of the i-th neuron at time t. The activation function of the neurons is represented by $g(x(t)) = (g_1(x_1(t)), \ldots, g_n(x_n(t)))^T$, capturing the non-linear response of each neuron to its input.

The matrix $A = \text{diag}(c_1, \ldots, c_n)$ illustrates the constant rate at which each i-th unit returns to its resting state when isolated from the network and external inputs, signifying the decay or damping factor specific to each neuron. The connection weights between the j-th and i-th neurons at time t are denoted by $D = (d_{ij}) \in \mathbb{R}^{n \times n}$, where d_{ij} specifies the influence of the j-th neuron on the i-th neuron.

Additionally, $\mathbf{I} = (I_1, I_2, \ldots, I_n)^T$ serves as an external bias vector, providing a constant input to each neuron that can model external stimuli or baseline activity levels.

Before advancing, we posit the following hypothesis:

(H_1): The activation functions g_j display Lipschitz continuity, ensuring the presence of positive constants κ_j, indexed by $j = 1, 2, \ldots, n$. These constants are defined as follows:

$$ |g_j(x) - g_j(y)| < {}_j|x - y|, \quad \forall x, y \in \mathbb{R} $$

.

The system represented by equation (7.1) functions as the driving system, which provides the primary dynamics and influences the behavior of the secondary system. In contrast, the secondary system, known as the slave system, is defined as follows:

$$ {}^{C}\nabla_{a}^{\alpha} y(t) = -Ay(t) + Dg(t, y(t)) + I + u(t). \tag{7.2} $$

In this context, $y(t) \in \mathbb{R}^n$ represents the state vector of the slave system, encapsulating the system's state variables at time t. Meanwhile, $u(t)$ denotes the controller, a control input that is yet to be determined and is designed to influence the behavior of the slave system to achieve a desired objective.

The synchronization error, which quantifies the discrepancy between the states of the master and slave systems, is defined as follows:

$$ e(t) = y(t) - x(t). \tag{7.3} $$

The error dynamics, derived from Equations (7.1) to (7.2), can be expressed as follows:

$$ {}^{C}\nabla_{a}^{\alpha} e(t) = -Ae(t) + B(g(t, y(t)) - f(t, x(t))) + u(t). \tag{7.4} $$

7.2.1 Synchronization Scheme

Our overarching goal is to devise a feedback control strategy that can effectively regulate the behavior of the system towards desired outcomes. This involves designing control mechanisms that leverage information about the system's states and dynamics to continuously adjust and optimize control inputs. By carefully crafting such a control approach, we aim to steer the system towards desired states, achieve precise performance objectives, and enhance robustness against disturbances or uncertainties.

$$u(t) = Ke(t), \tag{7.5}$$

here, $K = \text{diag}(k_1, k_2, \ldots, k_n)$ is a diagonal matrix, this matrix serves a pivotal role in shaping the subsequent error system, enabling it to take the following form:

$${}^{C}\nabla_a^{\alpha} e(t) = -(A - K)e(t) + D(g(t, y(t)) - g(t, x(t))). \tag{7.6}$$

Alternatively,

$${}^{C}\nabla_a^{\alpha} e_i(t) = -(c_i - k_i)e_i(t) + \sum_{j=1}^{n} d_{ij}(g_j(t, y_j(t)) - g_j(t, x_j(t))), \quad i = 1, 2, \ldots, n. \tag{7.7}$$

Asymptotic stability suggests that the trajectory of the slave system, governed by equation (7.2) and initiated at $y(\alpha)$, has the capability to steadily approach and eventually converge towards the behavior of the drive system delineated by equation (7.1), which commences at $x(\alpha)$.

$$\lim_{t\to\infty} \|e(t)\| = \lim_{t\to\infty} \|y(t) - x(t)\| = 0. \tag{7.8}$$

Theorem 7.1. *If condition (H_1) is satisfied, synchronization between the master-slave systems described by equations (7.1) and (7.2) is attained under the following condition:*

$$-1 < v + w < 0. \tag{7.9}$$

where

$$v = \max_{i=1,\ldots,n} -(c_i - k_i) \quad \text{and} \quad w = \max_{i=1,\ldots,n} \sum_{j=1}^{n} |d_{ij}|_j.$$

Proof. To establish this outcome, it's imperative to acknowledge that the system described by equation (7.7) can be equivalently represented as:

$$\begin{cases} {}_a^{C}\nabla^{\alpha} e_1(t) = -(c_1 - k_1)e_1(t) + \sum_{j=1}^{n} d_{1j}(g_j(t, y_j(t)) - g_j(t, x_j(t))), \\ {}_a^{C}\nabla^{\alpha} e_2(t) = -(c_2 - k_2)e_2(t) + \sum_{j=1}^{n} d_{2j}(g_j(t, y_j(t)) - g_j(t, x_j(t))), \\ \vdots \\ {}_a^{C}\nabla^{\alpha} e_n(t) = -(c_n - k_n)e_n(t) + \sum_{j=1}^{n} d_{nj}(g_j(t, y_j(t)) - g_j(t, x_j(t))). \end{cases} \tag{7.10}$$

By utilizing Lemma 4.1, the system can be transformed into:

$$\begin{cases} e_1(t) &= E_\alpha(-(c_1-k_1),t-a)e_{01} \\ &\quad + \sum_{k=a+1}^{t} E_{\alpha,\alpha}(-(c_1-k_1),t-\rho(k))\sum_{j=1}^{n} d_{1j}(g_j(k,y_j(k))-g_j(k,x_j(k))), \\ e_2(t) &= E_\alpha(-(c_2-k_2),t-a)e_{02} \\ &\quad + \sum_{k=a+1}^{t} E_{\alpha,\alpha}(-(c_2-k_2),t-\rho(k))\sum_{j=1}^{n} d_{2j}(g_j(k,y_j(k))-g_j(k,x_j(k))), \\ &\vdots \\ e_n(t) &= E_\alpha(-(c_n-k_n),t-a)e_{0n} \\ &\quad + \sum_{k=a+1}^{t} E_{\alpha,\alpha}(-(c_n-k_n),t-\rho(k))\sum_{j=1}^{n} d_{nj}(g_j(k,y_j(k))-g_j(k,x_j(k))). \end{cases} \tag{7.11}$$

This transformation leads us to

$$\begin{cases} e_1(t) &\le E_\alpha(-(c_1-k_1),t-a)e_{01} + \sum_{k=a+1}^{t} E_{\alpha,\alpha}(-(c_1-k_1),t-\rho(k))\sum_{j=1}^{n} |d_{1j}|_j|e_j(t)|, \\ e_2(t) &\le E_\alpha(-(c_2-k_2),t-a)e_{02} + \sum_{k=a+1}^{t} E_{\alpha,\alpha}(-(c_2-k_2),t-\rho(k))\sum_{j=1}^{n} |d_{2j}|_j|e_j(t)|, \\ &\vdots \\ e_n(t) &\le E_\alpha(-(c_n-k_n),t-a)e_{0n} + \sum_{k=a+1}^{t} E_{\alpha,\alpha}(-(c_n-k_n),t-\rho(k))\sum_{j=1}^{n} |d_{nj}|_j|e_j(t)|. \end{cases} \tag{7.12}$$

By applying Lemma 4.2 and taking the norm of both sides of the aforementioned inequality, we derive:

$$\|e(t)\| \le E_\alpha(w,t-a)\|e_0\| + v\sum_{k=a+1}^{t} E_{\alpha,\alpha}(w,t-\rho(k))\|e(t)\|, \tag{7.13}$$

$$\|e(t)\| \le \|e_0\|E_\alpha(w+v,t-a).$$

Given that $-1 < w+v < 0$ holds true, as per Theorem 4.1, $|e(t)| \to 0$ as $t \to +\infty$. This indicates that the master-slave systems achieve synchronization.

□

7.2.2 Applications

In this section, we leverage numerical simulations conducted in Matlab to comprehensively validate the theoretical findings elucidated in the preceding theorem. These simulations are instrumental in offering robust validation of the synchronization patterns anticipated by our theoretical framework. Through meticulous numerical experiments, our objective is to furnish deeper insights and comprehension into the synchronization dynamics expounded by our theoretical analysis.

Example 7.1. *The master system comprises a discrete fractional neural network consisting of two neurons:*

$$ {}^{C}\nabla_{a}^{\alpha} x(t) = -Ax(t) + D\sin(x(t)) + I. \tag{7.14} $$

The slave system is specified as:

$$ {}^{C}\nabla_{a}^{\alpha} y(t) = -Ay(t) + D\sin(y(t)) + K(t) + I, . \tag{7.15} $$

Furthermore, let's

$$ A = \begin{pmatrix} 0.45 & 0 \\ 0 & 0.5 \end{pmatrix}, \quad D = \begin{pmatrix} 0.1 & -0.2 \\ 0.3 & 0.05 \end{pmatrix}, e(0) = \begin{pmatrix} 1 \\ 0.3 \end{pmatrix}, \quad I = \begin{pmatrix} 0 \\ 0 \end{pmatrix} \quad \alpha = \frac{1}{3} $$

Having verified the fulfillment of assumptions (H_1) *and the condition in Theorem 7.1, the synchronization of the master-slave systems (7.14)-(7.15) is established, with the designated control matrix:*

$$ K = \begin{pmatrix} 0.04 & 0 \\ 0 & 0.01. \end{pmatrix} \tag{7.16} $$

To reinforce the aforementioned theoretical insights, we provide numerical demonstrations. Figure 7.1 illustrates the dynamic behavior of the master-slave systems, while Figure 7.2 exhibits the asymptotic behavior of the error system, converging to zero as $t \to \infty$. *These visualizations corroborate the synchronization of the analyzed systems.*

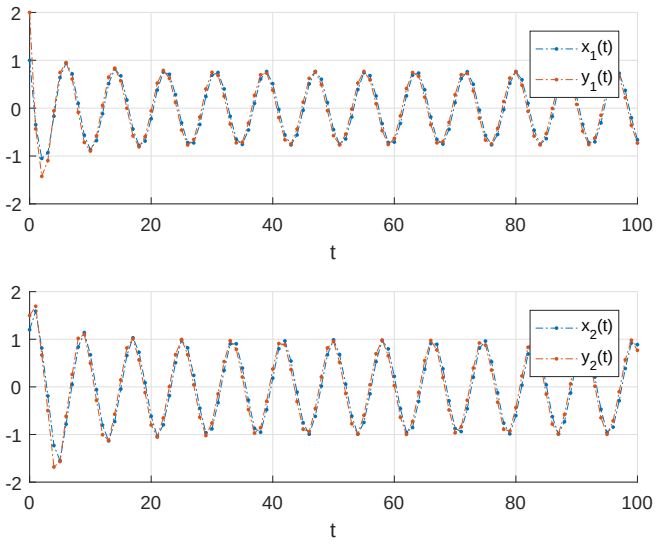

Figure 7.1: Trajectory of states in the master-slave system (7.14)-(7.15).

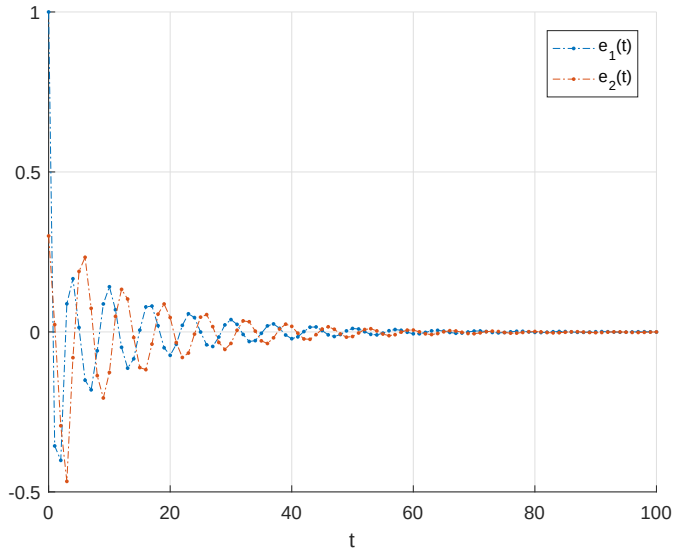

Figure 7.2: Temporal evolution of the error system.

7.3 Synchronization of Incommensurate Discrete Fractional Neural Networks with Variable Orders

In the forthcoming analysis, we delve into a thorough examination of the synchronization dynamics exhibited by incommensurate discrete fractional-order neural networks. These networks are distinguished by their fractional-order dynamics, which introduce non-integer degrees of differentiation into the system equations, adding complexity and richness to their behavior. By scrutinizing the synchronization behavior of such networks, we aim to unravel the interplay of their fractional-order dynamics and their impact on achieving coordinated behavior across disparate systems.

$$ {}^{C}\nabla_{a}^{\overline{\alpha}} x(t) = -Ax(t) + Dg(t, x(t)). \tag{7.17}$$

Before proceeding further, we introduce the following hypothesis:

(H_1): The activation functions g_j within the neural network demonstrate Lipschitz continuity, guaranteeing the existence of positive constants $_j$, with j ranging from 1 to n. These constants are characterized by:

$$|g_j(x) - g_j(y)| < {}_j|x - y|, \quad \forall x, y \in \mathbb{R}$$

.

The system represented by equation (7.17) acts as the driving force, whereas the slave system is defined as:

$$ {}^{C}\nabla_{a}^{\overline{\alpha}} y(t) = -Ay(t) + Dg(t, y(t)), + u(t). \tag{7.18}$$

In this context, $y(t) \in \mathbb{R}^n$ signifies the state vector of the slave system, while $u(t)$ denotes the yet-to-be-determined controller.

The difference in states between the master and slave systems defines the synchronization error, expressed as:

$$e(t) = y(t) - x(t). \tag{7.19}$$

The error dynamics, derived from Equations (7.17) to (7.18), can be formulated as follows:

$${}^{C}\nabla_{a}^{\overline{\alpha}} e(t) = -Ae(t) + D(g(t, y(t)) - g(t, x(t))) + u(t). \tag{7.20}$$

Our goal is to develop a suitable feedback control approach.

$$u(t) = Ke(t). \tag{7.21}$$

In this scenario, $K = \text{diag}(k_1, k_2, \ldots, k_n)$ represents a diagonal matrix, where $\kappa_1, \kappa_2, \ldots, k_n$, are individual coefficients. This matrix shapes the subsequent error system, resulting in the following form:

$${}^{C}\nabla_{a}^{\overline{\alpha}} e(t) = -(A - K)e(t) + D(g(t, y(t)) - g(t, x(t))). \tag{7.22}$$

Alternatively, we can express this as:

$${}^{C}\nabla_{a}^{\alpha_i} e_i(t) = -(c_i - k_i)e_i(t) + \sum_{j=1}^{n} d_{ij}(g_j(t, y_j(t)) - g_j(t, x_j(t))), \quad i = 1, 2, \ldots, n. \tag{7.23}$$

Asymptotic stability indicates that the path followed by the slave system, as governed by equation (7.18) and initiated at $y(a)$, possesses the ability to gradually converge towards the trajectory of the drive system described by equation (7.17), which commences at $x(a)$.

$$\lim_{t\to\infty} \|e(t)\| = \lim_{t\to\infty} \|y(t) - x(t)\| = 0. \tag{7.24}$$

7.3.1 Synchronization Control

Theorem 7.2. *If assumption (H_1) holds true, and the following condition is satisfied:*

$$k_i > c_i - \sum_{j=1}^{n} \frac{|d_{ij}|_j + |d_{ji}|_i}{2}, \tag{7.25}$$

then, the master-slave systems described by equations (7.17) to (7.18) achieve synchronization.

Proof. Select the auxiliary function:

$$V(t) = \sum_{i=1}^{n} V_i(t) = \frac{1}{2} \sum_{i=1}^{n} e_i^2(t). \tag{7.26}$$

Utilizing Lemma 2.1 and computing the difference of order α_i on V_i, we obtain

$$\begin{aligned}
{}^{C}\nabla_a^{\alpha_i} V_i(t) &\leq e_i(t)\, {}^{C}\nabla_a^{\alpha_i} e_i(t), \\
&= e_i(t)\left(-(c_i - k_i)e_i(t) + \sum_{j=1}^{n} d_{ij}(g_j(t, y_j(t)) - g_j(t, x_j(t)))\right) \\
&\leq -(c_i - k_1)e_i^2(t) + \sum_{j=1}^{n} |d_{ij}|_j e_i(t)e_j(t), \\
&\leq -(c_i - k_i)e_i^2(t) + \sum_{j=1}^{n} |d_{ij}|_j \frac{e_i^2(t) + e_j^2(t)}{2}, \\
&\leq -(c_i - k_i)e_i^2(t) + e_i^2(t)\sum_{j=1}^{n} \frac{|d_{ij}|_j + |d_{ji}|_i}{2}, \\
&\leq -\left(c_i - k_i - \sum_{j=1}^{n} \frac{|d_{ij}|_j + |d_{ji}|_1}{2}\right) e_i^2(t), \\
&= -\left(c_i - k_i - \sum_{j=1}^{n} \frac{|d_{ij}|_j + |d_{ji}|_i}{2}\right) V_i(t),
\end{aligned} \tag{7.27}$$

Using equation (7.27), we can formulate the corresponding comparative system as:

$$\begin{bmatrix} {}^{C}\nabla_a^{\alpha_1} W_1(t) \\ {}^{C}\nabla_a^{\alpha_2} W_2(t) \\ \vdots \\ {}^{C}\nabla_a^{\alpha_n} W_n(t) \end{bmatrix} = \begin{bmatrix} \epsilon_{11} & 0 & \cdots & 0 \\ 0 & \epsilon_{22} & \cdots & 0 \\ \vdots & \vdots & \ddots & \vdots \\ 0 & 0 & \cdots & \epsilon_{nn} \end{bmatrix} \begin{bmatrix} W_1(t) \\ W_2(t) \\ \vdots \\ W_n(t) \end{bmatrix}, \tag{7.28}$$

where

$$\epsilon_{ii} = -\left(c_i - k_i - \sum_{j=1}^{n} \frac{|d_{ij}|_j + |d_{ji}|_i}{2}\right), \tag{7.29}$$

System denoted by (7.28) can be rephrased as:

$${}^{C}\nabla_a^{\overline{\alpha}} W(t) = DW(t). \tag{7.30}$$

Let $W(t) = (W_1(t), W_2(t), \ldots, W_n(t))^T$ and $D = \text{diag}(e_{ii})_{n\times n}$. According to Lemma 1.15, the controlled system (7.30) is asymptotically stable under certain conditions, specifically when $W(t) \to 0$ as $k_i > c_i - \sum_{j=1}^{n} \frac{|d_{ij}|_j + |d_{ji}|_i}{2}$. Utilizing the comparison principle from Lemma 1.12, we infer that $V(t) \leq W(t)$ and $V(t) \to 0$. Since $V(t) = \sum_{i=1}^{n} V_i(t) = \sum_{i=1}^{n} e_i^2(t)$, it follows that $e_i(t) \to 0$. Consequently, the synchronization error system (7.20) is also stable, thus completing the proof. □

7.3.2 Numerical Examples

In this section, we utilize numerical simulations executed in Matlab to thoroughly validate the theoretical results outlined in the previous theorem. These simulations serve to provide an extensive validation of the synchronization behavior predicted by our theoretical

framework. By conducting detailed numerical experiments, we aim to offer deeper insights and understanding into the synchronization dynamics elucidated by our theoretical analysis.

Example 7.2. *The master system consists of an incommensurate discrete fractional neural network comprising two neurons:*

$$\begin{cases} {}^{C}\nabla_{a}^{\alpha_1} x_1(t) &= -0.25x_1(t) + 0.1\sin(x_1(t)) - 0.2\sin(x_2(t)), \\ {}^{C}\nabla_{a}^{\alpha_2} x_2(t) &= -0.3x_2(t) + 0.3\sin(x_1(t)) + 0.4\sin(x_2(t)). \end{cases} \tag{7.31}$$

The slave system is defined as:

$$\begin{cases} {}^{C}\nabla_{a}^{\alpha_1} y_1(t) &= -1y_1(t) + 0.1\sin(y_1(t)) - 0.2\sin(y_2(t)) + k_1(t), \\ {}^{C}\nabla_{a}^{\alpha_2} y_2(t) &= -1.5y_2(t) + 0.3\sin(y_1(t)) + 0.4\sin(y_2(t)) + k_2(t). \end{cases} \tag{7.32}$$

The synchronization state-feedback gain is calculated as follows:

$$K = \begin{bmatrix} 0.2 & 0 \\ 0 & 0.1 \end{bmatrix}. \tag{7.33}$$

This leads to the formation of the matrix A, characterized as:

$$A = \begin{bmatrix} 0.1 & 0 \\ 0 & 0.2 \end{bmatrix}. \tag{7.34}$$

Certainly, the matrix A satisfies the conditions outlined in both Theorem 1 and Theorem 2, indicating the asymptotic stability of the error system. This suggests the achievement of synchronization between the driving and responding systems. In our computational experiments, we initiate the driving and responding systems with $x(0) = (3, 1, 2)^T$ and $y(0) = (4, 2, 3)^T$, respectively. Figure 7.3 visually illustrates the evolution of state synchronization between these systems, while Figure 7.4 displays the synchronization error.

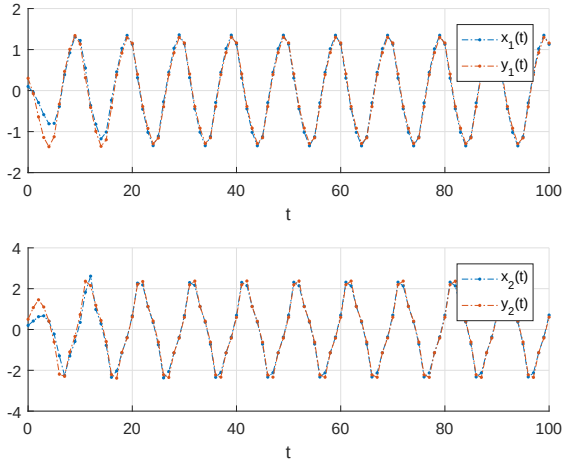

Figure 7.3: State trajectory of master-slave system (7.31)-(7.32).

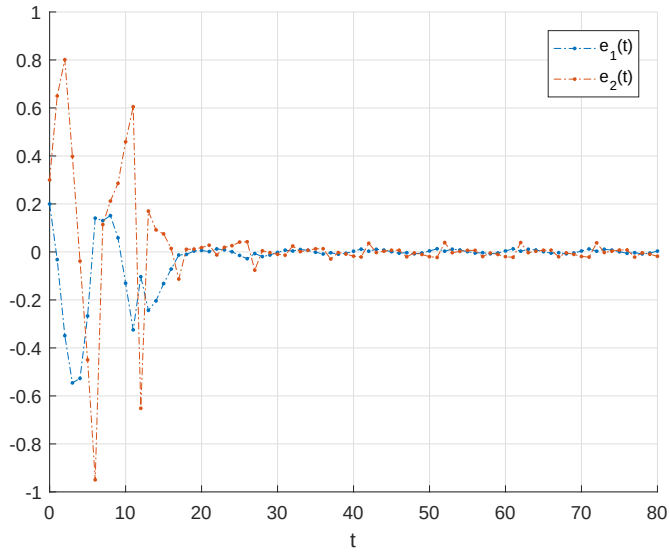

Figure 7.4: Time evolution of the error system.

7.4 Synchronization in Commensurate Nabla Discrete Variable-Order Neural Networks

Let's explore the complex dynamics of synchronization within a discrete-variable order neural network, characterized by Equation (7.35). Our focus will be on scrutinizing the dynamics of this network, treating it as the primary system for our examination.

$$ {}^{C}\nabla_{a}^{\alpha(t)} x(t) = -Ax(t) + Dg(t, x(t)) + I. \tag{7.35} $$

Conversely, we label the controlled discrete incommensurate variable-order neural network, delineated by Equation (7.36), as the slave system. Within this framework, n synchronization controllers, denoted as $L_1, L_2, \ldots, L_n$, are assigned the responsibility of regulating distinct aspects of the system's behavior.

$$ {}^{C}\nabla_{a}^{\alpha(t)} y(t) = -Ay(t) + Dg(t, y(t)) + L(t). \tag{7.36} $$

In pursuit of achieving full synchronization, we define the synchronization error as follows:

$$ e_i(t) = x_i(t) - y_i(t), \quad i = 1, ..., n. \tag{7.37} $$

The synchronization scheme is considered successful when the following condition is satisfied:

$$ \lim_{t \to +\infty} |e_i(t)| = 0, \text{ for } i = 1, ..., n. \tag{7.38} $$

To highlight the significant results of the proposed synchronization strategy, the following theorem is introduced to ensure synchronization between the master and slave neural networks.

7.4.1 Synchronization in Nabla Discrete Variable-Order Model

Theorem 7.3. *The master-slave systems described by equations (7.35) and (7.36) achieve synchronization when the controlled variables $L_i, i = 1, ..., n$ are selected as follows:*

$$L_i(t) = -\left(\sum_{j=1}^{n} \frac{|d_{ij}|_j + |d_{ji}|_i}{2}\right) e_i(t), \quad i = 1, ..., n. \tag{7.39}$$

Proof. □

To expedite the convergence of the synchronization errors detailed in equation (7.37), we commence by employing the nabla Caputo-type variable-order differences to equation (7.37), resulting in:

$${}^{C}\nabla_a^{\alpha(t)} e_i(t) = -c_i e_i(t) + \sum_{j=1}^{n} d_{ij}(g_j(t, y_j(t)) - g_j(t, x_j(t))) + L_i(t). \tag{7.40}$$

Incorporating the proposed control law (7.39) for $L_i, i = 1, ..., n$, into system (7.40) yields the following modified fractional discrete system:

$${}^{C}\nabla_a^{\alpha(t)} e_i(t) = -c_i e_i(t) + \sum_{j=1}^{n} d_{ij}(g_j(t, y_j(t)) - g_j(t, x_j(t))) - \left(\sum_{j=1}^{n} \frac{|d_{ij}|_j + |d_{ji}|_i}{2}\right) e_i(t). \tag{7.41}$$

Now, let's scrutinize the Lyapunov function, which encapsulates the overall error state.

$$V(t) = \frac{1}{2}\sum_{i=1}^{n} e_i^2(t). \tag{7.42}$$

Moreover, utilizing Lemma 4.10, we can derive the following inequality:

$$\begin{aligned}
{}^{C}\nabla_a^{\beta} V(t) &\leq \sum_{i=1}^{n} e_i(t)\, {}^{C}\nabla_a^{\alpha(t)} e_i(t), \\
&= \sum_{i=1}^{n} e_i(t) \left(-c_i e_i(t) + \sum_{j=1}^{n} d_{ij}(g_j(t, y_j(t)) - g_j(t, x_j(t))) - \left(\sum_{j=1}^{n} \frac{|d_{ij}|_j + |d_{ji}|_i}{2}\right) e_i(t)\right), \\
&\leq \sum_{i=1}^{n} -c_i e_i^2(t) + \sum_{j=1}^{n} |d_{ij}| e_i(t) e_j(t) - \left(\sum_{j=1}^{n} \frac{|d_{ij}|_j + |d_{ji}|_i}{2}\right) e_i^2(t), \\
&\leq \sum_{i=1}^{n} -c_i e_i^2(t) + \sum_{j=1}^{n} |d_{ij}| \frac{e_i^2(t) + e_j^2(t)}{2} - \left(\sum_{j=1}^{n} \frac{|d_{ij}|_j + |d_{ji}|_i}{2}\right) e_i^2(t), \\
&\leq -\sum_{i=1}^{n} c_i e_i^2(t) \leq -\gamma \sum_{i=1}^{n} e_i^2(t) = -\gamma \|e(t)\| < 0.
\end{aligned} \tag{7.43}$$

Furthermore, as per Theorem 4.10, the investigation of the error system (7.37) dynamics in discrete variable-order networks confirms that they eventually converge to zero, signifying stability. This convergence illustrates the effective synchronization between systems (7.35) - (7.36) of the discrete variable-order neural network. The synchronization is achieved through the application of linear control laws (7.39), which ensure the

alignment of network trajectories. Consequently, the established stability and synchronization validate the efficiency of the proposed control strategy. Therefore, with the error dynamics converging and synchronization being achieved, the proof confirms the robustness and dependability of the proposed approach.

7.4.2 Applications

In this section, we employ numerical simulations conducted in Matlab to rigorously verify the theoretical results presented in the preceding theorem. These simulations provide comprehensive validation of the synchronization behavior predicted by our theoretical framework. Through detailed numerical experiments, we aim to gain deeper insights and a better understanding of the synchronization dynamics as predicted by our theoretical analysis.

Example 7.3. *Consider the three-dimensional discrete variable-order neural network defined by equations* (7.44) *and* (7.45) *as the master-slave systems for our study.*

$$ {}^{C}\nabla_{a}^{\alpha(t)} x(t) = -Ax(t) + D\tanh(x(t)) + I, \tag{7.44} $$

while,

$$ {}^{C}\nabla_{a}^{\alpha(t)} y(t) = -Ay(t) + \tanh(y(t)) + L(t) + I. \tag{7.45} $$

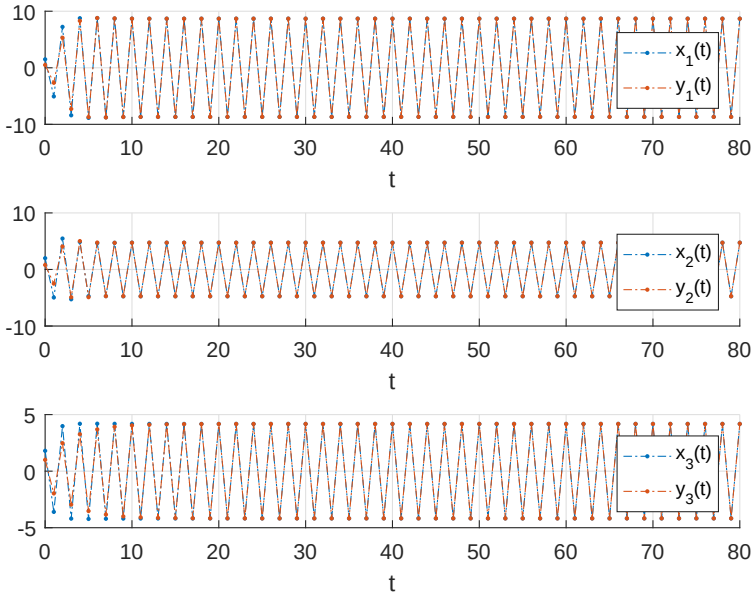

Figure 7.5: Trajectory of states in the master-slave system (7.44)-(7.45).

The initial conditions, represented by $e_1(0)$, $e_2(0)$, *and* $e_3(0)$, *serve as the starting points. To model the states of the variable-order error system and the synchronized systems described by equations* (7.44) *and* (7.45), *we apply the predictor-corrector method.*

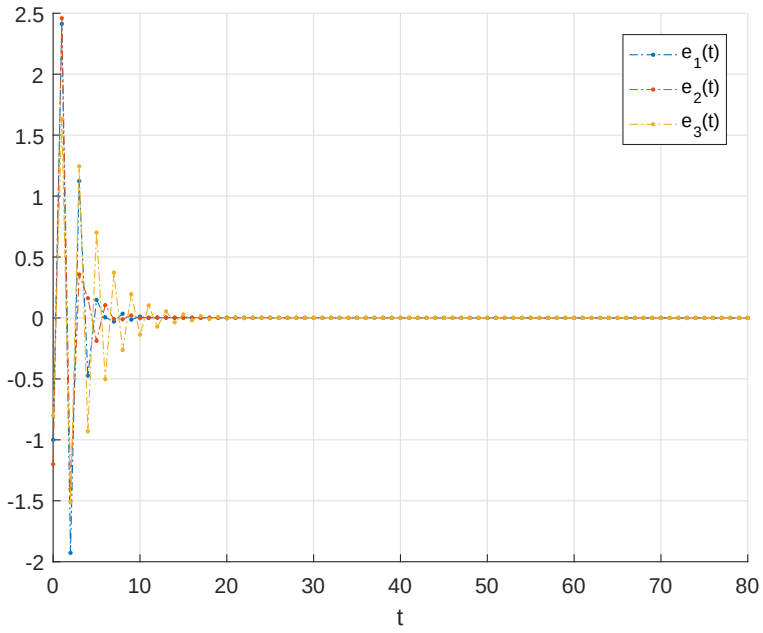

Figure 7.6: Temporal evolution of the error system.

The initial states are set to $x(0) = (1.5, 2, 1.8)^T$ *and* $y(0) = (0.5, 0.8, 1)^T$ *Furthermore, the variable-order parameter is defined as:* $\alpha(t) = \left|\frac{1}{2} - e^{-4(t+1)}\right|$, *along with the parameters:*

$$A = \begin{pmatrix} 1.4 & 0 & 0 \\ 0 & 1.3 & 0 \\ 0 & 0 & 1.5 \end{pmatrix}, \quad D = \begin{pmatrix} -0.5 & -0.7 & -0.5 \\ -0.5 & -1 & 0.1 \\ -0.6 & 0.5 & -0.3 \end{pmatrix}, \quad I = \begin{pmatrix} 0 \\ 0 \\ 0 \end{pmatrix}. \tag{7.46}$$

In Figure 7.5, we illustrate the numerical states of the discrete systems (7.44) and (7.45). Meanwhile, Figure 7.6 showcases the temporal evolution of the error system. These visual representations clearly demonstrate the synchronized dynamics achieved by the two chaotic fractional neural networks, affirming the effectiveness and simplicity of the linear control laws (7.39) in achieving synchronization.

7.5 Synchronization in Commensurate ABC type Discrete Variable-Order Neural Networks

In this part of the study, the primary system is described by the discrete neural network (7.47),

$$\prescript{ABC}{a}{\nabla^{\alpha}} x_i(t) = -c_i x_i(t) + \sum_{j=1}^{n} d_{ij} g_j(t, x_j(t)) + I_i. \tag{7.47}$$

whereas the secondary system is specified as follows:

$$\prescript{ABC}{a}{\nabla^{\alpha}} y(t) = -Ay(t) + Dg(t, y(t)) + I - U(t). \tag{7.48}$$

Given the primary system described by (7.47) and the secondary system by (7.48), we introduce the variable $e_i(t) = y_i(t) - x_i(t)$ for $i = 1, \ldots, n$. This leads to the following formulation for the error system:

$$ {}_{a}^{ABC}\nabla^{\alpha} e(t) = -Ae(t) + D(g(t, y(t)) - g(t, x(t))) - U(t). \tag{7.49} $$

We define the initial conditions for the error system as follows:

$$ \phi = e(a) = y(a) - x(a). \tag{7.50} $$

To achieve synchronization between system (7.47) and system (7.48), we utilize the state feedback control method. The controller employed in this context is defined as follows:

$$ U_i(t) = k_i e_i(t), \quad i = 1, ..., n, \tag{7.51} $$

while $k = (k_i)_{i=1,\ldots,n} \in \mathbb{R}^n$ represents the control gains. Thus, we derive the following.

$$ {}_{a}^{ABC}\nabla^{\alpha} e(t) = -(A + k)e(t) + D(g(t, y(t)) - g(t, x(t))). \tag{7.52} $$

To begin, let's introduce a condition that ensures master synchronization within a finite time frame.

7.5.1 Synchronization in Discrete ABC Type Variable-Order Neural Networks

Definition 7.1 ([390]). *System (7.47) accomplishes finite-time synchronization with system (7.48) employing the controller (7.51). If there exists $\epsilon\delta T$ with $\epsilon, T > 0$ and $0 < \delta < \epsilon$ such that*

$$ \|\phi\| < \delta, \tag{7.53} $$

which gives

$$ \|e(t)\| < \epsilon. \tag{7.54} $$

Theorem 7.4. *Let's suppose that conditions (A_1) and (A_3) are met. Assuming that $|\phi| \leq \delta$, then system (7.47) and system (7.48) achieve finite-time synchronization under controller (7.51) if the following inequality holds:*

$$ \frac{B(\alpha)}{B(\alpha) - (1-\alpha)\nu} V(a) E_{\bar{\alpha}}\left(\frac{\varsigma\nu}{B(\alpha) - (1-\alpha)\nu}, t - a\right) \leq \frac{\epsilon}{\delta}. $$

Proof. Let's define the Lyapunov function as follows:

$$ V(t) = \frac{1}{2}\sum_{i=1}^{n} e_i^2(t), \tag{7.55} $$

Utilizing Lemma 1, we obtain the following result.

$$\begin{aligned}
{}_{a}^{ABC}\nabla^{\alpha}V(t) &= \frac{1}{2}\sum_{i=1}^{n} {}_{a}^{ABC}\nabla^{\alpha}e_i^2(t),\\
&\leq \sum_{i=1}^{n} e_i(t)\,{}_{a}^{ABC}\nabla^{\alpha}e_i(t),\\
&= \sum_{i=1}^{n} e_i(t)\left(-(c_i+k_i)e_i(t)+\sum_{j=1}^{n} d_{ij}(g_i(t,y_j(t))-g_j(t,x_j(t)))\right),\\
&\leq \sum_{i=1}^{n} -(c_i+k_i)e_i^2(t)+\sum_{j=1}^{n} d_{ijj}e_i(t)e_j(t),\\
&\leq \sum_{i=1}^{n} -(c_i+k_i)e_i^2(t)+\sum_{j=1}^{n} d_{ijj}\frac{e_i^2(t)}{e_j^2(t)},\\
&\leq \sum_{i=1}^{n} -(c_i+k_i)e_i^2(t)+e_i^2(t)\sum_{j=1}^{n}\frac{d_{ijj}+d_{jii}}{2},\\
&\leq \left(\max_{i=1,\ldots,n}\left(-(c_i+k_i)+\sum_{j=1}^{n}\frac{d_{ijj}+d_{jii}}{2}\right)\right)\|e_i(t)\|^2.
\end{aligned}$$

This implies that

$$V(t)\leq V(a)+\left(\max_{i=1,\ldots,n}\left(-(c_i+k_i)+\frac{d_{ijj}+d_{jii}}{2}\right)\right){}_{a}^{AB}\nabla^{-x}V(t).$$

According to Theorem 5.1, this indicates

$$V(t)\leq \frac{B(\alpha)}{B(\alpha)-(1-\alpha)\nu}V(a)E_{\overline{\alpha}}\left(\frac{\alpha\nu}{B(\alpha)-(1-\alpha)\nu},t-a\right).$$

where $\nu=\left(\max_{i=1,\ldots,n}\left(-(c_i+k_i)+\frac{d_{ijj}+d_{jii}}{2}\right)\right)$,

Consequently, we can infer that $\|e_i(t)\|\leq\epsilon$

where $\epsilon=\frac{B(\alpha)}{B(\alpha)-(1-\alpha)\nu}V(a)E_{\overline{\alpha}}\left(\frac{\alpha\nu}{B(\alpha)-(1-\alpha)\nu},t-a\right)$. This concludes the proof. □

7.5.2 Computer Simulations

In this section, we present two numerical demonstrations to illustrate the practicality and effectiveness of our theoretical findings. These simulations encompass various scenarios and settings.

Example 7.4. *Consider the drive system illustrated in Figure 7.7, which can be expressed as:*

$$\begin{cases}
{}_{a}^{ABC}\nabla^{\alpha}x_1(t)=-c_1x(t)+d_{11}\tanh(x_1(t))+d_{12}\tanh(x_2(t))+I_1,\\
{}_{a}^{ABC}\nabla^{\alpha}x_2(t)=-c_2x(t)+d_{21}\tanh(x_1(t))+d_{22}\tanh(x_2(t))+I_2.
\end{cases}\tag{7.56}$$

The slave system is defined as follows:

$$\begin{cases} {}_{a}^{ABC}\nabla^{\alpha} y_1(t) = -c_1 y(t) + d_{11}\sin(y_1(t)) + d_{12}\sin(y_2(t)) + I_1 + U_1(t), \\ {}_{a}^{ABC}\nabla^{\alpha} y_2(t) = -c_2 y(t) + d_{21}\sin(y_1(t)) + d_{22}\sin(y_2(t)) + I_2 + U_2(t). \end{cases} \tag{7.57}$$

Additionally, the parameters are chosen as follows:

$$A = \begin{pmatrix} 0.6 & 0 \\ 0 & 0.65 \end{pmatrix}, \quad D = \begin{pmatrix} -0.02 & 0.01 \\ 0.01 & -0.03 \end{pmatrix}, \quad I = \begin{pmatrix} 0.1 \\ 0.1 \end{pmatrix}. \tag{7.58}$$

In order to achieve finite-time synchronization for systems (7.56) and (7.57), we introduce a feedback controller (7.59).

$$k = \begin{pmatrix} 0.2 & 0 \\ 0 & 0.3 \end{pmatrix}. \tag{7.59}$$

Computations reveal that $\dfrac{\alpha\nu}{B(\alpha) - (1-\alpha)\nu} \leq 1$, *which is greater than 0, when* $\alpha = 1 - \dfrac{\sqrt{\frac{5}{t+1}}}{t+5}$. *This indicates that the conditions of Theorem 4 are satisfied. According to Theorem 4, the settling time is determined to be* $T = 10$.
In Figure 7.8, the evolution of the slave system (7.57) is depicted, while Figure 7.9 displays the synchronization error $e(t)$. *The figures clearly demonstrate that systems (7.56) and (7.57) indeed achieve synchronization in finite time. These simulations underscore the practicality and effectiveness of the theoretical findings presented in this study.*

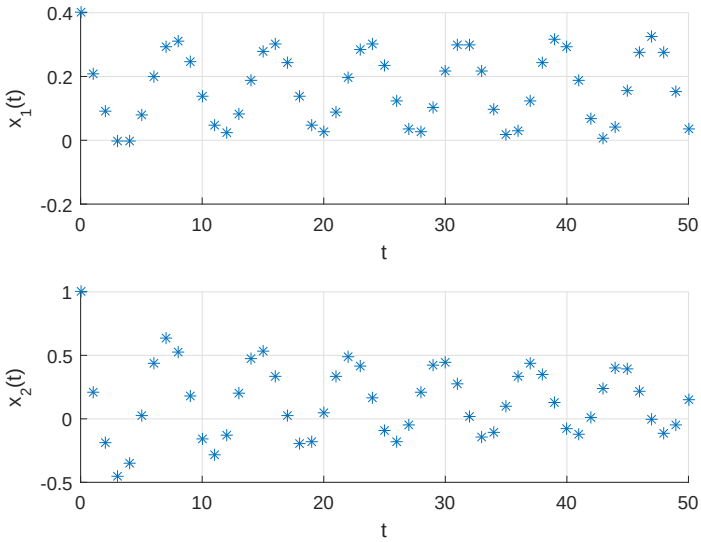

Figure 7.7: Numerical solution of the master system (7.56) for the initial condition $(0.4, 1)^T$.

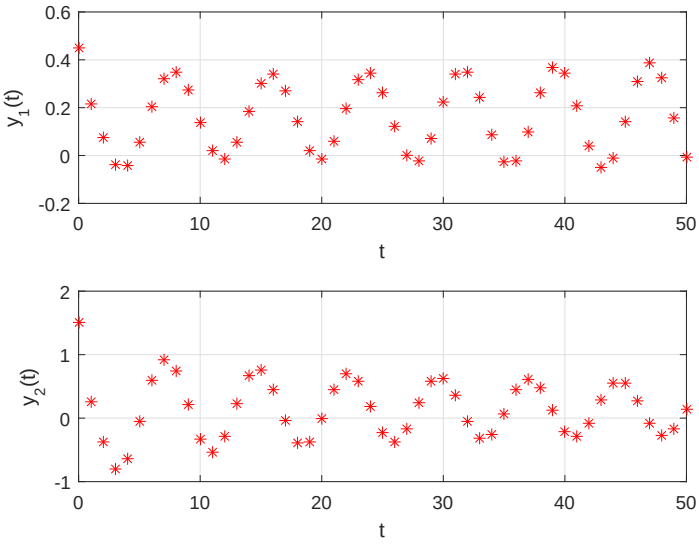

Figure 7.8: Numerical solution of slave system (7.57) for the initial condition $(0.45, 1.5)^T$.

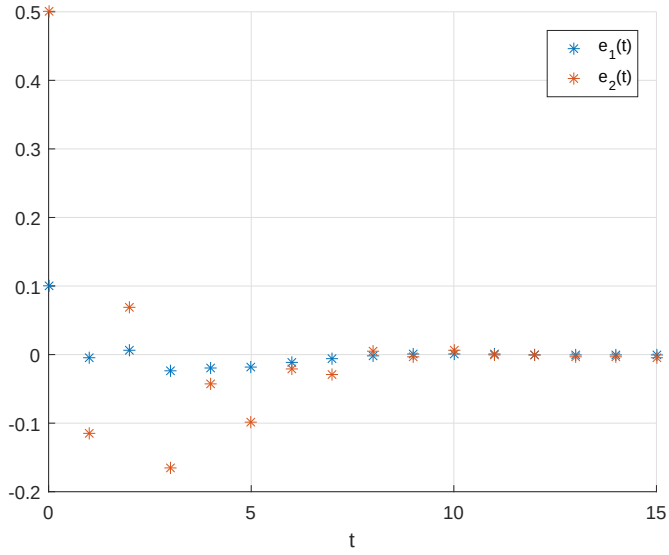

Figure 7.9: Numerical evolution of error system (7.52).

7.6 Synchronization in Incommensurate Discrete Variable-Order Neural Networks

Let's delve into the synchronization dynamics of a discrete incommensurate variable-order neural network, represented by Equation (7.60). We introduce a novel theorem aimed at ensuring synchronized dynamics between two chaotic neural networks using straightforward linear control laws. Consider the discrete incommensurate variable-order

neural network described by Equation (7.60) as the primary system.

$$\begin{cases} {}^{C}\nabla_{a}^{\alpha_1(t)} x_1(t) = -c_1 x_1(t) + \sum_{j=1}^{n} d_{ij} g_j(t, x_j(t)), \\ {}^{C}\nabla_{a}^{\alpha_2(t)} x_2(t) = -c_2 x_2(t) + \sum_{j=1}^{n} d_{2j} g_j(t, x_j(t)), \\ \ldots, \\ {}^{C}\nabla_{a}^{\alpha_n(t)} x_n(t) = -c_n x_n(t) + \sum_{j=1}^{n} d_{nj} g_j(t, x_j(t)). \end{cases} \tag{7.60}$$

Conversely, we regard the controlled discrete incommensurate variable-order neural network, depicted by Equation (1.45), as the slave system. Here, n synchronization controllers are denoted as $L_1, L_2, ..., L_n$, respectively.

$$\begin{cases} {}^{C}\nabla_{a}^{\alpha_1(t)} y_1(t) = -c_1 y_1(t) + \sum_{j=1}^{n} d_{ij} g_j(t, y_j(t)) + L_1(t), \\ {}^{C}\nabla_{a}^{\alpha_2(t)} y_2(t) = -c_2 y_2(t) + \sum_{j=1}^{n} d_{2j} g_j(t, y_j(t)) + L_2(t), \\ \ldots, \\ {}^{C}\nabla_{a}^{\alpha_n(t)} y_n(t) = -c_n y_n(t) + \sum_{j=1}^{n} d_{nj} g_j(t, y_j(t)) + L_n(t). \end{cases} \tag{7.61}$$

In order to achieve full synchronization, the synchronization error is defined as follows:

$$e_i(t) = y_i(t) - x_i(t), \quad i = 1, ..., n. \tag{7.62}$$

The synchronization scheme is considered successful when the following condition is met:

$$\lim_{s \to +\infty} |e_i(t)| = 0, \text{ for } i = 1, ..., n. \tag{7.63}$$

To underscore the significant results of the proposed synchronization strategy, the following theorem is introduced to ensure synchronization between the master and slave neural networks.

7.6.1 Incommensurate Discrete Variable-Order Model and its Synchronization

Theorem 7.5. *The master-slave systems described by equations (7.60) and (7.61) achieve synchronization when the controlled variables $L_i, i = 1, \ldots, n$, are selected as follows:*

$$L_i(t) = -\left(\sum_{j=1}^{n} \frac{|d_{ij}|_j + |d_{ji}|_i}{2} \right) e_i(t), \quad i = 1, ..., n. \tag{7.64}$$

Proof. To guarantee the convergence of the synchronization errors defined in equation (7.62), we start by applying the nabla Caputo-type variable-order differences to equation

(7.62), yielding:

$$\begin{cases} {}^{C}\nabla_a^{\alpha_1(t)} e_1(t) &= -c_1 e_1(t) + \sum_{j=1}^{n} d_{1j}(g_j(t, x_j(t)) - g_j(t, y_j(t))) + L_1(t), \\ {}^{C}\nabla_a^{\alpha_2(t)} e_2(t) &= -c_2 e_2(t) + \sum_{j=1}^{n} d_{2j}(g_j(t, x_j(t)) - g_j(t, y_j(t))) + L_2(t), \\ &\ldots, \\ {}^{C}\nabla_a^{\alpha_n(t)} e_n(t) &= -c_n e_n(t) + \sum_{j=1}^{n} d_{nj}(g_j(t, x_j(t)) - g_j(t, y_j(t))) + L_n(t). \end{cases} \tag{7.65}$$

Replacing the suggested control law (7.64) for $L_i, i = 1, \ldots, n$, in system (7.65) results in the following revised fractional discrete system:

$$\begin{cases} {}^{C}\nabla_a^{\alpha_1(t)} e_1(t) &= -c_1 e_1(t) + \sum_{j=1}^{n} b_{nj}(f_j(t, y_j(t)) - g_j(t, x_j(t))) - \left(\sum_{j=1}^{n} \frac{|d_{1j}|_j + |d_{j1}|_1}{2} \right) e_1(t), \\ {}^{C}\nabla_a^{\alpha_2(t)} e_2(t) &= -c_2 e_2(t) + \sum_{j=1}^{n} d_{nj}(g_j(t, y_j(t)) - g_j(t, x_j(t))) - \left(\sum_{j=1}^{n} \frac{|d_{2j}|_j + |d_{j2}|_2}{2} \right) e_2(t), \\ &\ldots, \\ {}^{C}\nabla_a^{\alpha_n(t)} e_n(t) &= -c_n e_n(t) + \sum_{j=1}^{n} d_{nj}(g_j(t, y_j(t)) - g_j(t, x_j(t))) - \left(\sum_{j=1}^{n} \frac{|g_{nj}|_j + |g_{jn}|_n}{2} \right) e_n(t). \end{cases} \tag{7.66}$$

Next, we proceed to analyze the Lyapunov function, which encompasses the overall error state.

$$V(t) = \frac{1}{2} \sum_{i=1}^{n} {}^{C}\nabla_a^{\alpha_i(t)-\beta} ei^2(t). \tag{7.67}$$

This yields:

$${}^{C}\nabla_a^{\beta} V(t) = \frac{1}{2} \sum_{i=1}^{n} {}^{C}\nabla_a^{\alpha_i(t)} e_i^2(t).$$

Furthermore, employing Lemma (4.10), we obtain the following inequality:

$$\begin{aligned} {}^{C}\nabla_a^{\beta} V(t) &\leq \sum_{i=1}^{n} e_i(t)\, {}^{C}\nabla_a^{\alpha_i(t)} e_i(t), \\ &= \sum_{i=1}^{n} e_i(t) \left(-c_i e_i(t) + \sum_{j=1}^{n} d_{ij}(g_j(t, y_j(t)) - g_j(t, x_j(t))) - \left(\sum_{j=1}^{n} \frac{|d_{ij}|_j + |d_{ji}|_i}{2} \right) e_i(t) \right), \\ &\leq \sum_{i=1}^{n} -c_i e_i^2(t) + \sum_{j=1}^{n} |d_{ij}| e_i(t) e_j(t) - \left(\sum_{j=1}^{n} \frac{|d_{ij}|_j + |d_{ji}|_i}{2} \right) e_i^2(t), \\ &\leq \sum_{i=1}^{n} -c_i e_i^2(t) + \sum_{j=1}^{n} |d_{ij}| \frac{e_i^2(t) + e_j^2(t)}{2} - \left(\sum_{j=1}^{n} \frac{|d_{ij}|_j + |d_{ji}|_i}{2} \right) e_i^2(t), \\ &\leq -\sum_{i=1}^{n} c_i e_i^2(t) \leq -\gamma \sum_{i=1}^{n} e_i^2(t) = -\gamma \|e(t)\| < 0. \end{aligned} \tag{7.68}$$

Moreover, according to Theorem 4.10, it can be asserted that the dynamics of the error system (7.62) for discrete incommensurate variable-order networks converge towards zero, indicating stability. Consequently, synchronization between the master system (7.60) and the slave system (7.61) of the discrete incommensurate variable-order neural network is successfully achieved through the utilization of linear control laws (7.64). Thus, the proof is hereby concluded.

□

7.6.2 Numerical Examples

In this section, we employ numerical simulations conducted in We utilize Matlab to comprehensively validate the theoretical findings presented in the preceding theorem. Through detailed numerical experiments, our goal is to offer a deeper understanding and insight into the synchronization behavior predicted by our theoretical framework.

Example 7.5. *Consider the three-dimensional discrete incommensurate variable-order neural network described by equations (7.69) and (7.70) as the master-slave systems for our investigation.*

$$\begin{cases} {}^{C}\nabla_{a}^{\alpha_1(t)} x_1(t) = -x_1(t) - 0.5\tanh(x_1(t)) - 0.7\tanh(x_2(t)) - 0.5\tanh(x_3(t)), \\ {}^{C}\nabla_{a}^{\alpha_2(t)} x_2(t) = -x_2(t) - 0.6\tanh(x_1(t)) - \tanh(x_2(t)) + 0.1\tanh(x_3(t)), \\ {}^{C}\nabla_{a}^{\alpha_3(t)} x_3(t) = -1.3x_3(t) - 0.6\tanh(x_1(t)) + 0.5\tanh(x_2(t)) - 0.3\tanh(x_3(t)), \end{cases} \tag{7.69}$$

while,

$$\begin{cases} {}^{C}\nabla_{a}^{\alpha_1(t)} y_1(t) = -y_1(t) - 0.5\tanh(y_1(t)) - 0.7\tanh(y_2(t)) - 0.5\tanh(y_3(t)) + L_1(t), \\ {}^{C}\nabla_{a}^{\alpha_2(t)} y_2(t) = -y_2(t) - 0.6\tanh(y_1(t)) - \tanh(y_2(t)) + 0.1\tanh(y_3(t)) + L_2(t), \\ {}^{C}\nabla_{a}^{\alpha_3(t)} y_3(t) = -1.3y_3(t) - 0.6\tanh(y_1(t)) + 0.5\tanh(y_2(t)) - 0.3\tanh(y_3(t)) + L_3(t). \end{cases} \tag{7.70}$$

The initial states, denoted by $e_1(0)$, $e_2(0)$, and $e_3(0)$, serve as the starting values. To simulate the states of the variable-order error system and the synchronized systems (7.69) and (7.70), we employ the predictor-corrector method. The initial values are set to $x(0) = (0.5, 0.3, 0.8)^T$ and $y(0) = (0.1, 0.3, 1)^T$, along with:

$$\begin{cases} \alpha_1(t) = \left| \dfrac{1}{2} - e^{-4(t+1)} \right|, \\ \alpha_2(t) = \dfrac{1}{5} |\log(t+3)|, \\ \alpha_3(t) = \dfrac{1}{2} - \dfrac{e^{\frac{-10}{t+1}}}{t+1}. \end{cases} \tag{7.71}$$

In Figure 7.10, we depict the numerical states of the discrete incommensurate systems (7.69)-(7.70). Meanwhile, Figure 7.11 illustrates the time evolution of the error system. These visualizations clearly demonstrate the synchronized dynamics achieved by the two chaotic fractional neural networks, confirming the effectiveness and simplicity of the linear control laws (7.64) in achieving synchronization.

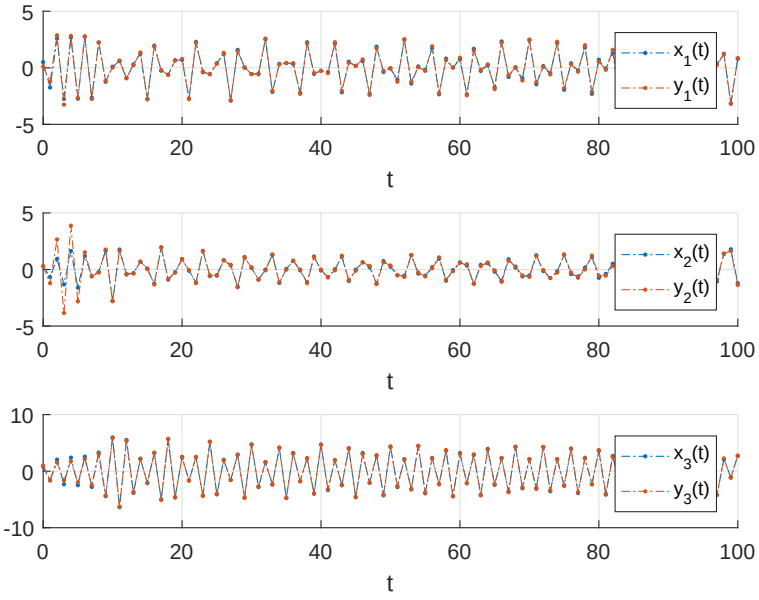

Figure 7.10: Trajectory of states in the master-slave system (7.69)-(7.70).

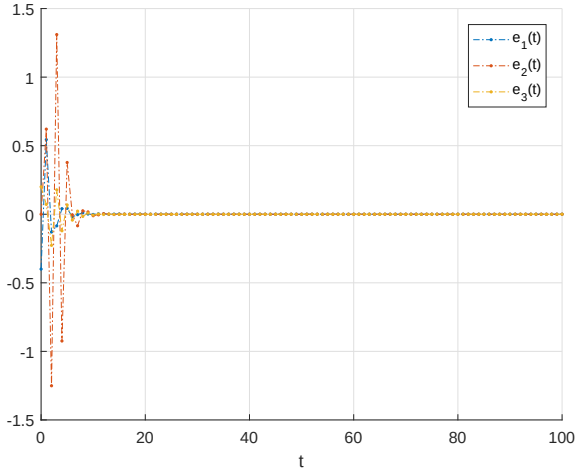

Figure 7.11: Temporal evolution of the error system.

7.7 Conclusion

In summary, this chapter adresses the critical phenomenon of synchronization within chaotic systems, specifically focusing on discrete fractional neural networks. We have explored various synchronization paradigms, including complete synchronization, projective synchronization, each contributing to a deeper understanding of complex system dynamics and opening new avenues for applications across diverse fields.

Complete synchronization, which ensures the convergence of all state variables in coupled systems to identical trajectories, has found extensive applications ranging from

secure communication systems to biomedical fields. Projective synchronization, with its ability to coordinate specific state variables while preserving the independence of others, offers tailored synchronization schemes for engineering and control applications.

Recent research has extended beyond commensurate systems to investigate synchronization in non-commensurate discrete fractional neural networks. These studies have highlighted the significance of finite-time synchronization, which enhances the robustness and stability of chaotic neural networks by ensuring synchronization within a defined time frame. This capability is particularly beneficial for practical engineering applications where predictability and interference suppression are crucial.

Motivated by these advancements, we have introduced novel discrete incommensurate network models based on the Nabla Caputo difference operator. These models provide effective strategies for synchronizing dynamic behaviors, paving the way for innovative applications in various domains.

The chapter is structured to present criteria and methodologies for achieving synchronization in discrete fractional neural networks, supported by numerical simulations to validate the proposed approaches. Finally, concluding remarks offer insights into the implications of our findings, underscoring the potential impact of this comprehensive investigation on future research and applications in the field of chaotic systems and neural networks.

General Conclusion and Future Perspectives

In conclusion, fractional calculus, which traces its origins to the 17th-century inquiries into fractional derivatives, has evolved into a cornerstone of mathematical analysis. This advanced field extends the capabilities of classical calculus by offering sophisticated tools to model systems with memory effects and hereditary properties, which are crucial for understanding and predicting the behavior of complex phenomena across a multitude of disciplines. Recent advancements in fractional-order dynamical systems underscore their significant role in mechanics, electrical engineering, and control theory, providing deeper insights and more precise models compared to traditional integer-order approaches.

The emergence of discrete fractional calculus has further broadened the scope of this field, presenting new frontiers in comprehending systems that evolve in discrete time steps. This burgeoning area not only extrapolates concepts from continuous fractional calculus but also uncovers new complexities and behaviors, such as the persistence and manifestation of chaotic dynamics. Integrating chaotic maps within the framework of discrete fractional calculus has enhanced our understanding, revealing robust chaotic behaviors and offering new perspectives on the dynamics of discrete systems.

Moreover, the study of fractional discrete neural networks represents a pivotal and innovative area of investigation within this context. These networks, inspired by the intricacies of biological neural systems, utilize fractional calculus to model and analyze complex behaviors and dynamics in discrete time domains. Research into their stability, synchronization, and finite-time behaviors provides profound insights into their potential applications, spanning across various fields such as artificial intelligence, cognitive sciences, and computational neuroscience.

Looking ahead, future research efforts will focus on refining theoretical frameworks and enhancing the practical applications of discrete fractional calculus. One promising direction is the physical implementation of variable-order systems and fractional discrete neural networks. These implementations are expected to validate theoretical insights and explore novel applications in a diverse array of fields, including robotics, finance, medical diagnostics, and advanced manufacturing processes. These advancements will not only deepen our understanding of complex systems but also inspire innovative solutions to real-world challenges, thereby solidifying fractional calculus as an indispensable tool in contemporary mathematical analysis and applied sciences.

The ongoing advancements in fractional calculus, particularly in its discrete forms, represent a significant leap forward in the ability to model, analyze, and control complex systems. By bridging theoretical developments with practical applications, this field

promises to unlock new possibilities and drive innovation across a wide spectrum of scientific and engineering disciplines. As such, fractional calculus is poised to remain a crucial and transformative tool in contemporary mathematical analysis, offering profound contributions to the understanding and management of complex phenomena in the modern world.

Bibliography

[1] Jesseph, D. M. (1998). Leibniz on the foundations of the calculus: The question of the reality of infinitesimal magnitudes. Perspectives on Science, 6(1), 6-40.

[2] Butzer, P. L., Westphal, U. (2000). An introduction to fractional calculus. In Applications of fractional calculus in physics (pp. 1-85).

[3] Podlubny, I., Magin, R. L., Trymorush, I. (2017). Niels Henrik Abel and the birth of fractional calculus. Fractional Calculus and Applied Analysis, 20(5), 1068-1075.

[4] Unnikrishnan, G., Joseph, J., Singh, K. (2000). Optical encryption by double-random phase encoding in the fractional Fourier domain. Optics letters, 25(12), 887-889.

[5] Das, S. (2011). Functional fractional calculus (Vol. 1). Berlin: Springer.

[6] Hilfer, R. (Ed.). (2000). Applications of fractional calculus in physics. World scientific.

[7] Zhang, Z. M., Zhang, Z. M., Luby. (2007). Nano/microscale heat transfer (Vol. 410). New York: McGraw-Hill.

[8] Fantoni, S., Fabrocini, A. (2007). Correlated basis function theory for fermion systems. In Microscopic Quantum Many-Body Theories and Their Applications: Proceedings of a European Summer School Held at Valencia, Spain, 8–19 September 1997 (pp. 119-186). Berlin, Heidelberg: Springer Berlin Heidelberg.

[9] Stancu-Minasian, I. M. (2012). Fractional programming: theory, methods and applications (Vol. 409). Springer Science & Business Media.

[10] Meral, F. C., Royston, T. J., Magin, R. (2010). Fractional calculus in viscoelasticity: an experimental study. Communications in nonlinear science and numerical simulation, 15(4), 939-945.

[11] Kaczorek, T., Rogowski, K. (2015). Fractional linear systems and electrical circuits (pp. 49-80). Cham, Switzerland: Springer International Publishing.

[12] Tenreiro Machado, J. A., Silva, M., Barbosa, R., Jesus, I. S., Reis, C., Marcos, M. D. G., Galhano, A. (2010). Some applications of fractional calculus in engineering. Mathematical problems in engineering, 2010, 1-34.

[13] Laskin, N. (2000). Fractional quantum mechanics. Physical Review E, 62(3), 3135.

[14] Bonfanti, A., Kaplan, J. L., Charras, G., Kabla, A. (2020). Fractional viscoelastic models for power-law materials. Soft Matter, 16(26), 6002-6020.

[15] Yang, X. J. (2012). Advanced local fractional calculus and its applications.

[16] Yang, X. J., Machado, J. T., Cattani, C., Gao, F. (2017). On a fractal LC-electric circuit modeled by local fractional calculus. Communications in Nonlinear Science and Numerical Simulation, 47, 200-206.

[17] Yang, X. J. (2011). Local Fractional Functional Analysis Its Applications (Vol. 1). Hong Kong: Asian Academic Publisher Limited.

[18] Coimbra, C. F. (2003). Mechanics with variable-order differential operators. Annalen der Physik, 515(11-12), 692-703.

[19] Atanackovic, T., Pilipovic, S. (2011). Hamilton's principle with variable order fractional derivatives. Fractional Calculus and Applied Analysis, 14(1), 94-109.

[20] Diaz, G., Coimbra, C. F. M. (2009). Nonlinear dynamics and control of a variable order oscillator with application to the van der Pol equation. Nonlinear Dynamics, 56, 145-157.

[21] Lorenzo, C. F., Hartley, T. T. (2002). Variable order and distributed order fractional operators. Nonlinear dynamics, 29, 57-98.

[22] Ramirez, L. E., Coimbra, C. F. (2011). On the variable order dynamics of the nonlinear wake caused by a sedimenting particle. Physica D: nonlinear phenomena, 240(13), 1111-1118.

[23] Ross, B., Samko, S. (1995). Fractional integration operator of variable order in the Holder spaces H (x). International Journal of Mathematics and Mathematical Sciences, 18(4), 777-788.

[24] Abdeljawad, T., Atici, F. M. (2012, January). On the definitions of nabla fractional operators. In Abstract and applied Analysis (Vol. 2012, No. SI01, pp. 1-13). Hindawi.

[25] Ferreira, R. A., Torres, D. F. (2011). Fractional h-difference equations arising from the calculus of variations. Applicable Analysis and Discrete Mathematics, 110-121.

[26] Anastassiou, G. A. (2010). Nabla discrete fractional calculus and nabla inequalities. Mathematical and Computer Modelling, 51(5-6), 562-571.

[27] Goodrich, C., Peterson, A. C. (2015). Discrete fractional calculus (Vol. 10, pp. 978-3). Cham: Springer.

[28] Miller, K. S., Ross, B. (1988, May). Fractional difference calculus. In Proceedings of the international symposium on univalent functions, fractional calculus and their applications (pp. 139-152).

[29] Atici, F. M., Eloe, P. (2009). Discrete fractional calculus with the nabla operator. Electronic Journal of Qualitative Theory of Differential Equations [electronic only], 2009, Paper-No.

[30] Abdeljawad, T. (2011). On Riemann and Caputo fractional differences. Computers & Mathematics with Applications, 62(3), 1602-1611.

[31] Abdeljawad, T., Baleanu, D. (2011). Fractional Differences and Integration by Parts. Journal of Computational Analysis & Applications, 13(3).

[32] Zhu, L., Jiang, D., Ni, J., Wang, X., Rong, X., Ahmad, M., Chen, Y. (2022). A stable meaningful image encryption scheme using the newly-designed 2D discrete fractional-order chaotic map and Bayesian compressive sensing. Signal Processing, 195, 108489.

[33] Ji, Y., Lai, L., Zhong, S., Zhang, L. (2018). Bifurcation and chaos of a new discrete fractional-order logistic map. Communications in Nonlinear Science and Numerical Simulation, 57, 352-358.

[34] Pötzsche, C. (2010). Geometric theory of discrete nonautonomous dynamical systems. Springer.

[35] Vignesh, D., Banerjee, S. (2023). Dynamical analysis of a fractional discrete-time vocal system. Nonlinear Dynamics, 111(5), 4501-4515.

[36] Stanisławski, R., Latawiec, K. J. (2021). A modified Mikhailov stability criterion for a class of discrete-time noncommensurate fractional-order systems. Communications in Nonlinear Science and Numerical Simulation, 96, 105697.

[37] Abbes, A., Ouannas, A., Shawagfeh, N. (2023). An incommensurate fractional discrete macroeconomic system: Bifurcation, chaos, and complexity. Chinese Physics B, 32(3), 030203.

[38] Qi, F., Qu, J., Chai, Y., Chen, L., Lopes, A. M. (2022). Synchronization of incommensurate fractional-order chaotic systems based on linear feedback control. Fractal and Fractional, 6(4), 221.

[39] Liu, X., Ma, L. (2020). Chaotic vibration, bifurcation, stabilization and synchronization control for fractional discrete-time systems. Applied Mathematics and Computation, 385, 125423.

[40] Jarad, F., Abdeljawad, T., Baleanu, D., Biçen, K. (2012, January). On the stability of some discrete fractional nonautonomous systems. In Abstract and Applied Analysis (Vol. 2012, pp. 1-9). Hindawi.

[41] Jarad, F., Abdeljawad, T., Gündoğdu, E., Baleanu, D. (2011). On the Mittag-Leffler stability of q-fractional nonlinear dynamical systems.

[42] Abdeljawad, T., Baleanu, D. (2011). Caputo q-fractional initial value problems and a q-analogue Mittag–Leffler function. Communications in Nonlinear Science and Numerical Simulation, 16(12), 4682-4688.

[43] Djenina, N., Ouannas, A., Batiha, I. M., Grassi, G., Pham, V. T. (2020). On the stability of linear incommensurate fractional-order difference systems. Mathematics, 8(10), 1754.

[44] Shatnawi, M. T., Djenina, N., Ouannas, A., Batiha, I. M., Grassi, G. (2022). Novel convenient conditions for the stability of nonlinear incommensurate fractional-order difference systems. Alexandria Engineering Journal, 61(2), 1655-1663.

[45] Djenina, N., Ouannas, A., Oussaeif, T. E., Grassi, G., Batiha, I. M., Momani, S., Albadarneh, R. B. (2022). On the stability of incommensurate h-nabla fractional-order difference systems. Fractal and Fractional, 6(3), 158.

[46] Wu, X., Yang, X., Song, Q., Chen, X. (2022). Stability analysis on nabla discrete distributed-order dynamical system. Fractal and Fractional, 6(8), 429.

[47] Wei, Y. (2022). Time-varying Lyapunov functions for nonautonomous nabla fractional order systems. ISA transactions, 126, 235-241.

[48] Wei, Y., Zhao, L., Wei, Y., Cao, J. (2023). Lyapunov theorem for stability analysis of nonlinear nabla fractional order systems. Communications in Nonlinear Science and Numerical Simulation, 126, 107443.

[49] Huang, L., Wang, L., Shi, D. (2016). Discrete fractional order chaotic systems synchronization based on the variable structure control with a new discrete reaching-law. IEEE/CAA Journal of Automatica Sinica.

[50] Ouannas, A., Khennaoui, A. A., Grassi, G., Bendoukha, S. (2018). On the Q–S Chaos Synchronization of Fractional-Order Discrete-Time Systems: General Method and Examples. Discrete Dynamics in Nature and Society, 2018(1), 2950357.

[51] Djennoune, S., Bettayeb, M., Al-Saggaf, U. M. (2019). Synchronization of fractional-order discrete-time chaotic systems by an exact delayed state reconstructor: Application to secure communication. International Journal of Applied Mathematics and Computer Science, 29(1), 179-194.

[52] Ouannas, A., Azar, A. T., Vaidyanathan, S. (2017). A robust method for new fractional hybrid chaos synchronization. Mathematical Methods in the Applied Sciences, 40(5), 1804-1812.

[53] Ouannas, A., Azar, A. T., Abu-Saris, R. (2017). A new type of hybrid synchronization between arbitrary hyperchaotic maps. International Journal of Machine Learning and Cybernetics, 8(6), 1887-1894.

[54] Ouannas, A., Azar, A. T., Vaidyanathan, S. (2017). New hybrid synchronisation schemes based on coexistence of various types of synchronisation between master-slave hyperchaotic systems. International Journal of Computer Applications in Technology, 55(2), 112-120.

[55] Azar, A. T., Volos, C., Gerodimos, N. A., Tombras, G. S., Pham, V. T., Radwan, A. G., Munoz-Pacheco, J. M. (2017). A novel chaotic system without equilibrium: dynamics, synchronization, and circuit realization. Complexity, 2017(1), 7871467.

[56] Ouannas, A., Khennaoui, A. A., Odibat, Z., Pham, V. T., Grassi, G. (2019). On the dynamics, control and synchronization of fractional-order Ikeda map. Chaos, Solitons & Fractals, 123, 108-115.

[57] Singh, S., Azar, A. T., Ouannas, A., Zhu, Q., Zhang, W., Na, J. (2017, July). Sliding mode control technique for multi-switching synchronization of chaotic systems. In 2017 9th international conference on modelling, identification and control (ICMIC) (pp. 880-885). IEEE.

[58] Pham, V. T., Ouannas, A., Volos, C., Kapitaniak, T. (2018). A simple fractional-order chaotic system without equilibrium and its synchronization. AEU-International Journal of Electronics and Communications, 86, 69-76.

[59] Ouannas, A., Azar, A. T., Ziar, T. (2020). On inverse full state hybrid function projective synchronization for continuous-time chaotic dynamical systems with arbitrary dimensions. Differential Equations and Dynamical Systems, 28(4), 1045-1058.

[60] Ouannas, A., Azar, A. T., Vaidyanathan, S. (2017). On a simple approach for QS synchronisation of chaotic dynamical systems in continuous-time. International Journal of Computing Science and Mathematics, 8(1), 20-27.

[61] Ouannas, A., Azar, A. T., Ziar, T., Radwan, A. G. (2017). Generalized synchronization of different dimensional integer-order and fractional order chaotic systems. Fractional order control and synchronization of chaotic systems, 671-697.

[62] Ouannas, A., Grassi, G. (2016). Inverse full state hybrid projective synchronization for chaotic maps with different dimensions. Chinese Physics B, 25(9), 090503.

[63] Ouannas, A., Karouma, A., Grassi, G., Pham, V. T. (2021). A novel secure communications scheme based on chaotic modulation, recursive encryption and chaotic masking. Alexandria Engineering Journal, 60(1), 1873-1884.

[64] Ouannas, A., Grassi, G., Ziar, T., Odibat, Z. (2017). On a function projective synchronization scheme for non-identical fractional-order chaotic (hyperchaotic) systems with different dimensions and orders. Optik, 136, 513-523.

[65] Ouannas, A., Azar, A. T., Ziar, T., Vaidyanathan, S. (2017). Fractional inverse generalized chaos synchronization between different dimensional systems. In Fractional Order Control and Synchronization of Chaotic Systems (pp. 525-551). Cham: Springer International Publishing.

[66] Ouannas, A., Ziar, T., Azar, A. T., Vaidyanathan, S. (2017). A new method to synchronize fractional chaotic systems with different dimensions. Fractional Order Control and Synchronization of Chaotic Systems, 581-611.

[67] Ouannas, A., Al-Sawalha, M. M., Ziar, T. (2016). Fractional chaos synchronization schemes for different dimensional systems with non-identical fractional-orders via two scaling matrices. Optik, 127(20), 8410-8418.

[68] Ouannas, A., Odibat, Z. (2016). On inverse generalized synchronization of continuous chaotic dynamical systems. International Journal of Applied and Computational Mathematics, 2, 1-11.

[69] Ouannas, A., Grassi, G. (2016). A new approach to study the coexistence of some synchronization types between chaotic maps with different dimensions. Nonlinear Dynamics, 86(2), 1319-1328.

[70] Ouannas, A., Al-sawalha, M. M. (2016). Synchronization between different dimensional chaotic systems using two scaling matrices. Optik, 127(2), 959-963.

[71] Khennaoui, A. A., Ouannas, A., Boulaaras, S., Pham, V. T., Taher Azar, A. (2020). A fractional map with hidden attractors: chaos and control. The European Physical Journal Special Topics, 229, 1083-1093.

[72] Ouannas, A. (2015). A new generalized-type of synchronization for discrete-time chaotic dynamical systems. Journal of Computational and Nonlinear Dynamics, 10(6), 061019.

[73] Debbouche, N., Ouannas, A., Batiha, I. M., Grassi, G. (2021). Chaotic dynamics in a novel COVID-19 pandemic model described by commensurate and incommensurate fractional-order derivatives. Nonlinear Dynamics, 1-13.

[74] Vaidyanathan, S., Azar, A. T., Ouannas, A. (2017). Hyperchaos and adaptive control of a novel hyperchaotic system with two quadratic nonlinearities. In Fractional Order Control and Synchronization of Chaotic Systems (pp. 773-803). Cham: Springer International Publishing.

[75] Jouini, L., Ouannas, A., Khennaoui, A. A., Wang, X., Grassi, G., Pham, V. T. (2019). The fractional form of a new three-dimensional generalized Hénon map. Advances in Difference Equations, 2019, 1-12.

[76] Vaidyanathan, S., Azar, A. T., Ouannas, A. (2017). An eight-term 3-D novel chaotic system with three quadratic nonlinearities, its adaptive feedback control and synchronization. In Fractional Order Control and Synchronization of Chaotic Systems (pp. 719-746). Cham: Springer International Publishing.

[77] Ouannas, A., Azar, A. T., Radwan, A. G. (2016, December). On inverse problem of generalized synchronization between different dimensional integer-order and fractional-order chaotic systems. In 2016 28th International Conference on Microelectronics (ICM) (pp. 193-196). IEEE.

[78] Ouannas, A., Azar, A. T., Ziar, T., Vaidyanathan, S. (2017). On new fractional inverse matrix projective synchronization schemes. Fractional Order Control and Synchronization of Chaotic Systems, 497-524.

[79] Ouannas, A., Khennaoui, A. A., Grassi, G., Bendoukha, S. (2019). On chaos in the fractional-order Grassi–Miller map and its control. Journal of Computational and Applied Mathematics, 358, 293-305.

[80] Ouannas, A., Odibat, Z., Hayat, T. (2017). Fractional analysis of co-existence of some types of chaos synchronization. Chaos, Solitons & Fractals, 105, 215-223.

[81] Ouannas, A., Azar, A. T., Ziar, T., Radwan, A. G. (2017). A study on coexistence of different types of synchronization between different dimensional fractional chaotic systems. Fractional Order Control and Synchronization of Chaotic Systems, 637-669.

[82] Ouannas, A., Azar, A. T., Vaidyanathan, S. (2017). A new fractional hybrid chaos synchronisation. International Journal of Modelling, Identification and Control, 27(4), 314-322.

[83] Wang, X., Ouannas, A., Pham, V. T., Abdolmohammadi, H. R. (2018). A fractional-order form of a system with stable equilibria and its synchronization. Advances in Difference Equations, 2018, 1-13.

[84] Ouannas, A., Al-Sawalha, M. M. (2015). A new approach to synchronize different dimensional chaotic maps using two scaling matrices. Nonlinear Dyn. Syst. Theory, 15(4), 400-408.

[85] Ouannas, A., Abdelmalek, S., Bendoukha, S. (2017). Coexistence of some chaos synchronization types in fractional-order differential equations.

[86] Ouannas, A., Wang, X., Khennaoui, A. A., Bendoukha, S., Pham, V. T., Alsaadi, F. E. (2018). Fractional form of a chaotic map without fixed points: Chaos, entropy and control. Entropy, 20(10), 720.

[87] Azar, A. T., Ouannas, A., Singh, S. (2018). Control of new type of fractional chaos synchronization. In Proceedings of the International Conference on Advanced Intelligent Systems and Informatics 2017 (pp. 47-56). Springer International Publishing.

[88] Ouannas, A., Wang, X., Pham, V. T., Ziar, T. (2017). Dynamic analysis of complex synchronization schemes between integer order and fractional order chaotic systems with different dimensions. Complexity, 2017(1), 4948392.

[89] Ouannas, A., Abu-Saris, R. (2016). On Matrix Projective Synchronization and Inverse Matrix Projective Synchronization for Different and Identical Dimensional Discrete-Time Chaotic Systems. Journal of Chaos, 2016(1), 4912520.

[90] Ouannas, A., Khennaoui, A. A., Momani, S., Grassi, G., Pham, V. T., El-Khazali, R., Vo Hoang, D. (2020). A quadratic fractional map without equilibria: Bifurcation, 0–1 test, complexity, entropy, and control. Electronics, 9(5), 748.

[91] Ouannas, A., Khennaoui, A. A., Bendoukha, S., Vo, T. P., Pham, V. T., Huynh, V. V. (2018). The fractional form of the Tinkerbell map is chaotic. Applied Sciences, 8(12), 2640.

[92] Khennaoui, A. A., Ouannas, A., Bendoukha, S., Grassi, G., Wang, X., Pham, V. T. (2018). Generalized and inverse generalized synchronization of fractional-order discrete-time chaotic systems with non-identical dimensions. Advances in Difference Equations, 2018, 1-14.

[93] Hadjabi, F., Ouannas, A., Shawagfeh, N., Khennaoui, A. A., Grassi, G. (2020). On two-dimensional fractional chaotic maps with symmetries. Symmetry, 12(5), 756.

[94] Ouannas, A., Khennaoui, A. A., Wang, X., Pham, V. T., Boulaaras, S., Momani, S. (2020). Bifurcation and chaos in the fractional form of Hénon-Lozi type map. The European Physical Journal Special Topics, 229, 2261-2273.

[95] Ouannas, A., Bendoukha, S., Volos, C., Boumaza, N., Karouma, A. (2019). Synchronization of fractional hyperchaotic Rabinovich systems via linear and nonlinear control with an application to secure communications. International Journal of Control, Automation and Systems, 17, 2211-2219.

[96] Huynh, V. V., Ouannas, A., Wang, X., Pham, V. T., Nguyen, X. Q., Alsaadi, F. E. (2019). Chaotic map with no fixed points: entropy, implementation and control. Entropy, 21(3), 279.

[97] Grassi, G., Ouannas, A., Azar, A. T., Radwan, A. G., Volos, C., Pham, V. T., Stouboulos, I. N. (2017, May). Chaos synchronisation of continuous systems via scalar signal. In 2017 6th International Conference on Modern Circuits and Systems Technologies (MOCAST) (pp. 1-4). IEEE.

[98] Ouannas, A. (2016). Co-existence of various types of synchronization between hyperchaotic maps. Nonlinear Dyn. Syst. Theory, 16, 312-321.

[99] Ahmad, I., Ouannas, A., Shafiq, M., Pham, V. T., Baleanu, D. (2021). Finite-time stabilization of a perturbed chaotic finance model. Journal of Advanced Research, 32, 1-14.

[100] Ouannas, A., Khennaoui, A. A., Bendoukha, S., Wang, Z., Pham, V. T. (2020). The dynamics and control of the fractional forms of some rational chaotic maps. Journal of Systems Science and Complexity, 33(3), 584-603.

[101] Bendoukha, S., Abdelmalek, S., Ouannas, A. (2019). Secure communication systems based on the synchronization of chaotic systems. Mathematics Applied to Engineering, Modelling, and Social Issues, 281-311.

[102] Different generalized synchronization schemes between integer-order and fractional-order chaotic systems with different dimensions A Ouannas, A Karouma Differential Equations and Dynamical Systems 26 (1), 125-137, 2018

[103] Ouannas, A., Karouma, A. (2018). Different generalized synchronization schemes between integer-order and fractional-order chaotic systems with different dimensions. Differential Equations and Dynamical Systems, 26(1), 125-137.

[104] Ouannas, A., Abu-Saris, R. (2015). A Robust Control Method for Q-S Synchronization between Different Dimensional Integer-Order and Fractional-Order Chaotic Systems. Journal of Control Science and Engineering, 2015(1), 703753.

[105] Ouannas, A. (2014). Chaos synchronization approach based on new criterion of stability. Nonlinear Dynamics and Systems Theory, 14(4), 395-401.

[106] Batiha, I. M., Alshorm, S., Ouannas, A., Momani, S., Ababneh, O. Y., Albdareen, M. (2022). Modified three-point fractional formulas with Richardson extrapolation. Mathematics, 10(19), 3489.

[107] Debbouche, N., Ouannas, A., Batiha, I. M., Grassi, G., Kaabar, M. K., Jahanshahi, H., Aljuaid, A. M. (2021). Chaotic Behavior Analysis of a New Incommensurate Fractional-Order Hopfield Neural Network System. Complexity, 2021(1), 3394666.

[108] Khennaoui, A. A., Ouannas, A., Odibat, Z., Pham, V. T., Grassi, G. (2020). On the three-dimensional fractional-order Hénon map with Lorenz-like attractors. International Journal of Bifurcation and Chaos, 30(11), 2050217.

[109] Ouannas, A., Al-sawalha, M. M. (2016). On $\Lambda - \psi$ generalized synchronization of chaotic dynamical systems in continuous–time. The European Physical Journal Special Topics, 225(1), 187-196.

[110] Padron, J. P., Perez, J. P., Pérez Díaz, J. J., Martinez Huerta, A. (2021). Time-delay synchronization and anti-synchronization of variable-order fractional discrete-time Chen–Rossler chaotic systems using variable-order fractional discrete-time PID control. Mathematics, 9(17), 2149.

[111] Ma, W., Li, Z., Ma, N. (2022). Synchronization of discrete fractional-order complex networks with and without unknown topology. Chaos: An Interdisciplinary Journal of Nonlinear Science, 32(1).

[112] Ouannas, A., Odibat, Z. (2015). Generalized synchronization of different dimensional chaotic dynamical systems in discrete time. Nonlinear Dynamics, 81, 765-771.

[113] Ouannas, A., Khennaoui, A. A., Momani, S., Grassi, G., Pham, V. T. (2020). Chaos and control of a three-dimensional fractional order discrete-time system with no equilibrium and its synchronization. AIP Advances, 10(4).

[114] Khennaoui, A. A., Ouannas, A., Bendoukha, S., Grassi, G., Wang, X., Pham, V. T., Alsaadi, F. E. (2019). Chaos, control, and synchronization in some fractional-order difference equations. Advances in Difference Equations, 2019, 1-23.

[115] Ouannas, A., Khennaoui, A. A., Momani, S., Pham, V. T., El-Khazali, R. (2020). Hidden attractors in a new fractional–order discrete system: Chaos, complexity, entropy, and control. Chinese Physics B, 29(5), 050504.

[116] Ouannas, A., Odibat, Z., Shawagfeh, N., Alsaedi, A., Ahmad, B. (2017). Universal chaos synchronization control laws for general quadratic discrete systems. Applied Mathematical Modelling, 45, 636-641.

[117] Khennaoui, A. A., Ouannas, A., Bendoukha, S., Wang, X., Pham, V. T. (2018). On chaos in the fractional-order discrete-time unified system and its control synchronization. Entropy, 20(7), 530.

[118] Ouannas, A. (2014). On Full-State Hybrid Projective Synchronization of General Discrete Chaotic Systems. Journal of Nonlinear Dynamics, 2014(1), 983293.

[119] Abbes, A., Ouannas, A., Shawagfeh, N., Khennaoui, A. A. (2022). Incommensurate fractional discrete neural network: chaos and complexity. The European Physical Journal Plus, 137(2), 235.

[120] Ouannas, A., Khennaoui, A. A., Momani, S., Pham, V. T. (2020). The discrete fractional duffing system: Chaos, 0–1 test, C complexity, entropy, and control. Chaos: An Interdisciplinary Journal of Nonlinear Science, 30(8).

[121] Ouannas, A., Khennaoui, A. A., Bendoukha, S., Grassi, G. (2019). On the dynamics and control of a fractional form of the discrete double scroll. International Journal of Bifurcation and Chaos, 29(06), 1950078.

[122] Ouannas, A., Odibat, Z., Shawagfeh, N. (2019). A new Q–S synchronization results for discrete chaotic systems. Differential Equations and Dynamical Systems, 27(4), 413-422.

[123] Bendoukha, S., Ouannas, A., Wang, X., Khennaoui, A. A., Pham, V. T., Grassi, G., Huynh, V. V. (2018). The co-existence of different synchronization types in fractional-order discrete-time chaotic systems with non–identical dimensions and orders. Entropy, 20(9), 710.

[124] Shatnawi, M. T., Abbes, A., Ouannas, A., Batiha, I. M. (2023). Hidden multistability of fractional discrete non-equilibrium point memristor based map. Physica Scripta, 98(3), 035213.

[125] Saadeh, R., Abbes, A., Al-Husban, A., Ouannas, A., Grassi, G. (2023). The fractional discrete predator–prey model: chaos, control and synchronization. Fractal and Fractional, 7(2), 120.

[126] Ouannas, A., Grassi, G., Azar, A. T., Radwan, A. G., Volos, C., Pham, V. T., Stouboulos, I. N. (2017, May). Dead-beat synchronization control in discrete-time chaotic systems. In 2017 6th International Conference on Modern Circuits and Systems Technologies (MOCAST) (pp. 1-4). IEEE.

[127] Ouannas, A., Khennaoui, A. A., Grassi, G., Bendoukha, S. (2018). On the Q–S Chaos Synchronization of Fractional-Order Discrete-Time Systems: General Method and Examples. Discrete Dynamics in Nature and Society, 2018(1), 2950357.

[128] Ouannas, A., Khennaoui, A. A., Zehrour, O., Bendoukha, S., Grassi, G., Pham, V. T. (2019). Synchronisation of integer-order and fractional-order discrete-time chaotic systems. Pramana, 92, 1-9.

[129] Ouannas, A., Grassi, G., Karouma, A., Ziar, T., Wang, X., Pham, V. T. (2018). New type of chaos synchronization in discrete-time systems: the FM synchronization. Open Physics, 16(1), 174-182.

[130] Ouannas, A., Mahmoud, E. E. (2014). Inverse matrix projective synchronization for discrete chaotic systems with different dimensions. Journal of Computational Intelligence and Electronic Systems, 3(3), 188-192.

[131]

[132] Dababneh, A., Djenina, N., Ouannas, A., Grassi, G., Batiha, I. M., Jebril, I. H. (2022). A new incommensurate fractional-order discrete COVID-19 model with vaccinated individuals compartment. Fractal and Fractional, 6(8), 456.

[133] Ouannas, A. (2015). A new synchronization scheme for general 3D quadratic chaotic systems in discrete-time. Nonlinear Dynamics and Systems Theory, 15(2), 163-170.

[134] Djenina, N., Ouannas, A., Batiha, I. M., Grassi, G., Oussaeif, T. E., Momani, S. (2022). A novel fractional-order discrete SIR model for predicting COVID-19 behavior. Mathematics, 10(13), 2224.

[135] Ouannas, A., Grassi, G., Azar, A. T., Radwan, A. G., Volos, C., Pham, V. T., Stouboulos, I. N. (2017, May). Dead-beat synchronization control in discrete-time chaotic systems. In 2017 6th International Conference on Modern Circuits and Systems Technologies (MOCAST) (pp. 1-4). IEEE.

[136] Khennaoui, A. A., Almatroud, A. O., Ouannas, A., Al-sawalha, M. M., Grassi, G., Pham, V. T., Batiha, I. M. (2021). An Unprecedented 2-Dimensional Discrete-Time Fractional-Order System and Its Hidden Chaotic Attractors. Mathematical Problems in Engineering, 2021(1), 6768215.

[137] Gurney, K. (2018). An introduction to neural networks. CRC press.

[138] Jansson, P. A. (1991). Neural networks: An overview. Analytical chemistry, 63(6), 357A-362A.

[139] Müller, B., Reinhardt, J., Strickland, M. T. (2012). Neural networks: an introduction. Springer Science & Business Media.

[140] Hecht-Nielsen, R. (1992). Theory of the backpropagation neural network. In Neural networks for perception (pp. 65-93). Academic Press.

[141] Hegazy, T., Fazio, P., Moselhi, O. (1994). Developing practical neural network applications using back-propagation. Computer-Aided Civil and Infrastructure Engineering, 9(2), 145-159.

[142] Goldberg, Y. (2022). Neural network methods for natural language processing. Springer Nature.

[143] Dunne, R. A. (2007). A statistical approach to neural networks for pattern recognition. John Wiley & Sons.

[144] Bishop, C. M. (1995). Neural networks for pattern recognition. Oxford university press.

[145] Widrow, B., Rumelhart, D. E., Lehr, M. A. (1994). Neural networks: applications in industry, business and science. Communications of the ACM, 37(3), 93-106.

[146] Bishop, C. M. (1994). Neural networks and their applications. Review of scientific instruments, 65(6), 1803-1832.

[147] Dreyfus, G. (2005). Neural networks: methodology and applications. Springer Science & Business Media.

[148] Rajchakit, G., Agarwal, P., Ramalingam, S. (2021). Stability analysis of neural networks. Singapore: Springer.

[149] Zheng, S., Song, Y., Leung, T., Goodfellow, I. (2016). Improving the robustness of deep neural networks via stability training. In Proceedings of the ieee conference on computer vision and pattern recognition (pp. 4480-4488).

[150] Zhang, S., Yu, Y., Wang, H. (2015). Mittag-Leffler stability of fractional-order Hopfield neural networks. Nonlinear Analysis: Hybrid Systems, 16, 104-121.

[151] Zhang, S., Yu, Y., Yu, J. (2016). LMI conditions for global stability of fractional-order neural networks. IEEE transactions on neural networks and learning systems, 28(10), 2423-2433.

[152] Wu, G. C., Abdeljawad, T., Liu, J., Baleanu, D., Wu, K. T. (2019). Mittag-Leffler stability analysis of fractional discrete-time neural networks via fixed point technique.

[153] You, X., Song, Q., Zhao, Z. (2020). Global Mittag-Leffler stability and synchronization of discrete-time fractional-order complex-valued neural networks with time delay. Neural Networks, 122, 382-394.

[154] Bhat, S. P., Bernstein, D. S. (2000). Finite-time stability of continuous autonomous systems. SIAM Journal on Control and optimization, 38(3), 751-766.

[155] Amato, F., Ambrosino, R., Ariola, M., Cosentino, C., De Tommasi, G. (2014). Finite-time stability and control (Vol. 453). London: Springer.

[156] Moulay, E., Perruquetti, W. (2006). Finite time stability and stabilization of a class of continuous systems. Journal of Mathematical analysis and applications, 323(2), 1430-1443.

[157] Wu, R., Lu, Y., Chen, L. (2015). Finite-time stability of fractional delayed neural networks. Neurocomputing, 149, 700-707.

[158] Shen, J., Lam, J. (2014). Non-existence of finite-time stable equilibria in fractional-order nonlinear systems. Automatica, 50(2), 547-551.

[159] Haddad, W. M., Lee, J. (2020). Finite-time stability of discrete autonomous systems. Automatica, 122, 109282.

[160] Wang, B., Jahanshahi, H., Arıcıoğlu, B., Boru, B., Kacar, S., Alotaibi, N. D. (2023). A variable-order fractional neural network: Dynamical properties, Data security application, and synchronization using a novel control algorithm with a finite-time estimator. Journal of the Franklin Institute, 360(17), 13648-13670.

[161] You, X., Song, Q., Zhao, Z. (2020). Existence and finite-time stability of discrete fractional-order complex-valued neural networks with time delays. Neural Networks, 123, 248-260.

[162] Hu, T., He, Z., Zhang, X., Zhong, S. (2020). Finite-time stability for fractional-order complex-valued neural networks with time delay. Applied Mathematics and Computation, 365, 124715.

[163] Bouvrie, J., Slotine, J. J. (2011). Synchronization and redundancy: implications for robustness of neural learning and decision making. Neural computation, 23(11), 2915-2941.

[164] Rossello, J. L., Canals, V., Oliver, A., Morro, A. (2014). Studying the role of synchronized and chaotic spiking neural ensembles in neural information processing. International journal of neural systems, 24(05), 1430003.

[165] Balootaki, M. A., Rahmani, H., Moeinkhah, H., Mohammadzadeh, A. (2020). On the synchronization and stabilization of fractional-order chaotic systems: Recent advances and future perspectives. Physica A: Statistical Mechanics and its Applications, 551, 124203.

[166] Xiao, J., Wu, L., Wu, A., Zeng, Z., Zhang, Z. (2022). Novel controller design for finite-time synchronization of fractional-order memristive neural networks. Neurocomputing, 512, 494-502.

[167] Narayanan, G., Muhiuddin, G., Ali, M. S., Diab, A. A. Z., Al-Amri, J. F., Abdul-Ghaffar, H. I. (2022). Impulsive synchronization control mechanism for fractional-order complex-valued reaction-diffusion systems with sampled-data control: its application to image encryption. IEEE Access, 10, 83620-83635.

[168] Liu, P., Zeng, Z., Wang, J. (2018). Global synchronization of coupled fractional-order recurrent neural networks. IEEE transactions on neural networks and learning systems, 30(8), 2358-2368.

[169] Chen, D., Zhang, R., Liu, X., Ma, X. (2014). Fractional order Lyapunov stability theorem and its applications in synchronization of complex dynamical networks. Communications in Nonlinear Science and Numerical Simulation, 19(12), 4105-4121.

[170] Wang, Y., Wang, Z., Liang, J. (2008). A delay fractioning approach to global synchronization of delayed complex networks with stochastic disturbances. Physics Letters A, 372(39), 6066-6073.

[171] Liu, N., Fang, J., Deng, W., Wu, Z. J., Ding, G. Q. (2018). Synchronization for a class of fractional-order linear complex networks via impulsive control. International Journal of Control, Automation and Systems, 16(6), 2839-2844.

[172] Atici, F. M., Eloe, P. W. (2007). A transform method in discrete fractional calculus. International Journal of Difference Equations, 2(2).

[173] Atici, F., Eloe, P. (2009). Initial value problems in discrete fractional calculus. Proceedings of the American Mathematical Society, 137(3), 981-989.

[174] Atici, F. M., Eloe, P. W. (2011). Linear systems of fractional nabla difference equations. The Rocky Mountain Journal of Mathematics, 353-370.

[175] Atıcı, F. M., Eloe, P. W. (2012). Gronwall's inequality on discrete fractional calculus. Computers & Mathematics with Applications, 64(10), 3193-3200.

[176] Goodrich, C. S. (2010). Existence of a positive solution to a class of fractional differential equations. Applied Mathematics Letters, 23(9), 1050-1055.

[177] Wu, G. C., Baleanu, D. (2014). Discrete fractional logistic map and its chaos. Nonlinear Dynamics, 75, 283-287.

[178] Hein, J., McCarthy, Z., Gaswick, N., McKain, B., Speer, K. (2011). Laplace transforms for the nabla-difference operator. Pan American Mathematical Journal, 21(3), 79-96.

[179] Abdeljawad, T. (2013). Dual identities in fractional difference calculus within Riemann. Advances in Difference Equations, 2013, 1-16.

[180] Abdeljawad, T. (2013). On delta and nabla Caputo fractional differences and dual identities. Discrete Dynamics in Nature and Society, 2013(1), 406910.

[181] Dahal, R., Goodrich, C. S. (2014). A monotonicity result for discrete fractional difference operators. Archiv der Mathematik, 102, 293-299.

[182] Jia, B., Erbe, L., Peterson, A. (2015). Two monotonicity results for nabla and delta fractional differences. Archiv der Mathematik, 104, 589-597.

[183] Erbe, L., Goodrich, C. S., Jia, B., Peterson, A. (2017). Monotonicity results for delta fractional differences revisited. Mathematica Slovaca, 67(4), 895-906.

[184] Atici, F. M., Uyanik, M. (2015). Analysis of discrete fractional operators. Applicable Analysis and Discrete Mathematics, 139-149.

[185] Dahal, R., Goodrich, C. S. (2017). An almost sharp monotonicity result for discrete sequential fractional delta differences. Journal of Difference Equations and Applications, 23(7), 1190-1203.

[186] Abdeljawad, T., Baleanu, D. (2017). On fractional derivatives with exponential kernel and their discrete versions. Reports on Mathematical Physics, 80(1), 11-27.

[187] Atangana, A., Baleanu, D. (2016). New fractional derivatives with nonlocal and non-singular kernel: theory and application to heat transfer model. arXiv preprint arXiv:1602.03408.

[188] Abdeljawad, T., Baleanu, D. (2016). Integration by parts and its applications of a new nonlocal fractional derivative with Mittag-Leffler nonsingular kernel. arXiv preprint arXiv:1607.00262.

[189] Abdeljawad, T., Baleanu, D. (2016). Discrete fractional differences with nonsingular discrete Mittag-Leffler kernels. Advances in Difference Equations, 2016, 1-18.

[190] Abdeljawad, T., Al-Mdallal, Q. M. (2018). Discrete Mittag-Leffler kernel type fractional difference initial value problems and Gronwall's inequality. Journal of Computational and Applied Mathematics, 339, 218-230.

[191] Abdeljawad, T., Baleanu, D. (2017). Monotonicity results for fractional difference operators with discrete exponential kernels. Advances in Difference Equations, 2017, 1-9.

[192] Abdeljawad, T., Baleanu, D. (2017). Monotonicity analysis of a nabla discrete fractional operator with discrete Mittag-Leffler kernel. Chaos, Solitons & Fractals, 102, 106-110.

[193] Holm, M. (2011). The theory of discrete fractional calculus: Development and application. The University of Nebraska-Lincoln.

[194] Caputo, M. (1967). Linear models of dissipation whose Q is almost frequency independent—II. Geophysical journal international, 13(5), 529-539.

[195] Agarwal, R. P. (2000). Difference equations and inequalities: theory, methods, and applications. CRC Press.

[196] Abdeljawad, T. (2018). Different type kernel h-fractional differences and their fractional h-sums. Chaos, Solitons & Fractals, 116, 146-156.

[197] Mozyrska, D., Girejko, E. (2013). Overview of fractional h-difference operators. In Advances in harmonic analysis and operator theory: the stefan samko anniversary volume (pp. 253-268). Springer Basel.

[198] Holm, M. T. (2011). The Laplace transform in discrete fractional calculus. Computers & Mathematics with Applications, 62(3), 1591-1601.

[199] Bohner, M., Peterson, A. Advances in Dynamic Equations on Time Scales [electronic resource].

[200] Bohner, M., Peterson, A. (2001). Dynamic equations on time scales: An introduction with applications. Springer Science & Business Media.

[201] Bohner, M., Peterson, A. C. (2003). Advances in Dynamic Equations on Time Scales, Birkäuser Boston. Inc., Boston, MA.

[202] Holm, M. (2011). Sum and difference compositions in discrete fractional calculus. Cubo (Temuco), 13(3), 153-184.

[203] Abdeljawad, T. (2011). On Riemann and Caputo fractional differences. Computers & Mathematics with Applications, 62(3), 1602-1611.

[204] Abdeljawad, T., Baleanu, D., Jarad, F., Agarwal, R. P. (2013). Fractional sums and differences with binomial coefficients. Discrete Dynamics in Nature and Society, 2013(1), 104173.

[205] Bohner, M., Peterson, A. (2001). Dynamic equations on time scales: An introduction with applications. Springer Science & Business Media.

[206] Eladyi, S. (2000). An introduction to difference equations.

[207] Mozyrska, D., Wyrwas, M. (2015). The Z-transform method and delta type fractional difference operators. Discrete Dynamics in Nature and Society, 2015(1), 852734.

[208] Ross, B., Samko, S. (1995). Fractional integration operator of variable order in the Holder spaces H (x). International Journal of Mathematics and Mathematical Sciences, 18(4), 777-788.

[209] Samko, S. G. (1995). Fractional integration and differentiation of variable order. Analysis Mathematica, 21(3), 213-236.

[210] Samko, S. G., Ross, B. (1993). Integration and differentiation to a variable fractional order. Integral transforms and special functions, 1(4), 277-300.

[211] Atanackovic, T., Pilipovic, S. (2011). Hamilton's principle with variable order fractional derivatives. Fractional Calculus and Applied Analysis, 14(1), 94-109.

[212] Coimbra, C. F. (2003). Mechanics with variable-order differential operators. Annalen der Physik, 515(11-12), 692-703.

[213] Diaz, G., Coimbra, C. F. M. (2009). Nonlinear dynamics and control of a variable order oscillator with application to the van der Pol equation. Nonlinear Dynamics, 56, 145-157.

[214] Lorenzo, C. F., Hartley, T. T. (2002). Variable order and distributed order fractional operators. Nonlinear dynamics, 29, 57-98.

[215] Ramirez, L. E., Coimbra, C. F. (2010). On the selection and meaning of variable order operators for dynamic modeling. International Journal of Differential Equations, 2010(SI1), 1-16.

[216] Ramirez, L. E., Coimbra, C. F. (2011). On the variable order dynamics of the nonlinear wake caused by a sedimenting particle. Physica D: nonlinear phenomena, 240(13), 1111-1118.

[217] Abdeljawad, T., Mert, R., Torres, D. F. (2019). Variable order Mittag–Leffler fractional operators on isolated time scales and application to the calculus of variations. Fractional Derivatives with Mittag-Leffler Kernel: Trends and Applications in Science and Engineering, 35-47.

[218] Abdeljawad, T., Baleanu, D. (2017). On fractional derivatives with exponential kernel and their discrete versions. Reports on Mathematical Physics, 80(1), 11-27.

[219] Atangana, A., Baleanu, D. (2016). New fractional derivatives with nonlocal and non-singular kernel: theory and application to heat transfer model. arXiv preprint arXiv:1602.03408.

[220] Ferreira, R. A. (2012). A discrete fractional Gronwall inequality. Proceedings of the American Mathematical Society, 1605-1612.

[221] Liao, H. L., McLean, W., Zhang, J. (2019). A discrete Gronwall inequality with applications to numerical schemes for subdiffusion problems. SIAM Journal on Numerical Analysis, 57(1), 218-237.

[222] Wu, G. C., Baleanu, D., Zeng, S. D. (2018). Finite-time stability of discrete fractional delay systems: Gronwall inequality and stability criterion. Communications in Nonlinear Science and Numerical Simulation, 57, 299-308.

[223] Busłowicz, M. (2010). Robust stability of positive discrete-time linear systems of fractional order. Bulletin of the Polish Academy of Sciences: Technical Sciences, 567-572.

[224] Rivero, M., Rogosin, S. V., Tenreiro Machado, J. A., Trujillo, J. J. (2013). Stability of fractional order systems. Mathematical Problems in Engineering, 2013(1), 356215.

[225] Mohammed, P. O., Srivastava, H. M., Baleanu, D., Al-Sarairah, E., Sahoo, S. K., Chorfi, N. (2023). Monotonicity and positivity analyses for two discrete fractional-order operator types with exponential and Mittag–Leffler kernels. Journal of King Saud University-Science, 35(7), 102794.

[226] Wei, Y., Wei, Y., Chen, Y., Wang, Y. (2020). Mittag–Leffler stability of nabla discrete fractional-order dynamic systems. Nonlinear Dynamics, 101, 407-417.

[227] Wu, G. C., Abdeljawad, T., Liu, J., Baleanu, D., Wu, K. T. (2019). Mittag-Leffler stability analysis of fractional discrete-time neural networks via fixed point technique.

[228] Khennaoui, A. A., Ouannas, A. (2021). Chaos, control and synchronization of discrete.

[229] Franco-Perez, L., Fernandez-Anaya, G., Quezada-Téllez, L. A. (2020). On stability of nonlinear nonautonomous discrete fractional Caputo systems. Journal of Mathematical Analysis and Applications, 487(2), 124021.

[230] Wei, Y., Zhao, L., Wei, Y., Cao, J. (2023). Lyapunov theorem for stability analysis of nonlinear nabla fractional order systems. Communications in Nonlinear Science and Numerical Simulation, 126, 107443.

[231] Liu, X., Jia, B., Erbe, L., Peterson, A. (2019). Stability analysis for a class of nabla (q, h)-fractional difference equations. Turkish Journal of Mathematics, 43(2), 664-687.

[232] Franco-Perez, L., Fernandez-Anaya, G., Quezada-Téllez, L. A. (2020). On stability of nonlinear nonautonomous discrete fractional Caputo systems. Journal of Mathematical Analysis and Applications, 487(2), 124021.

[233] Djenina, N., Ouannas, A., Batiha, I. M., Grassi, G., Pham, V. T. (2020). On the stability of linear incommensurate fractional-order difference systems. Mathematics, 8(10), 1754.

[234] Shatnawi, M. T., Djenina, N., Ouannas, A., Batiha, I. M., Grassi, G. (2022). Novel convenient conditions for the stability of nonlinear incommensurate fractional-order difference systems. Alexandria Engineering Journal, 61(2), 1655-1663.

[235] Djenina, N., Ouannas, A., Oussaeif, T. E., Grassi, G., Batiha, I. M., Momani, S., Albadarneh, R. B. (2022). On the stability of incommensurate h-nabla fractional-order difference systems. Fractal and Fractional, 6(3), 158.

[236] Simon, H. (2009). Neural networks and learning machines.

[237] Du, K. L., Swamy, M. N. (2006). Neural networks in a softcomputing framework (Vol. 501). London: Springer.

[238] Most, T. (2005). Approximation of complex nonlinear functions by means of neural networks. 2nd Weimar Optimization and Stochastic Days 2005.

[239] Nielsen, M. A. (2015). Neural networks and deep learning (Vol. 25, pp. 15-24). San Francisco, CA, USA: Determination press.

[240] Ferrari, S., Stengel, R. F. (2005). Smooth function approximation using neural networks. IEEE Transactions on Neural Networks, 16(1), 24-38.

[241] Hornik, K., Stinchcombe, M., White, H. (1990). Universal approximation of an unknown mapping and its derivatives using multilayer feedforward networks. Neural networks, 3(5), 551-560.

[242] Vemuri, A. T., Polycarpou, M. M. (1997). Neural-network-based robust fault diagnosis in robotic systems. IEEE Transactions on neural networks, 8(6), 1410-1420.

[243] Minsky, M. Papert., S.,(1969). Perceptrons: An introduction to computational geometry.

[244] Arena, P., Fortuna, L., Porto, D. (2000). Chaotic behavior in noninteger-order cellular neural networks. Physical Review E, 61(1), 776.

[245] Kaslik, E., Sivasundaram, S. (2011, July). Dynamics of fractional-order neural networks. In The 2011 International Joint Conference on Neural Networks (pp. 611-618). IEEE.

[246] Thanh, P. D., Thuong, C. P. (2015, October). Chaos in the fractional order cellular neural network and its sychronization. In 2015 15th International Conference on Control, Automation and Systems (ICCAS) (pp. 161-166). IEEE.

[247] Kaslik, E., Sivasundaram, S. (2011, July). Dynamics of fractional-order neural networks. In The 2011 International Joint Conference on Neural Networks (pp. 611-618). IEEE.

[248] Edelstein-Keshet, L. (2004). Featured review: mathematical biology.

[249] Xiao, M., Zheng, W. X. (2012, May). Nonlinear dynamics and limit cycle bifurcation of a fractional-order three-node recurrent neural network. In 2012 IEEE International Symposium on Circuits and Systems (ISCAS) (pp. 161-164). IEEE.

[250] El-Saka, H. A., Ahmed, E., Shehata, M. I., El-Sayed, A. M. A. (2009). On stability, persistence, and Hopf bifurcation in fractional order dynamical systems. Nonlinear Dynamics, 56, 121-126.

[251] Xiao, M., Zheng, W. X., Jiang, G., Cao, J. (2015). Undamped oscillations generated by Hopf bifurcations in fractional-order recurrent neural networks with Caputo derivative. IEEE transactions on neural networks and learning systems, 26(12), 3201-3214.

[252] Kaslik, E., Sivasundaram, S. (2012). Non-existence of periodic solutions in fractional-order dynamical systems and a remarkable difference between integer and fractional-order derivatives of periodic functions. Nonlinear Analysis: Real World Applications, 13(3), 1489-1497.

[253] Zhang, S., Yu, Y., Hu, W. (2014). Robust stability analysis of fractional-order Hopfield neural networks with parameter uncertainties. Mathematical Problems in Engineering, 2014(1), 302702.

[254] Zhang, S., Yu, Y., Hu, W. (2014). Robust stability analysis of fractional-order Hopfield neural networks with parameter uncertainties. Mathematical Problems in Engineering, 2014(1), 302702.

[255] Song, C., Cao, J., Fei, S. (2016, July). New stability results of fractional-order hopfield neural networks with delays. In 2016 35th Chinese Control Conference (CCC) (pp. 3561-3565). IEEE.

[256] Li, Y., Chen, Y., Podlubny, I. (2009). Mittag–Leffler stability of fractional order nonlinear dynamic systems. Automatica, 45(8), 1965-1969.

[257] Zhang, S., Yu, Y., Wang, H. (2015). Mittag-Leffler stability of fractional-order Hopfield neural networks. Nonlinear Analysis: Hybrid Systems, 16, 104-121.

[258] Aguila-Camacho, N., Duarte-Mermoud, M. A., Gallegos, J. A. (2014). Lyapunov functions for fractional order systems. Communications in Nonlinear Science and Numerical Simulation, 19(9), 2951-2957.

[259] Chen, J., Zeng, Z., Jiang, P. (2014). Global Mittag-Leffler stability and synchronization of memristor-based fractional-order neural networks. Neural Networks, 51, 1-8.

[260] Gonzalez, R. C. (2009). Digital image processing. Pearson education india.

[261] Anem, J., Kumar, G. S., Madhu, R. (2020). Cat Swarm Fractional Calculus optimization-based deep learning for artifact removal from EEG signal. Journal of Experimental & Theoretical Artificial Intelligence, 32(6), 939-958.

[262] Bohner, M. J., Stamova, I. M. (2018). An impulsive delay discrete stochastic neural network fractional-order model and applications in finance. Filomat, 32(18), 6339-6352.

[263] Bukhari, A. H., Raja, M. A. Z., Sulaiman, M., Islam, S., Shoaib, M., Kumam, P. (2020). Fractional neuro-sequential ARFIMA-LSTM for financial market forecasting. Ieee Access, 8, 71326-71338.

[264] Yaghoubi, Z., Zarabadipour, H. (2012). Phase and Antiphase Synchronization between 3-Cell CNN and Volta Fractional-Order Chaotic Systems via Active Control. Mathematical Problems in Engineering, 2012.

[265] Wang, H. (2019). Research on application of fractional calculus in signal real-time analysis and processing in stock financial market. Chaos, Solitons & Fractals, 128, 92-97.

[266] Yin, K. L., Pu, Y. F., Lu, L. (2020). Combination of fractional FLANN filters for solving the Van der Pol-Duffing oscillator. Neurocomputing, 399, 183-192.

[267] Aguilar, C. Z., Gómez-Aguilar, J. F., Alvarado-Martínez, V. M., Romero-Ugalde, H. M. (2020). Fractional order neural networks for system identification. Chaos, Solitons & Fractals, 130, 109444.

[268] Rahmani, M. R., Farrokhi, M. (2020). Fractional-order Hammerstein state-space modeling of nonlinear dynamic systems from input–output measurements. ISA transactions, 96, 177-184.

[269] Zúñiga-Aguilar, C. J., Gómez-Aguilar, J. F., Romero-Ugalde, H. M., Jahanshahi, H., Alsaadi, F. E. (2022). Fractal-fractional neuro-adaptive method for system identification. Engineering with Computers, 1-24.

[270] Sierociuk, D., Petráš, I. (2011, August). Modeling of heat transfer process by using discrete fractional-order neural networks. In 2011 16th International Conference on Methods & Models in Automation & Robotics (pp. 146-150). IEEE.

[271] Yu, J., Hu, C., Jiang, H. (2012). α-stability and α-synchronization for fractional-order neural networks. Neural Networks, 35, 82-87.

[272] Chen, L., Chai, Y., Wu, R., Ma, T., Zhai, H. (2013). Dynamic analysis of a class of fractional-order neural networks with delay. Neurocomputing, 111, 190-194.

[273] Wu, R. C., Hei, X. D., Chen, L. P. (2013). Finite-time stability of fractional-order neural networks with delay. Communications in Theoretical Physics, 60(2), 189.

[274] Chen, L., Liu, C., Wu, R., He, Y., Chai, Y. (2016). Finite-time stability criteria for a class of fractional-order neural networks with delay. Neural Computing and Applications, 27, 549-556.

[275] Zhang, H., Ye, R., Liu, S., Cao, J., Alsaedi, A., Li, X. (2018). LMI-based approach to stability analysis for fractional-order neural networks with discrete and distributed delays. International Journal of Systems Science, 49(3), 537-545.

[276] Yang, Y., He, Y., Wang, Y., Wu, M. (2018). Stability analysis of fractional-order neural networks: an LMI approach. Neurocomputing, 285, 82-93.

[277] Huang, C., Cao, J. (2020). Bifurcation mechanisation of a fractional-order neural network with unequal delays. Neural processing letters, 52, 1171-1187.

[278] Ma, W., Li, C., Wu, Y., Wu, Y. (2014). Adaptive synchronization of fractional neural networks with unknown parameters and time delays. Entropy, 16(12), 6286-6299.

[279] Yu, J., Hu, C., Jiang, H., Fan, X. (2014). Projective synchronization for fractional neural networks. Neural Networks, 49, 87-95.

[280] Ding, Z., Shen, Y. (2016). Projective synchronization of nonidentical fractional-order neural networks based on sliding mode controller. Neural Networks, 76, 97-105.

[281] Song, X., Song, S., Li, B., Tejado Balsera, I. (2018). Adaptive projective synchronization for time-delayed fractional-order neural networks with uncertain parameters and its application in secure communications. Transactions of the Institute of Measurement and Control, 40(10), 3078-3087.

[282] Liu, H., Li, S., Wang, H., Huo, Y., Luo, J. (2015). Adaptive synchronization for a class of uncertain fractional-order neural networks. Entropy, 17(10), 7185-7200.

[283] Ding, Z., Shen, Y., Wang, L. (2016). Global Mittag-Leffler synchronization of fractional-order neural networks with discontinuous activations. Neural Networks, 73, 77-85.

[284] Song, C., Cao, J. (2014). Dynamics in fractional-order neural networks. Neurocomputing, 142, 494-498.

[285] Zhang, S., Yu, Y., Yu, J. (2016). LMI conditions for global stability of fractional-order neural networks. IEEE transactions on neural networks and learning systems, 28(10), 2423-2433.

[286] Gu, Y., Yu, Y., Wang, H. (2017). Synchronization-based parameter estimation of fractional-order neural networks. Physica A: Statistical Mechanics and its Applications, 483, 351-361.

[287] Boroomand, A., Menhaj, M. B. (2009). Fractional-order Hopfield neural networks. In Advances in Neuro-Information Processing: 15th International Conference, ICONIP 2008, Auckland, New Zealand, November 25-28, 2008, Revised Selected Papers, Part I 15 (pp. 883-890). Springer Berlin Heidelberg.

[288] Kaslik, E., Sivasundaram, S. (2011, July). Dynamics of fractional-order neural networks. In The 2011 International Joint Conference on Neural Networks (pp. 611-618). IEEE.

[289] Kaslik, E., Sivasundaram, S. (2012). Nonlinear dynamics and chaos in fractional-order neural networks. Neural Networks, 32, 245-256.

[290] Chen, L., Qu, J., Chai, Y., Wu, R., Qi, G. (2013). Synchronization of a class of fractional-order chaotic neural networks. Entropy, 15(8), 3265-3276.

[291] Wang, H., Yu, Y., Wen, G. (2014). Stability analysis of fractional-order Hopfield neural networks with time delays. Neural Networks, 55, 98-109.

[292] Zhang, S., Yu, Y., Wang, Q. (2016). Stability analysis of fractional-order Hopfield neural networks with discontinuous activation functions. Neurocomputing, 171, 1075-1084.

[293] Wu, H., Zhang, X., Xue, S., Wang, L., Wang, Y. (2016). LMI conditions to global Mittag-Leffler stability of fractional-order neural networks with impulses. Neurocomputing, 193, 148-154.

[294] Petras, I. (2006, July). A note on the fractional-order cellular neural networks. In The 2006 IEEE International Joint Conference on Neural Network Proceedings (pp. 1021-1024). IEEE.

[295] Huang, X., Zhao, Z., Wang, Z., Li, Y. (2012). Chaos and hyperchaos in fractional-order cellular neural networks. Neurocomputing, 94, 13-21.

[296] Stamova, I. (2014). Global Mittag-Leffler stability and synchronization of impulsive fractional-order neural networks with time-varying delays. Nonlinear Dynamics, 77, 1251-1260.

[297] Hu, T., Zhang, X., Zhong, S. (2018). Global asymptotic synchronization of non-identical fractional-order neural networks. Neurocomputing, 313, 39-46.

[298] Pratap, A., Raja, R., Agarwal, R. P., Cao, J., Bagdasar, O. (2020). Multi-weighted complex structure on fractional order coupled neural networks with linear coupling delay: a robust synchronization problem. Neural Processing Letters, 51, 2453-2479.

[299] Qu, H., Zhang, T., Zhou, J. (2020). Global stability analysis of S-asymptotically ω-periodic oscillation in fractional-order cellular neural networks with time variable delays. Neurocomputing, 399, 390-398.

[300] Xiao, J., Li, Y., Wen, S. (2021). Mittag-Leffler synchronization and stability analysis for neural networks in the fractional-order multi-dimension field. Knowledge-Based Systems, 231, 107404.

[301] Hui, M., Wei, C., Zhang, J., Ho-Ching Iu, H., Luo, N., Yao, R., Bai, L. (2020). Finite-Time Projective Synchronization of Fractional-Order Memristive Neural Networks with Mixed Time-Varying Delays. Complexity, 2020(1), 4168705.

[302] Huang, X., Jia, J., Fan, Y., Wang, Z., Xia, J. (2020). Interval matrix method based synchronization criteria for fractional-order memristive neural networks with multiple time-varying delays. Journal of the Franklin Institute, 357(3), 1707-1733.

[303] Yang, X., Song, Q., Liu, Y., Zhao, Z. (2014). Uniform stability analysis of fractional-order BAM neural networks with delays in the leakage terms. In Abstract and applied analysis (Vol. 2014, No. 1, p. 261930). Hindawi Publishing Corporation.

[304] Chen, J., Zeng, Z., Jiang, P. (2014). Global Mittag-Leffler stability and synchronization of memristor-based fractional-order neural networks. Neural Networks, 51, 1-8.

[305] Cao, Y., Bai, C. (2014). Finite-time stability of fractional-order BAM neural networks with distributed delay. In Abstract and Applied Analysis (Vol. 2014, No. 1, p. 634803). Hindawi Publishing Corporation.

[306] Gu, Y., Yu, Y., Wang, H. (2016). Synchronization for fractional-order time-delayed memristor-based neural networks with parameter uncertainty. Journal of the Franklin Institute, 353(15), 3657-3684.

[307] Zhang, S., Yu, Y., Gu, Y. (2017). Global attractivity of memristor-based fractional-order neural networks. Neurocomputing, 227, 64-73.

[308] Yang, X., Li, C., Huang, T., Song, Q., Chen, X. (2017). Quasi-uniform synchronization of fractional-order memristor-based neural networks with delay. Neurocomputing, 234, 205-215.

[309] Pratap, A., Raja, R., Sowmiya, C., Bagdasar, O., Cao, J., Rajchakit, G. (2020). Global projective lag synchronization of fractional order memristor based BAM neural networks with mixed time varying delays. Asian Journal of Control, 22(1), 570-583.

[310] Li, H. L., Jiang, H., Cao, J. (2020). Global synchronization of fractional-order quaternion-valued neural networks with leakage and discrete delays. Neurocomputing, 385, 211-219.

[311] Gu, Y., Wang, H., Yu, Y. (2020). Synchronization for commensurate Riemann-Liouville fractional-order memristor-based neural networks with unknown parameters. Journal of the Franklin Institute, 357(13), 8870-8898.

[312] Xiao, J., Cheng, J., Shi, K., Zhang, R. (2021). A general approach to fixed-time synchronization problem for fractional-order multidimension-valued fuzzy neural networks based on memristor. IEEE Transactions on fuzzy systems, 30(4), 968-977.

[313] Rajchakit, G., Chanthorn, P., Niezabitowski, M., Raja, R., Baleanu, D., Pratap, A. (2020). Impulsive effects on stability and passivity analysis of memristor-based fractional-order competitive neural networks. Neurocomputing, 417, 290-301.

[314] Rakkiyappan, R., Velmurugan, G., Cao, J. (2014). Finite-time stability analysis of fractional-order complex-valued memristor-based neural networks with time delays. Nonlinear Dynamics, 78(4), 2823-2836.

[315] Rakkiyappan, R., Cao, J., Velmurugan, G. (2014). Existence and uniform stability analysis of fractional-order complex-valued neural networks with time delays. IEEE Transactions on Neural Networks and Learning Systems, 26(1), 84-97.

[316] Velmurugan, G., Rakkiyappan, R., Vembarasan, V., Cao, J., Alsaedi, A. (2017). Dissipativity and stability analysis of fractional-order complex-valued neural networks with time delay. Neural Networks, 86, 42-53.

[317] Wu, G. C., Abdeljawad, T., Liu, J., Baleanu, D., Wu, K. T. (2019). Mittag-Leffler stability analysis of fractional discrete-time neural networks via fixed point technique.

[318] Pratap, A., Raja, R., Cao, J., Huang, C., Niezabitowski, M., Bagdasar, O. (2021). Stability of discrete-time fractional-order time-delayed neural networks in complex field. Mathematical Methods in the Applied Sciences, 44(1), 419-440.

[319] Yang, D., Yu, Y., Hu, W., Yuan, X., Ren, G. (2023). Mean square asymptotic stability of discrete-time fractional order stochastic neural networks with multiple time-varying delays. Neural Processing Letters, 55(7), 9247-9268.

[320] You, X., Song, Q., Zhao, Z. (2020). Existence and finite-time stability of discrete fractional-order complex-valued neural networks with time delays. Neural Networks, 123, 248-260.

[321] Zhang, T., Li, Y. (2022). Global exponential stability of discrete-time almost automorphic Caputo–Fabrizio BAM fuzzy neural networks via exponential Euler technique. Knowledge-Based Systems, 246, 108675.

[322] Zhao, M., Li, H. L., Zhang, L., Hu, C., Jiang, H. (2023). Quasi-projective synchronization of discrete-time fractional-order quaternion-valued neural networks. Journal of the Franklin Institute, 360(4), 3263-3279.

[323] You, X., Song, Q., Zhao, Z. (2020). Global Mittag-Leffler stability and synchronization of discrete-time fractional-order complex-valued neural networks with time delay. Neural Networks, 122, 382-394.

[324] Zhang, X. L., Li, H. L., Kao, Y., Zhang, L., Jiang, H. (2022). Global Mittag-Leffler synchronization of discrete-time fractional-order neural networks with time delays. Applied Mathematics and Computation, 433, 127417.

[325] Li, H. L., Cao, J., Hu, C., Zhang, L., Jiang, H. (2023). Adaptive control-based synchronization of discrete-time fractional-order fuzzy neural networks with time-varying delays. Neural Networks, 168, 59-73.

[326] Xiao, Q., Huang, T., Zeng, Z. (2018). Global exponential stability and synchronization for discrete-time inertial neural networks with time delays: A timescale approach. IEEE Transactions on Neural Networks and Learning Systems, 30(6), 1854-1866.

[327] Perumal, R., Hymavathi, M., Ali, M. S., Mahmoud, B. A., Osman, W. M., Ibrahim, T. F. (2023). Synchronization of Discrete-Time Fractional-Order Complex-Valued Neural Networks with Distributed Delays. Fractal and Fractional, 7(6), 452.

[328] Chen, L., Yin, H., Huang, T., Yuan, L., Zheng, S., Yin, L. (2020). Chaos in fractional-order discrete neural networks with application to image encryption. Neural Networks, 125, 174-184.

[329] Hilfer, R. (Ed.). (2000). Applications of fractional calculus in physics. World scientific.

[330] West, B. J. (2016). Fractional calculus view of complexity: tomorrow's science. CRC Press.

[331] Kilbas, A. A., Srivastava, H. M., Trujillo, J. J. (2006). Theory and applications of fractional differential equations (Vol. 204). elsevier.

[332] Sabatier, J. A. T. M. J., Agrawal, O. P., Machado, J. T. (2007). Advances in fractional calculus (Vol. 4, No. 9). Dordrecht: Springer.

[333] Stancu-Minasian, I. M. (2012). Fractional programming: theory, methods and applications (Vol. 409). Springer Science & Business Media.

[334] Goodrich, C., & Peterson, A. C. (2015). Discrete fractional calculus (Vol. 10, pp. 978-3). Cham: Springer.

[335] Edelman, M., Macau, E. E., Sanjuan, M. A. (Eds.). (2018). Chaotic, fractional, and complex dynamics: new insights and perspectives. Berlin, Germany: Springer International Publishing.

[336] Chen, Y., Li, X., Liu, S. (2021). Finite-time stability of ABC type fractional delay difference equations. Chaos, Solitons & Fractals, 152, 111430.

[337] Wei, Y., Wei, Y., Chen, Y., Wang, Y. (2020). Mittag–Leffler stability of nabla discrete fractional-order dynamic systems. Nonlinear Dynamics, 101, 407-417.

[338] Rashid, S., Sultana, S., Karaca, Y., Khalid, A., Chu, Y. M. (2022). Some further extensions considering discrete proportional fractional operators. Fractals, 30(01), 2240026.

[339] You, X., Song, Q., Zhao, Z. (2020). Global Mittag-Leffler stability and synchronization of discrete-time fractional-order complex-valued neural networks with time delay. Neural Networks, 122, 382-394.

[340] Pratap, A., Raja, R., Cao, J., Huang, C., Niezabitowski, M., Bagdasar, O. (2021). Stability of discrete-time fractional-order time-delayed neural networks in complex field. Mathematical Methods in the Applied Sciences, 44(1), 419-440.

[341] Li, R., Cao, J., Xue, C., Manivannan, R. (2021). Quasi-stability and quasi-synchronization control of quaternion-valued fractional-order discrete-time memristive neural networks. Applied Mathematics and Computation, 395, 125851.

[342] You, X., Song, Q., Zhao, Z. (2020). Existence and finite-time stability of discrete fractional-order complex-valued neural networks with time delays. Neural Networks, 123, 248-260.

[343] Gu, Y., Wang, H., Yu, Y. (2020). Synchronization for fractional-order discrete-time neural networks with time delays. Applied Mathematics and Computation, 372, 124995.

[344] You, X., Dian, S., Guo, R., Li, S. (2021). Exponential stability analysis for discrete-time quaternion-valued neural networks with leakage delay and discrete time-varying delays. Neurocomputing, 430, 71-81.

[345] Wu, G. C., Abdeljawad, T., Liu, J., Baleanu, D., Wu, K. T. (2019). Mittag-Leffler stability analysis of fractional discrete-time neural networks via fixed point technique.

[346] Djenina, N., Ouannas, A., Batiha, I. M., Grassi, G., Pham, V. T. (2020). On the stability of linear incommensurate fractional-order difference systems. Mathematics, 8(10), 1754.

[347] Shatnawi, M. T., Djenina, N., Ouannas, A., Batiha, I. M., Grassi, G. (2022). Novel convenient conditions for the stability of nonlinear incommensurate fractional-order difference systems. Alexandria Engineering Journal, 61(2), 1655-1663.

[348] Stanisławski, R., Latawiec, K. J. (2021). A modified Mikhailov stability criterion for a class of discrete-time noncommensurate fractional-order systems. Communications in Nonlinear Science and Numerical Simulation, 96, 105697.

[349] Hamadneh, T., Hioual, A., Alsayyed, O., Al-Khassawneh, Y. A., Al-Husban, A., Ouannas, A. (2023). Finite Time Stability Results for Neural Networks Described by Variable-Order Fractional Difference Equations. Fractal and Fractional, 7(8), 616.

[350] Hioual, A., Ouannas, A., Oussaeif, T. E., Grassi, G., Batiha, I. M., Momani, S. (2022). On variable-order fractional discrete neural networks: solvability and stability. Fractal and Fractional, 6(2), 119.

[351] Chen, L., Gu, P., Lopes, A. M., Chai, Y., Xu, S., Ge, S. (2023). Asymptotic stability of fractional-order incommensurate neural networks. Neural Processing Letters, 55(5), 5499-5513.

[352] Karoun, R. C., Ouannas, A., Horani, M. A., Grassi, G. (2022). The effect of Caputo fractional variable difference operator on a discrete-time hopfield neural network with non-commensurate order. Fractal and Fractional, 6(10), 575.

[353] Wang, M., Wang, Y., Chu, R. (2023). Dynamical analysis of the incommensurate fractional-order Hopfield neural network system and its digital circuit realization. Fractal and Fractional, 7(6), 474.

[354] Liu, H., Shen, Y., Zhao, X. (2013). Finite-time stabilization and boundedness of switched linear system under state-dependent switching. Journal of the Franklin Institute, 350(3), 541-555.

[355] Amato, F., Ambrosino, R., Ariola, M., Cosentino, C. (2009). Finite-time stability of linear time-varying systems with jumps. Automatica, 45(5), 1354-1358.

[356] Wu, G. C., Baleanu, D., Zeng, S. D. (2018). Finite-time stability of discrete fractional delay systems: Gronwall inequality and stability criterion. Communications in Nonlinear Science and Numerical Simulation, 57, 299-308.

[357] Du, F., Jia, B. (2020). Finite time stability of fractional delay difference systems: A discrete delayed Mittag-Leffler matrix function approach. Chaos, Solitons & Fractals, 141, 110430.

[358] Chen, Y., Li, X., Liu, S. (2021). Finite-time stability of ABC type fractional delay difference equations. Chaos, Solitons & Fractals, 152, 111430.

[359] Wu, R. C., Hei, X. D., Chen, L. P. (2013). Finite-time stability of fractional-order neural networks with delay. Communications in Theoretical Physics, 60(2), 189.

[360] Wu, R., Lu, Y., Chen, L. (2015). Finite-time stability of fractional delayed neural networks. Neurocomputing, 149, 700–707.

[361] Yang, X., Song, Q., Liu, Y., Zhao, Z. (2015). Finite-time stability analysis of fractional-order neural networks with delay. Neurocomputing, 152, 19–26.

[362] Ding, X., Cao, J., Zhao, X., Alsaadi, F. E. (2017). Finite-time stability of fractional-order complexvalued neural networks with time delays. Neural Processing Letters, 46, 561–580.

[363] Rakkiyappan, R., Velmurugan, G., Cao, J. (2014). Finite-time stability analysis of fractional-order complex-valued memristor-based neural networks with time delays. Nonlinear Dynamics, 78(4), 2823-2836.

[364] Wang, L., Song, Q., Liu, Y., Zhao, Z., Alsaadi, F. E. (2017). Finite-time stability analysis of fractional-order complex-valued memristor-based neural networks with both leakage and time-varying delays. Neurocomputing, 245, 86-101.

[365] Wu, G. C., Baleanu, D., Zeng, S. D. (2018). Finite-time stability of discrete fractional delay systems: Gronwall inequality and stability criterion. Communications in Nonlinear Science and Numerical Simulation, 57, 299-308.

[366] Du, F., Jia, B. (2021). A generalized fractional (q, h)–Gronwall inequality and its applications to nonlinear fractional delay (q, h)–difference systems. Mathematical Methods in the Applied Sciences, 44(13), 10513-10529.

[367] Hioual, A., Ouannas, A., Grassi, G., Oussaeif, T. E. (2023). Nonlinear nabla variable-order fractional discrete systems: Asymptotic stability and application to neural networks. Journal of Computational and Applied Mathematics, 423, 114939.

[368] Hamadneh, T., Hioual, A., Alsayyed, O., Al-Khassawneh, Y. A., Al-Husban, A., Ouannas, A. (2023). Finite Time Stability Results for Neural Networks Described by Variable-Order Fractional Difference Equations. Fractal and Fractional, 7(8), 616.

[369] Hioual, A., Ouannas, A., Momani, S., Oussaeif, T. E. (2023, March). Finite-Time Stability of ABC Type h-Fractional Discrete Neural Networks: Gronwall Inequality and Stability Criterion. In 2023 International Conference on Fractional Differentiation and Its Applications (ICFDA) (pp. 1-6). IEEE.

[370] Chen, C., Bohner, M., Jia, B. (2019). Ulam-Hyers stability of Caputo fractional difference equations. Mathematical Methods in the Applied Sciences, 42(18), 7461-7470.

[371] Jonnalagadda, J. M. (2016). Hyers-Ulam Stability of Fractional Nabla Difference Equations. International Journal of Analysis, 2016(1), 7265307.

[372] Selvam, A. G. M., Baleanu, D., Alzabut, J., Vignesh, D., Abbas, S. (2020). On Hyers–Ulam Mittag-Leffler stability of discrete fractional Duffing equation with application on inverted pendulum. Advances in Difference Equations, 2020, 1-15.

[373] Hioual, A., Ouannas, A., Oussaeif, T. E., Grassi, G., Batiha, I. M., Momani, S. (2022). On variable-order fractional discrete neural networks: solvability and stability. Fractal and Fractional, 6(2), 119.

[374] Pratap, A., Raja, R., Cao, J., Huang, C., Niezabitowski, M., Bagdasar, O. (2021). Stability of discrete-time fractional-order time-delayed neural networks in complex field. Mathematical Methods in the Applied Sciences, 44(1), 419-440.

[375] Zhang, H., Ye, R., Liu, S., Cao, J., Alsaedi, A., Li, X. (2018). LMI-based approach to stability analysis for fractional-order neural networks with discrete and distributed delays. International Journal of Systems Science, 49(3), 537-545.

[376] Li, H., Kao, Y., Bao, H., Chen, Y. (2021). Uniform stability of complex-valued neural networks of fractional order with linear impulses and fixed time delays. IEEE Transactions on Neural Networks and Learning Systems, 33(10), 5321-5331.

[377] Almatroud, O. A., Hioual, A., Ouannas, A., Sawalha, M. M., Alshammari, S., Alshammari, M. (2023). On variable-order fractional discrete neural networks: existence, uniqueness and stability. Fractal and Fractional, 7(2), 118.

[378] Burton, T. A., Furumochi, T. (2002). Krasnoselskii's fixed point theorem and stability. Nonlinear Analysis-Theory Methods and Applications, 49(4), 445-454.

[379] Chen, C., Bohner, M., Jia, B. (2019). Ulam-Hyers stability of Caputo fractional difference equations. Mathematical Methods in the Applied Sciences, 42(18), 7461-7470.

[380] Franco-Perez, L., Fernandez-Anaya, G., Quezada-Téllez, L. A. (2020). On stability of nonlinear nonautonomous discrete fractional Caputo systems. Journal of Mathematical Analysis and Applications, 487(2), 124021.

[381] Djennoune, S., Bettayeb, M., Al-Saggaf, U. M. (2019). Synchronization of fractional-order discrete-time chaotic systems by an exact delayed state reconstructor: Application to secure communication. International Journal of Applied Mathematics and Computer Science, 29(1), 179-194.

[382] Megherbi, O., Hamiche, H., Djennoune, S., Bettayeb, M. (2017). A new contribution for the impulsive synchronization of fractional-order discrete-time chaotic systems. Nonlinear Dynamics, 90, 1519-1533.

via cross-coupled second-order discrete-time fractional-order sliding mode. IEEE/ASME Transactions on Mechatronics, 26(1), 358-368.

via cross-coupled second-order discrete-time fractional-order sliding mode. IEEE/ASME Transactions on Mechatronics, 26(1), 358-368.

[383] Xin, B., Wu, Z. (2015). Projective synchronization of chaotic discrete dynamical systems via linear state error feedback control. Entropy, 17(5), 2677-2687.

[384] Wang, S., Jian, J. (2023). Predefined-time synchronization of incommensurate fractionalorder competitive neural networks with time-varying delays. Chaos, Solitons & Fractals, 177, 114216.

[385] Gu, Y., Wang, H., Yu, Y. (2019). Synchronization for incommensurate Riemann–Liouville fractional-order time-delayed competitive neural networks with different time scales and known or unknown parameters. Journal of Computational and Nonlinear Dynamics, 14(5), 051002.

[386] Jia, J., Wang, F., Zeng, Z. (2022). Lag quasi-synchronization of incommensurate fractionalorder memristor-based neural networks with nonidentical characteristics via quantized control: A vector fractional Halanay inequality approach. Journal of the Franklin Institute, 359(12), 6392-6437.

[387] Wang, M., Wang, Y., Chu, R. (2023). Dynamical Analysis of the Incommensurate Fractional-Order Hopfield Neural Network System and Its Digital Circuit Realization. Fractal and Fractional, 7(6), 474.

[388] Hioual, A., Ouannas, A., Momani, S., Oussaeif, T. E. (2023, March). Finite-Time Stability of ABC Type h-Fractional Discrete Neural Networks: Gronwall Inequality and Stability Criterion. In 2023 International Conference on Fractional Differentiation and Its Applications (ICFDA) (pp. 1-6). IEEE.

[389] Momani, S., Batiha, I. M., Hioual, A., Ouannas, A. (2023, March). Fractional Neural Networks: Finite time stability and its application to synchronization. In 2023 International Conference on Fractional Differentiation and Its Applications (ICFDA) (pp. 1-5). IEEE.

[390] Popa, C. A., Kaslik, E. (2020). Finite-time Mittag–Leffler synchronization of neutral-type fractional-order neural networks with leakage delay and time-varying delays. Mathematics, 8(7), 1146.

Abstract

Thesis: On Nonlinear Fractional-Order Neural Networks

Option: **Mathematics**
Specialty: **Applied Mathematics**
Post graduate student: **Amel Hioual**
Supervisor: **Taki Eddine Oussaeif**

This thesis aims to investigate the existence, uniqueness, and stability of solutions for nonlinear fractional order neural networks. Additionally, it focuses on the numerical resolution of this problem and the dynamic simulation of solutions. Our study encompasses various cases, including fractional nonlinear partial differential neural networks, discrete-time fractional partial differential neural networks, and incommensurate fractional-order variable-order differential and discrete-time neural networks.

The study addresses several analytical and dynamic problems in nonlinear neural networks described by fractional order differential and difference equations. Utilizing robust analytical approaches, we present new results on the existence and uniqueness of solutions for fractional order neural networks. These findings are crucial for understanding the underlying behavior and characteristics of such complex systems.

Furthermore, significant attention is given to the stability analysis of these neural networks. We achieve notable results concerning the asymptotic stability, finite time stability, uniform stability, Ulam-Hyers stability, and synchronization of fractional order neural network models. These stability properties are essential for ensuring the reliability and predictability of the network's performance over time.

To substantiate our theoretical findings, we conduct extensive numerical simulations. These simulations are designed to illustrate the dynamic behavior of the solutions and to validate the theoretical predictions. The numerical results provide a visual and practical confirmation of the analytical outcomes, thereby bridging the gap between theory and practice. **Keywords:** Fractional-order neural networks ; Fractional-order differential equations ; Fractional-order difference equation; Stability; Asymptotical stability.

Résumé

Thèse : Sur les réseaux de neurones non linéaires d'ordre fractionnaire

Option : **Mathématiques**
Spécialité : **Mathématiques Appliquées**
Étudiant de troisième cycle : **Amel Hioual**
Encadrant : **Taki Eddine Oussaeif**

Cette thèse vise à étudier l'existence, l'unicité et la stabilité des solutions pour les réseaux de neurones non linéaires d'ordre fractionnaire. De plus, elle se concentre sur la résolution numérique de ce problème et la simulation dynamique des solutions. Notre étude englobe divers cas, notamment les réseaux de neurones non linéaires à dérivées partielles d'ordre fractionnaire, les réseaux de neurones à dérivées partielles d'ordre fractionnaire en temps discret, et les réseaux de neurones à ordre différentiel variable et à ordre fractionnaire incommensurable en temps discret.

L'étude aborde plusieurs problèmes analytiques et dynamiques dans les réseaux de neurones non linéaires décrits par des équations différentielles et des équations aux différences d'ordre fractionnaire. En utilisant des approches analytiques robustes, nous présentons de nouveaux résultats sur l'existence et l'unicité des solutions pour les réseaux de neurones d'ordre fractionnaire. Ces résultats sont essentiels pour comprendre le comportement et les caractéristiques sous-jacentes de ces systèmes complexes.

De plus, une attention particulière est accordée à l'analyse de la stabilité de ces réseaux de neurones. Nous obtenons des résultats notables concernant la stabilité asymptotique, la stabilité en temps fini, la stabilité uniforme, la stabilité d'Ulam-Hyers et la synchronisation des modèles de réseaux de neurones d'ordre fractionnaire. Ces propriétés de stabilité sont cruciales pour garantir la fiabilité et la prévisibilité des performances du réseau au fil du temps.

Pour étayer nos résultats théoriques, nous effectuons des simulations numériques approfondies. Ces simulations sont conçues pour illustrer le comportement dynamique des solutions et valider les prédictions théoriques. Les résultats numériques fournissent une confirmation visuelle et pratique des résultats analytiques, comblant ainsi le fossé entre la théorie et la pratique. **Keywords :** Réseaux de neurones d'ordre fractionnaire ; Équations différentielles d'ordre fractionnaire ; Équations aux différences d'ordre fractionnaire ; Stabilité ; Stabilité asymptotique

ملخص

الاطروحة :حول الشبكات العصبية غير الخطية من الرتبة الكسرية

الميدان : رياضيات

التخصص: رياضيات تطبيقية

طالبة الدكتوراه: امال حيوال

المؤطر: اوصيف تقي الدين

تهدف هذه الأطروحة إلى دراسة وجود وحيدة واستقرار الحلول لشبكات العصبية غير الخطية من الرتبة الكسرية. بالإضافة إلى ذلك، تركز على الحل العددي لهذه المشكلة والمحاكاة الديناميكية للحلول. تتضمن دراستنا عدة حالات، بما في ذلك شبكات العصبية غير الخطية ذات المشتقات الجزئية من الرتبة الكسرية، شبكات العصبية ذات المشتقات الجزئية من الرتبة الكسرية في الزمن المتقطع، وشبكات العصبية ذات الرتبة التفاضلية المتغيرة والمتفاوتة الكسرية في الزمن المتقطع.

تتناول الدراسة العديد من المشاكل التحليلية والديناميكية في الشبكات العصبية غير الخطية الموصوفة بالمعادلات التفاضلية ومعادلات الفروق من الرتبة الكسرية. باستخدام مناهج تحليلية قوية، نقدم نتائج جديدة حول وجود وحيدة الحلول لشبكات العصبية من الرتبة الكسرية. هذه النتائج ضرورية لفهم السلوك والخصائص الأساسية لهذه الأنظمة المعقدة.

بالإضافة إلى ذلك، يتم التركيز بشكل خاص على تحليل استقرار هذه الشبكات العصبية. نحصل على نتائج بارزة فيما يتعلق بالاستقرار المتزامن، الاستقرار في الوقت المحدود، الاستقرار المنتظم، استقرار يولام-هايرز والتزامن في نماذج الشبكات العصبية من الرتبة الكسرية. هذه الخصائص الاستقرارية ضرورية لضمان موثوقية وقابلية التنبؤ بأداء الشبكة مع مرور الوقت.

لتدعيم نتائجنا النظرية، نجري محاكاة عددية شاملة. هذه المحاكاة مصممة لتوضيح السلوك الديناميكي للحلول والتحقق من صحة التنبؤات النظرية. تقدم النتائج العددية تأكيدًا بصريًا وعمليًا للنتائج التحليلية، مما يجسر الفجوة بين النظرية والتطبيق.

تقدم هذه الدراسة الشاملة رؤى قيمة حول سلوك شبكات العصبية من الرتبة الكسرية. تساهم نتائجنا في فهم أفضل للديناميكيات لهذه الشبكات، مما يبرز إمكاناتها في التطبيقات المختلفة، بما في ذلك أنظمة التحكم، معالجة الإشارات والذكاء الاصطناعي. من خلال تقديم مزيج من التحليلات النظرية الدقيقة والمحاكاة العددية المفصلة، نؤسس أساسًا قويًا للأبحاث المستقبلية في مجال شبكات العصبية من الرتبة الكسرية.

الكلمات المفتاحية:

الشبكات العصبية ذات الترتيب الكسري; المعادلات التفاضلية ذات الترتيب الكسري; معادلات الفروق ذات الترتيب الكسري; الاستقرار ;الاستقرار التماثلي